DEVELOPING POLYMER BASED SURFACE MODIFIED COMPOSITE FOR DRUG ELUTING ORTHOPEDIC IMPLANTS

Ph.D. THESIS

by

MANOJ KUMAR R

DEPARTMENT OF METALLURGICAL AND MATERIALS ENGINEERING
INDIAN INSTITUTE OF TECHNOLOGY ROORKEE
ROORKEE – 247667, INDIA
JULY, 2019

DEVELOPING POLYMER BASED SURFACE MODIFIED COMPOSITE FOR DRUG ELUTING ORTHOPEDIC IMPLANTS

A THESIS

Submitted in partial fulfilment of the requirements for the award of the degree

of

DOCTOR OF PHILOSOPHY

in

METALLURGICAL AND MATERIALS ENGINEERING

by

MANOJ KUMAR R

DEPARTMENT OF METALLURGICAL AND MATERIALS ENGINEERING
INDIAN INSTITUTE OF TECHNOLOGY ROORKEE
ROORKEE – 247667, INDIA
JULY, 2019

©INDIAN INSTITUTE OF TECHNOLOGY ROORKEE, ROORKEE- 2019
ALL RIGHTS RESERVED

INDIAN INSTITUTE OF TECHNOLOGY ROORKEE
ROORKEE

CANDIDATE'S DECLARATION

I hereby certify that the work which is being presented in the thesis entitled **"Developing Polymer Based Surface Modified Composite for Drug Eluting Orthopedic Implants"** in partial fulfilment of the requirements for the award of the degree of Doctor of Philosophy and submitted in the Department of Metallurgical and Materials Engineering of the Indian Institute of Technology Roorkee, Roorkee is an authentic record of my own work carried out during a period from January, 2013 to July, 2019 under the supervision of Dr. Debrupa Lahiri, Associate Professor, Department of Metallurgical and Materials Engineering, Indian Institute of Technology Roorkee, Roorkee.

The matter presented in this thesis has not been submitted by me for the award of any other degree of this or any other Institution.

(MANOJ KUMAR R)

This is to certify that the above statement made by the candidate is correct to the best of my knowledge.

Date:

(Dr. Debrupa Lahiri)
Supervisor(s)

ABSTRACT

Osteoarthritis is a degenerative joint disease, caused due to wear and breaking down of the bone cartilage in a joint. Prosthetic joint replacement is the only solution after all non-surgical treatments fail to resolve the issue. Joint replacement alleviates the pain and restores the function of joints, improving the activeness in the patients. However, even after decades of successful track record, ~10% of these implant fail prematurely, within the first 10 to 20 years, thereby affecting many tens of thousands of patients annually. These premature failures lead to revision of surgeries. Aseptic loosening, fracture and implant associated infection are the main causes of arthroplasty failures. Despite sterilization and aseptic procedure, bacterial infection remains a key challenge in total hip arthroplasties. This fact emphasizes the urgent need for development of new implant systems, which should take care the infection by delivering the drug locally and improve structural stability to minimize the implant loosening and fracture. Hence, the major aim of the present investigation is to modifying the surfaces of polymeric acetabular cup liner for sustain delivery of drugs, while retaining the mechanical and tribological properties of clinically used ultra-high molecular weight polyethylene (UHMWPE) joint prostheses. The present work mainly includes four major parts.

In first part of the study, modified solvent based etching and lyophilization technique was used to engineer a thin porous surface layer on UHMWPE (PE) substrate, which is clinically used as acetabular cup lining. Gentamicin contained chitosan solution has been impregnated into modified surface, which suitably gets released over a long period. The main challenge was to keep the mechanical and tribological behavior of this lining material unaffected after the modification. Modified surface offers reduction in friction coefficient and wear rate, by 26% and 19%, respectively, in comparison to PE, which is encouraging towards the intended application. Hardness and elastic modulus decreases slightly, by 27% and 20%,

respectively, possibly due to improper impregnation of chitosan inside porous surface. However, after drug release, the modified surface regains the mechanical and tribological behavior similar to unmodified PE. Surface modified PE have shown an impressive release profile for drug up to 26 days and released ~94.11% of the total drug content. In vitro antibacterial tests have proven that the modified surface of PE can effectively release the drug and fight against infection. Besides, positive outcome of in-vitro cell culture shows potential of this material system in intended application.

In second part, electrostatic spray coating technique was used to construct the thin interconnected micro porous coating on PE substrate. Coating integrity, after curing, is expected to be good by considering the similarity in coating and substrate material. Uniform and deep pores were observed throughout the surface. Surface morphology on drug delivery kinetics, antibacterial efficacy, mechanical and tribological behavior was discussed extensively. This technique was compared with the former (modified solvent based etching technique) and competitive salient features of both were identified. Both the modified surfaces have shown slight decrease in hardness and elastic modulus, which may be attributed to improper impregnation of polymer inside porous surface. However, after the release of drug, the solvent-based etched surfaces regain its mechanical and tribological properties, in similar range to the unmodified PE surface, but not in case of electrostatic spray coating. Besides, the surfaces, modified by both techniques, have shown lower friction coefficient. But, higher wear rates were noticed for electrostatic sprayed coating. On the other hand, the drug release duration (860 h) was more for electrostatic spray modified surface than chemical etched surface (624 h).

In third part, an attempt has been made to improve the basic properties of conventional PE liner by preparing CNT-PE composite, to address issue related to decrease in mechanical property during surface modification of liner. CNTs are the great choice as reinforcement to prepare bio-composite because of its high in-plane-stiffness and strength, which helps in

toughening agent. Besides, their weaker out-of-plane integrity offers solid lubrication mechanism. Two different aspect ratios of CNTs, namely high aspect ratio (HAR-900) and low aspect ratio (LAR-75) ones were reinforced with PE matrix. A nominal 0.05–0.1 wt.% of CNT addition increases the hardness and elastic modulus of PE by 3–45% and 8–42%, respectively. Higher aspect ratio CNTs (HARCs) are found more effective in improving hardness (45%) and modulus (42%) of PE composite. On the other hand, significant improvement in tribological and thermal degradation property was also noticed for HARCs than LARCs (low aspect ratio CNTs) composite. Reasons for better performance of HARCs are their morphological similarity with polymer chains. The composite, containing 0.1 wt.% HARC have shown best mechanical and tribological behavior.

In fourth part, modified solvent based etching technique is used to engineer thin porous surface layer on 0.1 wt.% reinforced HARC composite. Modified test sample have shown an impressive gentamicin release profile up to 492 h (21 days). Around 89% of the total drug content got released in sustainable manner. Where as in surface modified PE, gentamicin released up to 624 h (26 days) and ~94.11% of the total drug content got released. The difference is directly related to surface morphology. In vitro antibacterial examination (Disc Diffusion Test) had proven the efficacy of drug release to eradicate the bacteria around the sample. Besides, modified surfaces of the HARC composite have shown reduction in friction coefficient and specific wear rate by 36% and 20%, respectively, as compared to PE. This was attributed due to improved mechanical properties of CNTs and their self-lubricating mechanism. Even after drug release, the mechanical and tribological properties of CNT-PE composite are much better than PE. In-vitro cytocompatibility results are also encouraging towards its intended application. Hence, these surfaces modified CNT-PE composite sample has shown great promise for fighting against initial infection after surgery.

The surface engineered acetabular cup lining is a promising candidate in the area of drug eluting implant, which can bring a significant advancement to the functionality of commercially used orthopedic implants by providing inherent capacity for fighting against infections in-vivo.

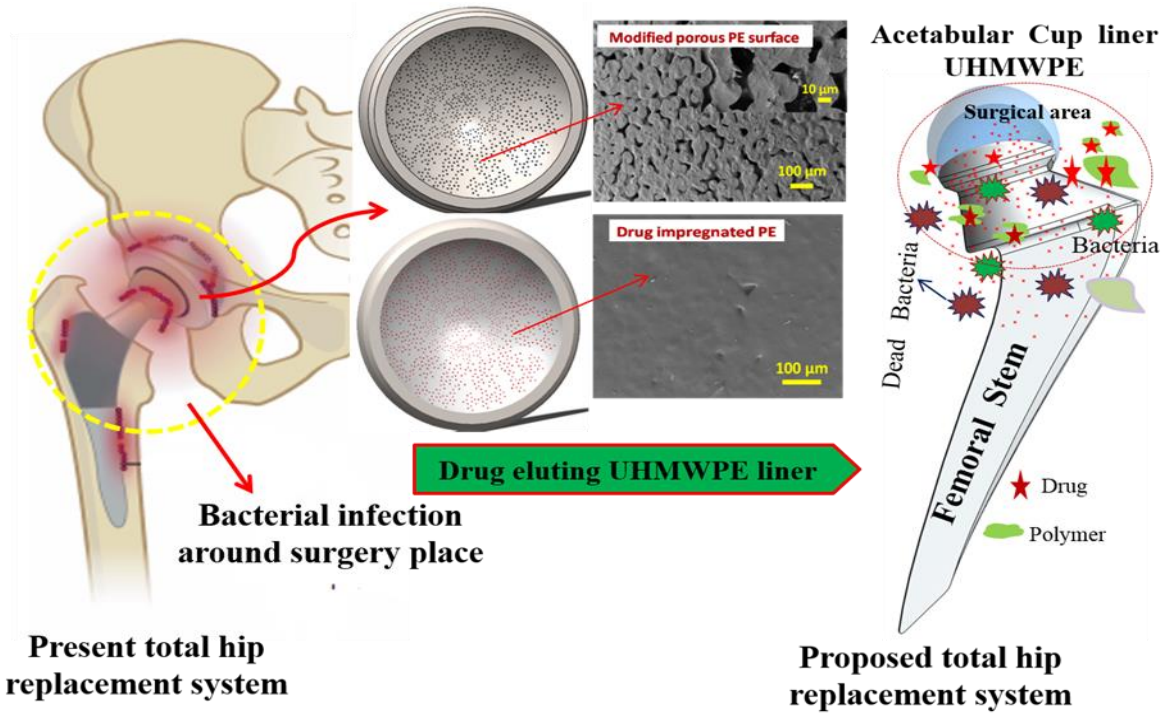

Figure shows the graphical representation of the proposed work

ACKNOWLEDGMENT

First of all, I would like to express my deepest gratitude, sincere thanks and acknowledgement to my respected supervisor Dr. Debrupa Lahiri, Associate Professor, Department of Metallurgical and Materials Engineering, Indian Institute of Technology Roorkee, for showing her faith in me and giving me the wonderful opportunity of doing research under her supervision. Her constant motivation and support throughout my entire research tuner helped me to achieve this milestone in my life. She gave me valuable time for discussions and suggestions for making the good explanation and easy understanding of research work. Her immense enthusiasm and unlimited zeal have been major driving force during my Ph.D. work which helped me a lot to develop myself professionally. I have learnt a lot from her, without her help I could not have finished my Ph.D. thesis successfully. It is very difficult for me to express my gratitude towards her in few words. I could not have imagined having a better advisor and mentor for my Ph.D. work than her. To her, I shall remain, professionally and emotionally obliged.

I would like to thank Dr. Ujjwal Prakash, Departmental Research Committee (DRC) chairman; Dr. B.V. Manoj Kumar, Internal Member and Dr. Partha Roy, External Member of my SRC committee for taking efforts in reading and providing the constructive suggestions with valuable comments throughout the thesis work. I would also like to thank Dr. Indranil Lahiri, Assistant Professor, Metallurgical and Materials Engineering Department, IIT Roorkee, for his valuable comments and suggestions throughout my research work.

I am deeply obliged to present my regards to Head of the Department Dr. G.P. Chaudhari, Professor, Metallurgical and Materials Engineering Department, for his help and providing the facilities in the department for my research work. I would also like to show my

appreciation to all our departmental faculties and our technical staff who have helped me through the experimental work, especially, Mr. R. K. Sharma for supporting me in the usage of departmental facilities.

Thanks are also due to my seniors, colleagues and friends Dr. Sandan Kumar Sharma, Dr. Vijeyesh Kumar, Dr. Raj Kumar, Dr. Rajanna siddaiah, Dr. Dhasharath, Dr. Yogesh K K, Dr. Neeraj, Dr. Swati Haldar, Dr. Muruli, Pallavi Gupta, Ankita Bhist, Sathish Jaiswal, Anshu Dubey, Vaibhav, Bisal, Rajesh Kanike, Sidharth, Souvik, Gurginder, Vinod, Promod, Rayapudi, Atif Suhael, Siddappa, Mukul, Sanjay, Akanksha, Palash and all BMML & NAL lab members for all the support and making my journey pleasant.

My heartfelt gratitude and sincere thanks goes to my parents, Shri. Rangaswamy and Smt. Rajamma, and my lovely brother Shri. Mahendra Kumar R, and my sisters Smt. Pankaja, Rekha and my Brother-In-Laws Mr. Puttaraju and Veerappa, Sister-In-Law Smt. Gheetha. I would also like to thank specially my wife Smt. Smitha V, for continuous support in all up and downs, and for their patience, love, guidance, encouragement and prayers during this research period.

I also like to thank everyone who supported me for completing this work successfully and I express my apology that I could not mention everyone individually.

Above all, to the great almighty, the author of knowledge and wisdom, for his everlasting love and strength that he bestowed upon me throughout my life.

MANOJ KUMAR R

TABLE OF CONTENTS

LIST OF FIGURES

LIST OF TABLES

CHAPTER 1

Introduction

During last five decades, biomaterials have seen a rapid growth, due to its direct impact on healthcare and advancements in the fabrication of synthetic biomaterials. The biomaterials market, including medical device and implants, is estimated to be greater than $130.17 billion US Dollars by the end of 2021 and is expected to increase by 13.2% every year [1][2]. The largest market size amongst all biomaterial products belongs to orthopedic devices and it is expected to reach $41.2 billion US Dollars by 2019.The current size of the Indian orthopedic devices market is ~$375 million US Dollars (Rs. 2,400 Crores) and it will grow ~ 20% every year for the next decade to reach $2.5 billion US Dollars (Rs. 16,000 Crores) by 2030 [3][4].

Owing to an increase in the aging population and active sedentary lifestyle, musculoskeletal (MSK) disorders are the second most cause of disability worldwide, according to a report by international experts, published in The Lancet on 15th December 2012 [5]. Musculoskeletal conditions, such as, osteoarthritis, osteoporosis, fragility fractures, back and neck pain, soft tissue rheumatism, injuries due to sports, workplace and road traffic accidents, so called joint diseases affect more than 1.7 billion people globally [4]. In India, 12-15% of the population seems to suffer from MSK [6]. Sharp increase in the number of primary total hip orthroplasties (THA) and primary total knee orthroplasties (TKA) are noticed in last two decades, due to increasing cases of osteoarthritis [7].

Osteoarthritis is degenerative joint syndrome, resulting from sickness, generic factors and obesity. It makes cartilage to worn out and creates severe pain during movement, due to bone to bone contact [8]. Implants are suggested medically as an option only when all non-surgical treatments have failed. The advantages of orthopedic implants are that they offer enhanced mobility to patient, reduce pain, restore function of the joint and resume back to

higher quality of life. According to 2007 estimation, ~1.5 million joint replacements have been performed annually around the world [7]. In India, over 70,000 hip and knee replacements are being performed every year [6]. However, even after decades of successful track record, ~10% of these implant fail prematurely, within the first 10 to 20 years, thereby affecting many tens of thousands of patients annually. These premature failures lead to revision of surgeries. Aseptic loosening, fracture, massive bone loss, dislocations and implant associated infection are the main causes of arthroplasty failures [7]-[14]. Relative distribution for the revision causes of THA (Total Hip Arthroplasties) in India during 2013 as shown in fig 1.1 [6]. Aseptic loosening, wear and fracture represent the predominant mode of failure in hip arthroplasty.

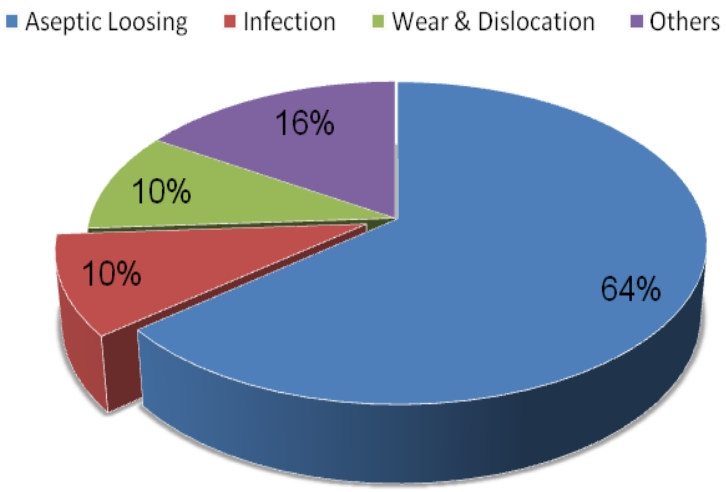

Fig. 1.1 *Different causes for total hip implant failure in India*

Infection rate of THA during the first two years is ~ 2 to 5%, in United States and Europe [15]-[17]. But, in India, the infection rate found little higher than US, around 10%. This is due to growing number of diabetes and obesity patients in India. Besides, the infection rates after revision of surgery, is considerably higher (5 to 40%) than the first surgery [16]. An implant associated infections occur due to microbes, particularly bacterial attachment on implant [17]. Aseptic loosening and implant associated infection looks to be mutually exclusive, but in recent research exploded the potential connection between them. Implants that

have been reported, fail due to aseptically, later found that, latent occult infections that may have been missed prior to the time of diagnosis [17][18]. Hence, even in cases of implant failure due to aseptic loosening, where infection was not the main cause, microbial presence in the implant may still play a key role in initiating or accelerating the failure pathway in later stage [17]. Once infection starts, it is difficult to treat and also tends to persist for a longer period. Moreover, an episode of infection severely reduces the quality of life in many patients. Currently, more number of patients has high risk of infection due to growing number of diabetes, obesity, dialysis and aging population. As a result, health care expenditure will also increases for revision of surgery and it is estimated to reach greater than 1.6 billion US dollar in 2020 [19], which is likely a worldwide valid prediction. Hence, prevention of infections is becoming more important.

Bacterial infection of a joint prosthesis occurs due to homeostatic imbalance between the host tissue and the presence of micro-organisms around the surgical site. Despite high sterilization and advances parenteral antibiotic prophylaxis, implant associated infection is still a clinical issues [20]. Most of the bacterial infection are caused by staphylococcus aureus and continue to be major complication after surgical procedure [21]. During “decisive period”, after the surgery, first 6 h of post implantation is more susceptible to bacterial adhesion, colonization and biofilms formation at the implant-tissue interface [22][23]. Biofilms are biologically active matrix for cells and major form of microbial life [24]. Once biofilms is established within surgical area or implant surface, it is difficult to stamp out the infection even with high dose of antibiotics, due its phenotypic resistance to antibiotics [25]. It can lead to prolonged hospitalization and sometimes implant failure also. Secondary surgery for its removal increases the economic burden and mortality rate [26]. Late infection, after 4 to 6 weeks of the surgery, leads to high joint pain, early loosening. This is mostly caused by hematogenously spread bacteria, such as, coagulase-negative staphylococci and propionibacterium acnes [27]-[29].

Inhibiting the initial bacterial adhesion on implant surface is often regarded as the most critical step to prevent the implant-associated infections. Hence, adequate supply of antibiotics around the surgery area is must for first couple of weeks to stop the initial infection.

In this connection, conventional or systematic drug administrative systems, such as, drug delivery by oral pills and injection has some drawbacks. High parenteral dose of antibiotic to achieve the effective therapeutic drug concentrations lead to renal and liver complications. Further, poor penetration of antibiotics into ischemic and necrotic tissue, due to lack of blood stream around the surgical site keeps delivery system challenge. All these often necessitates monitored hospitalization as well regular check-ups [30][31]. On other hand, in situ (local delivery) drug eluting devices overcomes all the limitation by effectively delivering the therapeutic dosage to the targeted place [32]. Initial burst release, followed by a relatively slower release, is an ideal drug delivery system. This type of antibiotic release profile is highly desirable for orthopedic implant surgery. Initially higher amount of antibiotics is required to prevent infection and eradicate the bacteria from the surgical area, as well as, from implant surface. Sustained release for many weeks is essential to fight against the late infection, which occurs at much lower magnitude [20]. To achieve this ideal drug delivery, several strategies have been proposed on orthopedic implants, including antibiotic loaded bone cement, drug molecules integrated with in the implant and loaded with porous coating structure [33].

In cemented joint arthroplasties, the femoral stem of the prosthesis is fitted into femur bone with the help of non-biodegradable polymeric bone cements, like, poly methyl methacrylate (PMMA). To reduce the deep infection, many clinical studies have incorporated the antibiotics into PMMA cement [16][34]. But PMMA has shown uncontrolled drug delivery, with initial burst followed by slow release up to months together [35]. Poor drug releasing efficiency is also noted with less than 50% of the loaded drug being releasing and remaining stuck within the cement. Further, heat generated during polymerization can inactivate the drugs

and kills the healthy bone cells. Besides, polymer dissolution due to water penetration into pore network of the cement leads poor implant stability and loosening [36]. In many cases, an antibiotic weakens the mechanical properties of the PMMA cement and third body wear is induced in acetabular cup due to cement wear debris. All of these accelerates the implant loosening [37][38]. In case of early clinical failure, secondary surgery would be required to remove the non-biodegradable PMMA cement. To overcome these drawbacks of bone cement, currently cementless (press fit fixation) procedures are in practice for hip replacement. Moreover, cemented procedure is essentially good for elder and inactive patients and not for young and active patients. Press-fit stems are used most frequently in today's market (fig 1.2).

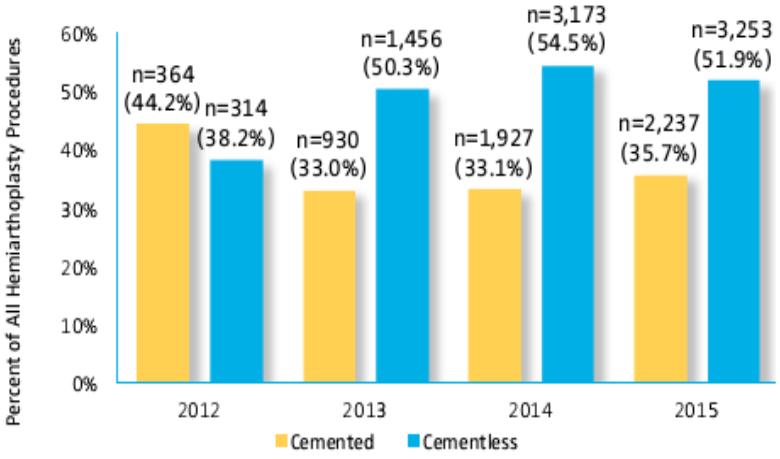

Fig. 1.2 *Cemented and cement-less femoral stems in hemi-arthroplasty (N=15,701)* [39].

Press-fit stems interface directly with the bone and achieve initial stability through an interference fit (mechanical) with the femur, thus giving long life to the implant. Progressive improvement in prosthesis design has been aimed for better osseointegration and reduction in the infection. Drug loaded bioceramic or bioresorbable coatings strategies are also evaluated for their potential to prevent the infection. The main problem with drug containing bioceramic coatings, like calcium phosphate or hydroxyapatite, is the processing of these coatings, which needs high temperature. These coatings, when synthesized at low temperature, do not provide enough fracture strength or adhesion to implant surface and thus prone to fast failure. In

addition, the drug release from these coatings is very fast and cannot sustain a long term release [30][32][40]–[42]. Soaking antibiotics in such coating surfaces also is suitable for only short-term release.

The second category of coating is bioresorbable or biodegradable polymers carrying the drug [17][43][44]. But, coating of such polymers, as film or as beads, covers the surface of the implant and thus reduces its functionality in terms of sparing the mechanical and tribological properties and even bioactivity also in specific cases.

Hence, there is great interest in finding new methods or strategies to inhibit biofilm formation with controlled drug delivery for longer period. In this connection, one of the ideal sites for drug loading would be those parts of an implant, which are not supposed to have bone grown on them and would be in direct contact with the body fluid to make the released drug available in the surrounding places of surgery. Such a part in a total hip implant can be the lining of the acetabular cup. Such liners are made of ultra-high molecular weight polyethylene (UHMWPE), which is clinically used in orthopedic implants. PE is chosen, based on its unique combinational properties against other polymer. Superior wear resistance, fracture toughness and good lubricity offered during rubbing action with the metallic femoral head of the implant gives long term performance [45][46]. Low friction coefficient and toughness of PE reduces the severity of abrasive and fatigue wear during complex loading and sliding motion. High impact strength (90-96 kJ/mm^2) and elongation to failure (370 to 420%) helps in avoiding the catastrophic failure of PE liner [47][48]. Besides, hydrophobic nature of PE, keeps most stable in any chemical environment and bio-inertness in the body. Relatively low cost and good process-ability are the additional characteristics of PE which attracts the medical industry [49]. Despite these superior properties, generation of wear debris cannot be avoided fully. The wear debris of PE can trigger macrophage induced resorption of bone and osteolysis [45]. In long run, it can lead to implant loosening and reduces the in vivo life of the implant [50]. New

material system with improved tribological, mechanical properties and additional antibacterial properties increases the service time of the implants and to avoid the frequency/need of revision surgeries. This is particularly important for younger and more active patients. Thus, modifying the inner surfaces of the PE lining of acetabular cup in total hip implant for carrying and delivering of the drugs, with improved mechanical and tribological behavior, would be a great solution for post operational infection problem. Developing such an acetabular cup liner would bring a significant advancement in the field of drug releasing total hip implants.

The total hip joint (fig 1.3) is the articulation of the acetabulum of the pelvis and the head of the femur. These two segments form a ball-on-socket synovial joint, which is enclosed by the joint capsule. The hip joint has a wide range of movements including flexion, extension, abduction, adduction and rotation. The stability of the hip joint is provided by numerous supporting structures, including a system of ligaments and muscles surrounding the hip joint. This arrangement allows motion and supports the weight of the body in both static and dynamic postures. During normal walking the hip is subjected to compressive loads of up to five times of body weight, and even greater loads can be reached when running, jumping or climbing stairs [51][52].

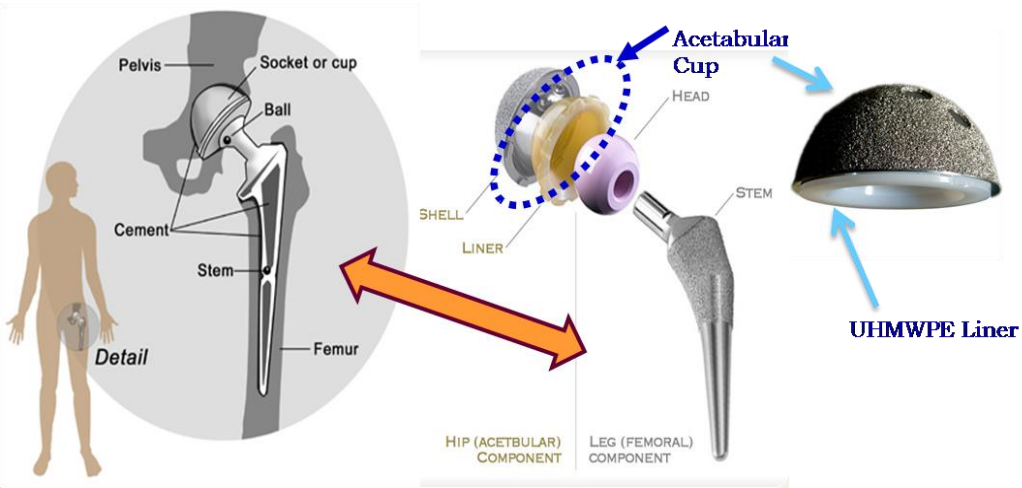

Fig. 1.3 *Schematic of total hip implant in human body and picture of a metallic hip implant*

A typical prosthetic implant system, used in hip replacements, consists of four different parts. The acetabular cup is inserted into the acetabulum of the pelvis [52]. Generally, the acetabular cup comprises a socket, which is usually made of titanium alloy, and a liner, which fits inside the socket and is usually made of high density polyethylene (PE). The femoral ball replaces the head of the original femur. This component is usually made up of cobalt-chromium alloy. The femoral stem is inserted into the shaft of the femur and it is usually made of titanium or titanium alloy. The area where the femoral ball and the liner connect is known as the bearing surface. Since the longevity of the implants has been directly related to wear, the major focus of orthopedic research during the recent years has been to improve the wear characteristics of joint bearings. On the other hand, liner of acetabular cup is the ideal sites for drug loading because these parts of an implant are not supposed to have bone grown on them and would be in direct contact with the body fluid to make the released drug available in the surrounding places of surgery. PE is the polymeric material that has been evolved after thorough scientific studies and it is in clinical use for last four decades as the liner of acetabular cup [45][53]-[55].

The overall objective of this research is to establish the potential use of surface modification of PE lining of acetabular cup for carrying and delivering the drugs to fight against bacterial infection around the surgical area. The surface of acetabular cup liner is to be modified for this purpose with an engineered microporous surface, which can carry drugs. biodegradable polymer is planned to be used as carrier for drugs and impregnated drug loaded polymer on modified surface (porous surface). Biodegradable polymer systems has gained considerable attention in recent years, particularly for controlled and sustained drug delivery [56], further, drug delivery kinetics, degradation rate and mechanical properties can be tailored easily by use of biodegradable polymer [57]. However, surface modification and drug loading should be achieved without compromising the mechanical and tribological behavior.

Developing such acetabular cup liner would bring a significant advancement in the field of drug releasing total hip implants.

Keeping the main aim in consideration, overall objective can be achieved through the following specific objectives:

- Engineering a porous layer on the surface of PE with optimized the porosity
- Impregnating the drug loaded biodegradable polymer solution on porous surface and evaluating the long term drug releasing capability, antibacterial effectiveness and biocompatibility of the modified surface
- Evaluating the modified surface mechanical and tribological behavior before and after drug release
- Comparing the surface modification results for different possible techniques – to establish the best one
- Considering the requirement of mechanical and tribological behavior of the modified PE surface, developing suitable ways in form of composites to improve properties of initial PE surface
- Analyzing the role of different aspect ratio of CNT reinforcement on mechanical and tribological behaviors of PE composite
- Engineering the porous layer on the surface of the best CNT reinforced PE composite and evaluating for mechanical, tribological, drug release kinetics and biocompatibility behaviors

The plan of research work is illustrated with the flow chart in fig. 1.4. The dissertation has been arranged in different chapters to present a clear picture about the background and the state of the art; the methods adopted in this study; the analysis of the outcomes with scientific interpretation and the future scope of research and improvement.

After brief introduction presented in **chapter 1,** critical review of the available literature on drug eluting orthopedic implant is presented in **chapter 2**. Different drug loading approach and surface modification of implants to achieve sustained drug delivery is also added. In addition, it contains the brief discussion on carbonaceous nano-particle reinforced PE polymer composite. Mechanical and tribological properties of CNT reinforced PE composite and limitations are discussed extensively. It also defines the motivation behind this research work, objectives and scope of the work based on the literature review.

Chapter 3 deals with the details of experimental procedure carried out for fabricating the PE surface with interconnected porosity to load the drug without compromising the mechanical and tribological property. Different surface modification technique, such as modified chemical etching technique and electrostatic spray coating technique included along with the CNT composite preparation. The instrumental setup and procedure to study the mechanical, tribological and microstructural behavior also covered. Detailed drug release kinetic procedure to improve the antibacterial efficacy and biocompatibility study are also explained in brief.

Chapter 4 describes the procedure of modified solvent based etching and lyophilization technique to engineer a thin porous surface layer on PE substrate. Drug loaded chitosan is impregnated on porous surface. The mechanical behavior of the modified PE surface is evaluated through instrumented indentation technique, while ball on disc tribometer is used to evaluate the wear behavior. In vitro drug release studies were carried out to analyze the releasing duration and kinetics. The objective of loading the drug in acetabular cup lining is to reduce the on-site bacterial infection. Thus, bacterial culture study has also been carried out to find out the effectiveness of this drug loaded surface in fighting against infection. Mechanical and tribological property variation after successful drug release study is also discussed extensively. In addition to that, biocompatibility results on modified PE surface are addressed.

This study thoroughly evaluates the modified PE surface for its potential application as a drug releasing acetabular liner in total hip implant.

Chapter 5 explains the procedure of electrostatic spray coating technique to engineer the porous surface on PE substrate. Drug loaded polymer is impregnated on coated surface through impregnation chamber. This chapter thoroughly compares the two different surface modification techniques, such as electrostatic spray coating technique and modified solvent based etching technique, in terms of modified surface characteristics. Mechanical and tribological behavior of the surfaces fabricated through two different routes are thoroughly analyzed and compared. In addition, a comparative in vitro drug release and antibacterial study is carried out to find out the most effective surface modification technique.

Chapter 6 discusses the effect of CNT morphology on mechanical and tribological behavior of PE matrix. Two different aspect ratios of MWCNTs and two different concentrations (0.05 and 0.1 wt.%) are used as reinforcements. Differential scanning calorimetry and thermos-gravimetric analysis is carried out to study the thermal, oxidation or degradation behaviors of the composite structure. Analysis of the results gave us an in-sight on the origin of structural change occurring in composites, due to different aspect ratio of CNTs used as reinforcement. Ball on disk tribometer and nano-indentation studies were conducted to study necessary properties required for artificial acetabular cup, e.g., COF, specific wear rate, hardness and elastic modulus. Finally, the obtained results were thoroughly analyzed to understand the mechanisms dominating mechanical and tribological behavior of the composite.

Chapter 7 deals with surface modification of PE-CNT composite surfaces for acetabular cup liner application. Modified and drug loaded surfaces are characterized for mechanical and tribological properties. In vitro drug releasing behavior and the efficacy to fight against bacterial infection is evaluated and discussed. Besides, in-vitro biocompatibility of surface modified CNT/PE composite is assed with osteoblasts. CNT-PE results are compared

with surface modified PE and highlighted the critical finding. The findings of this study leads to a solution for potential surface modification of acetabular cup liner in total hip implant, which can fight against bacterial infection and improve the in-vivo performance.

Chapter 8 presents the summary and conclusion of the entire work presented in the thesis and also proposes the future directions in which these studies can be extended.

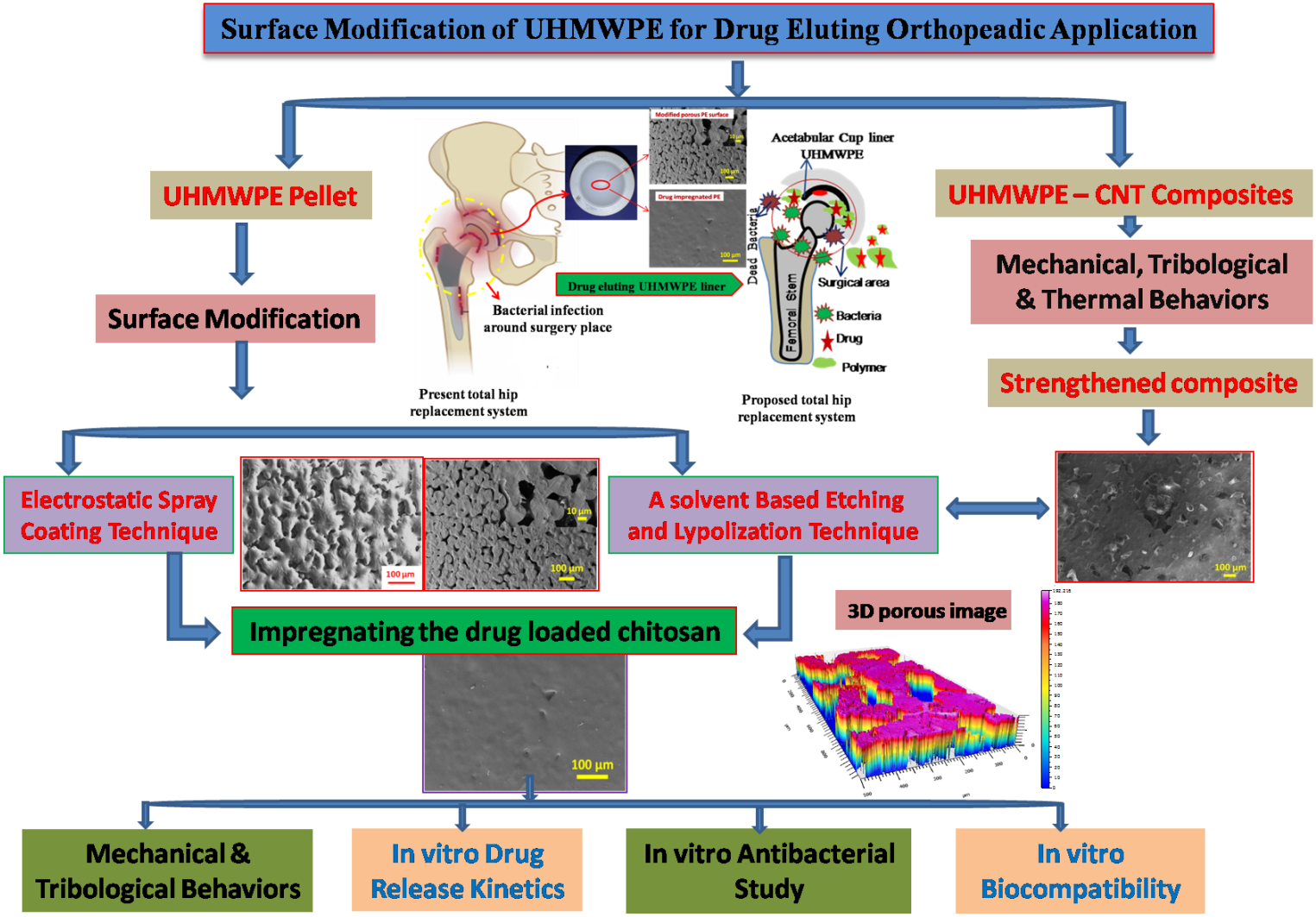

Fig. 1.4 *Flow chart of the research plan*

CHAPTER 2

Literature Review

In this chapter, a comprehensive summary of the available literature on drug eluting orthopedic implants and CNT-PE composite is discussed in detail. Different drug loading strategy and their limitations are highlighted. Besides, application of CNTs in orthopedic implants for improving the mechanical, tribological and biological properties are also discussed. A review and analysis of the past and on-going research in the field helped in finding the areas that need attention and led to the planning of this study.

2.1 Bone

Bones are the main organs of the body for giving structural support, permitting movement and locomotion by providing levers for the muscles, protecting vital internal organs and structures. Bone is basically composed with hard living tissue [58]. Hard tissues typically have a 3D complex hierarchical structure with an intertwined composite structure of the inorganic mineral phases, calcium phosphates based derivatives, like, hydroxyapatite (HA) and organic matrices like collagen and nano-collagen protein fibrils as depicted in fig 2.1 [59]. Inorganic minerals make bone rigid and proteins (collagen) offer strength and elasticity. Hard matrix of calcium salts deposited around protein fibers [58]. Bone tissues are generally divided into two types, trabecular or cancellous bone and cortical or compact bone. Cancellous bone has more porosity (50-95%) than cortical bone (5-10%), but both cancellous and cortical bone are composed of osteons (fig 2.1) [60]. Generally, an adult human skeleton is composed of 80% cortical bone and 20% cancellous bone. The ratio of cortical and cancellous bone also varies in different part of bone and it decides the strength of the bone. For example, femoral head is composed with 50:50 ratio, whereas vertebra is composed of 25% of cortical bone and 75% cancellous bone [58][61]. Cortical

bone is dense and solid, surrounding the cancellous (trabecular) bone, whereas trabecular bone is composed of a honeycomb-like network of trabecular plates and rods interspersed in the bone marrow compartment [58].

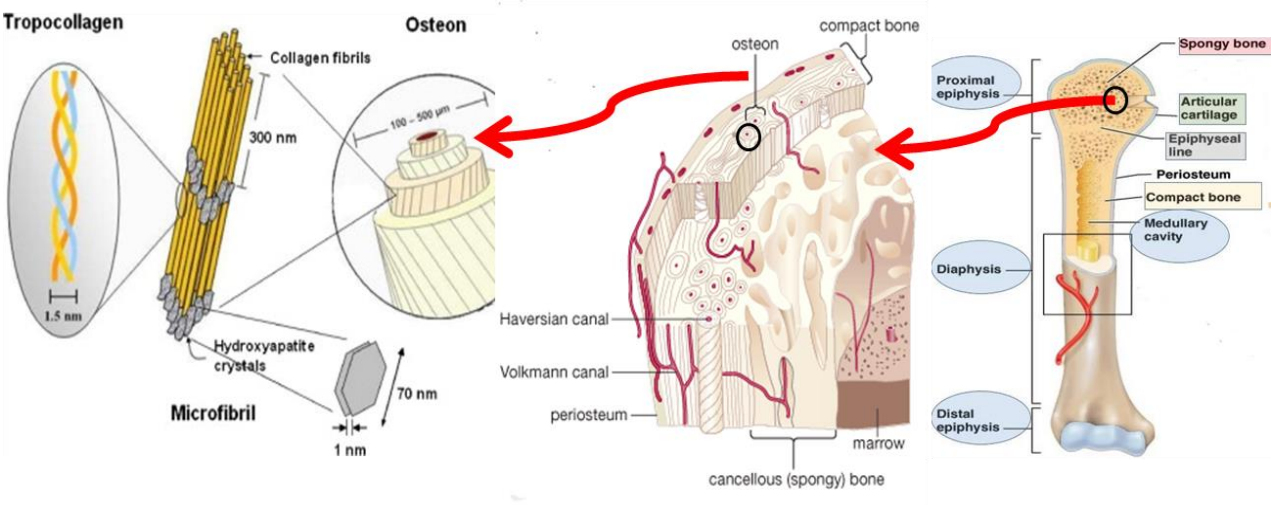

Fig. 2.1 *Structure of a typical long bone: hierarchical complex architecture of hydroxyapatite and collagen fibrils in natural bone*

Bone is a mineralized connective tissue that exhibits four types of cells: osteoblasts, osteoclast, osteocytes and bone lining cells [60][62][63][64]. Osteoblasts synthesize the bone tissue and this process is maintained by the osteocytes and bone-lining cells [65][66]. Osteoclasts cells take part in resorption and degradation of bone [62]. Bone is a highly dynamic organ that is continuously resorbed by osteoclasts and neobone formed by osteoblasts. Besides, osteocytes act as mechano-sensors and orchestrators of this bone remodeling process [67]. Bone undergoes continuous modelling and remodeling process during life. Modelling is the process by which bones change their overall shape in response to physiologic influences or mechanical forces, leading to gradual adjustment of the skeleton to the forces that it encounters [58]. Bone remodeling is the process by which bone is renewed to maintain bone strength and mineral homeostasis. The remodeling process resorbs old bone and forms new bone to prevent accumulation of bone micro damage [58][60]. Normal bone remodeling is necessary for fracture healing and skeleton

adaptation to mechanical use, as well as, for calcium homeostasis. On the other hand, an imbalance of bone resorption and formation results in detrimental bone diseases, like, osteoporosis [60][68].

2.2 History of the Total Hip Replacement

Disease and injury can damage the regular function of the hip joint and lead to severe local pain during bone to bone contact. This limits every day activity. Degenerative diseases, such as, osteoarthritis and rheumatoid arthritis are the most common causes of hip and knee disorders. Degenerative diseases, caused due to wearing or break down of the bone cartilage in a joint, and are found mostly in aged population [69]. In India, arthritis affects around 15% of the population, which is over 180 million people and globally ~1.7 billion people [4][70]. Most of these degenerative diseases will eventually require surgery (when all non-surgical treatments have failed) to replace one or both of the damaged surfaces of the hip joint using prosthetic components. Replacement of one half of the joint is termed hemi-arthroplasty, whereas, replacement of both components is known as total hip arthroplasty (THA) or total hip replacement (THR) [71][72]. A total hip replacement has two main components, the acetabular component, which fits into the hip socket and the femoral component, which is inserted into the femur (fig 2.2) [47].

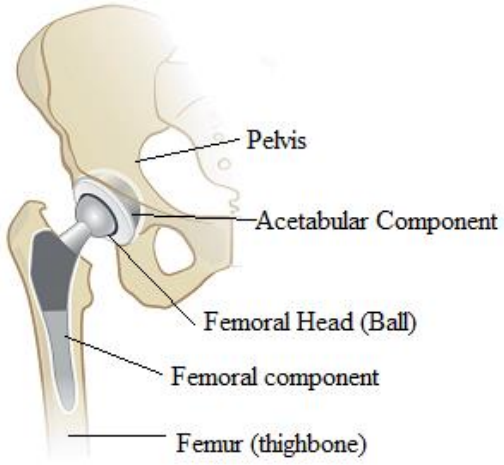

Fig. 2.2 *Components of total hip replacement*

The first hip joint replacement procedure was performed by a German physician, Thomas Gluck, in 1886 [71]. But, practicing of it was started widely after introducing Charnley's 'Low Friction Arthroplasty (LFA)' design in the 1960's. Today, the total hip replacement practice is one of the most frequently performed surgical procedures in the world. Over two million joint replacements are performed in every year [73]. In India, over 70,000 hip and knee replacements are being performed every year [6]. The procedure is widely regarded as one of the most important achievements in orthopedic surgery in the 21th century [71]. .

2.3 Fixation of Hip Replacements

According to fixation procedure, total hip replacement can be mainly categorized into two types, cemented and cementless. In cemented fixation, bone cement PMMA (poly-methyl-methacrylate) is used to hold the prosthesis in place. whereas cementless fixation relies on the interaction at the prosthesis-bone interface to hold the prosthesis in place as shown in fig 2.3 [5].

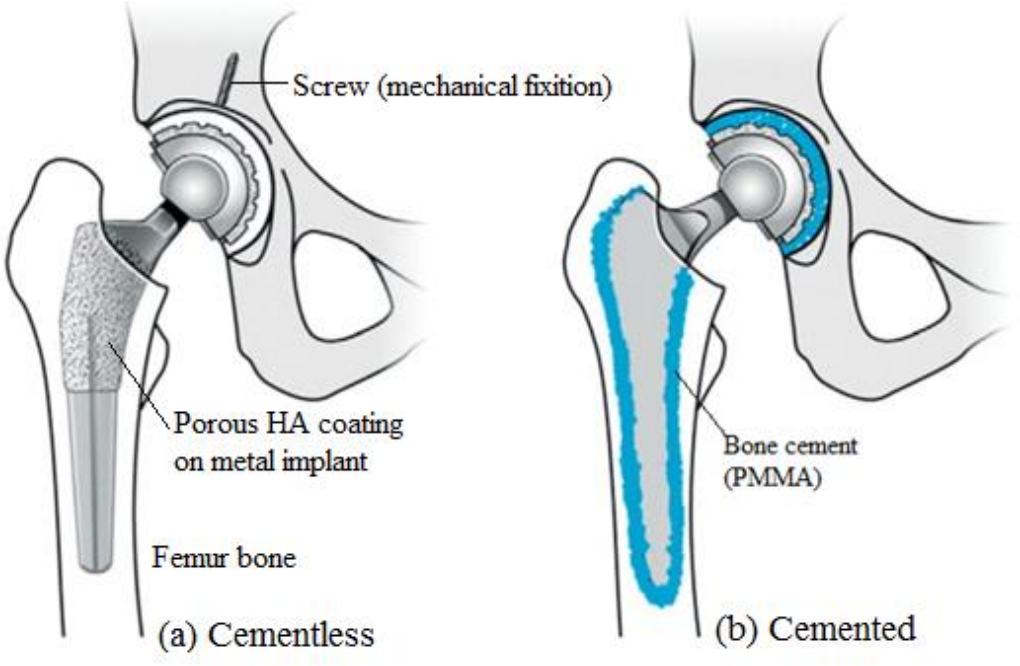

Fig. 2.3 *Shows cementless and cemented hip replacement design*

Acrylic cement PMMA is being used to fix the hip prosthesis for last 60 years [35][41]. Cemented replacements follow easy surgical procedure and cost effective treatment. But, interface between bone-cement-prosthesis is not smooth and contains lot of flaws, such as, pores and micro cracks [74][75]. As a result, under cyclic loading conditions, due to a patient's natural activities, bone-cement interface may result in fatigue crack nucleation and fracture. Besides, temperature rises up to 80 °C during polymerization, leading to death of immediately surrounded living tissue. According to 1970's reports, high radiographic failure rates and osteolysis led to a general dissatisfaction with the use of cement for fixation of total joint replacements [71]. The problems is more crucial particularly to young active patients, who usually outlives the fixation of a total hip or knee arthroplasty [76]. This dissatisfaction led to major developments in the areas of Cementless implants. Cementless (press fit fixation) procedures were extensively used in hip replacement and are used most frequently in today's market [39]. Success of cementless replacement lies in mechanical and biological fixation. Biological fixation involves specific biological reaction at the interface, which helps for the formation of bond between bone tissue and implant material [77]. Porous structures of bioactive material allow cells and tissue formation. The formation of this intimate bond is called as osseointegration and this can be enhanced by using bioactive material, such as bio-glass and hydroxyapatite (HA) [78][79]. Biological ingrowths into the porous cavities can bring a strong interlocking structure. Hence, it can withstand more complex stress conditions than mechanical fixation. Above advantages made the cementless hip replacement most successful in clinic. More than 60% of the patients, especially younger and active ones, and doctors prefer cementless practice at present [39].

2.4 The Clinical Need for Drug Eluting Orthopaedic Implant

Even after decades of successful track record, two common problems leading to implant failures are implant associated infection and implant loosening due to poor structural stability [17]. As a result, removal of the infected or loosened implant and follow-up surgery is essential to save the patient from severe consequences [80]. Infection rate of THA during the first two years is ~ 5 %, in United States and Europe [12][15]-[17]. But, in India, the infection rate is found to be 10%, which is significantly higher than US. This is due to growing number of diabetes and obesity patients in India. Besides, the infection rates after revision of surgery, is considerably higher (5 to 40%) than after the first one [16]. It is a burden for patient in terms of health, as well as economic consequences [81][82]. In near future, infections associated with prosthetic joint will further increase due to increase in residency time of prosthesis and growing number of patients with osteoarthritis [27]. Bacterial infection of a joint prosthesis occur post-operative by bacterial contamination of the operated place during the surgery or hematogenously, by microbials spreading through blood from a distant place [27]. Early infection, during first three weeks after the surgery, is generally caused due to highly virulent microorganisms, like, Staphylococcus aureus or gram-negative bacilli [28] . These result in local pain, erythema, fever and disturbance in wound healing. Late infection, after 6 weeks of the surgery, is typically caused due to microorganisms of low virulence, such as, coagulase-negative staphylococci and propionibacterium acnes. Outcome of this is high joint pain and early loosening, finally leading to implant failure and requirement of a secondary surgery to remove/replace the infected implants [27]-[29]. Infections are associated with bacterial biofilm formation on the surface of artificial implant and tissues surrounding the implant. Biofilms are biologically active matrix for cells and major form of microbial life [83]. Bacterial cells release an insoluble and shimy extra-cellular

polysaccharides (EPS). EPS offers necessary nutrients for cell growth and gives better protection from external environmental stresses, as well as, from antibiotics [84][85]. Once biofilms is established within surgical area or implant surface, it is difficult to eradicate the infection, even with high dose of antibiotics [26]. Thus, it is very important to stop the initial infection by adequate supply of antibiotics in the surrounding region of the implantation, after the surgery. This can be achieved most effectively by localized drug delivery.

In connection to above problems, drug eluting implants and accessories have greatly evolved in last two decades. But the successes of drug eluting implant mainly depend on ideal drug delivery system. An ideal system is defined as, initially high burst release to completely eradicate the bacteria from the surgical area, as well as, implant surface, followed by sustained release for several weeks at therapeutic concentration for inhibiting the occurrence of latent infection [20].

The improved local delivery system offers additional benefits over conventional or systematic drug administrative system. Drugs, delivered by oral (tablet), parenteral (injection) and inhalation require high dosage of drugs to achieve an actual optimized local concentration [20][86][87]. Besides, most of the newly discovered drugs are hydrophobic and water insoluble and hence their pharmacological efficiency is reduced [88]. Poor dug distribution at the site of infection, due to lack of blood circulation to the infected skeletal tissue, makes the drug delivery challenging [35]. On other hand, site-specific targeted drug delivery system have shown effective drug delivery to the targeted area with controlled therapeutic dosage and minimal side effects [20]. Implant associated infections are mainly caused due to well defined bacterial network formation on the implant surface, termed biofilms, which is extremely resistant to antibiotics [33]. This can be addressed by delivering the antibiotics locally.

Over the past decades, extensive research efforts have been made in developing drug eluting orthopedic implants. Various surface modification techniques and coating strategies have been adopted till date to deliver the drug locally after implantation [33][34][36][89][90]. However, it had been always a challenge to prepare a metallic orthopedic implant with sustained drug delivery capability. Thus, it becomes very necessary to exclusively review the studies dealing with drug releasing implants, which will serve as guideline to the researchers in the field to carry out further advancements. In this chapter, we attempted to review different techniques, used till date to prepare a drug eluting implant surface. These techniques include drug loaded bone cements, drug-eluting bioceramics and natural and synthetic antimicrobial loaded polymers. A comprehensive account of different techniques has been presented with emphasize on modifying the surface of the implants for loading drugs and release kinetics. The advantages and limitation of each process is also critically analyzed.

2.5 Bone Cement

Gaining the good knowledge about bone cement is primary important to all orthopedic researchers and surgeons. Bone cements are widely used to fasten the artificial joints (hip, knee and elbow joints) in cemented fixation method. Use of bone cement was started clinically since 1950 and it is gold standard in the field of joint replacement surgery [91][92]. Largely, the word “cement” is referred as a substance that bonds two things together. But, bone cements have no such intrinsic adhesive characteristics; it binds through mechanical interlock between the irregular bone surface and the implant. Bone cement fills the free space between the implant and the bone, that creates a tight space, which secured prosthesis against bone and ensures that the prosthesis remains in place over the long time [93]. Many commercial bone cements are available in present market. Poly-methyl-methacrylate (PMMA), plaster of paris, acrylic bone cement, calcium phosphate

cements (CPCs) and glass poly-alkenoate (ionomer) cements (GPCs) are extensively used for variety of orthopedic and dental application [91][94].

2.5.1 Poly Methyl Methacrylate (PMMA)

Poly-methyl-methacrylate (PMMA) is a synthetic thermosetting polymer. PMMA was primarily inserted in the body as a dental material. Later, famous English surgeon John Charnley used it for total hip arthroplasty in 1958 [91]. Charnley used cold-cured PMMA to attach an acetabular cup to the femoral head and to set a metallic femoral prosthesis (fig 2.4).

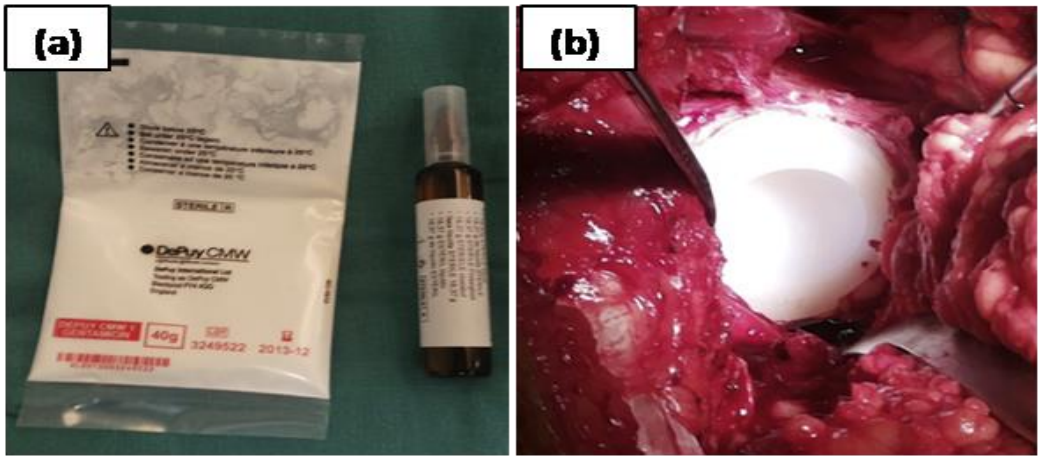

Fig. 2.4 *(a) Powder and liquid components of bone cement, (b) Cemented acetabular component*

This success was a great step for rapid advancement of orthopedic surgical practice. Charnley understood that PMMA could easily blend with the bone morphology and easily fill the medullary canal [95]. Later, in the 1970's, U.S food and drug administration (FDA) officially approved the use of bone cement for implant fixation. Since then, bone cement has become more popular all over the world and surgeons adopted them extensively for implant fixation [91]. PMMA is an acrylic polymer that is prepared by blending of two sterile components (Table 2.1). A powdered polymer (MMA-styrene co-polymer) and a liquid methyl-methacrylate (MMA) monomer are mixed, followed by 5 to 10 minutes of polymerization. Liquid monomer polymerizes

around the pre polymerized powder particles and form viscous dough like state, that can be safely used for required application and then finally hardens into solid hardened PMMA [96]. Viscosity and hardening time can be tailored to help the surgeon safely use the bone cement into required application. Nearly 80-86 °C of heat is generated during the exothermic free-radical polymerization process [91]. This increased temperature is higher than the critical level for protein denaturation in the body and also it can adversely affect surrounding tissues. Thin cement coating should not exceed more than 5 mm in order to lower the polymerization temperature in the body [97]. However, generated heat is dissipated through the large implant surface and the flow of blood. Besides, physical and chemical properties of the PMMA cement can be altered by adding various additives [91][95][96]. Usually, whenever PMMA is exposed to light and high temperature, premature polymerization of the liquid MMA was found. Hence, in order to prevent premature polymerization, hydroquinone is added to liquid as a stabilizer or inhibitor [91][97]. Besides, to start the polymerization process at room temperature (cold curing cement) an initiator, di-benzoyl peroxide (BPO) is added to the powder and an accelerator, typically, N-dimethyl-p-toluidine (DmpT) is added to the liquid monomer [98][99]. To follow up the in vivo performance of the bone cement, a contrast agent, such as zirconium dioxide (ZrO2) or barium sulphate (BaSO4) is added to make bone cement radiopaque [91][100].

Powder	**Liquid**
I) ***Polymer:*** Poly methyl methacrylate/co-polymer (PMMA)	I) ***Monomer:*** Methyl methacrylate (MMA)
II) ***Initiator:*** Benzoyl peroxide (BPO)	II) ***Accelerator:*** N, N-Dimethyl para-toluidine (DMPT)/diMethyl para-toluidine (DMpt)
III) ***Radio-opacifier:*** Barium sulphate (BaSO4)/Zirconia (ZrO2)	III) ***Stabilizer:*** Hydroquinone
IV) ***Antibiotics*** (e.g. Gentamycin)	

Table 2.1 *Components of bone cement*

The PMMA-based cements are currently the most suitable choice. Although successful track record was noticed for securing the prosthesis, implant failures do occur. A main reason for failure is poor bioactivity and poor dynamic mechanical property. Heat generation due to polymerization reaction and weak interface between bone and cement, bone necrosis and fibrous capsule can occur around the implant [101]. To improve the good interface and bioactivity, bioactive bone cement, such as, calcium phosphate cement (CPC) was discovered in the 1980s by Brown and Chow [102][103]. Since after, many CPCs with varying compositions have been introduced for other specific applications, such as, bone augmentation, reinforcement of osteoporotic bones, fixation of metallic implants in weakened bone, and spinal fractures and vertebroplasty [104].

2.5.2 Calcium Phosphate Based Cement (CPC)

The core advantages of CPCs over the PMMA is the ability to harden after being implanted with in the body, through a low temperature (body temperature) setting reaction [104]. Whereas PMMA cement harden through polymerization reaction. Besides, CPCs setting reaction is not, like, PMMA. Hence, incorporation of different drugs and biological molecules is easier and can be used effectively for drug delivery application [105][106]–[110]. CPCs are commonly hydraulic cements and are prepared by mixing with combination of one or more calcium orthophosphate powders and liquid phase, generally water or an aqueous solution. CPCs become moldable paste after proper mixing, which can be directly injecting to damaged bone or bone cavity during surgery, by using minimally invasive procedure [111]. Injected CPCs pastes can self-set *in vivo* due to dissolution and precipitation process. The entanglement of the precipitated crystals (needle-like or plate-like crystals) is responsible for cement hardening fig 2.5 [104].

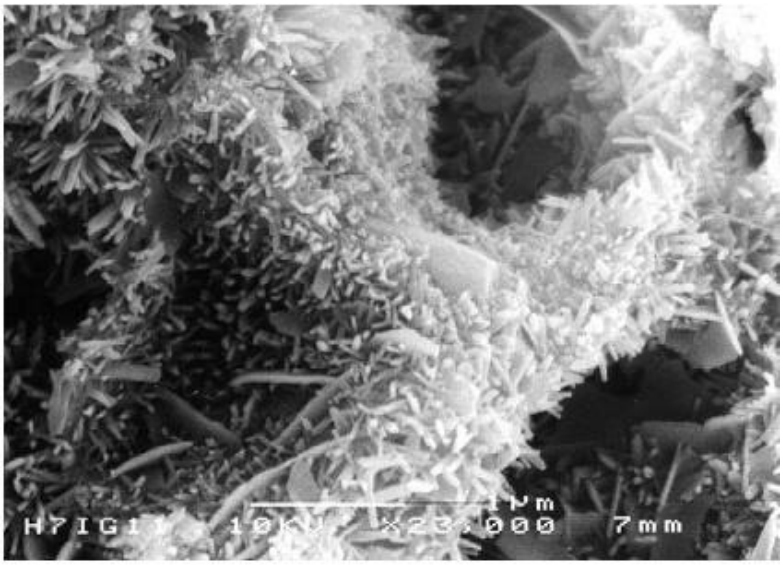

Fig. 2.5 *SEM image showing the microporous structure of an apatite CPC after self-setting*

Basically CPCs are porous in nature. Inter-granular spaces and left over extra aqueous solution generates micro/nanopores in CPCs after hardening. These porous structures are fundamentally helpful for loading drugs or biological molecules and porous structure also helps in bone colonization, mineralization and resorption of bone [103][104][112][113]. Porosity can be tailored (30 to 50%) through processing conditions and liquid to powder ratio. Besides, presence of nucleating agents and chemical composition of the reactants change the setting time and mechanical properties of the cement [114][115]. On the period of self-setting reaction various possible formulation can take place, predominantly precipitated apatite such as hydroxyapatite (HA) or calcium-deficient hydroxyapatite (CDHA) and brushite (Dicalcium Phosphate Dihydrate: DCPD). The key difference among these two products is their solubility. Hydroxyapatite is most stable CPC at physiological pH > 4.2. Brushite is generally a metastable phase, but it may be transformed to stable apatite at *in vivo* condition [104]. Hence, CPC are considered as one of the versatile materials, which can be modified to different medical requirements of several applications.

2.5.3 Drug Loaded PMMA Bone Cement

Bone cements are called as modern drug delivery system, because active substances, such as, antibiotics can be easily added to the powder component of the bone cement and it has capability to deliver the required drugs directly to the surgical site [91]. Drug loaded non-biodegradable polymer cements (PMMA) or beads have been used clinically to treat the osteomyelitis and is also one of the infection management method for nearly four decades [33]. Beside, bioactive agents, including anti-osteoporetic agents, proteins and growth factor can be loaded to PMMA along with different antibiotics to accelerate bone healing and reduce infection simultaneously [33]. Quantity of drug required for local delivery is significantly lower than clinical routine dosages for systemic single injections. Various drugs, like, Gentamicin, Tobramycin, Erythromycin, Cefuroxime and Vancomycin have been successfully mixed and used with bone cement. But the elementary conditions for mix ability is that the drug should be heat resistant during polymerization reaction and subsequently, in body's tissue. Drugs must be available as a powder because it mixes well with the powder cement polymer before adding of the methacrylate, rather than drug being in solution [93]. Besides, studies have shown that adding different drugs in different quantities to bone cement affects the mechanical properties. Mixing the antibiotics with lower than 2 g in standard packet of bone cement, does not adversely affect mechanical properties, but more than 2 g reduces compressive or diametrical tensile strengths [91][116]–[118].

There are many commercial drug loaded PMMA cement available in market. The most common types are Palacos (Merck KGaA, Darmstadt, Germany) and Simplex P (How-medica, Rutherford, N.J.), which are used in European countries. Commercially accessible gentamicin loaded Palacos PMMA cement (Pala-cos-Refobacin) and beads (Septopal) are manufactured in Germany. But, in current days, United States prepare drug loaded cement on site, as per patient

requirement, usually in operating room prior to use [93][119]. Many reports have been published on in vitro stability of antibiotic in cement beads or disks and their releasing kinetics [119]–[122][123].

Generally bi-phasic fashion of drug releasing characteristics was observed in non-biodegradable PMMA. Initial burst release followed by sustained release for months together and mainly incomplete release of drugs (retained within the cement) that continues for longer time [33]. These typical behavior is observed due to non-biodegradable matrices (PMMA), which slow down the drug release, as it is dominated by diffusion mechanism. Besides, release kinetics from bone cement is mainly influenced by porosity, surface roughness, area and relative loading amount [124][125].

In vivo reports also shown that drug loaded PMMA can effectively stop the infection from intraoperative challenge within a small period after implantation [33][126][127]. Surgeons from Europe and United States most frequently incorporate gentamicin and tobramycin into bone cements. Tobramycin is an aminoglycoside and its spectrum is closely related to gentamicin, but releasing characteristics are better than gentamicin. Pharmacokinetic studies specify that drug elution from gentamicin loaded bone cement or beads was not sustained. Further, less than 50% of the drug eluted within a month and thereafter no continuous drug release was observed [33][128]. Dimaio, Frank R. et al [122] have impregnated 0.2, 0.5 and 1 g of ciprofloxacin per 40 g of PMMA cement (standard 40 g packet of Simplex cement powder) beads and observed the sustained drug release up to 42 days in PBS. The study has also shown that the ciprofloxacin is heat stable up to 110 °C and remains biologically active. Besides, minimum inhibitory concentration (MIC) of ciprofloxacin is around 1 to 2 mcg/ml for effectively eradicating the many pathogens such as

Staphylococcus aureus, Streptococcus species, and Pseudomonas species which are mainly associated with chronic osteomyelitis.

Around 0.2 g of ciprofloxacin impregnated cement beads eluded at least 1-2 mcg/ml (MIC) concentration for 7 days, whereas 0.5 g for 30 days and 1 g for 42 days. The 1 g ciprofloxacin loaded cement beads released above MIC levels continuously for the entire 42 days as shown in fig 2.6.

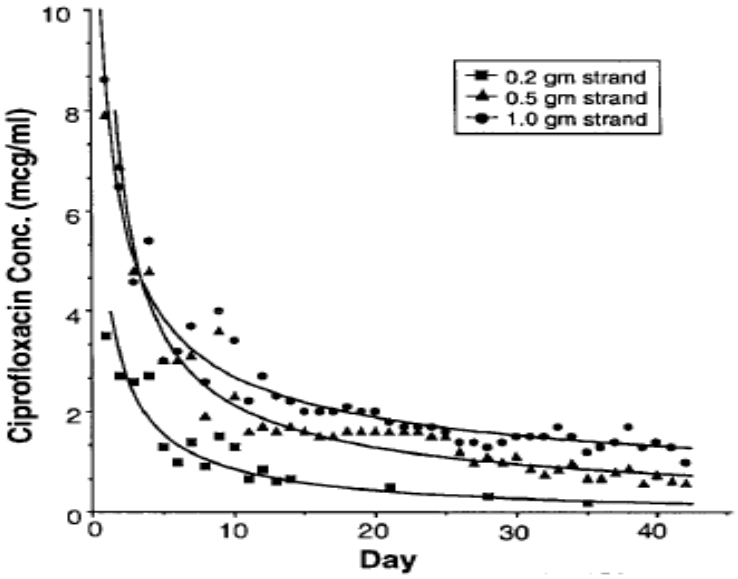

Fig. 2.6 *Shows ciprofloxacin release for all three concentration*

2.5.4 Drug Loaded CaP Bone Cement

Regardless of many drug loaded PMMA and its successful clinical use in orthopedic device fixation since four decades, inherent limitations of PMMA, such as, fragmentation and foreign body reaction to wear debris causes prosthetic loosening and peri-prosthetic osteolysis [122][129]. Besides, PMMA is not a biodegradable and secondary surgery is very essential to remove the PMMA if any clinical failure occurs before new bone regeneration in the defect. Bone cement (PMMA) generates heat and residual MMA monomer, which is toxic and can kill surrounding healthy bone cells and also pose potential chances for creating allergic reactions [33][130]. In

addition to that, during removal of PMMA, bone tissue also gets damaged/lost, as the PMMA gets well encapsulated within surrounding soft tissues, rather than implant surface. These all reduced the clinical enthusiasm for using PMMA cement [33].

On the other hand, excellent bioactivity, osteoconductivity and resorption property of calcium phosphate (CaP) and their derivatives like hydroxyapatites and tricalcium phosphate have also shown sustained drug release [131]. Tailorable biodegradability of CaP, as compared to other ceramics, and compositional similarities to bone mineral are some reasons behind the use of calcium phosphate and its derivatives extensively as drug delivery system for orthopedics. Calcium phosphates are used as drug carrier either as nanoparticle, coatings, cements and scaffold. Calcium phosphate cements (CPC) and CaP scaffolds are considered as 3-D construct, whereas CaP coatings and nanoparticle as 2-D and 1-D, respectively, as represented in fig 2.7 [132].

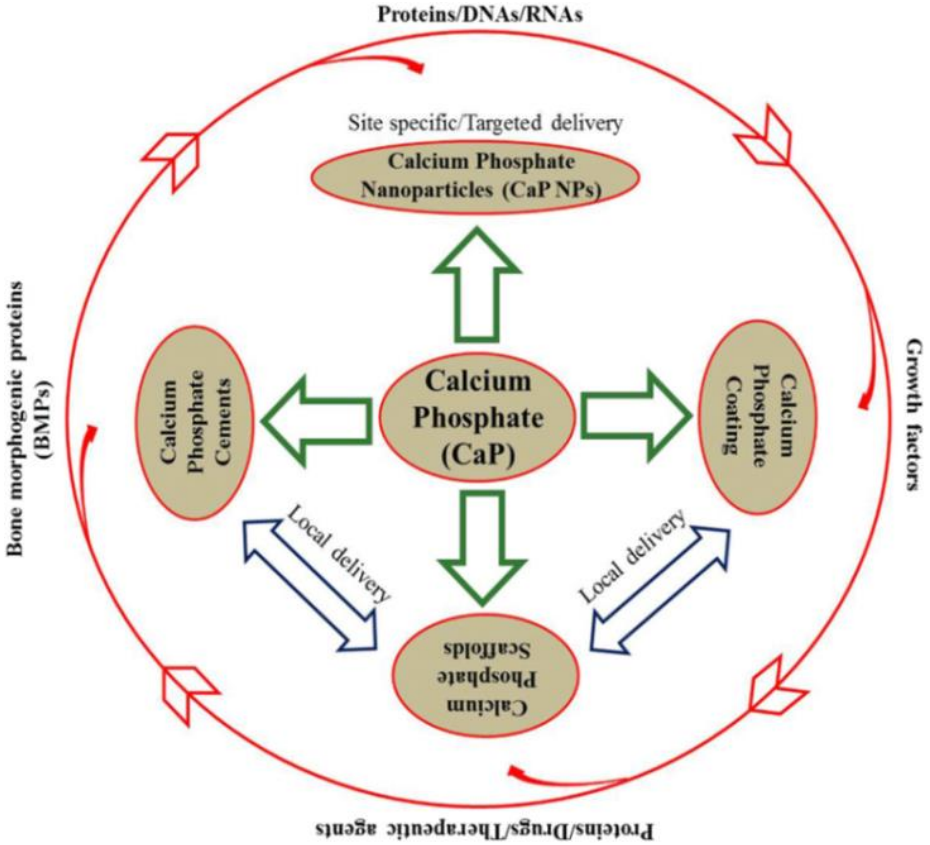

Fig. 2.7 *Shows different approaches of CaP as drug carrier*

Currently, a lot of research is focused on nanoparticle-based drug delivery, especially for targeted drug delivery application. Drug loaded nanoparticles are effectively used to kill tumor or cancers cells, as it is not used for orthopedic implants for fixing permanent implant. Besides, CaP scaffolds was successfully used for tissue engineering application and not as permanent implant. Hence, the discussion over here is restricted to drug release through cements and coatings.

Intrinsic porosity of CPC is helpful for incorporating different antibiotics, biologically active molecules or even cells [104]. Yu, Duncan, et al [133] have investigated in vitro elution behavior of cephalexin and norfloxacin incorporated HA cement and correlated release pattern with the Higuchi model [134]. The 4.8 wt.% norfloxacin added HA eluted the drug continuously up to 250 h. Prolonged release of drugs was observed in cements, because drugs were mixed well with two cement phases and drugs was incorporated throughout the whole material volume instead of surface [135]. Besides, it also depends on microstructure, type of bond among the drug and matrix, degradation mechanism of matrix and drugs. Whereas, in CPC, the release kinetics mainly taken place through diffusion controlled and partially matrix (CPC) degradation mechanism [135]. Doadrio et al. [136] have studied cephalexin release behavior by impregnating 1 wt% cephalexin drug into calcium sulphate (gypsum) cement and HA/gypsum composite cement. Burst release (80-90%) of drug was observed in SBF within 8 h, whereas HA/calcium phosphate composite cement shown 25% of drug release within 8 h and remaining drug (90%) was released after week. HA changes the release kinetics and it slows down the release significantly. In table 2.2 summarizes the various antibiotics and cements used for analyzing the in vitro and in vivo release characteristics of bone cement [104].

Solid phase	Liquid phase	Drug incorporation	Release method	In vitro release profile	In vitro release time	Other studies: microbial / celular / in vivo	Ref.
Antibiotics							
Aminoglicosides - **Gentamicin**							
Biobon (α-TCP)	NaCl 0.9%	S	6 x 12 mm in 5 ml PBS, †	☆	51 – 58% in 60 days SS not reached	In vivo efficacy towards S. Aureus bone infection	[108]
Equimolar DCPA + TTCP 1%wt Na_2PO_4	H_2O	PLGA microcapsules	6 x 12 mm in 5ml PBS, 7.4, ●	No burst release 1 – 2% in 24h Nearly zero order	16 – 17% in 96 days. SS not reached	In vitro fibroblast cell viability	[86]
β – TCP + MCPM	H_2O or polymer	L	12.5 x 18 mm, Paddle method, PBS, ●	☆ 70% in 24h. Diffusion controlled release.	100% in 80 h	–	[102]
β – TCP + MCPM	PAA	L	12.5 x 10 mm, USP paddle method, PBS, ●	☆ 40% – 100% in 24h. Diffusion controlled release. PAA did not modify release kinetics.	Reaching SS. Release between 100% and 50% depending on PAA contents.	–	[77]
Bone source	H_2O	L	Cylinders, 5 ml PBS, 7.4, 15 cycles/min	☆ 40% in 24h.	50% in 30 days	Higher release than PMMA beads. Release above MIC for 30 days	[84]
74.9% α-TCP, 5% DCP	Solution A	S blended with PLA	6 x 6 mm, PBS, 7.4, †	☆	Sustained release for 2 months. SS not reached.	Release in bone marrow above MIC	[81]
75% α-TCP, 20% TTCP, 5% DCPD	Solution A	S and/or PLA	6 x 6 mm, 5 ml PBS, †	☆ 70% in 24h	Release up to 60 days, SS not reached.	Implant in rabbit tibia. High [Drug] in bone marrow up to 8 weeks	[249]
$CaCO_3$, MCPM 7:3	Na_2HPO_4 1M	S	5 ml PBS	☆ 51 – 70% in 24h	85 – 95% released. SS reached in 4 – 6 days.	Reduced COX-2 cell response.Good cell viability.	[103]
Biobon Biofil Bonesource Calcibon Chronos Norian	Drug solution	L	6 x 5 mm, 500 ml H_2O, ●, †, ambient T°C	☆ 40% in 24h ☆ 95% in 24h ☆ 70% in 24h ☆ 90% in 24h ☆ 95% in 24h ☆ 90% in 24h	All reach SS between 50 and 400h. Initial release fits Higuchi	Antimicrobial activity vs. Staph Aureus.	[54]
Aminoglicosides - **Kanamycin**							
74.9% α-TCP, 5% DCP, 18% TTCP, 2% HA, 0.1% MgP	Solution A	S or L	7 x 14 mm in 10 ml SBF (7.4) †	☆ 37 – 45% in 24h drug in liquid phase 37 – 42% in 24h drug in solid phase	Drug in L: SS reached at 57 – 64% after 30 days Drug in S: 49 – 53% after 12 days	Elution above MIC in all cases during 36 days	[89]
Aminoglicosides - **Amikacin**							
BoneSource	H_2O	L	Cylinders, 5 ml PBS, ●	☆ 30 – 40% in 24h	50 – 60% in 30 days	Elution above MIC for 30 days.	[84]
Cephalosporins - **Cephalexin**							
Equimolar DCPA + TTCP	6% Na_2HPO_4 (+ SDS for macropores)	S	5 x 3 mm discs. 25 ml SBF pH = 7.4, †	☆ 42% in 10h	SS not reached 70% in 12 days (or 79% if macroporous)	–	[96]
Equimolar DCPA + TTCP	6% Na_2HPO_4 (+ SDS for macropores)	S	5 x 3 mm discs. 25 ml SBF pH = 7.4, †	☆ Higuchi initially. Weibull for whole release	70 – 90% released in 12 days	Released drug above MIC for S. Aureus and E.Coli	[55]
TTCP, CDPD, HA 3:3:2	H_3PO_4 20 mm	–	9 x 20 mm, 50ml PBS, ● Rotating disk apparatus	☆ 22% in 24h	41% released in 100h. SS reached.	–	[250]
BoneSource	–	S	Cylinders, 5 ml PBS, ●	☆ 9 – 20%	10 – 30% in 30 days	Released drug above MIC for 7 days.	[84]
α-TCP	H_2O, NaCMC or acidic sol.	S(not pure active principle)	10 x 1 mm, 50 ml H_2O, †	☆	SS reached between 5 and 30 days		[95]
Cephalosporins - **Flomoxef**							
Equimolar TTCP + DCPA	NaH_2PO_4, Na_2HPO_4 Sodium alginate	L	6 x 3 mm, 100 ml saline ● †	☆ 29 – 35% in 24h Without sodium alginate: 31% in 24h & 55% in 72	54 – 57% in 72h. SS reached.	–	[79]
Equimolar TTCP + DCPA	0,2MNaH_2PO_4, 0,2MNa_2HPO4 0,5% Chitosan	L	6x3mm, 100ml saline, ●	☆ 26-34% in 24h	SS reached in 7h	-	[99]
Glycopeptides - **Vancomycin**							
Equimolar β-TCP + MCPM	500 - 800 mM Citric acid	S	6 x 12 mm in 50 ml PBS, ●	☆ 60 – 80% in 24 h	SS reached for high L/P 4 days	–	[109]
Equimolar TTCP+DCPA	–	S	6 x 12 mm, 15 ml TBS (7.4) ● †	☆ 20% in 24 h	70% in 7 days. SS not reached.	No bactericidal properties	[87]
β-TCP	4 M H_3PO_4+ 1 mM Citric ac	S	6 x 12 mm,15 ml TBS (7.4) ● †	☆ 40% in 24 h	60% SS not reached.	Bactericidal properties for 5 days	[87]
α-TCP, DCPA, $CaCO_3$, HA (Biopex)	Solution A	S	10 mm beads of 2 g. 10 ml saline, †		5% in 13 days.	Successful treatment of MRSA osteomyelitis in 2 human patients	[114]

Solid Phase	Liquid phase	Drug Incorporation	Release method	In vitro release profile	In vitro release time	Other studies: microbial / celular / in vivo	Ref.
Antibiotics							
Glycopeptides–**Vancomycin**							
α TCP, DCPA, $CaCO_3$, HA (Biopex)	Solution A	L	10 ml PBS / g sample., †	☆ Stationary stage reached after 8 weeks.	Elution duration is greater and much longer in CPC than in PMMA	Antibacterial activity maintained after setting	[90]
TTCP, DCPD, HA	20 mM H_3PO_4	S	8 x 3 mm / 4 x 2 mm, 5 ml PBS or SBF, †, ●	☆ 60, 42, 30% in 24 h	95% released in 60 days	Antibacterial activity above MIC between 17 and more than 40 days	[85]
Quinolones–**Ciprofloxacin**							
Equimolarβ–TCP + MCPM	500–800 mM Citric acid	S	6 x 12 mm in 50 ml PBS, ●	☆ 30–60% in 24 h	SS reached for high L/P 14 days		[109]
α – TCP	H_2O, NaCMC or acidic solution	S preformulated drug	10 x 1 mm, 50 ml water, †.	☆	SS not reached		[95]
Quinolones–**Norfloxacin**							
TTCP, DCPD, HA 3:3:2	H_3PO_4 20 mM	–	9 x 20 mm, 50 mL PBS, ● Rotating disk apparatus	☆	SS reached after 450 h	–	[250]
Tetracyclines–**Tetracyclin**							
49% TTCP, 38% α–TCP, 13% sodium glycerophosphate	32% $Ca(OH)_2$, 68% H_3PO_4	S	Flow cell apparatus 6 x 6 mm, H_2O, 0.5 ml/min	☆ 22–30% release in 24 h. Then linear release.	60% in 6 days. SS not reached.		[93]
Tetracyclines–**Doxycycline hyclate**							
Sr–β–TCP + MCPM	H_2O + 7.5 mg Doxy/simple	L	10 x 5 mm, 8 ml PBS (pH7.4) ● †	☆	100% in 25 days	Inhibition of P. Gingivalis	[94]
β–TCP + MCP + sodium pyrophosphate	0.5M Citric acid	L	10 x 5 mm, Variable volume PBS, ●, †	☆ (50%) the first 10h fitting Higuchi.	75% released in 4 days, SS not reached.	Bacterial growth inhibition of different bacteria.	[56]
Nitroimidazole–**Metronidazole**							
α–TCP	H_2O, NaCMC or acidic solution	S	10 x 1 mm, 50 ml water, regular media change.	☆	Reaches SS between 1 and 5 days	–	[95]
Anti–inflammatory							
Ibuprofen							
49% TTCP, 38% α–TCP, 13% sodium glycerophosphate	32% $Ca(OH)_2$, 68% H_3PO_4	4% in LMAP microspheres	15 ml SBF pH=7.25, ● 100 rpm 45 days	Higuchi No burst release (12–7% released in the first 24 h)	31–69% in 45 days depending on initial concentration (2% or 6% microspheres in CPC)	–	[57]
Indomethacin							
TTCP, DCPD, Bovine collagen	11 mM H_3PO_4	S	10 x 10 x 7.5 mm, 25 mL SBF, ● †	☆ moderate, 4–10% in 24 h.Faster if macropores. Higuchi <30%	SS not reached in 325 h	–	[58]
TTCP, DCPD, 40% HA	25 mM H_3PO_4	S	2 o 4 o 15 x 2 mm, 25 mL SBF, ● †	☆ 46%, 29%, 5% in 24 h. Follows Higuchi initially	SS reached in 2.5–14 days. 92, 54, 18% release in 2 weeks	Subcutaneous in rats show higher C_{max} when CPC is smaller, but total release is lower. 28, 58, 84% in 2 weeks	[59]
TTCP, DCPD, 40% HA	25 mM H_3PO_4	S	25 mL SBF, ● †	☆ Low 4–6% in 24 h. Diffusion controlled in initial stages	32–45% in 21 days. SS reached for low concentrations	Subcutaneously implanted in rats showed continued release for 3 weeks	[72]
TTCP, DCPD, 40% HA	25 mM H_3PO_4	S	25 mL SBF, ● †	☆ 2–15% in 24 h (unsure) Higuchi fits up to 90% release	Release up to 5 weeks. SS not reached in most cases.	–	[60]
TTCP, DCPD, HA, $NaHCO_3$	20 mM H_3PO_4	S	16 x 2 mm, 25 mL SBF, ● †	☆ 35–90% in 24 h.	60–100% in 72h. SS reached for high concentrations between 24 and 40h.	–	[71]
Anticancer							
Cisplatin							
Cerapaste, Kobayashi Med. Japan	Aqueous solution	S	7 x 14 mm, 10 mL PBS (7.4), †	☆ 9% in 24 h	13% released. SS reached after 3 weeks	Rat osteosarcoma cells proliferation inhibited with CPC+drug. Cell death when Cisplatin + Caffeine	[135]
75% TCP, 20% TTCP, DCP	Solution A	S	5 x 4 mm, 100 ml PBS (7.4)	☆ 11% in 24 h	24–60% in 4 weeks. SS reached for low drug concentrations	↑[Drug] in bone marrow from implanted CPC than when systemic admin.	[133]
Doxorubicin							
TCP, TTCP, DCP	Solution A	S	5 x 14 mm, 10 ml cell media, †	–	–	Inhibition of cell proliferation for 14 days. Higher survival in mice implanted with CPC+drug	[134]

Solid phase	Liquid phase	Drug incorporation	Release method	In vitro release profile	In vitro release time	Other studies: microbial / celular / in vivo	Ref.
Anticancer							
Methotrexate							
TCP, DCPD, HA	0.05% H_3PO	S	3 x 10 mm	-	-	In Rabbits CPC–Drug inhibited osteogenesis initially after implantation.	[137]
6–Mercaptopurine							
TTCP, DCPD, 40% HAP	20 mM H_3PO_4	S	8.5 x 3 mm, 25 mL SBF, ● †	☆ 7.5–13% in 24 h planar surface ☆ 20–30% in 24 h cylinder Higuchi	15–25% in 92 h planar surface 38–55% in 92 h cylinder SS not reached.	-	[132]
TTCP, DCPD, 40% HAP	20 mM H_3PO_4	S	15 mm dia., 25 mL SBF, ● †	☆ 14% in 24 h Fits Higuchi up to 100 h	65% in 600h SS not reached	-	[61]
Anti-osteoporotic							
Alendronate							
78% a -TCP, 10% CDHA, 5% DCPD, 5% MCPM, 2% HPMC	5% Na_2HPO_4	S–chemisorption	Column desorption was studied by passing 33 ml PBS.	-	-	-	[141]
β–TCP, TTCP, HA, DCPA	-	S	6 x 12 mm, 2 mL PBS (7.25), ● †	☆ 13–18% in 24h.	33–21% released after 21 days. Release close to SS after 7 days.	No cytotoxicity for rat MSCs, thus, good biocompatibility in terms of cell proliferation.	[140]
Estradiol							
Equimolar TTCP + DCPD	20 mM H_3PO_4	S	SBF + Ca^{2+}, †	Higuchi		In vivo in diseased rats.	[62]
TTCP, DCPD, 40% HAP	20 mM H_3PO_4	S	155 mm dia., SBF + Ca^{2+}, ● †	Higuchi	SS not reached in 24 days	In vivo release in rats: ↑ Ca^{2+}, ↓ drug release	[63]
Salmon-calcitonin							
TTCP, DCPD, HA CHT/Collagen	-	-	6x12 mm, SBF	4–10% in 24 h. Sustained release 60 days: 50–70%.	SS not reached.	-	[144]
Other							
Vitamins **–Metatetrenone VK2**							
TTCP, DCPD, bovine collagen	11 mM H_3PO_4	S	10 x 10 x 7.5+holes. 25 ml SBF alternating with Acetate Buffer (4.5),● †	Greater release in Acetate Buffer.	-	-	[150]
Ca^{2+} Blocker **–Nifedipine**							
TTCP, DCPD, 40% HA	25 mM H_3PO_4	S	15 x 2 mm SBF Shaking method Paddle method Flow through method	Faster release in flow through cell method. Higuchi.	SS not reached after 7 days.	-	[64]
Caffeine							
Cerapaste, Kobayashi Medical Japan	Aqueous solution	S	7 x 14 mm, 10 mL PBS, †	☆18% in 24h	Release for 8 weeks up to 90%. SS not reached.	Good rat osteosarcoma cell proliferation in CPC + caffeine. Cell death when caffeine + cysplatin.	[135]
Clorhexidine							
Equimolar β–TCP, MCPM	800 mM citric acid	S	8 x 1 mm, 10 ml H_2O	☆ 60% in 24h Initially fits Higuchi	100% released after 7 days	-	[65]

Table 2.2 *Different combination of drug and calcium phosphate cements used to study the in vitro and in vivo drug release behavior [96]. ([] apatite CPC, () Brushite CPC. S: drug loaded from solid phase. L: drug incorporated from liquid phase. ☆ Burst release. ●Shaking or stirring. † Periodical media renewal. HPC: hydroxypropylcellulose, PAA: polyacrylic acid, CMC: carboxymethylcellulose, SDS: sodium dodecylsulfate, LMAP: Low methoxy-amidated pectin, PLGA: polylactide-co-glycolide, SS: Stationary Stage)*

Gaining the progress research knowledge on bone cements is significant to all orthopedic surgeons and researcher. Though bone cements have been gold standard in orthopedic field, the uses of bone cement in current days decreased due to the start of cementless implants (press-fit), which support good bone in growth. To address the drawbacks, side effects and toxicity of bone cement advance research is required.

2.6 Surface delivery through coating

Presently used all metallic implants are biologically compatible but biologically inert. This may lead to weak interface with the bone and cause aseptic loosening. Besides, to avoid the fibrous tissue encapsulation around the implant, CaP and polymer coating had been introduced. These coatings are often being evaluated for their potential use for delivering the drug in-vivo.

2.6.1 Drug loaded biodegradable polymer coating

In the past three decades, a considerable amount of research work has been carried out for development of biodegradable polymeric materials for orthopedic applications. Degradable polymers are preferred candidates for potential drug delivery vehicle in scaffolds for tissue engineering application [137]. Based on their origin, biodegradable polymers can be categorized as natural and synthetic polymers. Natural polymers include polysaccharides (starch, alginate, chitosan, hyaluronic acid derivatives) and proteins (collagen, fibrin gels, silk, gelatin etc.) [138]. But, their applications are limited due to fast degradation rate, low mechanical properties and high physiological activity [139]. On other hand, synthetic biodegradable polymers can be produced under controlled conditions and careful design. They can be tailored to exhibit predictable mechanical property and degradation rate. In general, synthetic biodegradable polymers include polyesters, polyanhydrides, polyorthoesters, polyphosphazenes, and polyurethanes. Amongst the

members of polyesters family, polylactic acid (PLA), polyglycolic acid (PGA), poly-ε-caprolactone (PCL) and poly-β-hydroxybutyrate (PHB and their copolymer, like, poly (lactic acid-co-glycolic acid) (PLGA) are widely used in tissue engineering and drug delivery, due to their controllable degradation through hydrolysis of the ester linkage, biocompatibility and nontoxic degradation products [139][140].

Efficient way of drug loading on metal implant is still a challenge to biomedical engineers. Key factors affecting the drug loading are (a) choice of a suitable carrier system, (b) effective surface modification of implant prior to loading and (c) techniques used for loading the drug. For controlled release of drugs, a variety of biodegradable polymers, in the form of liposomes, gel beads, films, microspheres and hydrogels, have been introduced by different research groups [139]–[142].

Use of micro or nano spheres of polymers as a coating on metal implant is a promising method for the drug delivery system [142]. In this coating, the surface texture of the metallic implant can be maintained, as well as, potential drug release profile can be obtained. Such coatings can be directly used on the bone implant, or integrated into allograft material to stimulate tissue integration because it will be degraded once the drug is released [142]. Di Silvio et al. [141] prepared the human growth hormone (hGH) loaded gelatin microspheres in a pre-heated syringe. The solidified microspheres were cross linked with 25% glutaraldeyhyde vapour under vacuum for 24 h. The release profile of microspheres was checked in 5ml phosphate buffered saline (PBS). Ultrasound exposed microsphere shown increased release of GH due to penetration of water through cavitation, which promotes hydrolytic degradation of gelation. Ling Ting et al. [143] have prepared vancomycin hydrochloride (VH) loaded PLGA-PEG-PLGA (PPP) micelles by solvent dialysis and direct dissolution method. The 50 μL VH containing micelles solution was

incorporated into porous mineralized collagen (MC) coated Ti substrate by electrochemical deposition. The drug releasing profile showed the decrease in burst release from 81% to 58% in the initial 8 h, compared to the MC coating alone and controlled release was prolonged from 3 days to 1 week. The VH releasing kinetic was reported to be adjusted by changing the concentration and size of micelles. Antibacterial activity was not statistically affected due to the less initial release of VH. In addition, the drug carrying PPP coated surface offered enhanced cell activity and bioactivity.

Price et al. [30] have used the gentamicin as an antibiotic and PLGA as the biodegradable polymer carrier and dip coated them on orthopedic implant and checked the in vitro bacterial growth. 20 wt.% gentamicin containing polymer coating showed more than 99% antibacterial activity over 24 h, in comparison to uncoated implant. Drug released profile exhibited considerable burst release with a concentration of about 200 μg/mL (in 10 mL PBS at 37°) for first 6 days, followed by a high concentration for the rest 20 days' period with an average of 133 μg/mL. Many studies have reported the drug release behavior of gentamicin, triclosan and chlorhexi-dine (CHX) loaded biodegradable polymer [144]–[147]. Releasing pattern of polymer coating is also a biphasic, with initial burst release phase, followed by and sustained release up to weeks to months as shown in fig 2.8 [148]. Gollwitzer et al. [149] have incorporated 5 wt.% of gentamicin and teicoplanin into PDLLA. SS Kirschner-wires (K-wires) was coated through solvent casting technique with drug loaded biodegradable polymer. Release profile in PBS shown initial burst release within 6 h, later observed continuous slow release up to 100 h (fig 2.8)

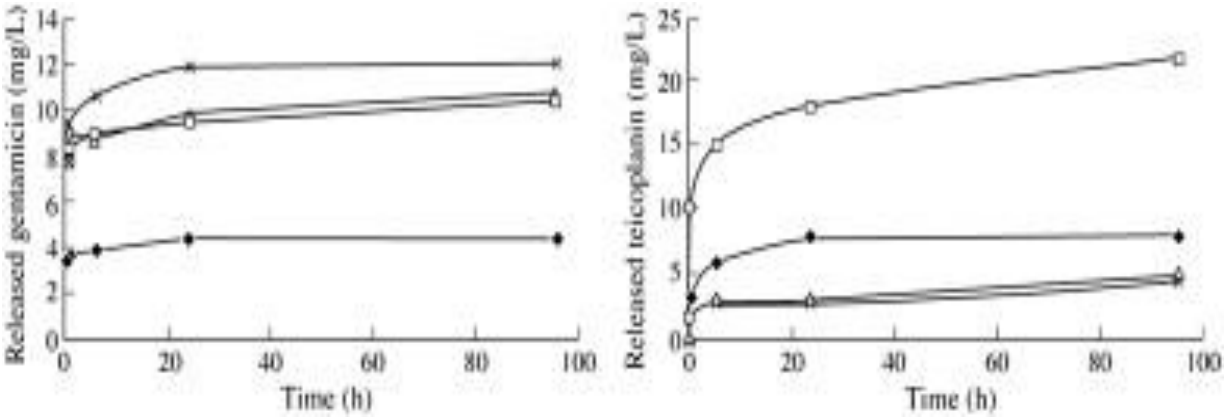

Fig. 2.8 *Release pattern of gentamicin (left hand panel) and teicoplanin (right-hand panel). (four different lines indicates four test sample release profile)*

The requirements for such coatings to be successful are the coating should not get damaged during implant insertion in surgery and loaded drug should remain stable within coating and get released in required manner, without any side effects [148]. Further, the degradation products of biodegradable polymer should not be harmful for any cell growth. Strategies to limit the degradation rates of polymer as well sustained control release fashion can be tailored with innovative fabrication of coating on metal implant and also it provides suitable mechanical property to fit the needs of implant coating. However, some studies have displayed burst with a short range of drug delivery and few of them established persistent drug profile. In other side's lack of in vivo studies and certain mechanical properties like coating strength, corrosion and anti-wear behavior of drug loaded biodegradable polymer coating on load bearing implant limit their clinical applications.

2.6.2 Drug Loaded Bioactive Ceramic Coating

Biomaterials used in orthopedic implant applications are classified as bio-inert, bio-tolerant and bioactive materials. Bio-inert materials remain inert while in direct contact with contiguous

tissue and hence does not induce any fibrous tissue around the implant. Some examples of such materials are alumina, zirconia and titanium. Bio-tolerant materials, like, poly-methyl-methacrylate (PMMA) bone cement acts as connecting tissue layer around the implant and bone. Bioactive materials, like, bioactive ceramics and bioactive glass, provoke direct chemical bond with the surrounding bone tissue and start the secondary reactions around the host bone as well as help in new bone formation. Thus, bioactive materials are an ideal candidate for replacing the damaged bone [150]. To overcome the problems associated with the metallic implants, like, biocompatibility and osteoconductivity, calcium phosphate based bio-ceramics and silica based bioactive glass coatings were suggested in late 1960s [151].

The earth's surface contains nearly about 3.4 wt.% of calcium and 0.10 wt.% of phosphorus and its widely scattered around the planet. The combination of these two oxide elements, with or without water incorporation, gives different calcium phosphate compounds and it belongs to the family of orthophosphates [152]. The family of calcium phosphate includes numerous compounds, differentiated by Ca/P ratios. Monocalcium phosphate monohydrate ($Ca(H_2PO_4)_2H_2O$) and dicalcium phosphate dehydrate ($CaHPO_42H_2O$) compounds has the ratio less than one. Hence, it is more acidic and water soluble and not suitable for biological application. On the other side, bioactive and bioresorbable tricalcium phosphate, with respect to their solubility and biological stability, exists in several states like α and β tricalcium phosphate and has the ratio 1.5. Besides, hydroxyapatite ($Ca_{10}(PO_4)_6(OH)_2$) has Ca/P ratio 1.67. It has a chemical composition and Ca/P ratio similar to apatite in human bone [153]. Bio-glasses, composed of sodium oxide, calcium oxide, phosphorus pentoxide and silica, have shown biocompatibility, osteoconductivity and potential to form bonds to bone without an intervening fibrous connective tissue interface [154][155].

However, HA and bioglasses generally suffer from brittleness, poor strength and low fracture toughness, limiting their use in load bearing implant. To overcome this problem, thin bioactive ceramic coating is proposed on metallic implant, to get the biological advantage of ceramics as well as strength of metal combined [150][150] Numerous techniques have been studied for coating the bioactive ceramics on metal implant such as plasma spraying processing [156], thermal spray coating [157], sputter coating [158], pulsed laser ablation [159], dip coating [160], sol- gel coating [161], elecrophoretic deposition [162] and biomimetic coating [163]. These coatings can be used as a good carrier of drugs for a targeted delivery.

Duan et al. [164] have developed the new method for local and sustained delivery of drugs. Calcium etidronate (family of bisphosphanate) were coated on titanium substrate through electrophoretic deposition. Coating showed amorphous globular morphology with a Ca/P ratio of 0.78 and there was no etidronate molecular structure change after deposition process. In vitro release profile showed continuous release up to 8 days. Xiao et al. [165] have prepared the asymmetric coating on titanium alloy by immersing the samples for 30 and 60 minutes into a dipping solution. Dipping solution was prepared by adding 1 g of hydroxyapatite and 10 g gelatin in 50 ml of deionized water. The samples were again dipped ibuprofen solution for four days and cross-linked with glutaraldehyde. Asymmetric coating has two layers. Outer layer was about 130 µm thick and composed of a thin dense structure, due to evaporation of solvent in a quiescent air. Inner layers (10 µm) was composed of thick pores, due to phase inversion by ethanol-water change in quench environment. The loading efficiency of the drug is directly dependent on the concentration of the drug in the solution, as well as, immersion time. In vitro release profile showed zero order release kinetics and lasted till 30 days from an asymmetric coating, due to osmotic pressure effect. Avés et al. [166] have deposited porous HA films on titanium implant

through sol-gel spin coating. Heat treating the coating at 450 °C leads to crystalline apatite structure. Coating strength was achieved on sand blasted Ti substrate through both mechanical interlocking and chemical bonding. Interconnected porous surface was formed due to gas evolution during thermal decomposition. This structure helps for loading the gentamicin sulfate and pores acts as potential drug carrier. Release kinetics shown 30 % to 40 % burst release in first 3 h and continuous release up to week. It is due to drug molecules attached in superficial layers of the samples and were easily accessible through voids and cracks.

The modern biomedical technology is driving the field towards cementless implantation procedure, which does not allow using cements as drug delivery system. However, in cementless prostheses, bioactive ceramics coatings on metal implants can take over the role of drug carrier. The success of these coated implants depends upon minimizing the early micromotion to improve the bonding strength as well as to avoid the fiber tissue encapsulation around the implant and boosting the fixation of the implant. On other hand, controlled drug delivery from these ceramic coated implants is facing several challenges. Stability of the coating is the critical limitation in wet chemical coating techniques, such as, biomimetic coating, sol-gel coating, dip coating and electrophoretic deposition. Wet chemical coating is solution based and low temperature process, where drugs can be easily incorporated into the coating. On other hand, physical deposition techniques, such as, pulsed laser deposition, sputtering and plasma spraying offer a greater interfacial bond strength and crystallinity. However, antibiotics cannot be incorporated into these coatings due to elevated temperature processing conditions. The drugs and bone growth factors can only be loaded after the coating is synthesized, by immersing the coated sample into concentrated drug containing solution. In this process, drugs get adsorbed only on the surface of the coating and it leads to a sizeable burst release, uncontrolled elution profile from loosely bonded drugs [167],

[168]. In this regard, research has to focus mainly to overcome this problem and bring the successful implant for future generation.

Briefly, several strategies have been proposed for orthopedic implants, including antibiotic loaded bone cement, drug molecules integrated within the implant and loaded with porous coating structure [33]. In cemented joint arthroplasties, antibiotics were traditionally doped into poly-methyl-methacrylate (PMMA) cement, but it offers unreliable release profile and weakening the polymer strength. Further, in long run, cements come out as particles, inducing third body wear. Wear debris invite immunological reaction and implant loosening [169][170].This rules out the use of bone cement for localized drug delivery. On the other hand, cement less (press fit fixation) procedure are most suitable to younger and active patient, as it interfaces directly with bone, offering good initial stability and avoiding aseptic loosening. Progressive improvement in prosthesis design offers drug loaded bioceramic or bioresorbable coatings for fighting against bacterial infection. However, local drug delivery from these coatings is very fast and without any control [171][172].

Hence, there is great interest in finding new methods or strategies to inhibit biofilms formation through controlled drug delivery for longer period. In this connection, one of the ideal sites for drug loading would be those parts of an implant, which are not supposed to have bone grown on them and would be in direct contact with the body fluid to make the released drug available in the surrounding sites of surgery. Such part in a total hip implant can be the lining of the acetabular cup. These liners are commercially made of ultra-high molecular weight polyethylene (UHMWPE).

2.7 Acetabular Cup (UHMWPE)

Ultra-high molecular weight polyethylene (UHMWPE) is the polymeric material that has been evolved after thorough scientific studies and it is in clinical use for last four decades as the liner of acetabular cup (bearing surface) [173][174]. UHMWPE belongs to a family of polymers with a simple chemical formulation of carbon and hydrogen molecules. UHMWPE (PE) is a linear homo-polymer. Carbon acts as backbone in polymer chain, which can rotate, twist, fold into crystalline phase and provide a more complex structure at the molecular level. Mechanical properties, such as, elastic modulus, yield strength and fatigue, creep resistance and thermal properties are directly related the degree of crystallinity in polymeric materials. PE can be synthetized from ethylene gas (C_2H_4) using the Ziegler-Natta process in a solvent using titanium tetra chloride ($TiCl_4$) as a catalyst (fig 2.9) [175][176]. Impurities of titanium, aluminium and

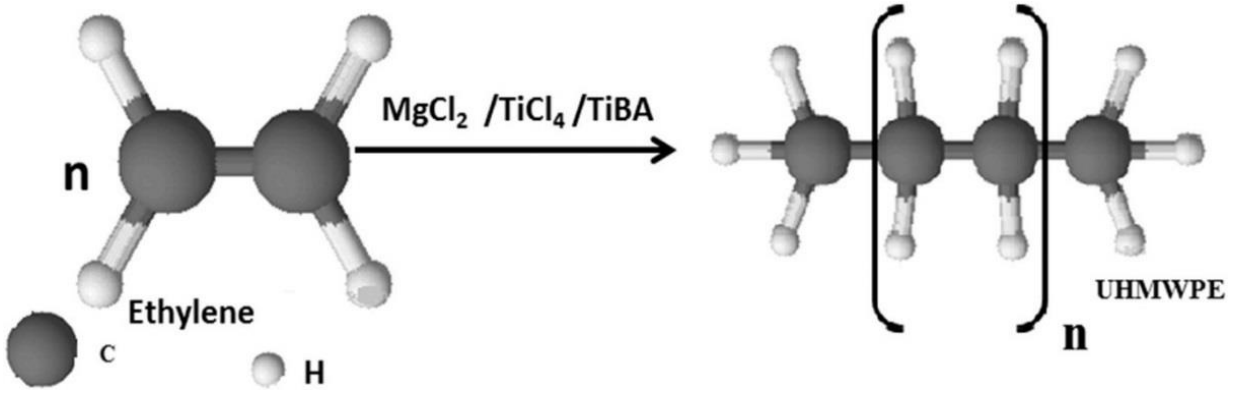

Fig. 2.9 *Synthesis of UHMWPE from ethylene gas*

chloride come from the catalyst. Two common PE resins are used for medical applications, namely, GUR 1020 and GUR 1050. Molecular weight, density, yield strength, ultimate tensile strength and elongation to failure of GUR 1020 are 3.5×10^6 g/mol, 935 kg/m^3, 21.9 - 22.3 MPa, 51.1 - 53.7 MPa and 440 - 452 %, respectively. The GUR 1050 resin has a higher Molecular

weight of 5.5-6×10^6 g/mol, density of 930-931 kg/m^3, yield strength 21 - 21.5 MPa, ultimate tensile strength 46.8 - 50.7 MPa and elongation to failure 373 - 395 % [174][177].

PE is very popular as the inner lining of the acetabular cup due to its unique combination of wear resistance, fracture toughness, bio-inertness and good processability, along with the lubricity offered during rubbing action with the metallic femoral head of the implant. Fracture toughness and wear resistance ensures generation of less wear debris, which can otherwise trigger macrophage induced re-sorption of bone and osteolysis [173][174][178][179]. Tribological behavior of PE lining plays a critical role in deciding life span of modular acetabular cup in total hip implants. Though PE is in clinical application for long time, its performance in extended period has been limited due to its inherent low yield strength, leading to permanent deformation, severe wear and ultimately premature failure of implant. Relative motion between the metal/ceramic femoral head and polyethylene lining surfaces generates wear debris. Generated debris migrates to the tissues around the implant through blood and invites inflammatory reactions, leading to osteolysis and gradual aseptic loosening of the implant as shown in fig 2.10 [180][181].

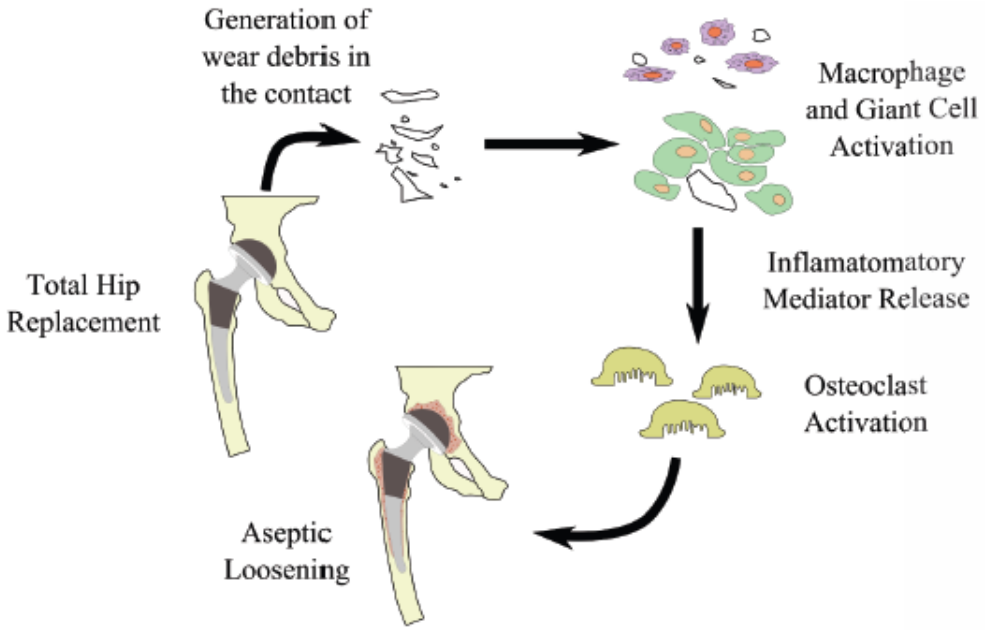

Fig. 2.10 *Key failure mechanism of total joint replacements*

Thus, a drive always exists to improve the stiffness and wear resistance of PE lining without increasing the coefficient of friction (COF), which is a challenging goal in itself. Over the past decades, significant efforts have been taken up for the enhancement of tribological and mechanical properties of PE bearing. Various techniques are explored for this purpose, namely, cross linking of polymer [182][183], increasing the degree of crystallinity through ionizing radiation [184] and chemical methods [185][186]. These modifications decreased the risk of wear rate of PE. But a negative effect on ductility and strength is noted, resulting into catastrophic failure of the implant [187]–[189]. However, main aim with the PE surfaces, to be used in orthopedic joints, is to have a unique combination of high wear resistance and low coefficient of friction, which apparently appears contradictory.

Polymer matrix composite is an alternate solution, where PE matrix is reinforced with either PE fiber itself [190] or various other carbonaceous nanoparticles and fibers, e.g., nano-diamonds, graphite, GNP and carbon nanotubes [140]–[142][181]. Cross linking PE fiber and nano particle reinforcement reduced the wear significantly. However, the reduction of strain to failure and fracture toughness had shown negative effective on its potential use [194]. Among stated reinforcements, CNTs have been used extensively for PE due to its unique properties; high elastic modulus (200–1000 GPa), tensile strength (11–63 GPa) and good lubrication [195][196][197]. Different processing routes, namely, solvent casting, ultra-sonication, in situ polymerization and ball milling, are employed to synthesize these composites with an aim of improving mechanical and wear behavior of PE matrix [198]. Tribological properties of CNT reinforced PE composite is a highly relevant characteristic for potential bearing application.

2.8 Carbon Nano-Tubes (CNTs) and Composite

CNTs are structurally defined as sheets of six-membered carbon atom rings (i.e., graphene) rolled up into cylinders. CNTs, having one layer, are called as single walled CNTs (SWCNTs) and more than one are called as multi walled CNTs (MWCNTs) [199]. Now days carbon based nanomaterials are used many product development applications. The key reasons beyond this is, its exceptional mechanical, thermal and electrical property. CNTs reinforced composite materials have been using already in market as sporting goods (tennis rackets), automobiles parts, body and in aircraft due its excellent mechanical properties [199].

Currently, wide range of research activities are ongoing in the world to develop a new CNTs based biomaterials for diagnosing the disease, cancer treatment, drug delivery and in vivo imaging [199][200]. Besides, CNTs were found brilliant as scaffold materials for nerve and bone tissue regeneration and regenerative medicine. Lot of research are still going on to expand the mechanical strength and durability of implants by joining CNTs with current biomaterials [200]. Further, many novel ideas have been put forward to explore use of CNTs in the treatment of different diseases. Fig 2.11 indicates the trend in the number of research articles found in the Pub Med database (http://www.ncbi.nlm.nih.gov/pubmed/ (accessed on 20 March 2014) by search using “carbon nanotubes” and “biomaterials” as keywords.

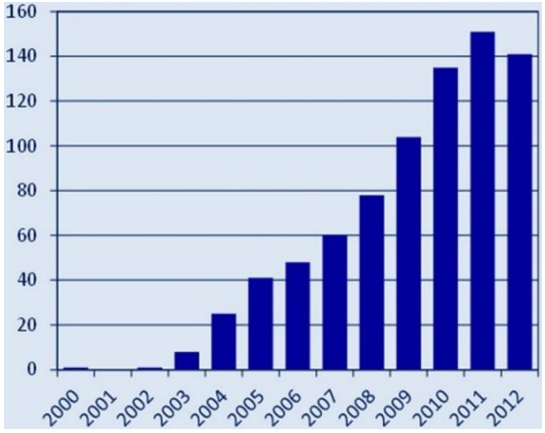

Fig. 2.11 *Indicates the trend in the number of research articles published*

2.8.1 Benefits of CNTs for Biomaterials Applications

The primary advantage of using CNTs is due to its small size, nanometers in diameter and micrometers in length, high aspect ratio. The following capabilities can be attributed to the small size of CNTs [199][200]:

(1) Reacting with cells by entering the cells or adhering to cell surfaces

(2) Acting on biological macromolecules and cell organelles of similar size

(3) Acting on parts of the body with fine structures

(4) Distributed via the bloodstream after intravenous injection and the like; thus they may be used in targeted drug delivery systems and in vivo imaging

(5) Rapidly eliminated from the body

(6) Having effects when combined with other biomaterials, for example, on fine structures to increase their mechanical strength

Many research works are carried out to improve the mechanical and tribological properties of PE composite. Ruanet et al. [201] reported 38% increase in elastic modulus and 49% in yield strength by addition of 1 wt.% MWCNT in solution casted PE films. In another study, addition of 5 wt.% of CNT in HDPE reduced wear rate by 50% and frictional coefficient by 12% [197]. On the other hand, a very small amount (0.2 wt.%) of single wall carbon nanotube (SWCNT) addition to PE increases hardness and elastic modulus by ~66% and 58%, respectively [202]. Wear durability is also improved impressively in this composite by more than two orders of magnitude [202]. CNTs can also offer the unique combination of improved toughness and decreased co-efficient of friction on surface by acting as a solid lubricant. However, effective utilization of CNTs in composite is strongly dependent on their uniform dispersion in the matrix, without disturbing their structural integrity [203]. Homogeneous reinforcement of phases and good

interfacial bonding enhance the load transfer efficiency from matrix to CNTs and show improved mechanical properties in the composite [204]. Strong interfacial bonding between polymer matrix and CNT is highly influenced by the aspect ratio of CNTs [205]. Hence, aspect ratio of the reinforcement is considered as a dominating factor for developing the theoretical and experimental models [206]. A few studies have explored the influence of CNT diameter and aspect ratio on mechanical properties of polymer composites. Diameter of CNTs have shown significant effect on fatigue behavior of an epoxy and 2.5 wt.% multi wall carbon nanotube (MWCNT) composite. A 10-fold reduction in the fatigue crack growth rate is observed for CNTs having diameter in the range of 5–8 nm, while only 2-fold improvement was recorded for thicker CNTs with diameter of 20–30 nm [207]. Both the CNTs possessed similar length of 10–15 μm. Thus, fatigue resistance and fracture toughness of epoxy is found to be functions of the aspect ratio of the filler phase. Ayatollahi et al. [205] have studied the epoxy-0.5 wt.% MWCNT composite with different aspect ratio of CNTs. A maximum of 32% increase in fracture toughness was observed with MWCNTs having aspect ratio of 1000 and it is decreased to 21% for a lower aspect ratio of 455. Both modulus of elasticity and tensile strength were increased with decreasing tube diameter. Small diameter and higher surface to volume ratio of CNTs form a percolated network in the composites and build strong interfacial bond with polymer chains, thus increasing the load transfer sites between the matrix and reinforcement [192].

Tribological properties of CNT reinforced PE composite is a highly relevant characteristic for potential bearing application. Only a few studies have dealt so far with the influence of CNT concentrations on wear and thermal stability of the polymer composite. All of these studies explored effect of CNT addition on the surface hardness, strength, plowing and cutting resistance of PE matrix. The reports mostly include improvement in wear resistance and increase in

coefficient of friction (COF). Few exceptions to this trend were also observed by Wei et al. [208] and Lee et al. [209] who reported decrease in COF by ~20% with addition of 5 wt.% CNTs. This decrease in COF is attributed to the self-lubrication offered by CNTs.

2.9 Summary of Literature Reviewed

Despite advances in orthopedic materials, the development of drug-eluting bone and joint implants that can sustain the delivery of the drug and maintain the necessary mechanical strength to withstand loading has remained elusive. In this regard, a significant amount of research has been devoted for developing drug releasing orthopedic scaffolds which has led to successful long term drug delivery also. However, it is easier to introduce drug in scaffold due to its structure, which is very porous and often made of organic and inorganic parts. Especially wide use of polymers in scaffolds made it easy to introduce drug and control its release for longer period. However, the function of scaffold and implant is very different and implant is often used to replace a bone permanently, as large as a limb. Thus, the implants are mostly made of metallic materials, and sometimes with hard polymers or ceramics forming a part of it. Due to the nature of structure and expected performance of the implants, it is not so easy to make them releasing drug for a longer period. On the other hand, the complete healing after surgery for a limb and similar parts takes 3 – 6 months and this is the period when drug release is needed. A very common and easy way, which has been tried to introduce drugs and growth factors to orthopedic implants, is through the bone cement. Non-biodegradable polymeric bone cements, like poly-methyl-methacrylate (PMMA), have been employed clinically for long time. But the problem with these type of medium is multifold: (a) uncontrolled delivery of drugs; (b) most of the delivery within 3 weeks with no long term release; (c) less than 50% of the loaded drug is released with rest being unused remaining inside non-biodegradable carrier; (d) requirement of surgery to remove the non-biodegradable

polymer during revision. In addition, the recent development in orthopedics towards cement-less implants leaves no scope for introducing drugs through bone-cement. The other options are drug loaded bioceramic or bioresorbable coatings. The main problem with drug containing bioceramic coatings, like calcium phosphate or hydroxyapaptite, is the processing of these coatings, which need high temperature. These coatings, when synthesized at low temperature, do not provide enough fracture strength or adhesion to implant surface and thus prone to fast failure. In addition, the drug release from these coatings is very fast and cannot sustain a long term release. Soaking antibiotics in such coating surfaces also is suitable for only short-term release. The second category of coating is bioresorbable or biodegradable polymers carrying the drug. But, coating of such polymers covers the surface of the implant and thus reduces its functionality in terms of sparing the mechanical and Tribological properties and even bioactivity also in specific cases. Thus, it is very important at this point to engineer the surfaces of different parts of orthopedic implants to carry and elute drugs and other necessary factors, still maintaining the functionality for osteoconduction and osteogenesis.

Our goal here was to develop methods by which therapeutic agents are incorporated into PE bearing surfaces but not increase any risk associated with their use while adding the benefit of antibacterial properties. However, it is also expected that any changes to the structure of the polymer may result in the compromise of one or more properties. Hence, reinforcing the different aspect ratio of CNT into PE to enhance the basic mechanical and tribological properties of PE. Further, engineering the surface of CNT-PE composite liner (acetabular cup) would lead to an efficient drug releasing device without compromising the mechanical and tribological behavior of the liner. Such acetabular cup liner would bring a significant advancement in field of drug releasing total hip implants.

2.10 Work Plan

This work aims to modify the surface of acetabular cup for carrying and sustained delivery of drugs without sparing functionality of the surface. The base material chosen for this work was ultra-high molecular weight polyethylene (PE), which is clinically used as lining to acetabular cup. The gentamicin (drug) was chosen because it is used to treat many types of bacterial infection particularly those caused by gram positive organisms. Biodegradable polymer chitosan was chosen for drug delivery carrier due to its compatibility with bone. Both (gentamicin and chitosan) are in clinical use in orthopedics and drug delivery. The critical part in this research is to modify the surface of PE in a way to incorporate these drug loaded biodegradable polymers in them. However, it is not intended to coat the surface of PE with biodegradable polymer, to avoid loss of functionality in terms of mechanical and Tribological behavior. In this regard vacuum impregnation technique was used to load the drug contained polymer into pores. The curing of PE needs high temperature, whereas the drugs cannot sustain heat. Thus, the PE free standing body (pellet) prepared and cured at high temperature with surface porosity to impregnate with drug loaded polymer at room temperature followed by curing through drying.

The modified surface was primarily being characterized for mechanical, tribological properties and it was compared with control sample, which is PE itself without surface modification, in order to assess their potential application in total hip implant. The tribological behavior of these materials was evaluated with pin-on-disc tribometer. The mechanical properties (hardness and elastic modulus) was measured using an instrumented indentation technique. Further, analyzed the drug release kinetics and mechanism, and its antibacterial efficacy for different days through disc diffusion method. In vitro cell culture studies also carried out to check its biocompatibility.

CHAPTER 3

Experimental Technique

This chapter describes the experimental techniques that are used to develop the drug eluting PE liner of acetabular cup for reducing the bacterial infection. The details of materials composition and processing route followed to prepare the composite are being explained. Methods used to engineer the interconnected micro porous surface layer on PE and CNT-PE composite substrate are also included. This is followed by details of techniques used for characterizing the microstructural, mechanical and tribological behavior of the modified surface is covered. The procedure followed to check in vitro drug release kinetics, antibacterial and biocompatibility are also given.

3.1 Materials

Medical grade ultra-high molecular weight polyethylene (PE) powder was procured from J.P polymer, Mumbai, India. It was in the form of white powder with an average granular particle size of 90 ± 30 µm and average molecular weight ~6 million g/mol. Density of the powder was found to be 0.953 g/cm^3, as estimated using helium pycnometer (SMART PYCNO-32, Smart Instrument Pvt. Ltd, Mumbai, India). Fig 3.1 shows powder particle and fibril structure of PE.

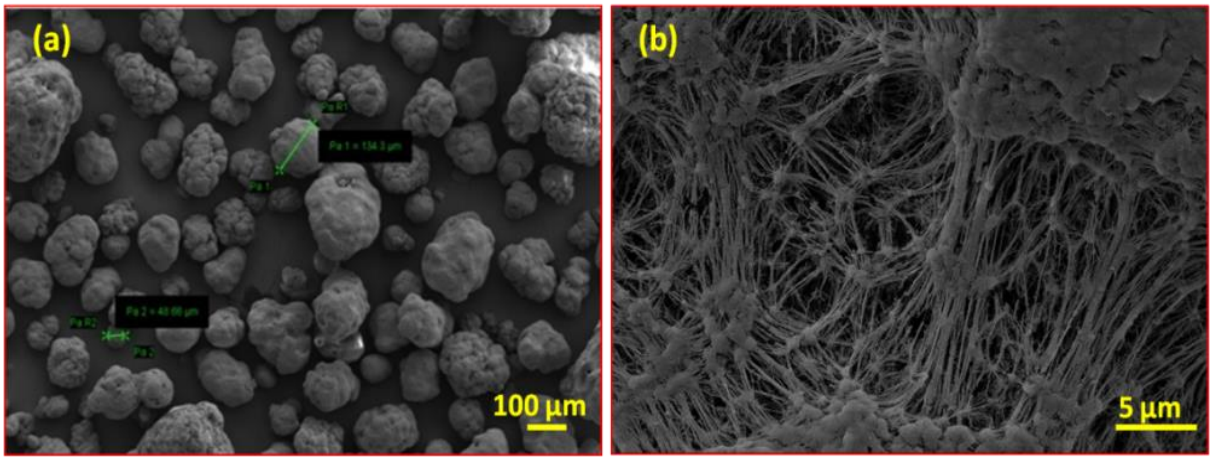

Fig. 3.1 *(a) PE powder particle and (b) PE powder fibril structure*

Two different aspect ratios of multi walled carbon nanotubes (MWCNTs), with more than 95% purity, are used in this study to prepare the composite. High aspect ratio CNTs (HARC), with outer diameter of 10-12 nm, length of 8-12 µm and density 1.8 g/cm^3, were procured from C-Nano Technology Limited, Beijing, China. Low aspect ratio CNTs (LARC), with outer diameter of 40-70 nm, length of 1-3 µm and density 2.1 g/cm^3, were procured from Inframat Corporation (Willington, CT). Their average aspect ratios (ratio of average length to diameter) are about 900 and 75, respectively. Fig.3.2a and b shows the FE-SEM images of as received MWCNTs. An inset in fig.3.2a and b clearly reveals the difference in aspect ratios of two types of CNTs used in this study.

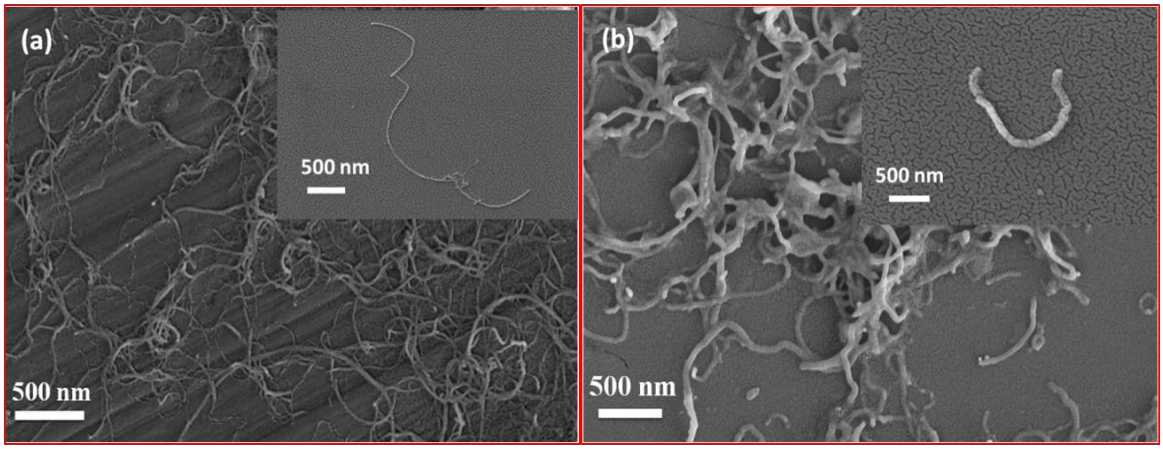

Fig. 3.2 *FE-SEM images of (a) high aspect ratio CNT, (b) low aspect ratio CNT*

3.2 Sample Preparation

CNT-PE composite was prepared by dispersing the CNTs homogeneously with acetone by using a probe sonicator for 60 minutes (Power - 500 Watts and 20 kHz frequency). During this CNTs were dispersed uniformly in acetone. This was followed by another 30 minutes of sonication, after mixing the PE powder in the dispersed CNT solution. Ultra-sonication technique is an established technique to disperse and breaking the nano particle agglomerates. High energy in the tip of probe produces shock waves and it promotes separation of CNTs from the

agglomerates/bundles. The composite powders were dried completely by keeping it in hot air oven at 60 °C. Fig. 3.3a and b shows homogeneous dispersion, attachment of HARC and LARC to PE powder respectively. Fig. 3.3c shows the digital image of the cured PE and composite pellet. Compositions with low reinforcement content (0.05 and 0.1 wt.%) were chosen for this study to avoid agglomeration and negative effect on biocompatibility.

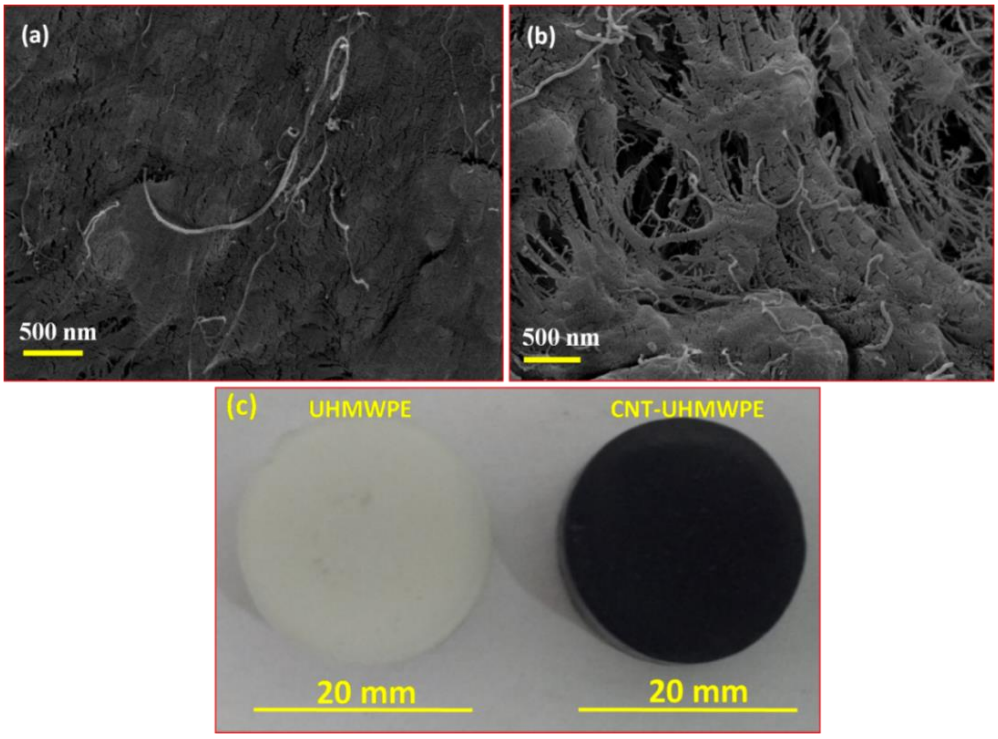

Fig. 3.3 *(a and b) Shows the 0.1 wt.% HARC and LARC dispersion on PE powder, respectively, before sintering and (c) digital image of the cured pellet.*

Following nomenclatures would be used for these different compositions throughout the manuscript: pure UHMWPE as (PE), PE-0.05 wt.% of HARC as (PE-0.05HARC) and LARC (PE-0.05LARC), UHMWPE-0.1 wt.% of HARC (PE-0.1HARC) and LARC (PE-0.1LARC). Disk shaped pellets (20 mm diameter and 5 mm thickness) were fabricated by compression molding of the composite powder with pressure of 300 MPa at room temperature, followed by curing at 160 °C for 60 minutes in hot air oven.

3.3 Thermal Characterization

Thermal behavior of PE and CNT-PE plays an important role in the mechanical and tribological property. For example, it is well known that degree of crystallinity and degradative oxidation behavior of PE leads to poor fracture toughness and low wear resistance, which ultimately lead to the aseptic loosening of the implant [210][211]. Besides, many literatures highlighted that addition of CNTs in PE can affect the degree of crystallinity through nucleation and crystals growing process [212][213]. Hence, differential scanning calorimetry (DSC) and thermos-gravimetric analysis (TGA) was performed using SEIKO 6300 EXTAR TG/DSC instrument. TGA is well known method to study the thermal stability and oxidative resistance of the polymer composite [5]. DSC is another thermal analysis technique for measuring the temperature and heat flow associated with material transitions as a function of time and temperature [215]. Melting temperatures, crystallization temperatures and crystallinity were analyzed by calorimetric study. About 10 mg of the test samples was sealed in aluminum pans; the samples were heated from 35º to 500° C at a heating rate of 5° C/min under nitrogen atmosphere. Degree of crystallinity was calculated by using the equation 1 [216] and assumed that no melting or crystallization occurs during heating.

$$X_C = \frac{\Delta H_C}{\Delta H_{100}} \times 100\% \quad \text{..... (1)}$$

where, X_C is degree of crystallization, ΔHc is the heat energy per unit mass (enthalpy) of composite and ΔH_{100} is the enthalpy of fusion 289 J/g for a 100 % crystalline PE [216].

The final properties of any polymer composite are mainly dependent on the interfacial bonding between the reinforcement and the matrix. Hence, curing temperature of the matrix is one of the critical parameter in preparing the composite. Differential scanning calorimetry (DSC) test was carried out on as-received PE powder (fig 3.4a). The melting temperature of PE is nearly

123 ºC, but it is very viscous at this point. Whereas, proper curing and wrapping of the reinforcement phase by polymer matrix needs more flow and lesser viscosity. Thus, a higher temperature of 160 ºC was used for curing. This was optimized by trial and error at a range of temperatures (130 to 180 ºC) and by observing the integrity of cured structure through microscopic investigation at the cross section of the PE pellets (fig 3.4c). Strong integrity between the PE particles demands optimization of curing time and temperature. In this context, the green pellet cured at 140 ºC for 60 minutes causes partial melting of PE particles, creating the bonding between other particles. Fig 3.4c clearly shows the lot of porosity inside the cured pellet. Poor melting of PE particles leads to poor fracture strength. On other hand, curing at 180 ºC for 60 minutes causes intensive melting of PE particles. Fractured surface had shown complete curing and no individual PE particles observed in the cured pellet (Fig 3.4d). Even though good curing was observed at 180 ºC, the pellet shape was distorted due to high melting temperature. Hence, 160 ºC was optimized for curing all PE and CNT-PE pellet (Fig 4b).

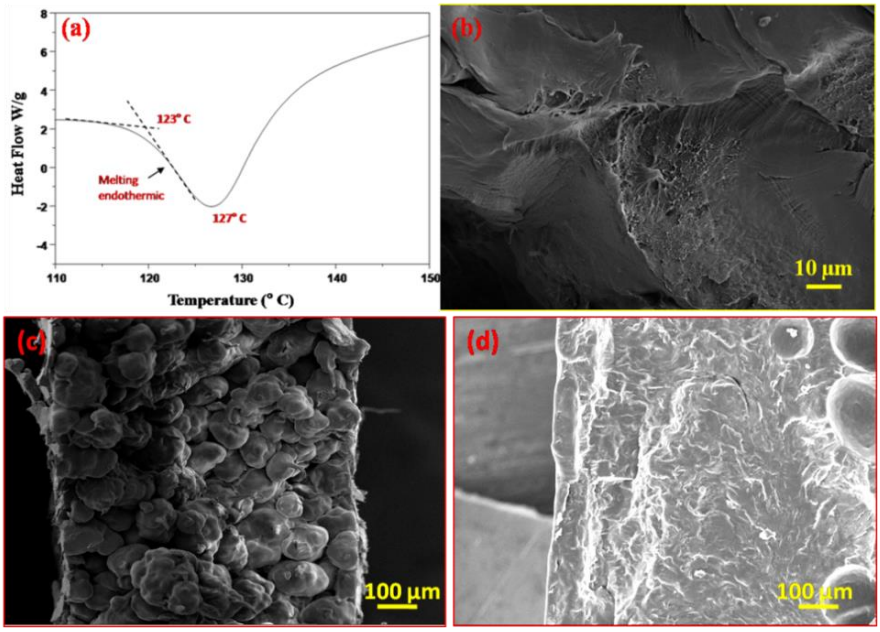

Fig. 3.4*a DSC curve recorded with PE powder;(b) cross section FE-SEM images of PE pellet cured at 160 ºC and (c & d) cross section FE-SEM images of PE pellet cured at 140 ºC and 180 ºC, respectively*

3.4 Preparation of Porous Surface

3.4.1 Modified Chemical Etching and Lyophilization

Micron sized pores were engineered on the surface of the cured PE and CNT-PE composite pellet through modified chemical etching followed by lyophilization technique. Micro pipette is used to pour ~75 µl of boiling (138 ^{0}C) paraxylene (procured from Sigma Aldrich, India) by drop-wise on surface of each PE pellet. Around 8-10 drops (~75 µl) were poured throughout the surface in 90 seconds and thereafter placed the samples in freezer. The samples were kept for freezing nearly 24 h, followed by lyophilizing (LYODEL, Delvac Pumps Pvt. Ltd, Chennai, India). Boiling paraxylene dissolved some amorphous regions on the surface of PE. This step was followed by freezing the material system at -20 °C in order to crystallize the paraxylene inside polymer pellet and thus stopping the full dissolution of surface. Fine pores were generated on the pellet surface after lyophilization process, whole process shown with the help of flow chart in fig 3.5. Lyophilization helps in vaporizing the crystallized paraxylene and thus leaving interconnected pores on PE and CNT-PE composite surface. Amount of average porosity (32 ± 5%) was calculated through Radical Meta check 5.0 software (Radical Instruments, Ambala Cant., India) by using SEM micrographs of the surface and also 3D optical profile. To get the optimized porosity all over the surface, different amount of boiling paraxylene was dropped and hold for different time to melt the surface. Pouring higher amount (≥150 µl) of paraxylene and longer holding time (2 to 3 minutes) leads to increase in porosity (40 ± 6%), by dissolving more PE surface (fig 3.6a). In case of lesser paraxylene (≤ 50 µl) and holding time (≤ 1 minutes), percentage of porosity (27 ± 5%) was decreased (fig 3.6b).

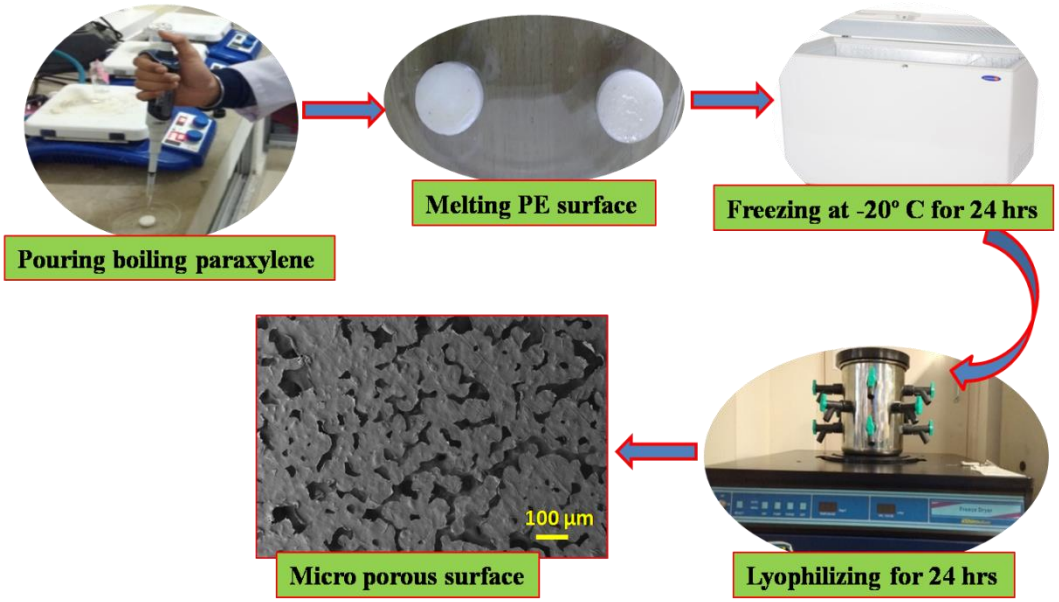

Fig. 3.5 *Flow chart shows the modified chemical etching and lyophilization process*

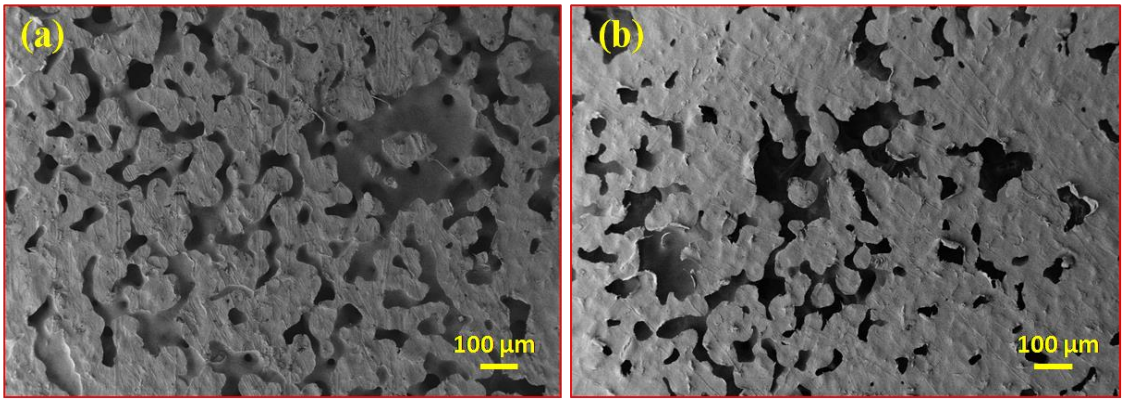

Fig. 3.6 *(a) FE-SEM images of higher loading of paraxylene and hold time; (b) lower loading paraxylene and holding time*

3.4.2 Electrostatic Spray Coating

Author idea here was to find other effective ways to modify the inner lining of acetabular cup to load antibiotic in it. The search was for a technique that can give the best drug release kinetics, while retaining mechanical and tribological attributes of the acetabular cup liner. In this context, electrostatic spray coating (ESC) technique was found logically suitable for fabricating such porous coating on PE liner surface. ESC offers uniform deposition rate, because all powder

particles are charged with same electrical polarity when they are ejected from spray gun and deposited uniformly on the substrate through charge repulsion. Further, the coating process offers controlled micro pores on the substrate [217][218][219]. Very strong integrity between porous coating and substrate is expected during curing, considering the fact that the substrate and coating material are same. Corona charge electrostatic powder spray system (Harbor Freight Tools Ltd, California, USA) was used to coat the cured PE pellet with PE powder.

ESC process consists of three steps: powder charging, spraying and deposition. During the operation, PE powders are supplied to the spray gun from a feeder unit through carrier gas (air), with the gas pressure of two bars. Carrier gas pressure is used to transport the PE powder from feeder chamber to spray gun and electrostatically charged powders were sprayed from the gun to grounded substrates to achieve a powder layer on the substrate [217]–[221]. High electrostatic voltage (80 KV) was applied to the spray gun by high voltage generator. Schematic diagram of ESC is shown in as fig 3.7. The charged particles follow the electrostatic field lines in 3D and get deposited on the grounded substrate, due to electrical field of attraction. However, PE being electrically insulating in nature, it was not easy to deposit the charged particles on it. Hence, NaCl solution was sprayed externally on PE substrate to makes it conductive. Same electrical polarity of the charged particles helps in uniform dispersion of particles on the substrate by mutual repulsion of charged particles and thus drawing the uniform coating (fig 3.8). The powder sprayed surface was cured to get the integrity in the coating. However, the curing parameters were optimized to have the porous structure, instead of having the powder particles fully melted and making a solid layer on the pellet surface and it is discussed in detail in result and discussion part (chapter 6).

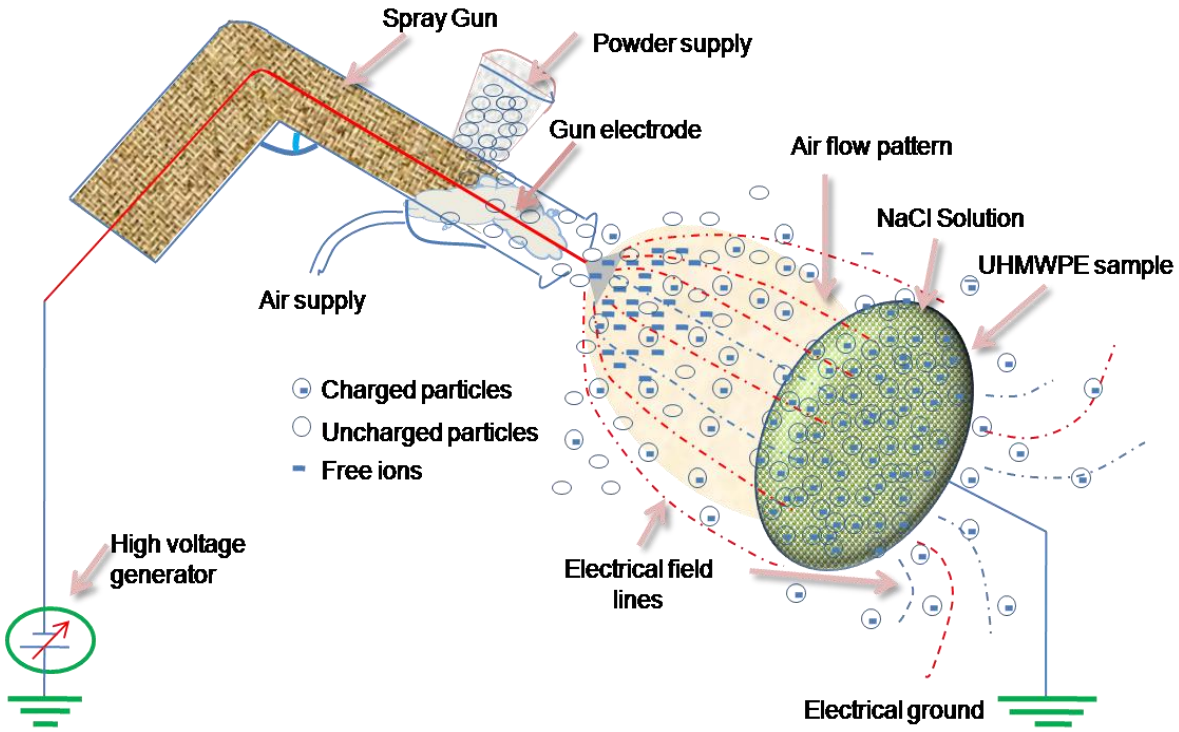

Fig. 3.7 *Schematic diagram of electrostatic spray coating (ESC) system*

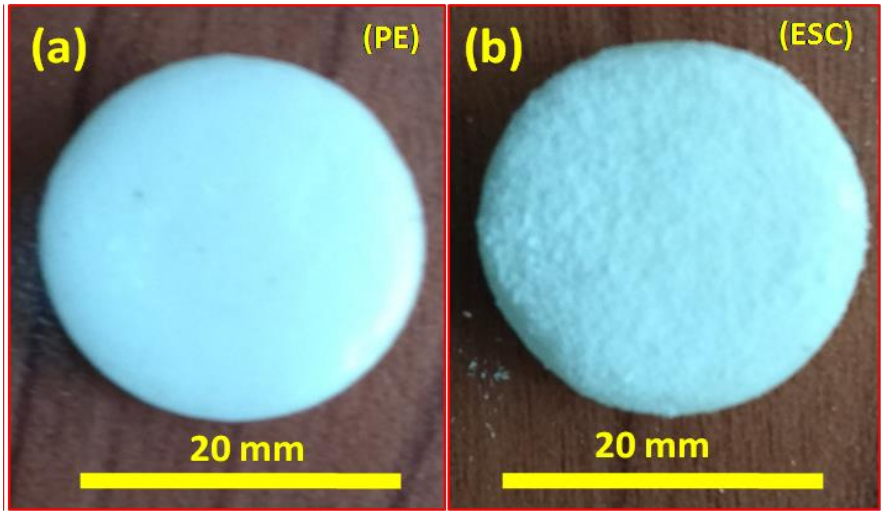

Fig. 3.8 *(a) Digital images of the PE pellet, (b) electrostatic powder spray coated pellet before curing*

3.5 Preparation of Gentamicin Loaded Chitosan

Chitosan (medium molecular weight of 240 to 280 kDa and 80% deacetylation) was procured from Sigma Aldrich, India. Chitosan is a biodegradable polymer and is reported to have some antibiotic characteristics [222]. Different concentration of chitosan solutions was prepared to optimize the viscosity and flow-ability of the solution. This was done to ensure that during impregnation the solution easily flows inside the pores and fill them. Finally, 10 ml of 3 % w/v chitosan solution was prepared as an optimized condition by dissolving the 0.3 g of chitosan in 1 % acetic acid. The mixture was stirred for 12 h at 70 ºC, using a magnetic stirrer, to get homogenous solution.

Gentamicin (molecular weight 463.6 Da) is a prototype of aminoglycoside with a broad spectrum of antibiotic drug and is used to treat many types of bacterial infection, particularly those caused by gram positive organisms. Gentamicin is used in this research to study the drug releasing efficiency of the modified PE surface. A measured amount (20 mg) of gentamicin sulphate (procured from Sigma Aldrich) was mixed well with the 1 ml of chitosan solution (3 wt% of chitosan in 1% acetic acid) through vortex shaker, for 30 minutes.

3.6 Characterization of Gentamicin Loaded Chitosan Solution

Fourier-transform infrared spectroscopy (FTIR) is the most useful technique for identifying the chemical components (bonds), present in the unknown mixture. Besides, it is used to find the chemical bonds in molecules, by producing an infrared absorption spectrum, which is like a molecular "finger print". The wavelength of light absorbed is characteristic of the chemical bond, as can be seen in this annotated spectrum. FTIR spectra over the wavelength range of 4000– 400 cm^{-1} were recorded using an FTIR spectrometer (Perkin Elmer Spectrum, Germany) to characterize the chemical interaction of gentamicin loaded chitosan. Individual solutions of

chitosan, gentamicin and gentamicin loaded chitosan was mixed well with potassium bromide powder using agate mortar & pestle and compressed to a 10 mm semi-transparent disk to carry out the test. Surface potentials of the same were determined using zeta-sizer (Nano ZS90, Malvern Instruments, UK).

3.7 Impregnation Procedure

This research aims to impregnate the drug containing biodegradable polymer in the interconnected pores, created on the surface of PE. Impregnation system was designed to load the drug effectively in the pores. The custom made impregnation chamber (Vacuum Systems and Products, Bangalore, India) and process shown with the help of flow chart in fig 3.9. Before impregnating the chitosan solution, the PE pellet was kept in high vacuum (1 mbar) inside impregnation chamber to remove entrapped air from the interconnected micro pores in the surface of the sample. After evacuation, chitosan solution was slowly incorporated in the chamber in controlled manner through the nozzle, to be sucked in and loaded in the pores. Finally, 3 bar pressure was applied on the impregnated samples to further drive the solution in the pores. The samples were allowed to cure at room temperature.

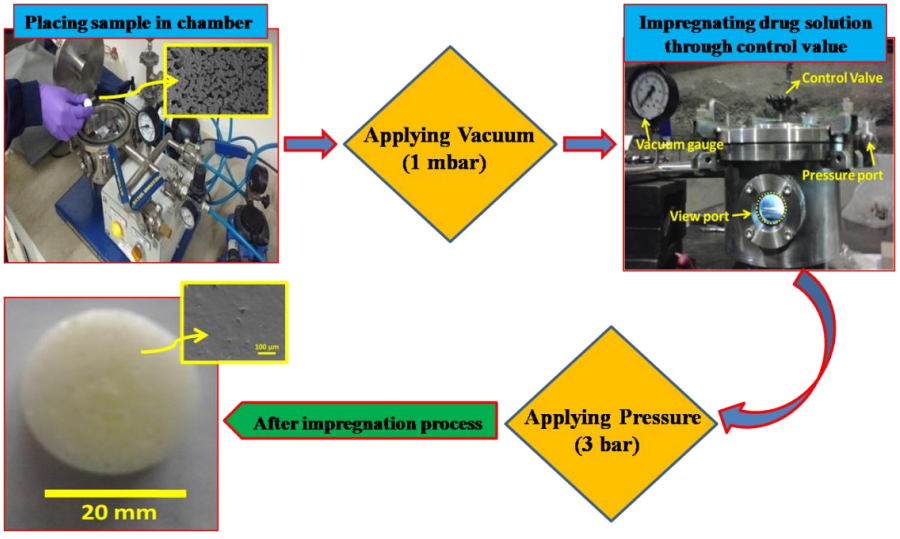

Fig. 3.9 *Flow chart describes the complete impregnation process*

3.8 Evaluating the Drug Release Kinetics

In vitro drug release study was carried out by immersing the drug-loaded samples into 10 ml of phosphate buffered saline (PBS, sigma P4417-100 TAB) solution. All immersed sample (Triplicates in each set) were stored in individual falcon tubes and placed in an incubator shaker with a speed of 80 rpm for better prediction of *in vitro* release kinetics. In specified time intervals, 2 ml of solution from each set of samples were withdrawn and 2 ml of fresh PBS solution were added in the falcon tubes to replenish the amount being withdrawn. The released drug concentration, from the withdrawn solution was analyzed via UV-Visible Spectrophotometer (Model Hitachi- 5330). Standard Calibration curve of gentamicin solution were prepared with different concentration and their absorbance values recorded at 250 nm wave lengths (Table 3. 1) [44]. Standard solution of gentamicin showed linear relationships between peak absorbance and gentamicin concentration in the ranges of 0.01 to 2 µg/ml (R^2 = 0.961), as presented in fig 3.10. Based on this calibration study, the amount of drug released from the modified surface, at specified intervals, was calculated. Cumulative drug release is plotted as a function of time.

Concentration of gentamicin solution (mg/ml)	Absorbance (nm)
1	0.095
0.5	0.048
0.3	0.046
0.1	0.019
0.05	0.01
0.01	0.005

Table 3.1 *Absorbance value of gentamicin solution with different concentration at 250nm*

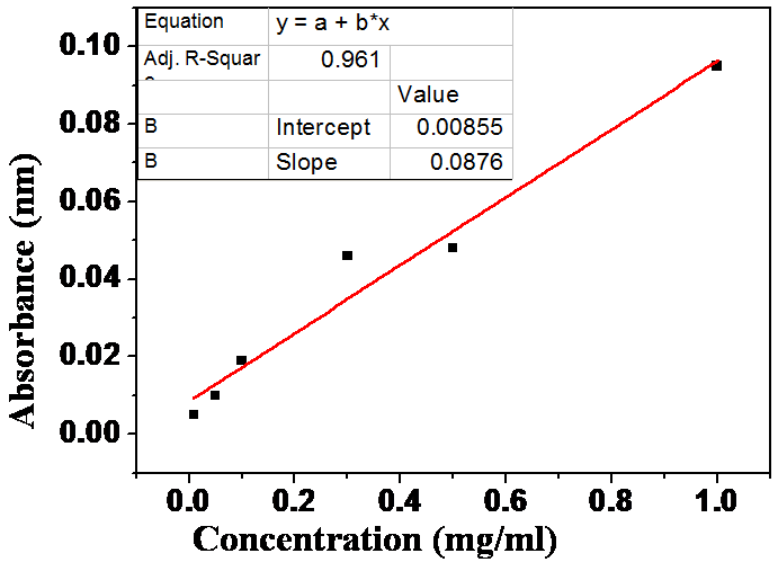

Fig. 3.10 *Standard calibration curve of gentamicin concentration in the range of 0.01 to 2 µg/ml*

3.9 Antimicrobial Activity

Antimicrobial study was carried out to evaluate the efficacy and stability of the drug released from the modified surface. Agar Disc Diffusion method was used to assess the antibacterial activity against gram-positive Staphylococcus aureus (*S. aureus*) bacteria. *S. aureus* was cultured in Luria Bertani Broth (LB) media and incubated in a shaking incubator at 37 °C overnight. After one day, the bacterial cells were brought into log phase by re-inoculating the overnight culture with 1:100 volume ratio, in fresh media, before further experiments. The experiments were started after achieving the optical density of 0.5 at 600 nm (OD 600), as confirmed using UV–vis-spectrophotometer (Lasany®, UV–vis double beam spectrophotometer). Modified drug loaded samples and unmodified PE samples were placed on freshly prepared nutrient agar lawned with S. aureus. All specimens were sterilized under ultraviolet rays before placing into agar plate. Efficacy of the gentamicin, released from modified surface, was assessed by measuring the zone of bacterial inhibition in the culture plate after 1, 3 and 5 days of bacterial incubation. SEM images were also captured after incubation.

In addition to that, antibacterial activity against gram negative (Escherichia Coli) bacteria was also assessed by the disc diffusion technique. E. coli was cultured in Luria Bertani Broth (LB) and incubated in a shaking incubator at 37 °C overnight. After one day, the bacterial cells were brought into log phase by re-inoculating the overnight culture 1:100 volumes into fresh media, before further experiments. The experiments were started after achieving the optical density of 0.5 at 600 nm (OD600), as confirmed using UV–vis-spectrophotometer (Lasany®, UV–vis double beam spectrophotometer). Unmodified PE surface and drug impregnated PE surfaces were used to study antibacterial activity for E. coli DH5α strain. The samples were sterilized under ultraviolet rays and incubated with 100 µl E. coli culture at 37 ºC. Antibiotic release of the specimens was assessed by the disc diffusion technique after 24, 48, 72, 96 and 120 h of bacterial incubation.

3.10 Evaluation of Cytocompatibility of the Implants

In vitro cell culture study was carried out in order to estimate the expected in vivo response to the modified surface produced in this study. Probable cytotoxic effect of the orthopedic implants was checked on osteogenic MG-63 cells through viability (MTT) and proliferation (DAPI staining) assays. Cells were cultured in Dulbecco's Modified Eagle Medium containing 1g/L glucose (DMEM low glucose, GibcoTM), and supplemented with 10% fetal bovine serum (FBS) (heat inactivated) (Invitrogen, Carlsbad, CA, USA), 1% antibiotic (100 U/ml of penicillin and 100 µg/ml streptomycin) (Hi-Media, India) and 0.3mg/ml Geneticin (GibcoTM). Cells were grown at 37 ºC in a 5% CO_2 incubator with 95% relative humidity (FormaSeriesThermoFisher, India). The implants were sterilized by overnight UV irradiation, followed by a round of pre-incubation in complete growth medium before seeding cells on them. 10 X 10^3, 8 X 10^3 and 6 X 10^3cells/implant/well were seeded in 24 well plate to check the viability after 1, 3 and 5 days, respectively. 3-(4,5-dimethylthiazol-2-yl)-2,5 diphenyltetrazolium bromide (MTT) assay was carried out as described

earlier [223]. Accordingly, MTT reagent was added to every sample to a final concentration of 200µg/ml from a 10mg/ml stock and incubated for 4 h at 37ºC. Formazan crystals thus formed were dissolved in 800µl DMSO. 200µl of this purple solution was aliquot into a 96-well plate and optical density (OD) measured at 570 nm in ELISA plate reader (Fluostar Optima, BMG Lab tech, Germany). Percentage cell survival was calculated as following:

$$\% \text{ Cell Survival} = \frac{\text{OD from cells grown on implant}}{\text{OD from cells growm on regular tissue culture well}} \times 100 \qquad \ldots\ldots\ldots (2)$$

To check the effect on proliferation, 5 X 10^3 cells were grown on the implants, fixed with 4% formaldehyde after1, 3 and 5 days of incubation and stained with 4',6-diamidino-2-phenylindole (DAPI).

3.11 Evaluation of Mechanical Properties

Nanoindentation and microindentation techniques were used to evaluate hardness and elastic modulus of the CNT reinforced composite and surface modified (coating) test samples.

3.11.1 Nano-Indentation: Elastic Modulus and Hardness

Nanoindentation test was conducted to measure the mechanical properties of the CNT-PE composite. Hysitron TI-950 triboindenter (HysitronInc, USA) equipped with three-sided berkovich diamond indenter with a tip radius of 100 nm. Tip-area calibration was done using a standard fused quartz substrate of known modulus (69.6 GPa). Indentations were made in the depth controlled mode to achieve same depth of penetration in all the indents. The maximum penetration depth of 150 nm was achieved in 10 s followed by holding for 2 s after attaining the peak displacement. A minimum of 25 indents were taken on each pellet to evaluate the hardness (H) and elastic modulus (E). E is calculated from the slope of the initial portion of unloading curve of load versus displacement plots using Oliver and Pharr method [224].

3.11.2 Instrumented Micro-Indentation

Instrumented micro-indentation test (M1 Mechanical Tester, Nanovea, USA) was carried out to measure the mechanical properties of different surface modified test samples, using a four-sided vickers diamond indenter with tip radius of 20 µm. Micro-indentation technique was chosen here to study the effect of porous structure on mechanical properties. In this instrument, the applied load is higher and indenter tip is 200 times bigger than nano indentation tip (berkovich). Hence, this indention covers the larger area and depth; as a result, it avoids the localized porosity effect on mechanical properties of the modified surface. A minimum of 15 indents were performed at different areas of each test sample to evaluate the hardness (H) and elastic modulus (E). Peak force of 2N was reached in the rate of 2N/min, followed by 10 s dwell time to avoid the overlapping of loading and unloading plot. Elastic modulus was measured from the unloading part of the load versus displacement curve of the indents, using Oliver –Pharr method [224]

3.12 Sliding Wear Test

Ball-on-disk tribometer (Ducom tribometer, Bangalore, India (fig 3.11)) test was performed to evaluate the friction and wear behavior of the CNT-PE composite and surface modified test sample. One of the intended applications of this PE based material system is in acetabular cup lining of hip implant. This lining goes through several rubbing action with the femoral head, which can be properly addressed through the macro scale wear studies with the rounded (spherical) surface. That is why ball-on-disk tests were chosen for evaluating tribological behavior of the composite. Before tribological testing, the disk samples and balls were cleaned using acetone in an ultrasonic bath for 15 minutes, followed by drying in a hot air stream. Commercially available EN-31 forged steel ball (hardness – 63 HRC) with 6mm diameter was used as counter body and sliding wear tests were done in ambient conditions (28 ±5^{o}C and 40 ±10% RH) without any lubricant.

Normal load and speed was used for the tests were 5 N and 200 rpm, respectively. The track diameter was approximately 6mm and test duration was 2 h. At least three tests were performed in each composition. Contact profile meter (SJ 400, Mitutoyo, Japan) was used to determine the depth and width of the wear track. At least ten profiles across the track were recorded in each of the three tracks for all the compositions to measure the average width and depth of the wear track. Wear volume (V) of the track was calculated using the following formula.

$$V = 2\pi \cdot r \times W \times D \quad \ldots\ldots\ldots\ldots\ldots\ldots\ldots\ldots\ldots\ldots (3)$$

Where r is the radius of the wear track; W and D is the width and depth of the wear track respectively. The variation in wear volume, thus measured, is reported as error bars in the corresponding calculations of wear rate.

Electronic sensor was attached to tribometer to record the continuous frictional force. The co-efficient of friction with respect to sliding distance is obtained from there. The specific wear rate was calculated from the following relationship;

$$W = \frac{V}{P \times S} \quad \ldots\ldots\ldots\ldots\ldots\ldots\ldots\ldots\ldots\ldots\ldots\ldots (4)$$

Where W is the specific wear rate, V is the total wear volume, P is the normal load and S sliding distance travelled in 2 hours. The worn surfaces were thoroughly studied through FE-SEM to identify the mechanisms dominating their tribological behavior. The worn surfaces and debris were studied to identify the dominant mechanisms of material removal using SEM equipped with energy dispersive X-ray spectroscopy (EDS) (ULTRA plus, Carl Zeiss, Germany).

On the other hand, optical profiler (Nanovea ST400, USA) was used to obtain the wear volume from wear track. With the help of optical pen (P1-OP3500D) and Mech 3D scan software, scan the whole worn area with the X-Y speed of 0.1 mm/s. Optical pen works with chromatic

confocal technique, where white light source (LED) passes through a series of lenses inside the optical pen and generates high degree of chromatic aberration. The refractive index of the lenses will vary the focal distance of each wavelength of the white light. Each separate wavelength of the white light will focus at a different distance from optical pen and create the measurement range (height). The measurement ranges of wavelength changes according to surface roughness level. The white light reflection and wave length change is used to measure the surface waviness. After scanning the worn surface, professional 3D.7 software (Mountains Technology Pvt. Ltd) was used for analyzing the track depth and for calculating the wear track volume (V).

Fig. 3.11 *Digital image of the ball-on-disk tribometer to perform continuous sliding wear test*

3.13 Roughness Measurement

Surface roughness (Ra) and wear track depth of CNT reinforced PE composite was calculated using Mitutoyo Surftest 400 surface roughness tester. This instrument consists of a contact type stylus, which has 2 µm radius diamond tip and it run over the surface. The sample was firmly fixed with double sided tape to prevent movement during measurement. Prior to start the measurement, standard calibration block was used to check the accuracy of roughness tester. At least five measurements were taken on each test sample to calculate the average roughness.

3.14 Density Determination

The density of the PE powder and CNT-PE composite was calculated using the helium pycnometer (SMART PYCNO-32, Smart Instrument Pvt. Ltd, Mumbai, India). The helium pycnometry technique involves forcing helium into the voids in a sample, as the helium can enter even the smallest voids and pores; it can be used to measure the volume per unit weight of a sample.

3.15 Scanning Electron Microscopy

Field emission scanning electron microscope (FE-SEM, Carl Zeiss Ultra Plus, Germany) and SEM (S4300, Hitachi Ltd., Japan) was used for characterizing the powders, cured composites and coatings at 15 kV operating voltage. All samples were sputter coated with gold before observing in SEM. Microscopic characterization of powders and CNTs was performed by dispersing them on a glass slide or silicon wafer. Fracture surface of the cured pellet and worn surface after wear testing was also checked under SEM to analyze the quality of CNT dispersion and its bonding with PE matrix. Influence of solid lubrication on friction and wear mechanism was well understood by SEM analysis. Further, Surface porous morphology before and after drug releasing well studied with the help of SEM.

3.16 Transmission Electron Microscopy (TEM)

To get the information, which is not accessible using optical microscopy and SEM, transmission electron microscopy (TEM) was used. It can magnify the specimens in the region of 10^{-6} m to 10^{-9} m by diffraction and imaging techniques. TEM is used to analyze the drug particle interaction in the chitosan matrix, using Tecnai G2 20s-TWIN (FEI Netherlands). For TEM, 2 μl of drug dispersed chitosan solution was dropped on a carbon-coated TEM grid and grids were air-dried prior to imaging. The images were captured at an accelerating voltage of 200 kV.

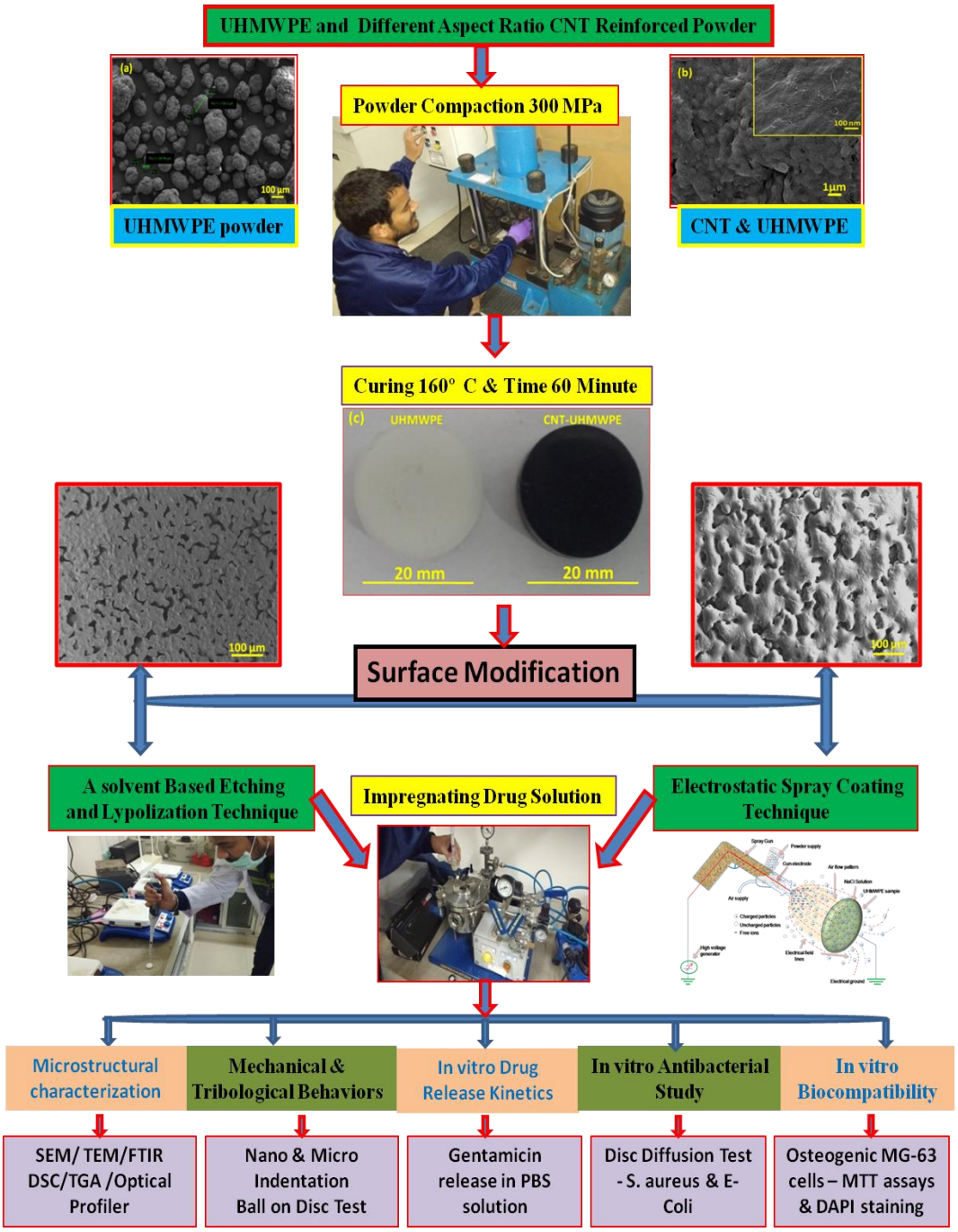

Fig. 3.12 Pictorial representation of experimental procedure carried out in present work

CHAPTER 4

Surface Modified on PE by Chemical Etching and Lyophilization Technique

This chapter deals with modifying the surface of PE lining for acetabular cup in total hip implant, for local delivering of drugs in the surrounding of the surgical area to fight against the initial infection. The majority of the surfaces of the metallic implant parts in total hip implant is generally surrounded by bones and is supposed to work as active site for growth of new bone. Once being covered by neobone, these surfaces are not as efficient in delivering the drug in the whole surrounding region to take care of all infections around. Thus, one of the ideal sites for drug loading would be those parts of an implant, which are not supposed to have bone grown on them and would be in direct contact with the body fluid to make the released drug available in the surrounding places of surgery. Such a part in a total hip implant can be the lining of the acetabular cup. Hence, surface modification of such material for holding and releasing the drug in controlled manner, without compromising its mechanical and tribological behavior, would bring a significant advancement in the field of drug releasing total hip implants. However, this is the first attempt in exploring the potential of polymeric acetabular cup liner as drug releasing part of a total hip implant and this very fact emphasizes the uniqueness of the research work being presented here. The modified surface released the drug in a controlled manner up to 26 days and shown improvement in the tribological property by reducing the coefficient of friction and wear rate. The in vitro antibacterial study with E. coli DH5α strain and S. aureus *confirms the effectiveness of drug release from the modified surface. After drug release (around 26 days), the modified surface has shown almost similar tribological and mechanical property as like unmodified surface. Hence, this study would offer new dimensions to polymeric acetabular cup liner as drug eluting part in total hip implant to treat the initial infection around the surgical area.*

R. Manoj Kumar *et al. "Sustained drug release from surface modified UHMWPE for acetabular cup lining in total hip implant."* ***Materials Science and Engineering: C,*** *77 (2017): 649-661.*

4.1 Results and Discussion

4.1.1 Microstructural Characterization of the Porous Surface

The PE powder compaction pressure and curing temperature of the green pellet was optimized by observing the integrity of the cured structure through microscopic investigation at the cross section, and it was clearly mentioned in experimental procedure section (chapter 3). Chemical dissolution and etching route was chosen to engineer the thin layer with interconnected micro pores on the surface of cured PE. Mechanical integrity and tribological behavior of the PE surface are important criteria for its use in acetabular cup lining. Thus, the aim was to avoid having a whole new layer of a biodegradable polymer, as coating, on the surface. It was rather assumed more prudential to have the biodegradable polymer impregnated in the open and beneath-the-surface pores on the PE surface. This helps in retaining PE on the maximum fraction of exposed surface area. This is only possible if one can obtain a thin porous layer on PE surface with interconnected pores, which can be filled with drug loaded biodegradable polymer. This construction helps in retaining the original structure and properties of inner liner of the acetabular cup, as much as possible.

Paraxylene is chosen for partial chemical dissolution of PE surface to fabricate a thin porous layer. It dissolves the amorphous region of the PE surface at elevated temperature. The aromatic hydrocarbon, paraxylene, interacts with hydrocarbon chains of PE at high temperature and breaks them [225][226]. The boiling point of paraxylene (138 ^{o}C) is higher than the melting temperature of PE (127 ^{o}C) [198]. Chemical dissolution was achieved by adding boiling paraxylene drop by drop on the surface of PE. This was followed by sudden freezing of paraxylene etched PE surface to avoid full melting of the surface. The remaining paraxylene crystallizes during freezing. Surface was lyophilized after freezing. Crystallized paraxylene evaporates during

lyophilization, leaving porous surface behind instead of fully melted layer. Lyophilized surface of PE shows porous layer with few tens of micron sized interconnected pores (fig 4.1a). An inset in fig 4.1a clearly indicates the interconnectivity of the pores beneath the surface, which are created by faster dissolution of amorphous region of the PE surface. Several trials were attempted in terms of number of boiling paraxylene drop casting on the surface, holding time and surface roughness of PE to get the optimized and interconnected porosity on the surface. It is assumed that ~1/3 of surface area of porosity would be optimum for holding enough drug loaded biodegradable polymer without losing the mechanical and tribological behavior of the PE surface significantly. The average depth of pores is around 190 ± 30 µm as measured using three dimensional optical profiles (fig 4.1g). The porosity is found to be 32 ± 6%, calculated from optical micrographs.

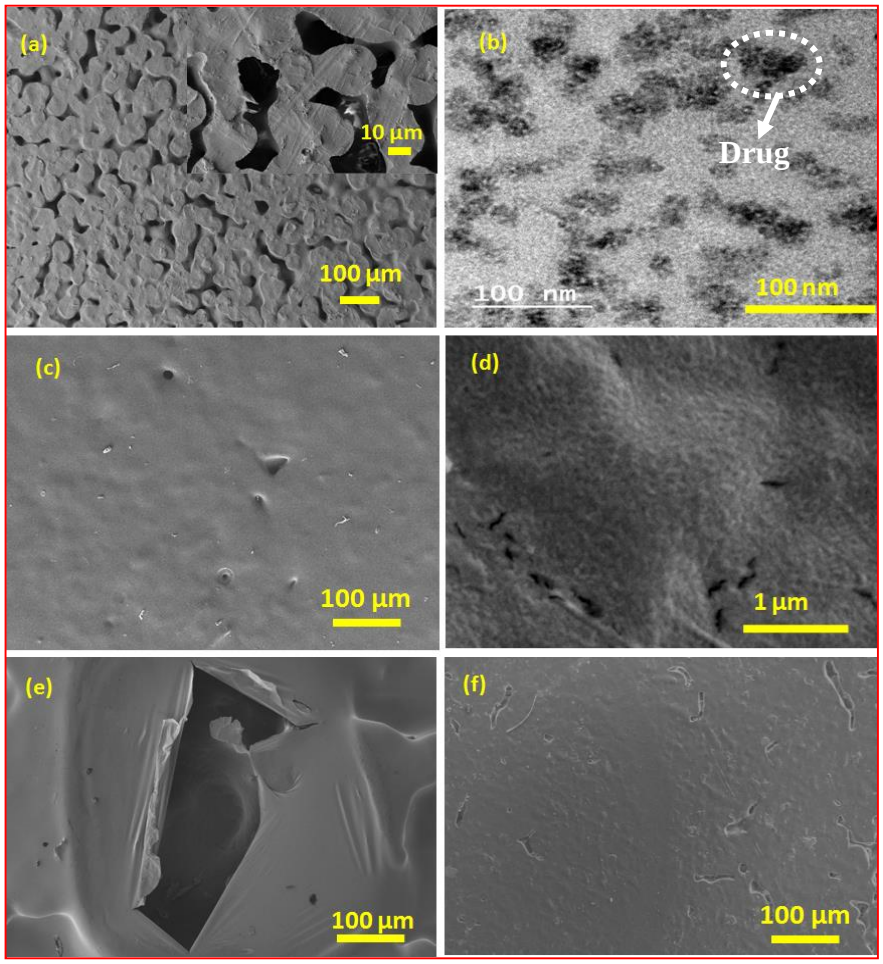

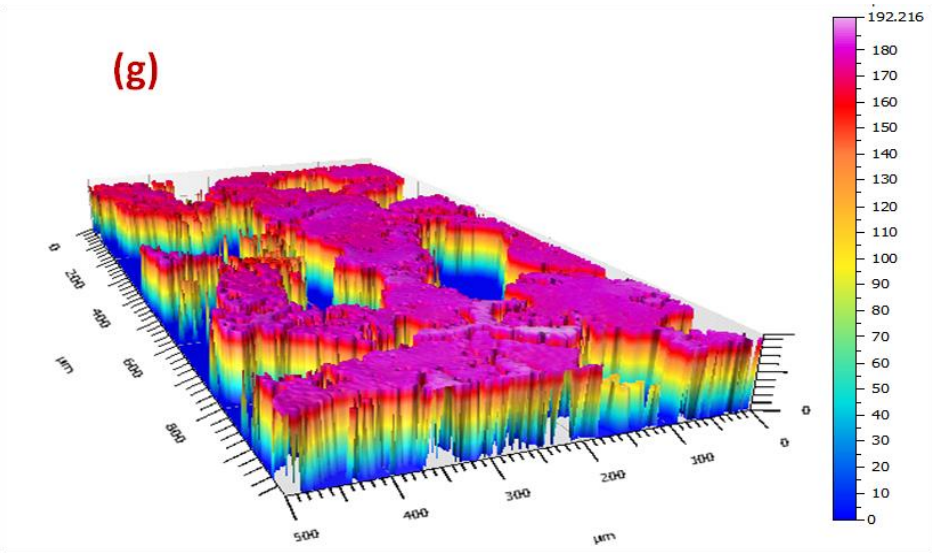

Fig. 4.1 *SEM micrographs of (a) modified PE surface with interconnected micro pores ; (b) TEM image of drug loaded chitosan; (c) SEM images drug loaded chitosan impregnated surface (CI-PE); (d) higher magnification image of (c); (e) dip coated drug loaded chitosan surface (CI-PE) and (f) PE surface after drug release (AD-PE); (g) Three dimensional optical profile of the porous surface*

The morphological characteristics of gentamicin loaded chitosan was imaged using TEM. TEM image (fig 4.1b) shows uniform dispersion of gentamicin in chitosan matrix. The drug particles were some extent spherical in nature with the average particles size of 27 ± 6 nm.

FTIR spectrum of gentamicin loaded chitosan is illustrated in fig 4.2. The main absorption peaks of gentamicin and chitosan solution are depicted in the spectra. fig 4.2a shows a peak at 620 cm^{-1}, which is considered as characteristics peak for gentamicin [227]. Three more peaks at 1137, 1653 and 3400 cm^{-1} were also detected for gentamicin. These peaks can be attributed to the N-H and O-H vibrational bonding of primary aromatic amines. Most important peaks in chitosan (fig 4.2b) are O-H from carbohydrate ring and N-H stretching in amine and amide groups (around 3500 cm^{-1}). An absorption peak for vibration of carbonyl bond (C-O-C) in amide group is also present at 1100 cm^{-1} [228]. However, no additional peak is observed in gentamicin loaded chitosan than the

ones present in either gentamicin or chitosan individually (fig 4.2c). Thus, the FTIR results do not suggest formation of an extra covalent bond between chitosan and gentamicin.

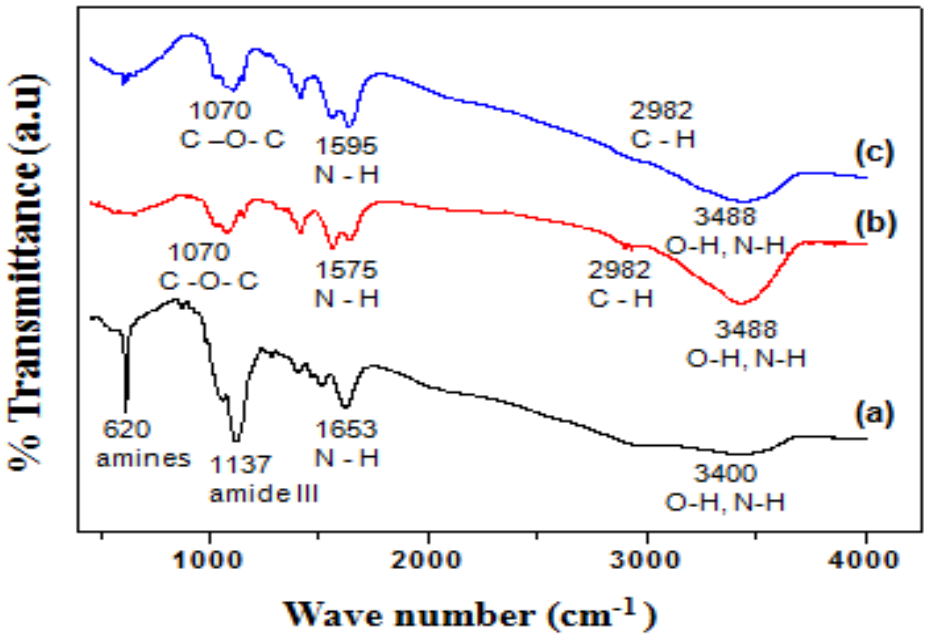

Fig. 4.2 *FTIR spectra of (a) gentamicin, (b) Chitosan and (c) gentamicin loaded chitosan*

Zeta potential analysis was further carried out to understand the possibility of any electrostatic binding between chitosan and gentamicin. Zeta potential of gentamicin, chitosan and gentamicin loaded chitosan was +1.11±0.4, +24.5±2.2 and +20.8±1.3 mV, respectively. This result clearly shows all are positively charged entities. Hence, there is no possibility to form strong interaction between chitosan and gentamicin. This fact helps in release of non-reacted gentamicin from chitosan matrix.

During impregnation process, drug loaded polymers were filled effectively in the interconnected micro pores, by creating the vacuum and applying the pressure after dropping the polymer solution in impregnation chamber. It has been clearly explained with the help of schematic diagram in experimental section (chapter 3). All the interconnected pores on the surface of PE were evacuated before filling. This step helps the poured polymer to be sucked inside the

pores. Application of external pressure, in the next step, further helps in forcing the polymer to fill the pores more effectively. Fig 4.1c shows chitosan impregnated PE surface (CI-PE), where drug loaded chitosan has completely filled the pores. A comparison of this impregnation process is made with normal dip coating of the porous PE surface in chitosan solution (fig 4.1e). The entrapped air bubbles, in the latter process, did not allow the polymer solution to fill the pores. As a result, upon drying, the thin coating got ruptured on the surface of the pore, revealing the void inside (fig 4.1e). It is evident from the comparative observations made in fig 4.1c and e that vacuum impregnation is a very efficient method for loading the drug in micro-porous surface. In addition, it allows the original surface composition to be exposed, thus helping in retaining the tribological and mechanical behavior of the original surface. Fig 4.1f presents the modified surface after the release of drug (AD-PE). It reveals almost smooth surface with rare traces of pores, from which drug is released. Thus, it is assumed that the surface of modified PE gets modified again during drug release, with the pores getting collapsed and surface retaining its original morphology. This observation is interesting as it might help in retaining the original properties of the acetabular cup lining after release of drug. This fact has been investigated further by evaluating mechanical and tribological behavior of all the surfaces.

4.1.2 Hardness and Elastic Modulus of the Modified Surface

The hardness and elastic modulus of different surfaces are analyzed through instrumented indentation. Fig 4.3 shows the representative load-displacement plots obtained from micro indentation test. Chitosan impregnated PE (CI-PE) is observed to have lower gradient of the loading curves as compare to PE. It is also noticed that with application of 2 N load, the depth of penetration has reached up to 50 μm in CI-PE, which is 19% higher than PE. The above mentioned responses suggest that resistance of the CI-PE samples to indentation is decreased as compared to

unmodified PE surface. However, the surface after releasing the drug for 624 h (AD-PE), shows similar response as PE with the representative load-displacement plots of the two almost overlapping.

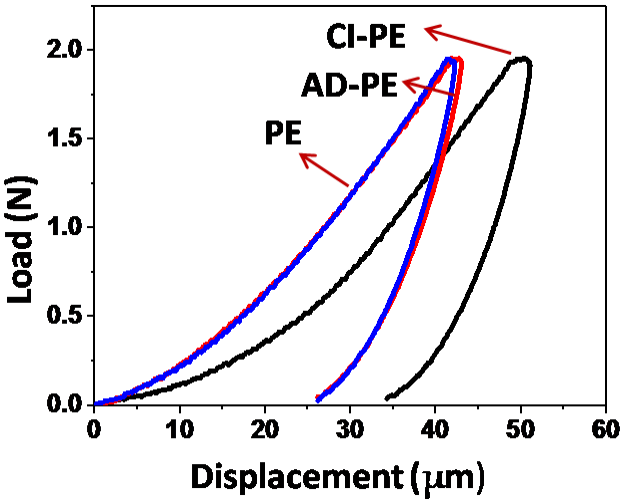

Fig. 4.3 *Representative load vs. displacement plots obtained from instrumented micro indentation on different surfaces*

Fig 4.4 presents the hardness and elastic modulus for all the three surfaces, calculated from the load-displacement plots [229]. The error bars in the plots denote standard deviation in the E and H values, obtained from at least 25 measurements in spatially different regions in each surface.

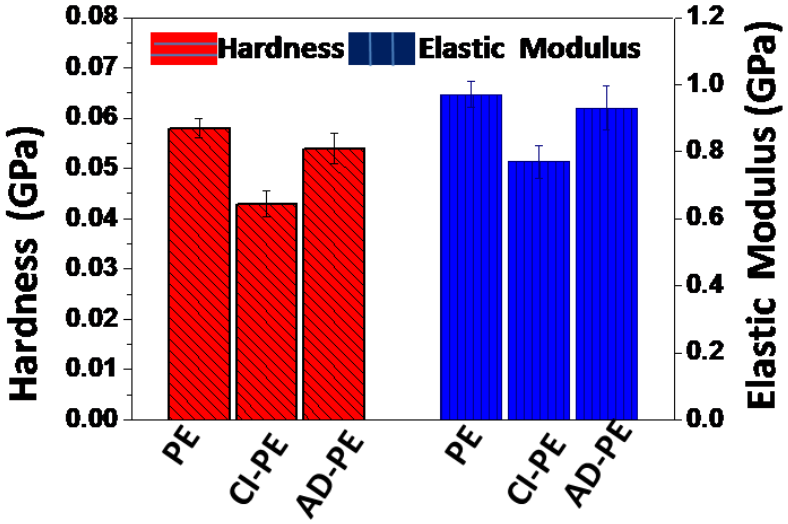

Fig. 4.4 *Hardness and elastic modulus of different surfaces obtained from instrumented micro indentation*

The decrease in hardness and elastic modulus noted for CI-PE surface is ~27% and 20%, respectively, as compared to PE. The decrease in hardness and elastic modulus of CI-PE surface is partially due to chitosan filled in the pores of modified PE surface. However, the elastic modulus and hardness of pure chitosan is 1.08 ± 0.04 GPa and 0.12 ± 0.05 GPa, respectively, which is comparable to that of PE, as reported in literature [230]. Thus, the decrease in E and H of CI-PE surface is not expected purely due to the chitosan impregnation but also attributed to the presence of partially unfilled pores on PE surface. It is interesting to note that AD-PE shows less decrease in H and E, by 7 and 6%, respectively, as compared to PE. Considering the standard deviations in the results, the mechanical behavior of PE and AD-PE is almost similar. This finding is specifically very interesting as it reveals the fact that after release of the drug, the acetabular cup liner would regain its original mechanical behavior and would bear no adverse effect in its natural function due to drug release. Similar characteristics in PE and AD-PE can be explained based on hypothesis presented as schematic in fig 4.5. While exposed to simulated body fluid (SBF) during drug release, biodegradable chitosan starts swelling substantially due to its hydrophilic and gel forming nature. During this swelling process, the pore walls experience high amount of compressive stress and starts deforming into thinner plates to accommodate the expanded volume. After drug release and chitosan degradation, these thin walls cannot retain their integrity and collapses. The procedure of collapsing takes place over a time period, simultaneously with degradation of chitosan. This happening makes the final surface smoother, reduces the volume and existence of pores. As a result, the surface appears relatively similar to the unmodified PE surface with little higher roughness.

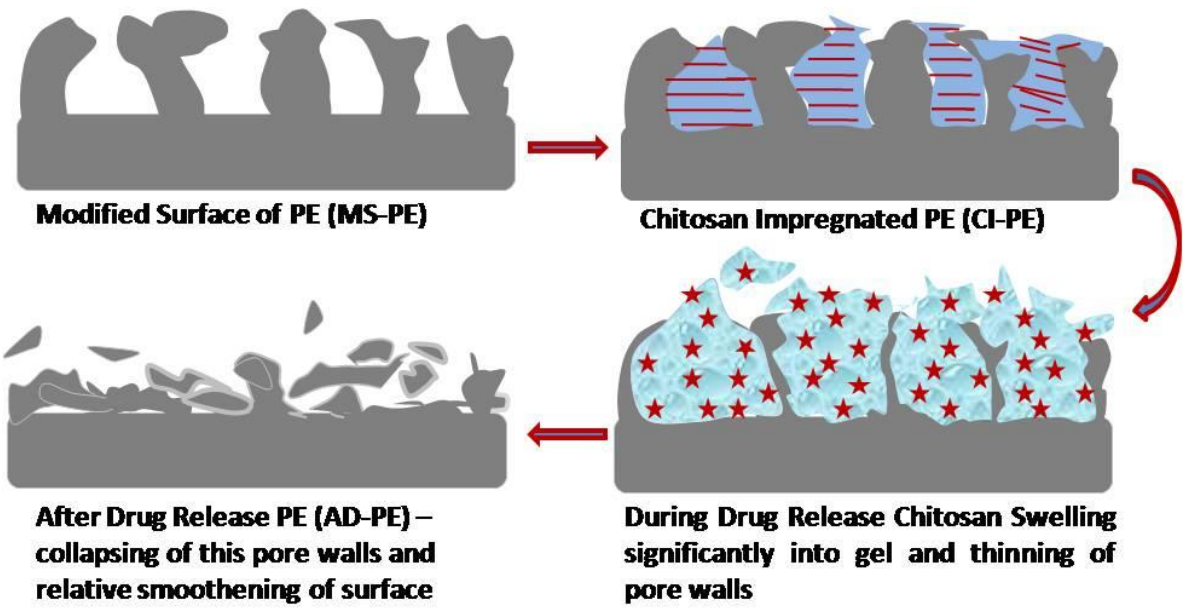

Fig. 4.5 *graphical representation of pores collapsing during drug releasing*

4.1.3 Friction and Wear Studies on Modified Surface

Hip joint is one of the main load bearing parts in the human body and it faces severe frictional forces during the movement. The surfaces that are under continuous frictional movement during the action of limbs are the femoral head and inner lining of the acetabular cup. PE is usually used as inner lining material of acetabular cup of the total hip implant to reduce the wear of the liner and coefficient of friction. Thus, it is important to evaluate the wear behavior of the modified PE surface, which is being proposed for acetabular cup lining. Measuring and comparing the coefficient of friction (CoF) and specific wear rate, followed by detailed microstructural analysis of worn surface and wear debris, provide insight into the wear mechanism dominating the tribological behavior of any material. Fig 4.6 shows the variation of CoF with sliding distance for different surfaces, as recorded continuously during the test.

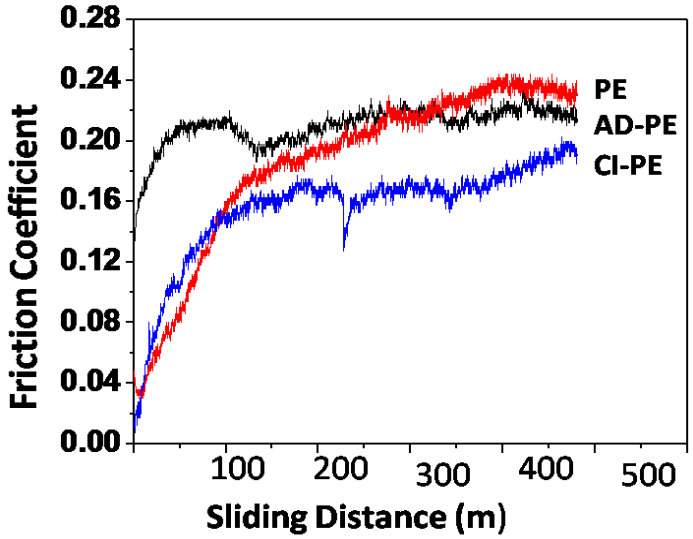

Fig. 4.6 *Coefficient of friction for different surfaces plotted against sliding distance*

Coefficient of friction (CoF) increased in initial ~100 m and thereafter achieved steady state for surfaces in all conditions. The average CoF values in steady state are 0.23, 0.17 and 0.21 for PE, CI-PE and AD-PE, respectively. Drug loaded chitosan coating on the PE surface (CI-PE) reduced steady state CoF by 26%, as compared to unmodified PE surface. It indicates that the chitosan helps as lubricating agent by avoiding the stick-slip mechanism [231][232]. On the other hand, the interconnected pores are filled effectively and attached nicely with the chitosan during impregnation process, which reduces the surface delamination. The combined effect of less wear debris and lubrication reduces CoF of CI-PE, as compared to PE. This speculation is visually confirmed through the wear rate analysis and microstructural observation of wear track and debris, which is explained later. After drug release, the AD-PE surface has also shown 8% decrease in CoF as compared to unmodified PE surface. This might be due to some chitosan left over inside the pores after drug release and also due to less contact surface of the counter body. AD-PE recorded the surface roughness (R_a) of 1.366 ± 0.300 µm, which is higher as compared to PE (0.361±0.070 µm) and CI-PE (0.260±0.050 µm), as observe in fig 4.7. The SEM images of wear

track are found to be smoother in CI-PE as compare to AD-PE and PE, which augments to the above mentioned reasoning.

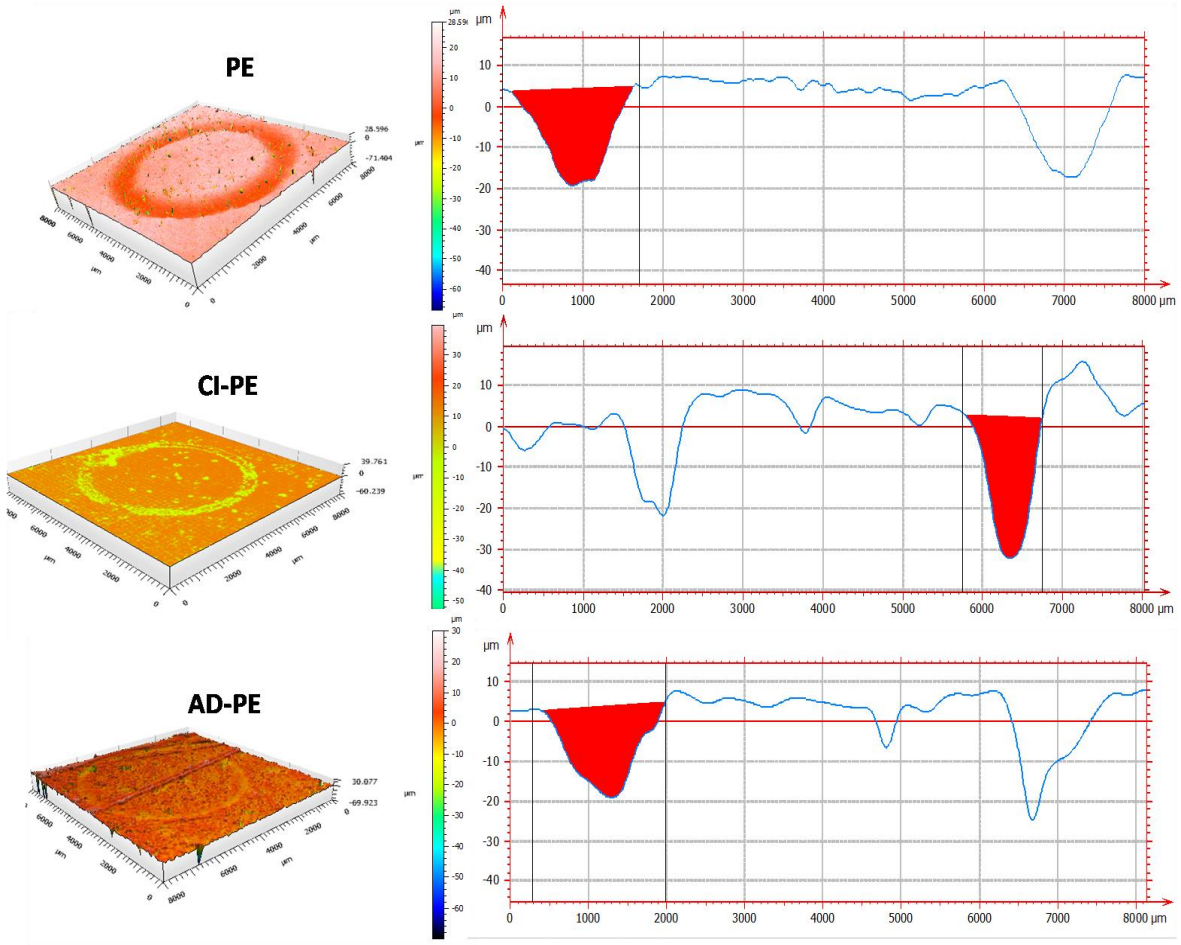

Fig. 4.7 *Three dimensional optical profiles of the wear tracks and corresponding two dimensional profiles across the track on different surfaces*

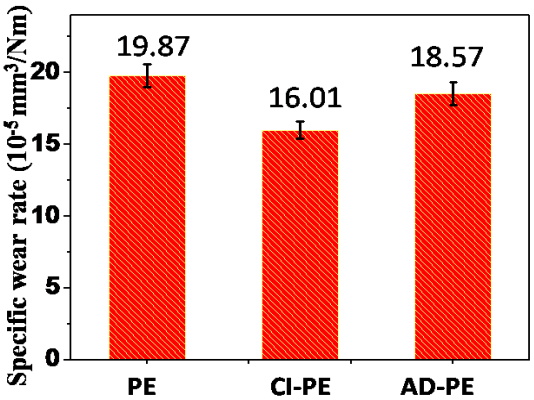

Fig. 4.8 *Specific wear rate calculated from ball-on-disc wear tests on different surfaces*

Fig 4.7 reveals 3D profile of the wear track and 2D line profile across the wear scar for PE, CI-PE and AD-PE samples. The average wear volume of PE, CI-PE and AD-PE is 0.448, and 0.362 and 0.418 mm^3 respectively. Fig 4.8 shows the specific wear rate values in bar chart for each type of surface. The small error bars in these chart denotes uniform tribological behavior for all the surfaces. CI-PE shows the lowest wear rate, which is in agreement with its low CoF value. Better lubrication on surface helps in reducing the linear force applied and thus results in less mass removal. As it can be observed, specific wear rate of CI-PE decrease 19% as compared to unmodified PE surface. AD-PE sample has shown 5% reduction in wear rate as compared to PE. However, considering the standard deviation, it can be assumed unmodified and drug released surfaces show similar wear rates. These observations have been correlated with micrographs of wear tracks and debris.

Fig 4.9 and 4.10 present FE-SEM images of worn surfaces and wear debris, respectively. The worn surface of PE reveals grooves in normal direction to sliding (fig 4.9a and a'). Grooves are formed due to the micro-cutting or micro-plowing of the PE surface by the abrasion of the hard steel ball [233]. In addition, the worn surface also consists of thin and weekly adherent layered material. It is a well-established understanding in sliding of polymers that such material transfers and adheres as films onto the hard counter body [1][2]. Platelets of transfer film, along with small particles, found as wear debris, (fig 4.10a) confirm the contribution of adhesion and abrasion as mechanisms of material removal for the PE surface, while sliding against steel ball.

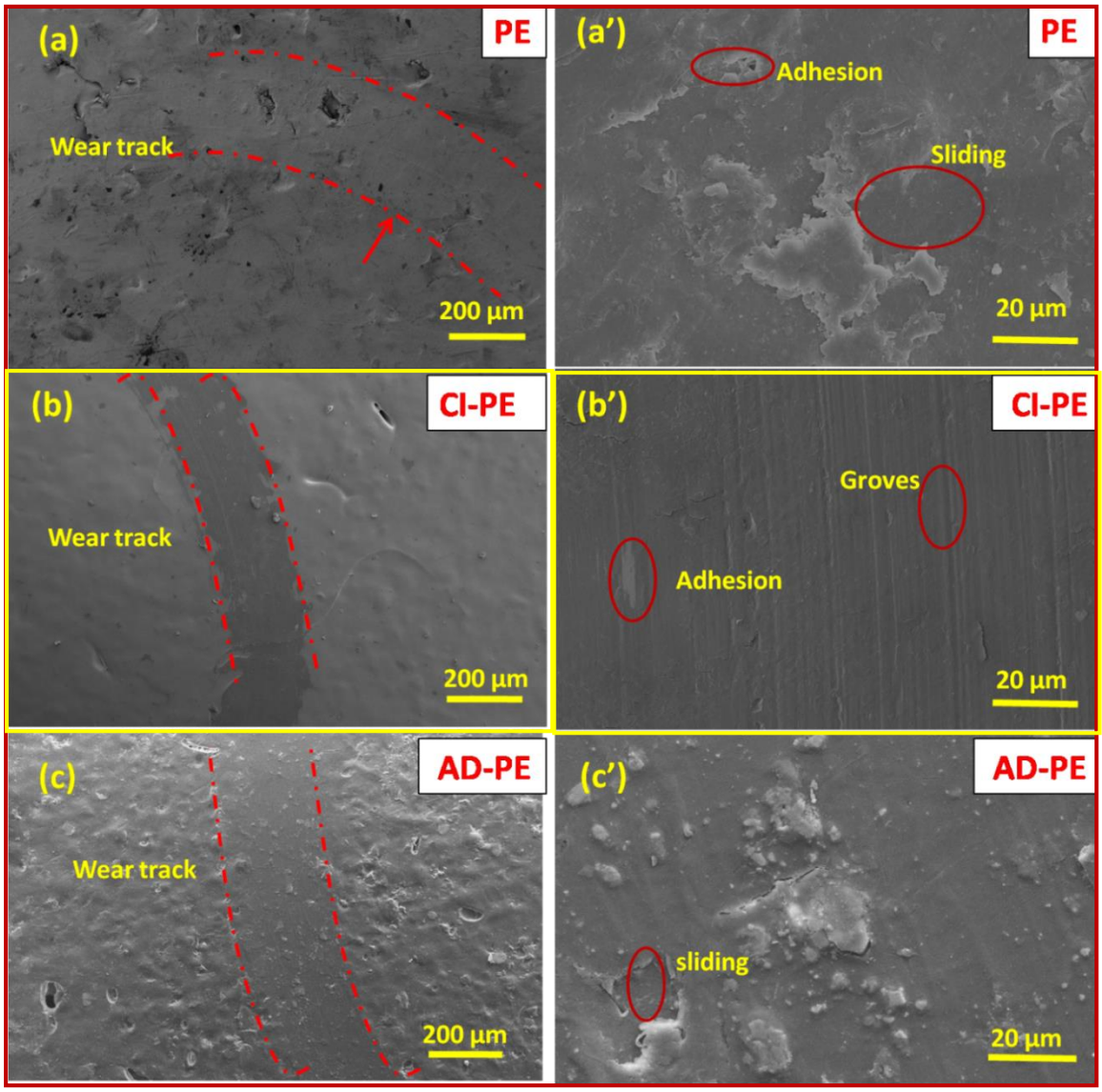

Fig. 4.9 *FE-SEM micrographs of wear track for different surfaces revealing wear mechanism*

On the contrary, the worn surface of chitosan impregnated PE (CI-PE) shows mild adhesion and abrasion. However, wear debris analysis, obtained during sliding of CI-PE, reveals only platelets transfer films on the ball surface are worn during sliding, while CI-PE surface is protected. For the given conditions of sliding and surface of hard counter body, the extent of transfer films is known to depend on mechanical properties of the polymer surface [234]. Relatively soft surface of CI-PE, in the present study, is easily removed in initial stages of sliding

and large amount of material is transferred onto the steel ball surface. The large extent of transferred material on the steel ball surface avoids contact of steel with CI-PE surface during further sliding. Thus, reduced friction and wear are recorded (fig 4.6 and 4.8) for CI-PE surface as compared to unmodified PE surface. Fig 4.9 (c and c') show worn surfaces of AD-PE sample. The presence of both abrasion and adhesion can be observed. After releasing drug, the surface becomes porous and results in increased wear as compared to CI-PE. The morphological features of debris collected during sliding of AD-PE (fig 4.10c), are also having combination features of those obtained for PE and CI-PE.

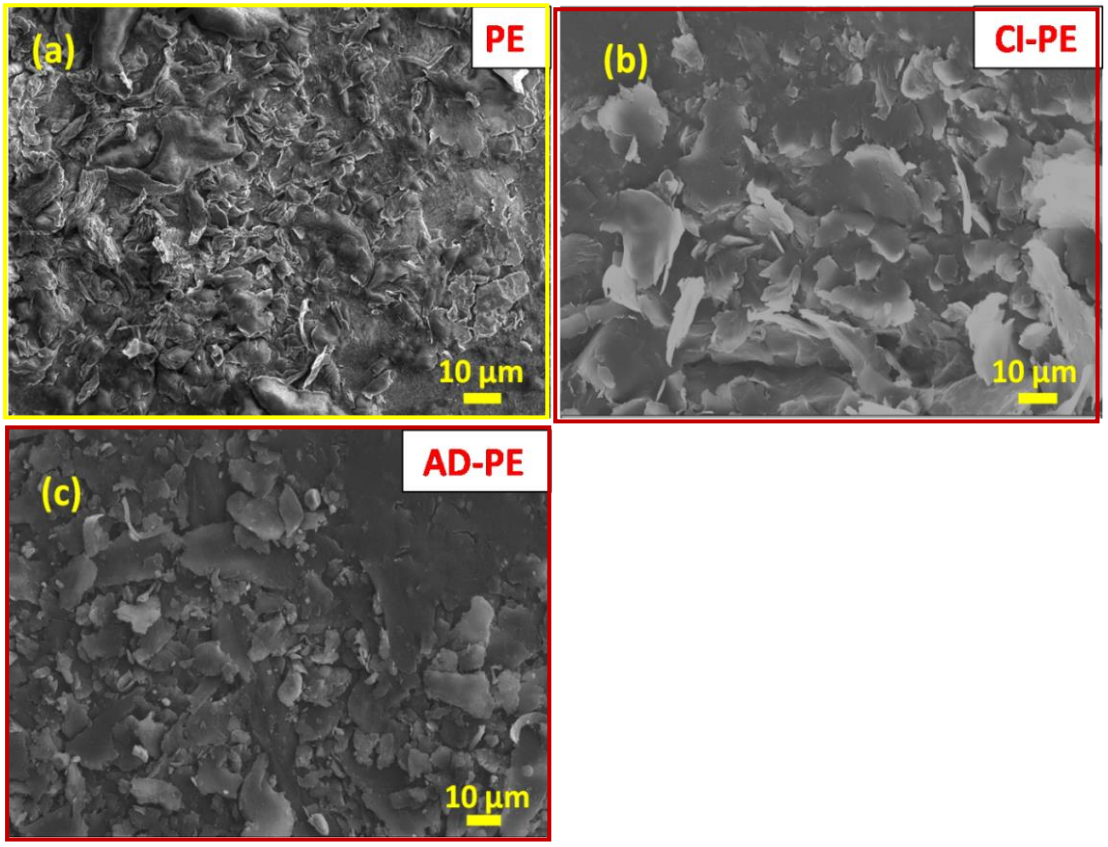

Fig. 4.10 *FE-SEM micrographs of wear debris generated during wear tests on different surfaces*

4.1.4 Percentage of Drug Loading and in Vitro Releasing Kinetics

Different surfaces, at least in triplicates, were impregnated with 1 ml of chitosan solution containing 20 mg of gentamicin. An average percentage of drug adsorption on the surface is calculated by using weight difference method. An example of such calculation is as following: Initial weight of the modified PE (without drug loaded chitosan) is 1.4830 gm and weight of PE after impregnation of drug loaded chitosan is 1.5185 gm. Total weight of drug loaded chitosan filled in the pores is 0.0355 gm. Total drug adsorption (14.2 mg) is calculated by multiplying the ratio of chitosan to drug (3:2) and weight of drug loaded chitosan (35.5 mg). The drug loading capacity is found to be ~70%, with respect to the amount of drug used for each pellet. Drug loading capacity decreased due to small sample size as compared to impregnation chamber. Therefore, excess drug containing chitosan solution was over flown and remained unutilized. However, sample size and more efficient design of impregnation chamber can significantly improve the drug loading efficiency.

The main interest behind fabrication of this surface modified PE sample is to release the drug in a controlled manner for longer period to treat the initial bacterial infection around the surgical area. *In vitro* drug release is recorded in terms of cumulative percentage of gentamicin released with respect to time (fig 4.11). All the test samples showed sustained release of gentamicin until 624 h (26 days).

The release rate is found to be a function of time and biodegradability of chitosan. Several drug delivery systems (DDS) are presented in the literature [13][15]. The ideal DDS should have a high initial drug release rate to eradicate the initial bacterial infection, followed by sustained release for several weeks to fight against the delayed infection.

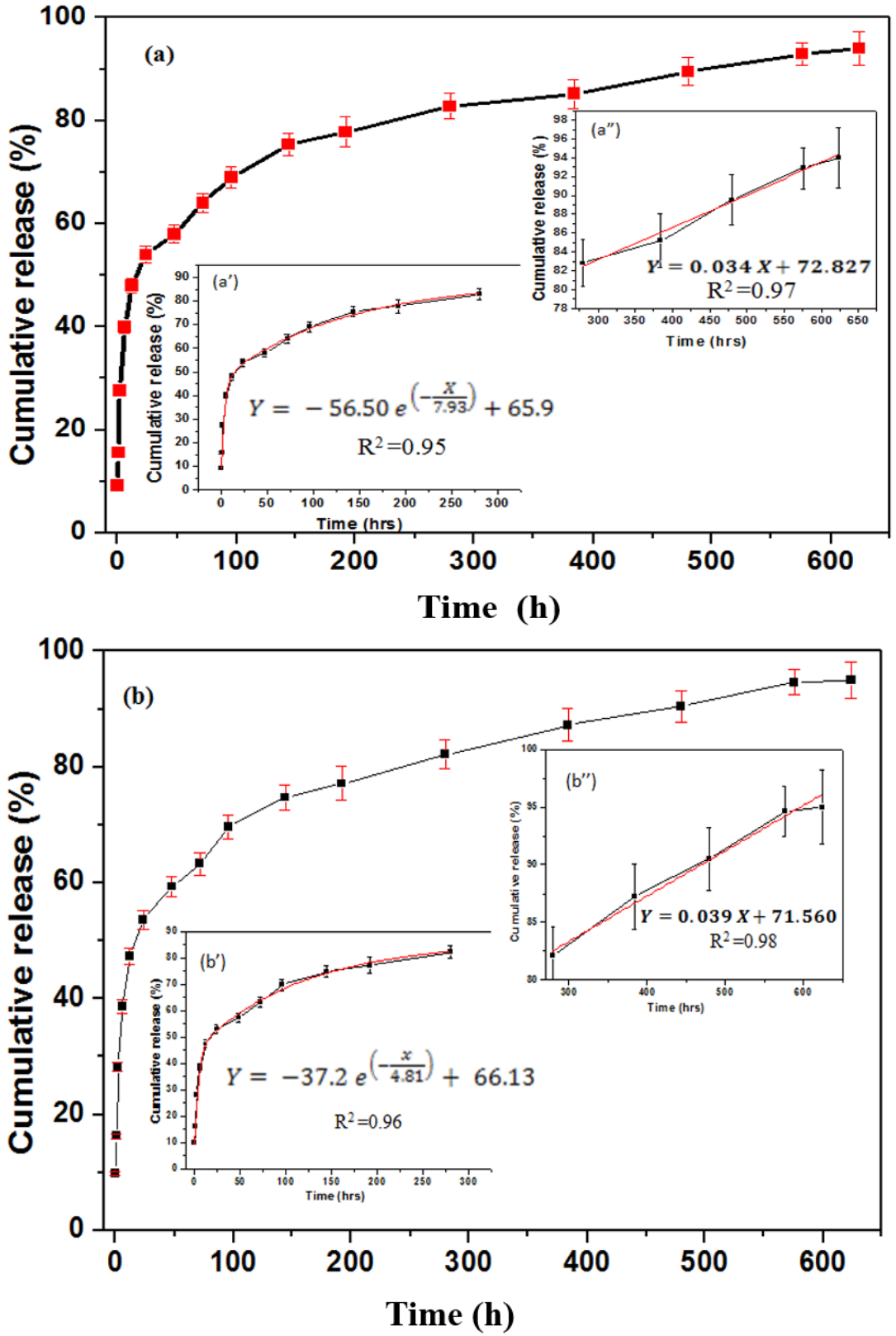

Fig. 4.11 *In vitro drug release kinetic profile of modified surface up to 624 h; (b) drug release profile for checking the drug stability in the sample after 7 days*

In the present study, a very fast release of the drug is noted during the first 24 h. Approximately 54% of the drug got released by diffusion mechanism, followed by sustained release up to 624 h (fig 4.11a). The complete release profile can be divided into two distinct behavioral categories. In the first phase up to 280 h, the release amount decreases gradually with time showing a behavior best defined as exponential decay. An inset (a`) in fig 4.11a clearly shows the best fit with high R^2 value of 0.95 (coefficient of determination). During this period ~83% of the gentamicin is released in fast and sustained manner. This behavior is typical to that of drug release being dominated by diffusion. Second phase of the release profile (280 to 624 h) follows the linear fit equation (R^2 = 0.97) (fig 4.11a``). The percentage of drug released per hour is calculated from slope of the equation. Around 1.513 mg (13.2 %) of drug is released in continuous manner during this time with a rate of 0.0043 mg/hr. This release is dominated by gradual degradation of the drug containing polymer, which happens at a constant rate over time.

Chitosan is biodegradable, non-toxic and biocompatible polymer. It serves as an ideal carrier for the controlled release of gentamicin. Various factors may affect the release kinetics of gentamicin from chitosan. The initial fast releasing of gentamicin can be attributed to high solubility and low molecular weight of the drug. The sustained gentamicin releases up to 624 h is due to degradation of chitosan. The cumulative percentage release of gentamicin from the test samples was about 94.1% over 624 h. This proves chitosan to be a very effective drug carrier for modified PE surfaces, as it releases almost the entire amount of loaded drug.

In addition to the above mentioned study, one more set of drug loaded samples (CI-PE) were kept for 7 days at 2 ºC in dried condition after fabrication, followed by drug release study in PBS. This was done in order to assess if the drug is leaked from the surface, when the implant is stored for some time before use. Fig 4.11b shows the cumulative drug release of this second set of

sample with respect to time. The release profile is almost identical to the first set of samples (fig 4.11a) and percentage of drug released is about 95%. This confirms there is no leakage of drugs from this material system during storage in dry state. It is emphasized here that; this research is more about proving the concept of using the inner liner of the acetabular cup as drug eluting part. Being an open surface, the drugs released from this liner gets direct access to the synovial and body fluid and thus can attack any infection around the total hip implant site after surgery. The modified liner, proposed here, can be further tailored for catering to specific requirement, i.e., sustained release for longer time; fast release over short period or a suitable combination of both. This can be achieved by optimizing the surface porosity and/or by using different biodegradable polymer with varying degradation rate. However, while modifying the liner, the mechanical and tribological behavior of the same should not be sacrificed.

4.1.5 Antimicrobial Activity

The antibiotic resistance study for *S. aureus* was designed to assess the *in vitro* antibacterial activity of gentamicin impregnated PE (CI-PE) surface. S. aureus (gram positive) is the pathogen that is responsible for about two thirds of chronic osteomyelitis infections [227]. The modified and drug loaded PE surface (CI-PE) was exposed to culture of *S. aureus* to evaluate the effectiveness of released drug in fighting infection, up to 10 days. Unmodified PE surface was used as control sample for this observation. The evaluation was performed using agar disc diffusion method. Released gentamicin from CI-PE was found killing *S. aureus* bacterial strains (fig 4.12). Distinctly clear and bacteria free area (zone of inhibition) is observed in the agar plate in the vicinity the drug loaded PE pellet, as marked in fig 4.12. On the contrary, no such bacteria free region was observed around the unmodified PE pellet. Same trend is observed throughout, up to 10 days of culture. This observation evidenced the potential of the drug loaded PE surface in combating bacterial infection.

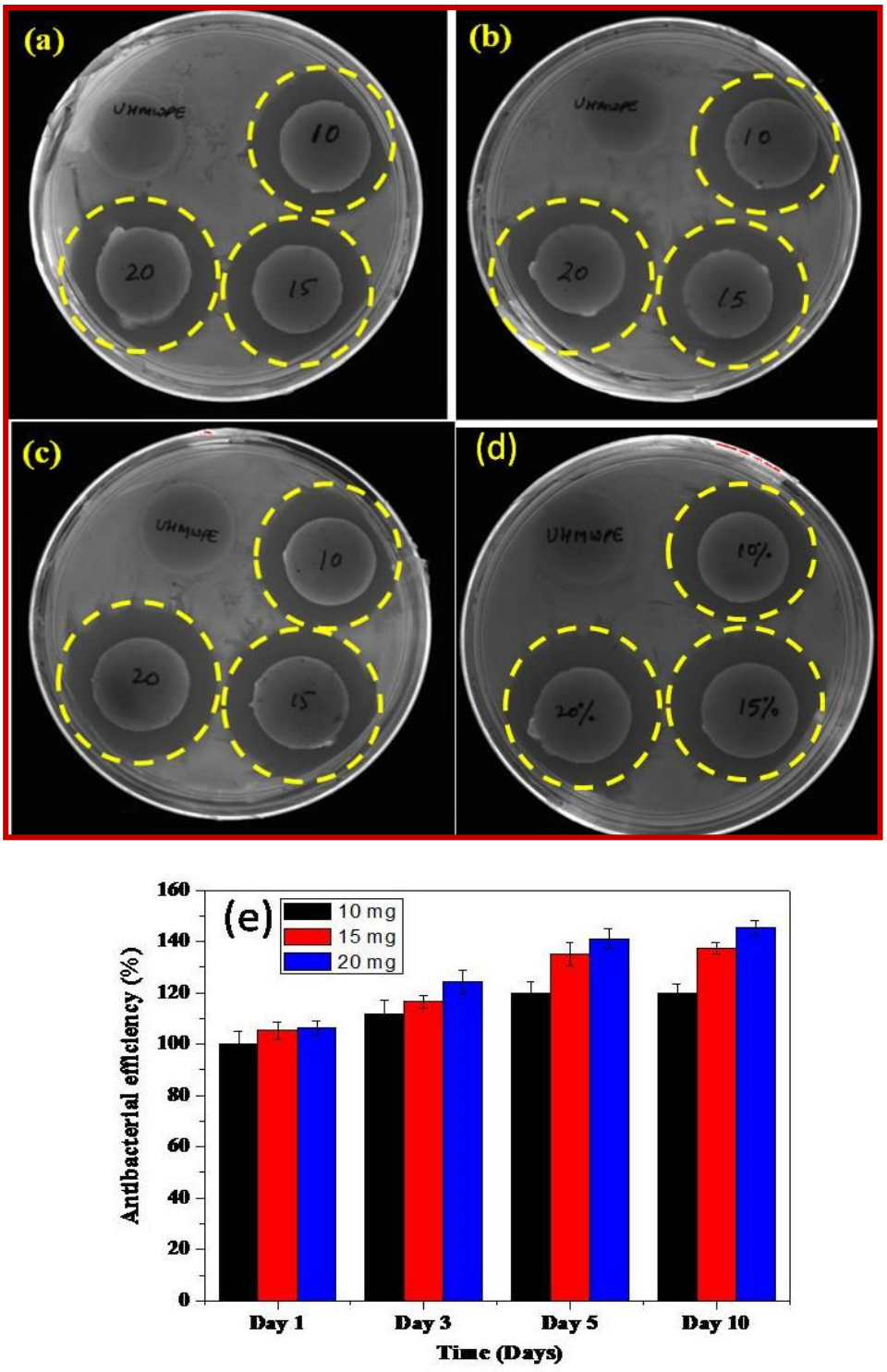

Fig. 4.12 *Bacterial activity for PE and CI-PE (10, 15, 20 mg of gentamicin) samples for 1, 3, 5 and 10 days (a-d) evaluated through agar disc diffusion tests. Inhibition zones are marked with yellow dotted circles in all the CI-PE images (for better visualization); (e) antibacterial efficiency rate as a function of different gentamicin concentration in for 1, 3, 5 and 10 days of culture.*

SEM analysis of the pellets is also performed after incubation to observe the PE surfaces with bacteria grown on it. The PE surface reveals a high population of bacteria grown on it with the passage of time (fig 4.13a). In contrast, no bacterial cells and trace of biofilm were found on the CI-PE surface (fig 4.13b). Furthermore, the amount of *S. aureus remained* at null level and did not increase with time, suggesting the antimicrobial effectiveness of gentamicin impregnated PE implant in long run. Modified surface effectively eradicated infection induced by gram-positive bacteria, even when exposed to high concentrations of microbes. The comparative antibacterial analysis is represented in the graph (fig 4.12e). The results show the increase in antibacterial efficiency with increasing drug amount from 10 to 20 mg/ml as well as with time i.e. from day 1 to day 10. This study also suggests that the drug does not get inactivated during the impregnation procedure. The established drug release profile for extended period of time, with an initial fast release, will enable the sterilization of the operated area at an early stage and effectively prevent any bacterial infection and biofilm formation around the implant.

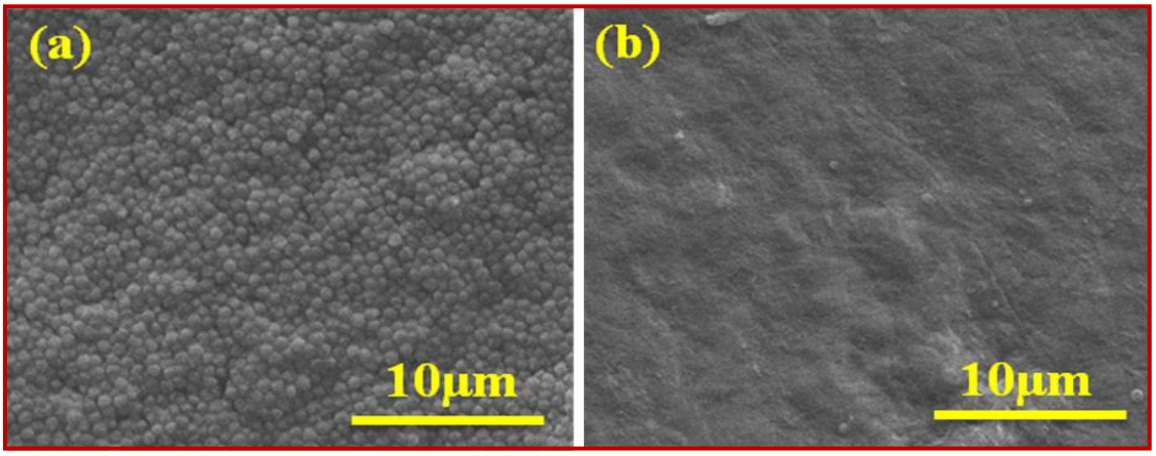

Fig. 4.13 *FE-SEM micrographs revealing the antibacterial activity on (a) unmodified PE surface and (b) drug loaded (10 mg/ml) surface, for 3 days of culture.*

On the other hand, to evaluate the antibacterial effectiveness of the modified surface against the gram negative bacteria, the modified and drug loaded PE surface (CI-PE) was exposed to culture of E. coli. Unmodified PE surface was used here also as control sample for antibacterial

observation. The evaluation was performed using agar disc diffusion method. Released gentamicin from CI-PE was found killing E. coli bacterial strains (fig 4.14). Distinctly clear and bacteria free area (Zone of inhibition) is observed in the agar plate in the vicinity the drug loaded PE pellet, as marked in fig 4.14. On the contrary, no such bacteria free region was observed in the whole agar plate, in case of the unmodified PE pellet. Same trend is observed throughout, up to 120 h of culture. This observation evinces the potential of the drug loaded PE surface in fighting against bacterial infection.

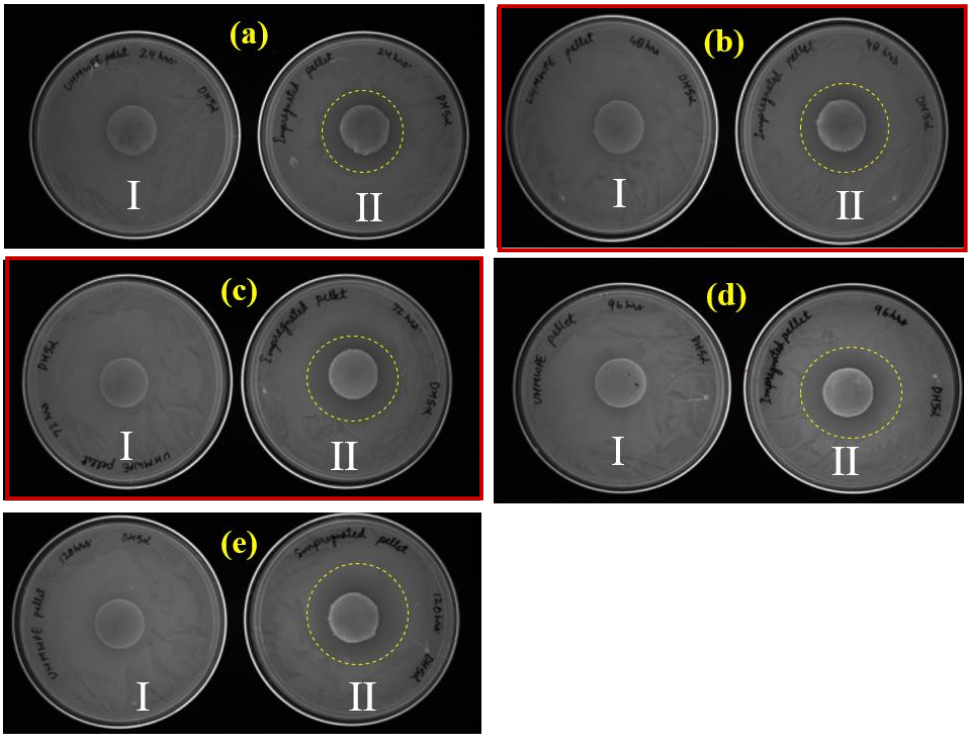

Fig. 4.14 *Bacterial activities for (I) PE and (II) CI-PE (20 mg of gentamicin) samples for 24, 48, 72, 96 and 120 hrs (a-e) evaluated through Agar disc diffusion tests. Inhibition zones are marked with yellow dotted circles in all the CI-PE images (for better visualization) and the plates containing PE samples are covered with bacterial lawn all over.*

SEM analysis of the pellets is also performed after incubation to observe the PE surfaces with bacteria grown on it. The PE surface reveals a high population of bacteria grown on it with the passage of time (fig 4.15 a & c). In contrast, no bacterial cells and trace of biofilm were found on the CI-PE surface (fig 4.15b & d). Furthermore, the amount of *E. coli* remained at null level and

did not increase with time suggesting the antimicrobial effectiveness of gentamicin impregnated PE implant in long run. Modified surface effectively eradicated infection induced by Gram-negative bacteria, even when exposed to high concentrations of microbes. This study also proves that the drug does not get ineffective during the impregnation procedure and killing effectively all kinds of bacterial stain.

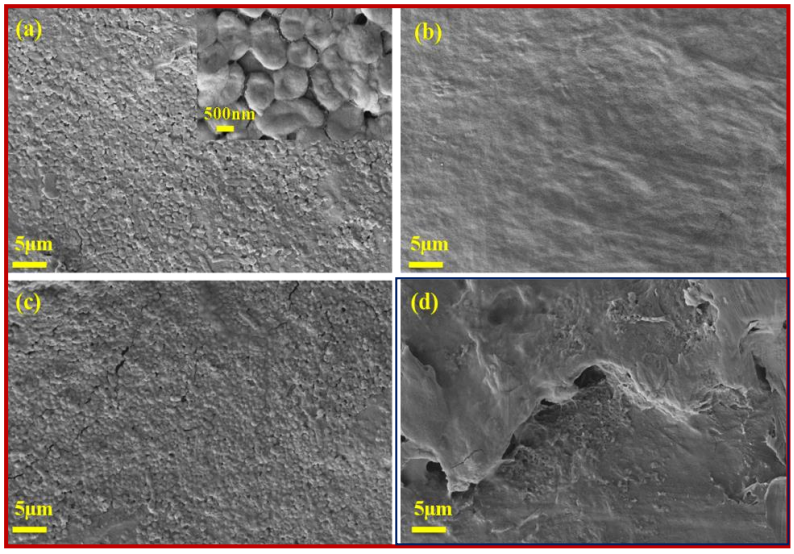

Fig. 4.15 *FE-SEM micrographs revealing the antibacterial activity on (a & c) unmodified PE surface and (b & d) drug loaded one for 24 and 96 hrs respectively. Inset in (a) shows the E. coli DH5α bacteria at higher magnification.*

4.1.6 Evaluation of Cytocompatibility

The surface modified PE liner of the acetabular cup in the present work is intended for orthopedic application. Therefore, it is very important to make sure that they are cytocompatible. We chose MG-63 cells for this study because they can be directed towards osteogenic differentiation. Cell survival and proliferation in the presence of the implants were evaluated through MTT assay and DAPI staining, respectively. MTT is a colorimetric assay to assess the metabolic state of cells. NAD(P)H dependent mitochondrial membrane associated oxido-reductase enzymes can reduce 3-(4,5-dimethylthiazol-2-yl)-2,5 diphenyltetrazolium bromide (MTT) to water insoluble purple formazan crystals, which are then dissolved in DMSO. Amount of formazan

crystals formed is indirectly measured and its OD at 570 nm gives a quantitative idea of the metabolic state of the cells under treatment (here, grown on implants) relative to untreated/ control cells (here, grown on regular tissue culture surface). This can be represented as percentage cell survival. DAPI is a fluorescent dye that stains DNA strongly, by binding to the A-T rich regions. This gives blue appearance to the nucleus. Cells take up DAPI stain proportionate to the proliferation rate. Moreover, any chromosomal damage that could eventually translate to reduced cell proliferation due to experimental conditions can also be followed through this staining. Healthy living cells have a typical DAPI stained profile of their nuclei. Any deviation from this would reflect as alteration in the nuclear integrity of the cells. This will be a strong indication of lack of cytocompatibility of the biomaterial under study. Cells grown on tissue culture treated plate were taken as positive control for both the assays.

Unmodified PE and surface modified with drug contained chitosan impregnated (CI-PE) samples used in the current study to analyze and compare the cytocompatibility results. After incubating on these implants for 1, 3 and 5 days, cells show an overall survival comparable to the positive control (fig. 4.16). Cells grown well on both the sample, PE and C-PE, initially PE sample showed around 92-95% survivability after first two days of incubation. But survival rates of PE became almost comparable to positive control (fig 4.16), and cells became significantly proliferative (fig 4.17G & H) after 5 days. Besides, our observations show overall better survival and proliferation on surface modified chitosan impregnated (CI-PE) sample (fig 4.16, fig 4.17 panels C, F, I with rest). The cells appear to be more proliferative when grown on chitosan impregnated CI-PE sample. It indicates drug loaded chitosan surface is more biocompatible than PE and their survivability is also higher (~108%) even compared to the control. Our observations on cell survival on the implants fall in line with those from DAPI staining of the cells' nuclei.

Magnified single nuclei from a representative cell from each implant and control show a healthy nuclear integrity (fig 4.18A-C). A healthy DAPI stained nucleus shows an unstained spot amidst intense blue background. The unstained spot is the nucleolus populated by more rRNA (a type of RNA) and less DNA (fig 4.18, shown with white arrows). A dying or unhealthy nucleolus will have fragmented nucleolus. Thus, the surface modified implant (CI-PE) is highly cytocompatible, supports cell proliferation and do not affect the nuclear integrities of the cells. Concluding that even after surface modification, it retains the biocompatibility nature.

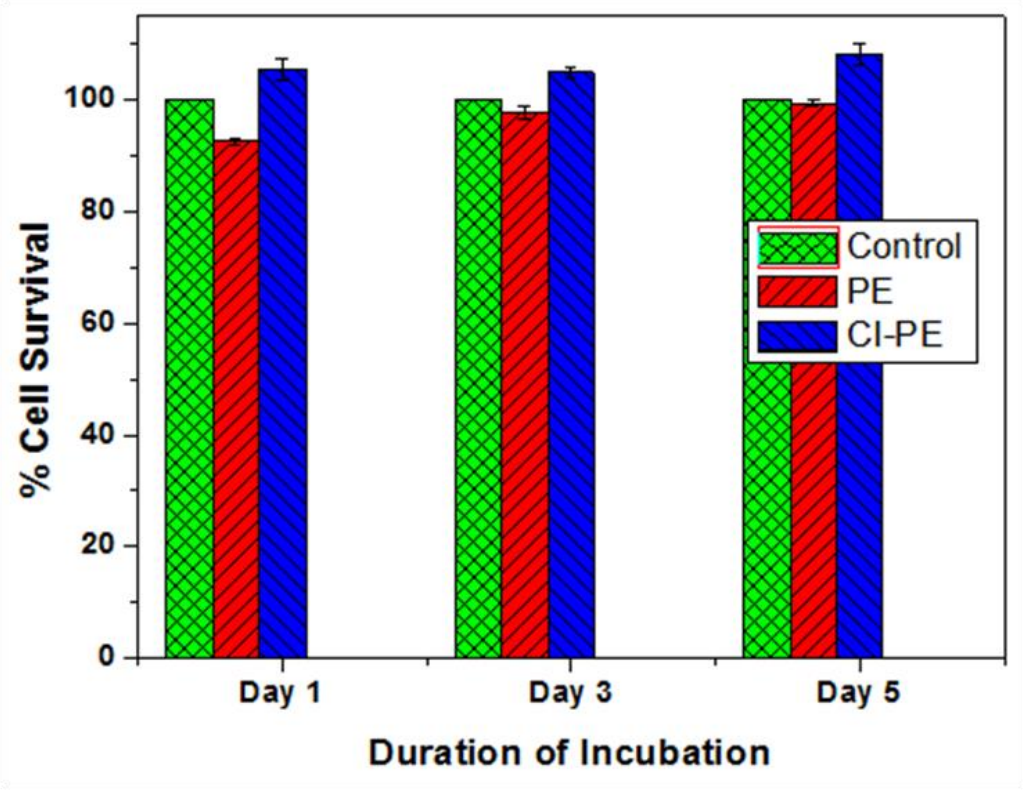

Fig. 4.16 *Cytotoxicity assay for evaluating the effect of implant surface modification on cell survival. Quantitative representations of MTT assay as % cell survival of MG-63 cells grown on different surface for 1, 3 and 5 days relative to control cells grown on regular tissue culture plastic ware. Data represents mean ± SD of 3 sets of independent experiments.*

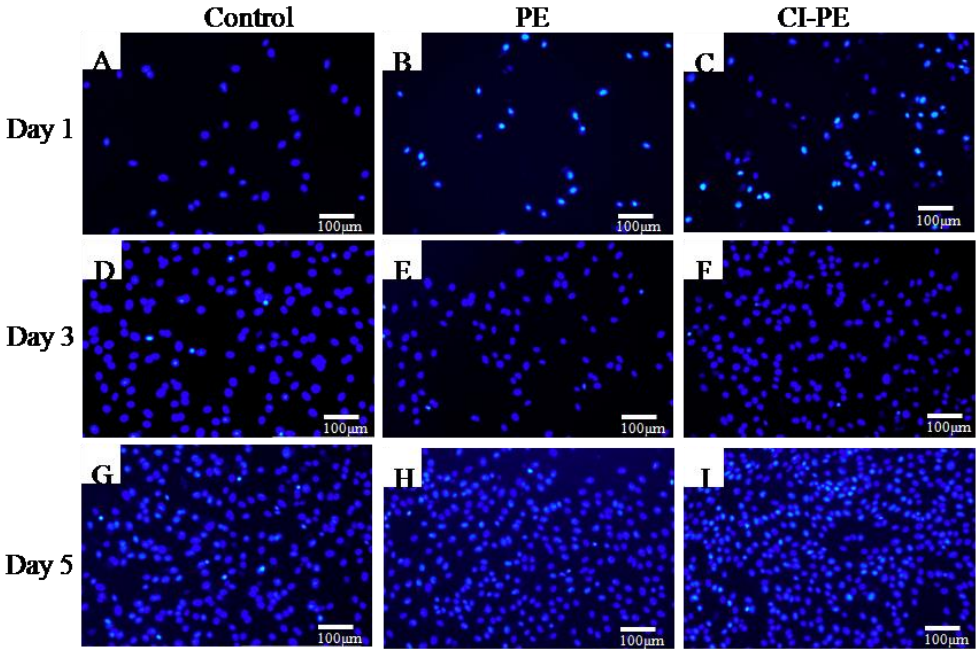

Fig. 4.17 *Nuclear staining shows the proliferation of cells over 5 days. Panels A-C, D-F and G-I shows DAPI stained nuclei of living cells after 1, 3 and 5 day of incubation, without implants: control (A, D & G) and on implants: PE (B,E & H), CI-PE (C, F& I).Scale bar =100µm.*

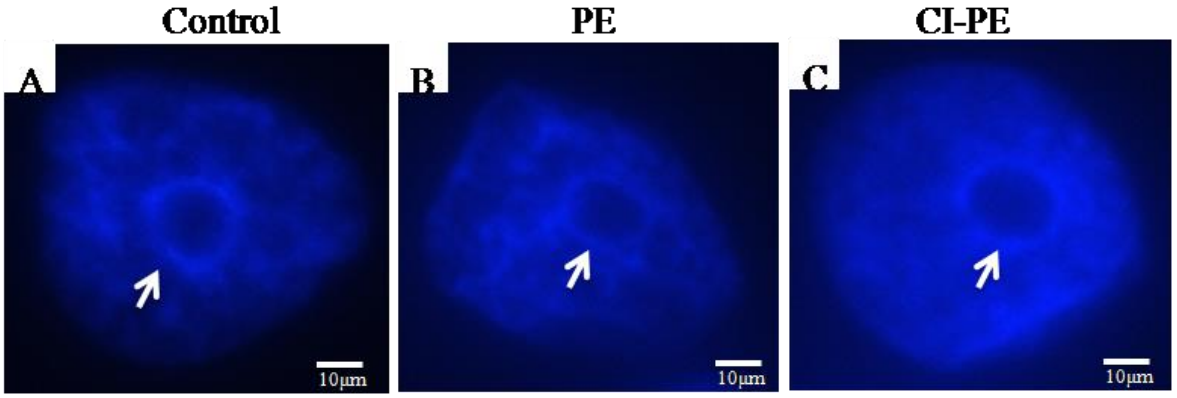

Fig. 4.18 *Nuclear staining shows the nucleolar integrity. Panels A-C, show representative single DAPI- stained nuclei from each group of cells. White arrow head in each panel points towards the intact nucleolar region pertaining to healthy cells in each case. Scale bar =10 µm*

A thorough analysis of different PE surfaces reveals that modifying the PE surface with drug loaded chitosan increases wear resistance, but registers slight decrease in hardness and elastic modulus. After the release of drug, the PE surface regains similar mechanical and tribological behavior as the unmodified PE surface. Tribological properties are most important for the inner

lining material of the acetabular cup, as it mainly faces the rubbing actions with femoral head. It is interesting to observe that drug loaded PE surface actually improves the tribological behavior, due to better lubrication offered by modification. Moreover, after drug release (up to 26 days), the liner surface recovers its property with reference to normal PE surface. Thus, the modified inner lining material of acetabular cup, with additional functionality in terms of drug releasing capability for longer time, should be a very potential means to treat the initial infection around the surgical area in cases of total hip replacement.

A concern might arise related to the differential *in-vivo* and *in-vitro* behavior of this lining material. However, the pores were filled effectively with drug loaded chitosan during impregnation. The surface roughness (Ra) of CI-PE is 0.260 μm as compared to 0.36 μm without surface modification and the pores got collapsed after the drug is released (fig 4.1f). Thus, the pores never remain with their bare morphology to influence the degradation or the behavior of body fluid, immune cells and reactive oxygen species significantly.

The other concern could be related to the biodegradation of the structure. PE, being non-biodegradable polymer, would not have any role in this process. On the other hand, chitosan is a biodegradable polymer and is reported to degrade faster in-vivo [16][17]. However, in the present case, most of the chitosan mass is not exposed to the body environment as they remain inside the pores and often inside the interconnection regions beneath PE surface. Only a small volume of chitosan in exposed at a time through the opening of the pore cavity and the part beneath is exposed only after the degradation of the top layer. Thus, the degradation rate should not vary widely due to differential degradation rate of chitosan between *in-vitro* and *in-vivo* conditions.

4.1.7 Summary

The present study introduces, for the first time, the concept of surface modification of the inner lining material of the acetabular cup to show the additional functionalities, required to meet the future demand. The modified surface released the drug in a controlled manner for up to 26 days. This improved functionality of the acetabular cup will be the key for a successful hip implant for treating the initial infection around surgical area. Inner lining material of acetabular cup of total hip implant faces severe frictional forces and load during the movement of limbs. The modified surface has shown good improvement in the tribological property by reducing the coefficient of friction (26%) and wear rate (19%), respectively. However, hardness and elastic modulus decreased 27% and 20%, respectively. After drug release, the modified surface has shown almost similar tribological and mechanical behavior as unmodified surface. Hence, based on the current data it could be concluded with conformity that the modified surface of the acetabular cup is one of the new generations of drug eluting implants, to treat the initial infection around the surgical area. The antibacterial study with *S. aureus* confirms the effectiveness of gentamicin, released from the modified surfaces, in inhibiting the bacterial infection. Besides, positive cytocompatility results give the new dimension for surface modification. In summary, while there is still significant potential for surface modification through different routes and process optimization, results of this study provide a foundation to use inner lining material of the acetabular cup as drug eluting material to treat post-operative infections *in-vivo*.

CHAPTER 5
Comparison Study – Modified Chemical Etching and Electrostatic Spraying Technique

This chapter deals with comparison of two methods for modifying the surface of polymeric acetabular cup liner PE as drug eluting part in total hip implant to treat the initial infection around the surgical area. In previous chapter, successful modification of the surface of PE for sustained drug release has been presented [1]. Briefly, a modified solvent-based etching and lyophilization technique was used to engineer a thin porous surface layer on PE. Drug containing chitosan solution was impregnated to the pores through impregnation chamber. Modified surface of PE have shown an impressive drug release profile for 26 days. It also offered reduction in friction coefficient and wear rate by 26% and 19%, respectively, in comparison to unmodified PE, which is encouraging towards the intended application. Modified surfaces did not affect the mechanical and tribological behavior significantly.

However, there might be other effective ways to modify the inner lining of the acetabular cup to load antibiotic in it. In this context, electrostatic spray coating (ES) can be a useful tool for fabricating such porous coating on PE liner surface. Electrostatic spray coating offers uniform deposition rate, because all powder particles are charged with same electrical polarity, when they are ejected from spray gun and deposited uniformly on the substrate through charge repulsion. Further, the coating process offers controlled micro pores on the substrate.

Manoj Kumar R, et al. ***"Comparative Study on the Efficacy of the UHMWPE Surface Modification by Chemical Etching and Electrostatic Spraying Method for Drug Release by Orthopedic Implants"*** *under review in Materials Science and Engineering: C*

In ES technique, very strong integrity between porous coating and substrate is expected during curing, considering the fact that the substrate and coating material are same. The coated surface is loaded with antibiotic containing biodegradable polymer. Such coated surface is characterized for mechanical and tribological behavior with drug loaded into it and after release of the same. The drug releasing behavior of such surface and their efficacy infighting against bacterial infection is also evaluated and analyzed.

Finally, this study thoroughly compares the effect of surface modification by electrostatic spraying route with the previously used solvent-based etching route, in terms of mechanical and tribological behavior, as well as drug releasing and antibacterial potential. The findings of this study leads to the identification of the most efficient surface modification technique for acetabular cup liner in total hip implant, which can fight bacterial infection in-vivo.

5.1 Results and Discussion

5.1.1 Microstructural Characterization of the Porous Surfaces

The PE powders are compacted through hydraulic press and cured at 160 ºC in hot air oven. Integrity of the cured pellet was investigated by observing the cross section in microscope. Interconnected micro porous coating is engineered on cured PE substrate through electrostatic spray coating (ES) technique. Integrity of the coating and wear characteristics are the two most essential criteria to offer the performance required by acetabular cup lining. Thus, it is important to have the surface mainly constituted of PE, which is achieved by engineering the PE coating on PE substrate. Filling the drug loaded biodegradable polymer into pores and modifying the surface without altering its basic mechanical and tribological property is the aim of this research.

In the above context, electrostatic spray coating appears to be the effective and easy technique to modify the surface of PE. During the operation, same (PE) powders were

electrostatically deposited on PE substrate [2]. Such coating is supposed to have very strong integrity at the interface between coating and substrate, after curing. This is due to the same physical, chemical and melting nature of both the substrate (PE) and the coating. Visual and SEM observation shows uniform coating with interconnected porosity. However, synthesis of such porous, yet integrated coating demands optimization of curing time and temperature. Hence, different range of temperature (140 to 180 ºC) and time (30 to 80 min) was chosen to optimize it (Table 5.1).

Trial	Temperature	Time	Remarks
Trial 1	140 °C	60 min	Powdery appearance on the surface. Surface in under cured (Fig 5.1a).
Trial 2	200 °C	60 min	Surface over cured with very less pores was visible (Fig 5.1b).
Trial 3	180 °C	30 min	Pores Visible in some areas, but lot of powdery appearance found (Fig 5.1c)
Trial 4	180 °C	80 min	Fully melted surface was observed (Fig 5.1d) and sample (substrate) started distorting
Trial 5	180 °C	60 min	Uniform and micro pores was observed through out surface (Fig 5.2a)

Table 5.1 *Shows the different curing parameter to optimized the coating porosity*

Curing at low temperature (e.g., <180 ºC) takes prolonged time for melting of the PE powders and unmelted particles makes surface uneven, as well as, increases the surface roughness. In this context, at a curing temperature lesser than 140 ºC, no acceptable porosity was obtained even after 3 h of curing time. At high curing temperature (>200 ºC), intensive melting, blistering and surface smoothening was observed on the coating. All these results were observed on coating subjected to a 60 min curing time. Finally, 180 ºC was chosen as curing temperature, from the temperature range of 140ºC to 200ºC. On the other hand, at a curing temperature of 180 ºC, the

coating porosity and integrity also depends on the curing time. For a low curing time (30 min), unmelted crystallite of PE was clearly observed in SEM (fig 5.1c). At higher curing time (>70 min), the density of the porosity decreases, because polymer melt viscosity is high enough to provide a good contact between macromolecules. The SEM micrographs of these optimization processes are presented in fig 5.1. Optimized porosity (37 ± 5%) was obtained at 180 ºC with 60 min curing time (fig 5.2a).

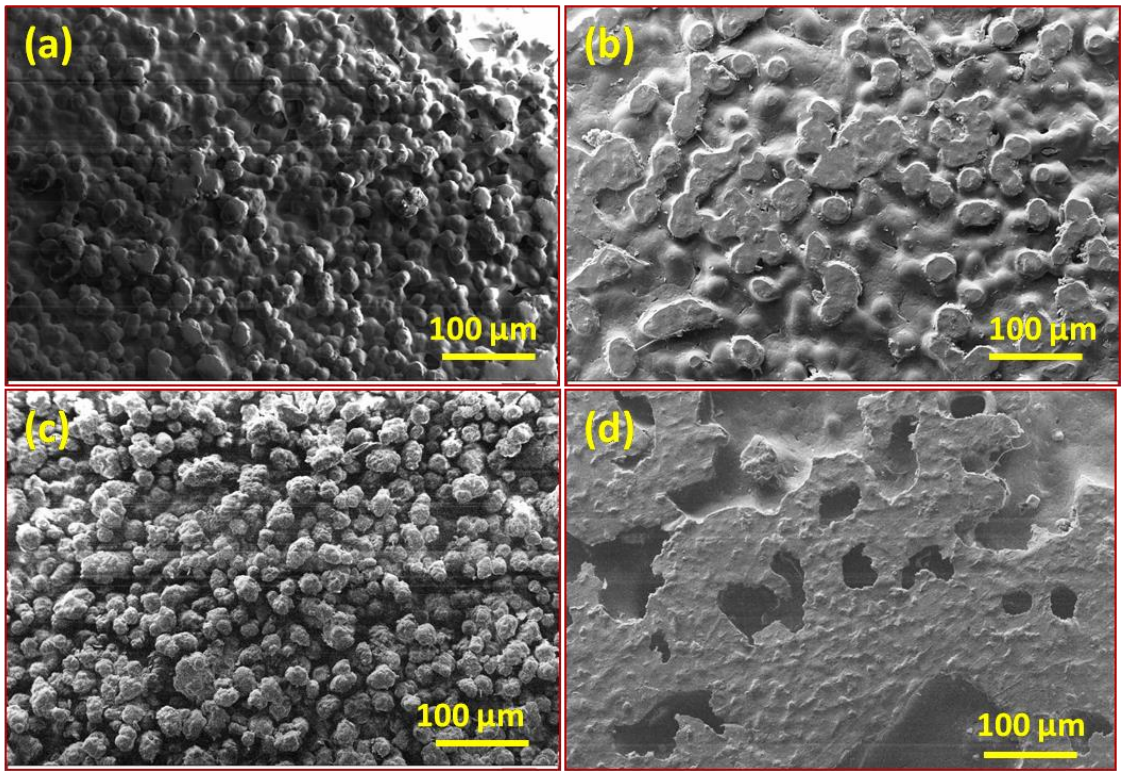

Fig. 5.1 *SEM micrographs of electrostatic spray coating prepared with different temperature and curing time (a) 140 ºC with 60 min (b) 200 ºC with 60 min (c) 180 ºC with 30 min and (d) 180 ºC with 70 min*

On other hand, chemical etching and lyophilization technique (CL) uses boiling paraxylene to partially etch PE surface [1]. Paraxylene is added drop by drop to avoid full melting of the surface, followed by freezing the remaining paraxylene. Lyophilizing process is used to evaporate the crystallized paraxylene and thus, leaving interconnected pores in the surface. Few tens of micron sized pores were observed in SEM image (fig 5.2b). Comparing both the surface

modification technique, electrostatic spray coating (ES) has shown 10 ± 4% higher percentage of porosity as compare to chemical etching technique. The increase in porosity is observed in the former due to the big size of pores in the surface and uneven surface due to partially melted particles (fig 5.2a).

Fig 5.2c and d shows the drug impregnated PE surface of the both coating, where drug contained polymer has completely filled in the pores. Fig 5.2c has shown little higher surface roughness (0.440 ± 0.30 µm), as compared to fig 5.2d (0.260 ± 0.090 µm), which is due to higher roughness offered by partially melted PE particles in ES coated surface.

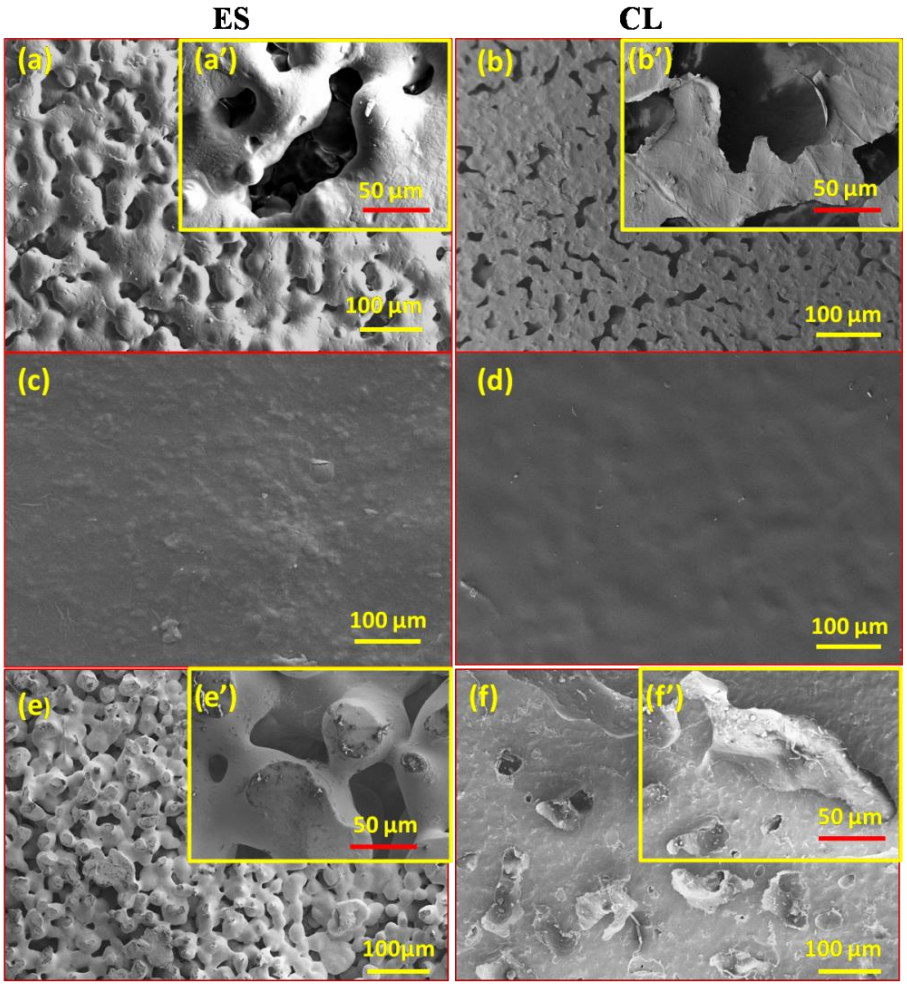

Fig 5.2 *SEM micrographs PE surface (a) electrostatic spray coating with interconnected pores; (b) chemical etching and lyophilization technique; (c & d) after impregnating the drug loaded polymer and, (e & f) after drug releasing, respectively*

After the drug is released (AD-PE), the chemically etched (CL-PE) surface is smoothened with rare traces of pores. Collapsing of the thin walls of pores modifies the surface morphology of CL-AD-PE (fig 5.2f). Walls collapsing mechanism was explained in detail in the previous chapter. But, in case electrostatic spray (ES-PE) coating, the pores remain unchanged even after drug release (fig 5.2e), due to thicker walls of pores and coating morphology (inset image of fig 5.2e). These differential evolutions of surface morphologies are supposed to have different effect on drug releasing, mechanical and tribological behavior, which are investigated and analyzed in following sections.

5.1.2 Drug Loading and Releasing Kinetics

The aim behind this surface modification of PE lining is to release the loaded drug in a controlled manner over a time, to fight against the initial bacterial infection around the surgical area. The amount of drug release is represented in terms of percentage of cumulative release and total quantity (mg) of release with respect to time (fig 5.3A and B). Electrostatic spray coated surfaces (ES-CI-PE) adsorb 16.34 ± 0.4 mg of drug (~82% ± 2), whereas chemically etched (CL-CI-PE) surfaces absorb 14.02± 0.5 mg (70%± 3) of drug. So, the former is loaded with 12% more amount of drug. Surface morphology and big size of pores in ES-CI-PE allows holding higher quantity of drug-loaded chitosan. Both ES-CI-PE and CL-CI-PE had shown sustained release of gentamicin until 860 h (35 days) and 624 h (26 days), respectively. In all the triplicate experiments, the obtained release profiles have shown good reproducibility with relatively small deviation, presented as error bar in fig 5.3.

Initial burst release, followed by a relatively slower release, is ideal drug delivery kinetics. This type of antibiotic release profile is highly desirable for orthopedic implant surgery. Higher

amount of antibiotics is required initially to prevent infection and eradicate the bacteria from the surgical area, as well as, from implant surface. Sustained release for several weeks is required to fight against the delayed infection [5].

Surface modification techniques have shown marked differences in the drug release behavior. ES coated surface shows a longer release profile. This observation can be explained with respect to surface morphology and pores structure. The complete release profile can be divided into two distinct behavioral categories. In first phase, up to 400 h, the amount of gentamicin released decreases slowly with time. This typical characteristic graph is best fitted with an exponential curve fit, as seen in fig 5.3a'. This fit indicates the dominance of diffusion mechanism in the drug release profile. During this period, ~70% of drug is released in fast and sustained manner from ES coated surface. In the similar region, CL-CI-PE had shown 83% of drug release in 280 h (fig 5.3b'). An increase in release percentage is observed due to higher diffusion rate in chemically modified surface. Open pores and lower depth of pores structure helps fast dissolution of chitosan. As a result, an antibiotic inside the chitosan dissolves and gives rise to burst release effect. Second phase of release profile continues 460 h onward till 860 h in ES-CI-PE and the release graph is best fitted with linear equation ($R^2 = 0.88$). The percentage of gentamicin released is calculated from the slope, which is ~2.94 mg (20%) of gentamicin released in continuous manner with a rate of 0.00684 mg/h. This behavior is dominated by gradual degradation of the drug-containing polymer. On the other hand, the second release phase of CL-CI-PE continues only up to 624 h (280 to 624). The drug release rate is noted as 0.0043 mg/h with ~1.513 mg (13.2 %) is being eluted in the whole period.

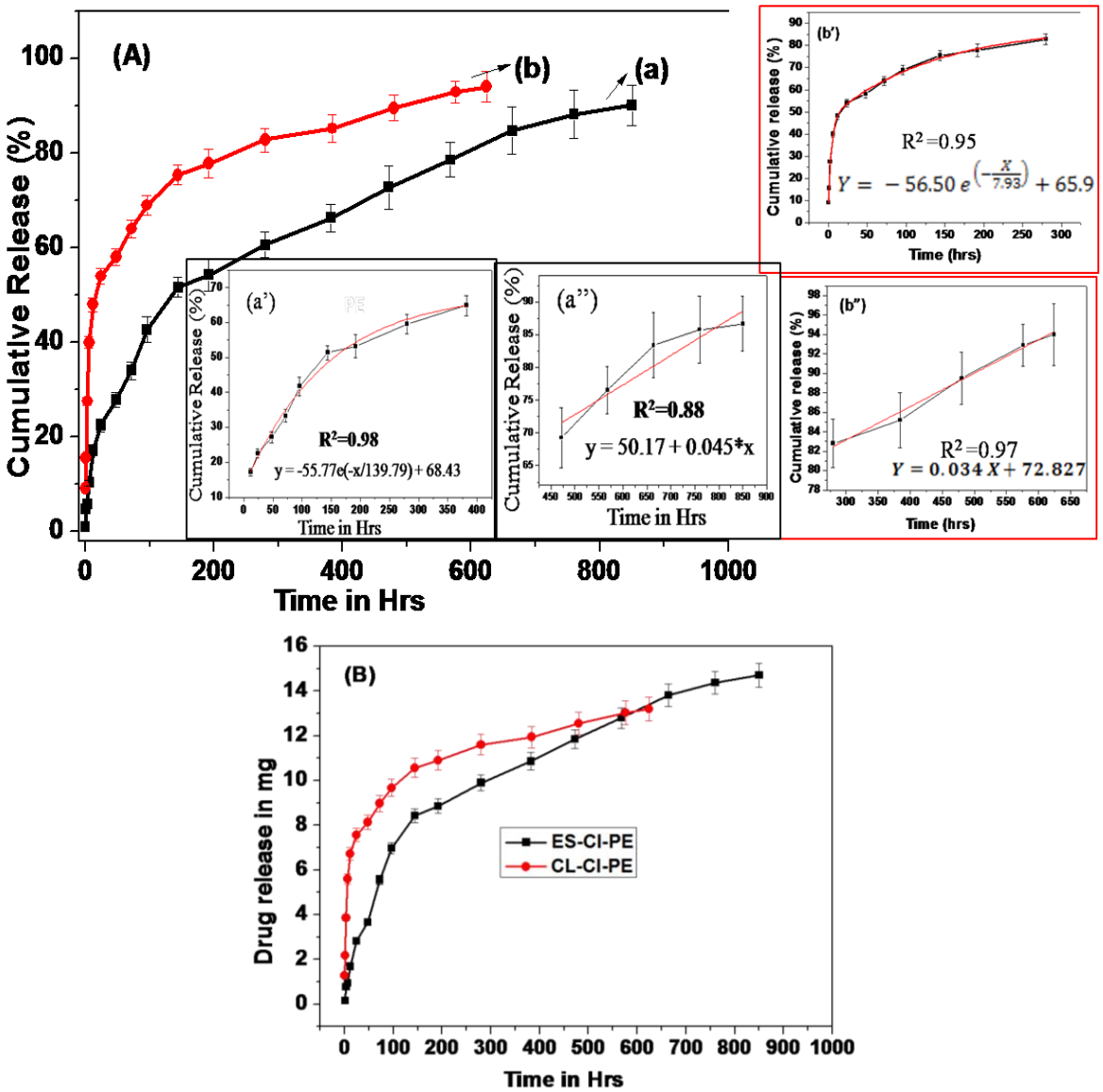

Fig. 5.3 *In vitro cumulative gentamicin release profile of (a) ES-CI-PE modified surface up to 860 h; (b) CL-CI-PE modified surface up to 624 h; (B) shows drug release in terms of total content*

Various factors may affect the release kinetics of gentamicin from chitosan. The initial fast releasing of gentamicin can be attributed to high solubility and low molecular weight of the drug. The sustained gentamicin release is due to slow degradation of chitosan. During drug release, the reaction between amine groups of chitosan and phosphate $(PO_4)^{3-}$ ions in PBS might lead to crosslinking of the chitosan, which leads to lower and sustained release of antibiotic [6]. The total cumulative percentage release of gentamicin from ES-CI-PE test samples was about 90% for 860

h. But, it was 94.1% for 624 h in CL-CI-PE test sample. Increase in total release by 4% was observed for CL-CI-PE, due to complete degradation of chitosan by collapsing of pores. Even though ES-CI-PE shown 4% less cumulative release, the amount of gentamicin release is 14.7 mg (Fig 5.3B), which is 10.27% higher than CL-CI-PE (13.19 mg). Deep pores and highly interconnected structure in ES-CI-PE allows slow degradation of chitosan and some left over chitosan inside deep pores, leading to slow and less cumulative release.

5.1.3 Antimicrobial Activity

The antibiotic resistance study, against *S. aureus,* was carried out to assess the effectiveness of gentamicin release from ES-CI-PE and CL-CI-PE. S. aureus is the pathogen that is responsible for about two thirds of chronic osteomyelitis infections. Fig 5.4 shows the antibacterial activity of ES-CI-PE and CL-CI-PE samples. All test samples were exposed to culture of S. aureus for up to 5 days, with unmodified PE sample being used as control for this observation. The test was performed by using agar disc diffusion technique.

Three different drug concentrations (10, 15 and 20 mg/ml) were used to test efficacy of low to high drug content to eradicate bacterial strains. Both (techniques) of the modified surfaces (20 mg concentration) displayed bacterial inhibition rings in the agar plate (marked in yellow dotted line in fig 5.4a and b). However, the inhibition zone of the S. aureus for CL-CI-PE at fifth day is slightly larger (4%) as compare to ES-CI-PE. It can be attributed to higher gentamicin release (20%) rate for the former in the starting 125 h, as discussed earlier in section 3.2. On the contrary, no such bacteria free region was observed around the unmodified PE surface. Same trend is observed throughout, up to 5 days of culture in both the coating method. Lower drug concentration (10 and 15 mg) was also checked to observe the effectiveness of lower concentration against S.

aureus. Inhibition zone is proportional to drug concentration. This observation evidenced the potential of the drug loaded PE surface in combating bacterial infection. The comparative antibacterial efficiency is represented in fig 5.4c, d and e for 20 mg, 15 mg and 10 mg respectively. Inhibition area is found increasing with increasing drug concentration and days, and it's clearly observed in percentage of antibacterial efficiency with respect to time.

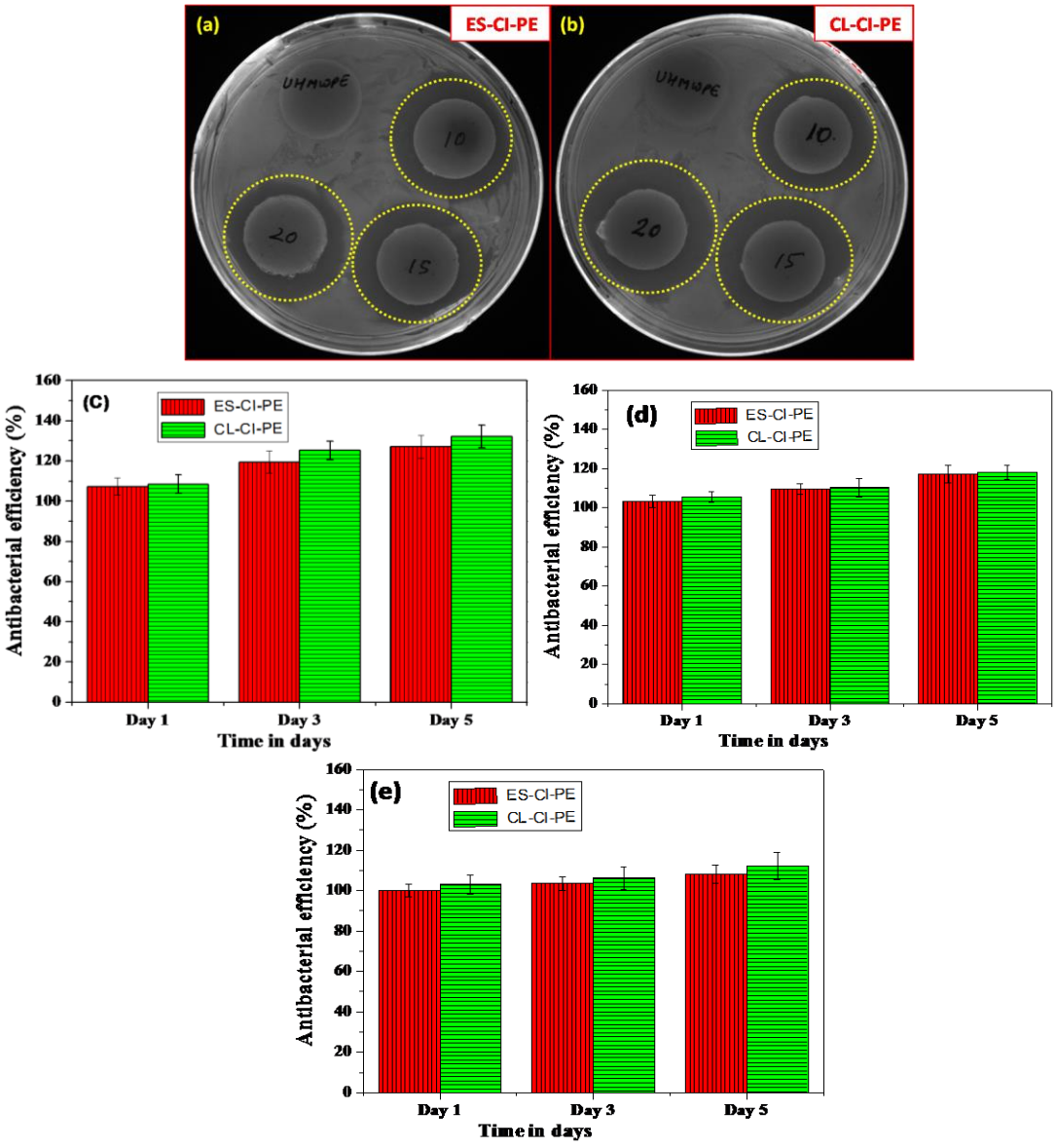

Fig. 5.4 *Antibacterial activity after 5 days of incubation on (a) ES-CI-PE and (b) CL-CI-PE samples. Inhibition zones are marked with yellow dotted circles for better visualization; (c) antibacterial efficiency rate for 20 mg of gentamicin concentration as a function of time, (d) for 15 mg of gentamicin and (e) 10 mg of gentamicin concentration*

SEM investigation was also performed after incubation to examine the grown bacteria on each test sample. High population of bacteria growth with the passage of time was found on the surface of unmodified PE (fig 5.5a). In contrast, no bacterial cells and trace of biofilm were found on the drug loaded PE surfaces (fig 5.5b). No traces of S. aureus were found at extended culture period of 5 days, suggesting the antimicrobial effectiveness of gentamicin impregnated PE implant in long run. Modified surface of both coating techniques effectively eradicated infection induced by gram-positive bacteria, even when exposed to high concentrations of microbes. This study also suggests that the drug does not get inactivated during mixing with chitosan and impregnation procedure. The established drug release profile for ES-CI-PE and CL-CI-PE shows the potential for sterilization of the operated area at an early stage and effective prevention of any bacterial infection and biofilms formation around the implant.

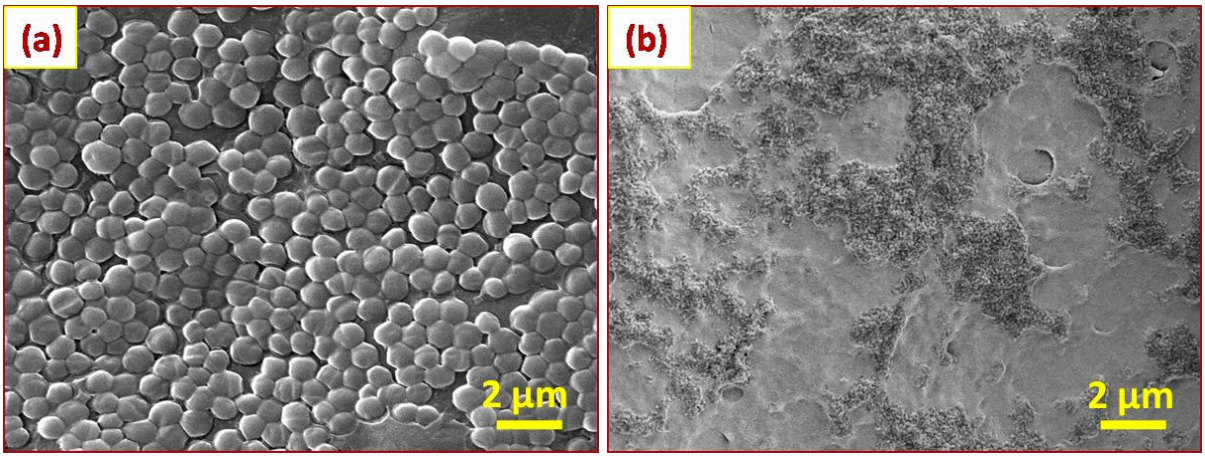

Fig. 5.5 *SEM micrographs revealing the antibacterial activity on (a) unmodified PE surface and (b) drug loaded (20 mg/ml) surface of ES-CI-PE, after 5 days of culture*

5.1.4 Mechanical Properties of Modified Surfaces

The mechanical properties of liner in acetabular cup are critically important to support skeleton and to bear the body weight, as well as, to bear frictional forces during operational condition. The hardness (H) and elastic modulus (E) of different surface modified PE was measured through instrumented indentation technique. Fig 5.6 shows typical indentation load-displacement behavior of different surfaces. Chitosan impregnated ES-CI-PE and CL-CI-PE surfaces have shown lower gradient in unloading curves and higher depth of penetration with the application of 2 N load. A 23% (ES-CI-PE) and 19% (CL-CI-PE) higher displacement is recorded, as compared to PE surface. The above mentioned responses suggest that resistance of the impregnated surface to indentation is decreased as compared to unmodified PE surface. However, after releasing the drug for 860 h, ES-AD-PE has shown further lower slope in the unloading part of the curve, because of porous surface morphology. But, in case of CL-AD-PE, the slope of unloading curve and depth of penetration is almost same as PE after drug release, due to surface re-modification after drug release [1].

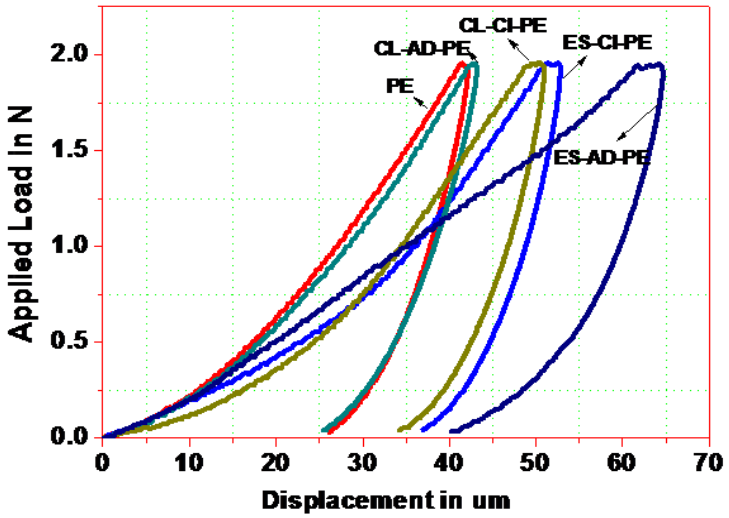

Fig. 5.6 *Representative load vs. displacement curves obtained from instrumented micro indentation test*

Unmodified surface of PE has shown hardness of 0.057 ± 0019 GPa and elastic modulus of 0.95 ± 0.38 GPa, which was considered as reference for all modified surfaces. Fig 5.7 shows the average values of hardness and elastic modulus for all prepared samples, with the standard deviations presented as error bars. Decrease in hardness and modulus is noted in all chitosan-impregnated samples as compare to PE. Around 27% and 29.2% decrease in hardness and 20% and 16% decrease in modulus is found in CL-CI-PE and ES-CI-PE, respectively, as compare to PE. The hardness and modulus of pure chitosan is 0.12 ± 0.05 GPa and 1.08 ± 0.04 GPa, respectively, which is comparable to PE [7]. Thus, the negative effect of impregnation on H and E can be explained as the improper impregnation of chitosan in pores.

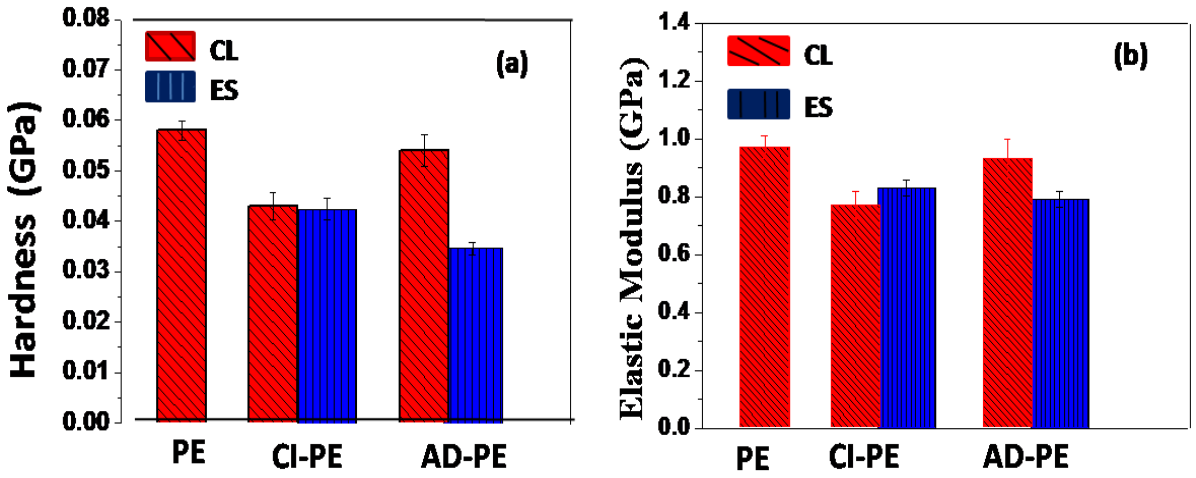

Fig. 5.7 *Hardness and elastic modulus of different surfaces obtained from instrumented micro indentation*

It is interesting to note that after drug release, CL-AD-PE regains its H and E values almost similar to PE. This finding is specifically very interesting as it reveals the fact that after release of the drug, the acetabular cup liner would bear no adverse effect in its natural function due to drug release. The reason behind this is proposed in detail earlier in chapter 4. Briefly, when samples are exposed to PBS during drug release study, biodegradable chitosan starts swelling substantially due to its hydrophilic and gel forming nature. During this swelling process, the pore walls experience

high amount of compressive stress and starts deforming into thinner plates to accommodate the expanded volume. After drug release and chitosan degradation, the thin walls cannot retain their integrity and collapses. The procedure of collapsing takes place over a time period, simultaneously with degradation of chitosan. This happening makes the final surface smoother, reduces the volume and existence of pores. As a result, the surface appears relatively smooth with slight increase in surface roughness (R_a = 1.366 ± 0.300 µm) than that of unmodified PE surface (R_a = 0.391 ± 0.070 µm).

On other hand, after drug release, ES-AD-PE had shown further decrease in H (42%) and E (19%) as compared to PE, because of porosity in the surface. In this case, the surface did not get modified by collapsing of the pore walls. The surface pores remained similar as before impregnation of chitosan and roughness noted as ~3.26 ± 0.900 µm (fig 5.2e). It was possible due to higher thickness of pore walls (pores generated between PE melted particles, fig 5.2a'), which made them strong enough to withstand compressive forces during swelling. Comparison of mechanical behavior of both modified surfaces reveal that CL is better than ES, as after specific periods of drug delivery the former is able to regains its mechanical property, which is required for this application.

5.1.5 Friction and Wear Studies on Modified Surface

Total hip and knee joints are the two main load-bearing parts of the human body, which are continuously experiencing severe dynamic frictional forces during movement of limbs. The mating parts of the total hip implants, namely, femoral head and inner lining of the acetabular cup, is continuously facing severe frictional forces during limb movement.

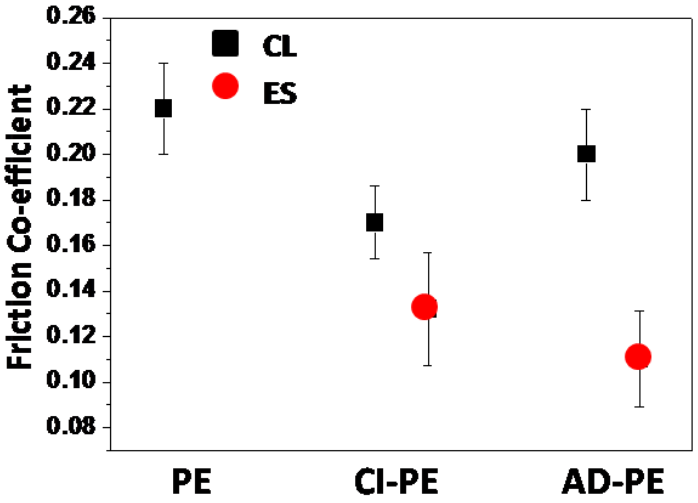

Fig. 5.8 *Coefficient of friction for different surfaces*

PE is clinically used as inner lining material of acetabular cup to reduce the friction and wear of hip prosthesis. Hence, it is important to assess the tribological performance of the modified PE surfaces, which are being proposed for acetabular cup lining. Fig 5.8 shows the average friction coefficient for different surfaces with standard deviation marked as error bars. For unmodified PE surface, the average CoF in steady state is 0.23 ± 0.02, which is 35% and 26% higher than ES-CI-PE and CL-AD-PE, respectively. It was clearly observed that impregnating the drug loaded chitosan on PE has significantly reduced the frictional forces. This observation indicates that drug contained chitosan might be acting as lubricating agent on PE surface, by avoiding the stick-slip mechanism. Further, drug and chitosan films have lower shear strength due to the inherent property of its molecules, as compared to ultra-high density PE. Hence, flexible molecules of drug containing chitosan offers lower resistance to the shearing force, leading to reduction in friction coefficient [8]. Further, ES-CI-PE has shown 11% lower CoF than CL-CI-PE. This could be related to lesser contact area, higher surface roughness and uneven surface morphology of the former, due to presence of partially melted PE particles on the surface. The combined effect of smooth worn surface and chitosan lubricant behavior reduced the CoF of chitosan impregnated PE

samples. After drug releasing, the friction coefficient of ES-AD-PE decreased to 45%, whereas, CL-AD-PE decreased to 8%. Higher decrease in CoF in former is found due to less contact area on porous surface. The left over chitosan inside the pores may also play a role. But in case of CL-CI-PE, pores got collapsed during drug release and surface regained its morphology similar to unmodified PE. Hence, the frictional characteristics are almost similar to PE.

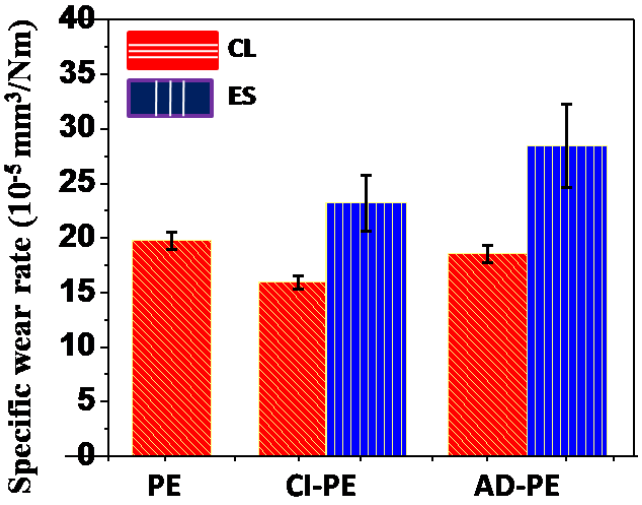

Fig. 5.9 *Specific wear rate of different test surface calculated from 2D line profile*

Fig 5.9 shows specific wear rate of different surfaces and it was calculated through wear track profiles. 2D track profiles are shown in fig 5.10. The 2D wear track profile clearly shows the amount of material removed from each test surfaces. Deep and broad worn scar was seen in ES-AD-PE as compare to other surfaces. On the other hand, least worn surface was observed on CL-CI-PE sample. The error bar of the respective bar chart denotes the variation of tribological behavior of the surface. The specific wear rate of PE is ~20 x 10^{-5} mm^3/Nm, which is 19% higher than CL-CI-PE, while 15% lower than ES-CI-PE. Besides, it was interesting to note the wear rate after drug release. The CL-AD-PE surface regains its surface morphology, as like PE, and offers wear rate in similar range. However, ES-AD-PE has shown further increase in wear rate (29%)

along with larger error bars than PE. These remarkable observations of wear rates have been further analyzed by correlating with micrographs of wear tracks and debris.

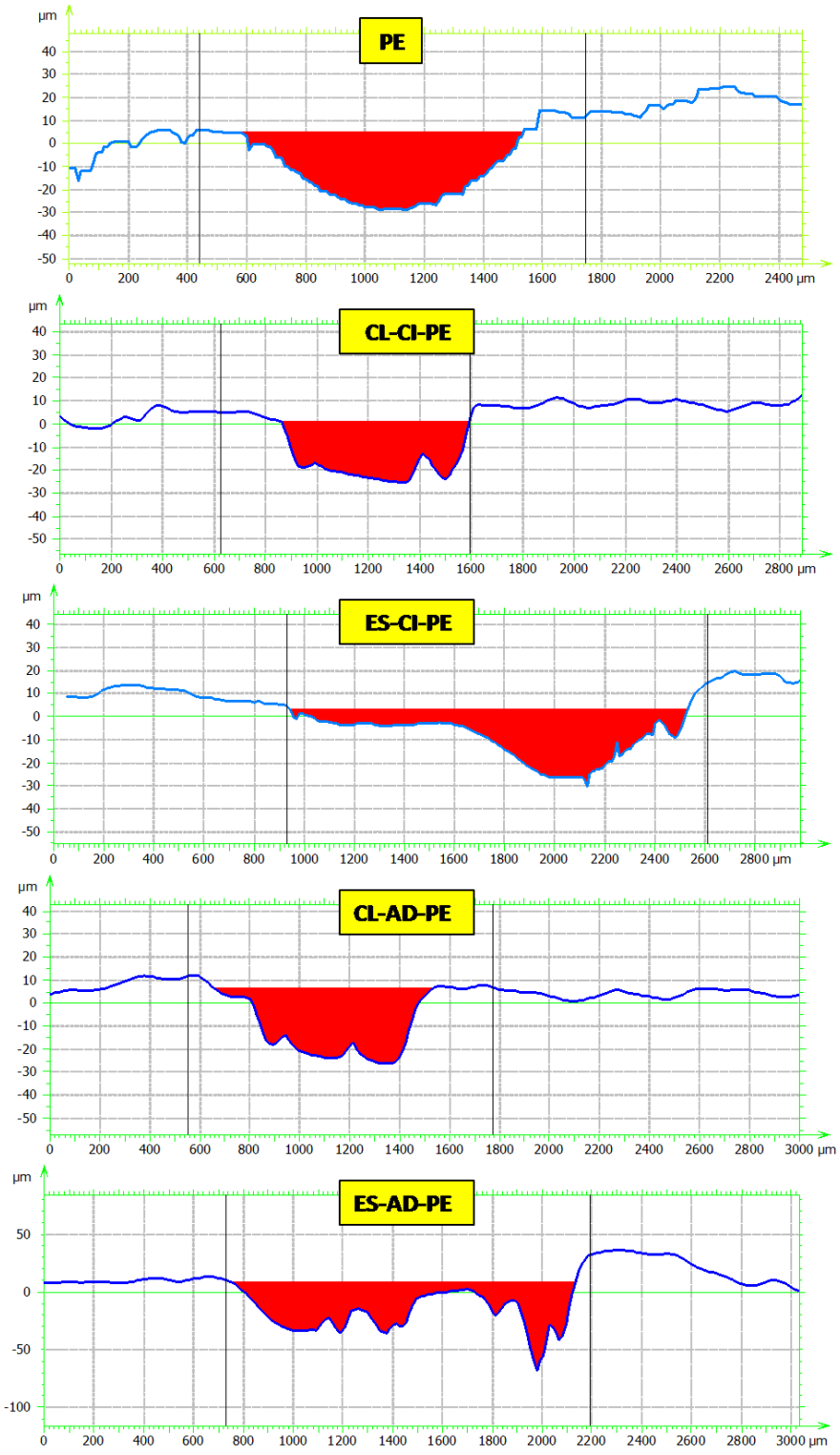

Fig. 5.10 *Represents the wear track surface profile of different test surfaces*

Fig 5.11 shows SEM images of worn surfaces as well as wear debris for all surfaces. The micrographs reveal different wear mechanism and microstructural effect on wear behavior. The worn surface of PE is relatively broader and shows deeper track profile. It shows that PE surface asperities experience severe compression and plastic deformation during sliding of counter body. As a result, adhesion and abrasive wear mechanism dominated on the worn surface, which can be validated by observing lot of tiny deformed wear debris (fig 5.11a and f). It is an established sliding wear mechanism of PE [9]. On the contrary, the scale of deformation differs markedly in case of chitosan impregnated PE samples. CL-CI-PE has shown almost no deformation and mild adhesion on the worn surface fig 5.11c. In addition to that, wear debris analysis reveals the platelets of transfer films (fig 5.11h). Combining these observations, it is understood that during initial sliding large extent of chitosan films adhere onto the surface of hard steel ball. The transferred material on the steel ball surface avoids contact of steel with CL-CI-PE surface during further sliding. Thus, reduced friction and wear rate were recorded (fig 5.8 and 5.9) for CL-CI-PE surface as compared to unmodified PE surface. In addition to that, impregnated chitosan did not get pulled out during the sliding process, which may suggest a good impregnation of chitosan in the pores. But in case of ES-CI-PE, though great reduction in CoF and mild adhesion wear was found, ~15% of increase in wear rate was noted. Reason for the latter case was surface roughness and scuffing (fig 5.11b). Besides, after drug release, damaged porous surface lead to increase in abrasion and adhesion wear on the surface of ES-AD-PE. This can be validated by observing the worn surface and deformed debris in fig5.11d and e. Hence, ES-AD-PE surface shown higher wear rate than ES-CI-PE and PE. But, it was not found in case of CL-AD-PE; the wear rate is lesser or almost similar to PE. Because, the surface of CL-CI-PE is modified during drug release and became almost similar like PE surface (fig 11e). In short, modified chemical etching and

lyophilization technique (CL) shown better tribological property than electrostatic spray coating technique (ES). Thus, the study suggests CL-CI-PE surfaces are more suitable for drug eluting acetabular cup liner.

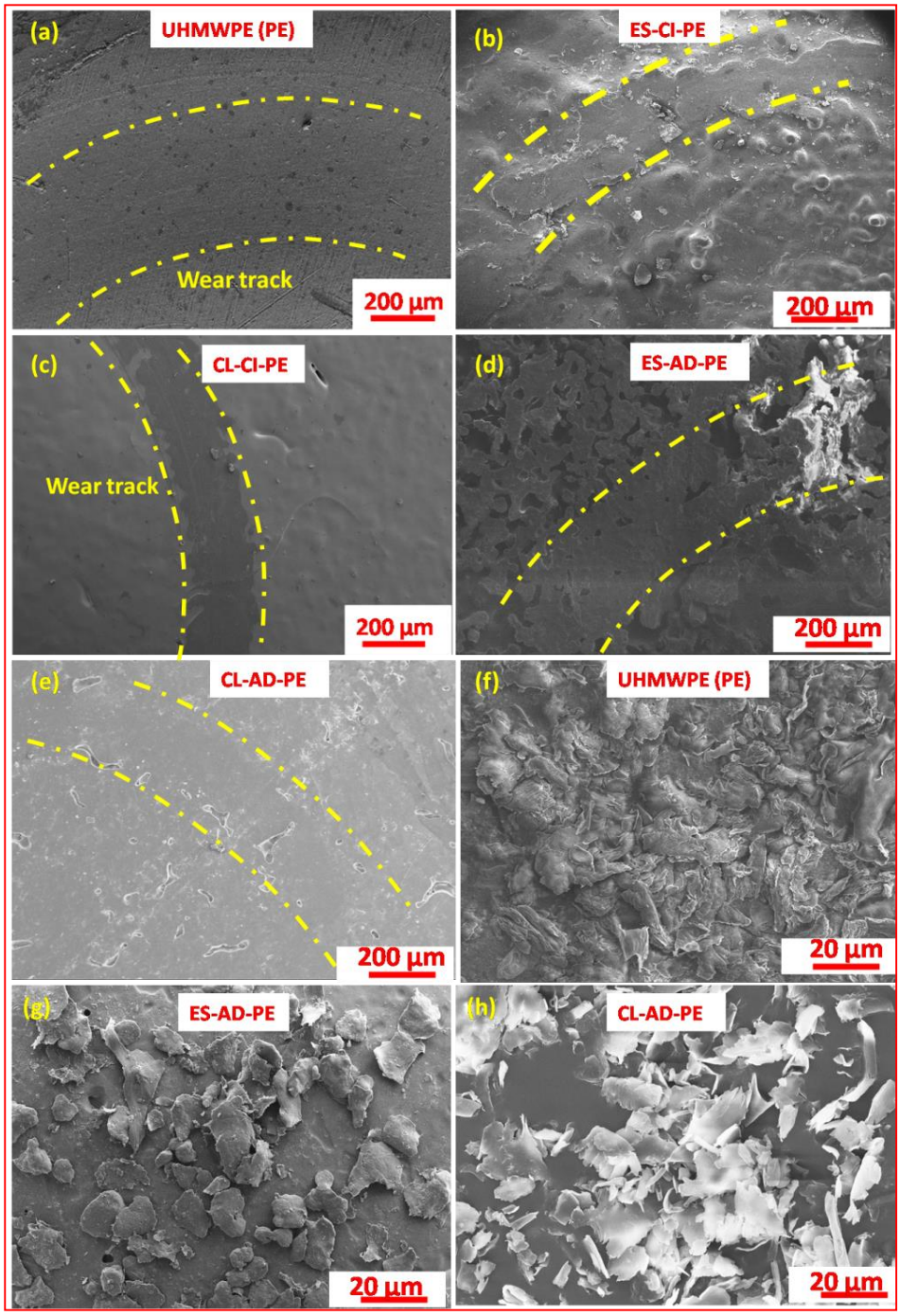

Fig 5.11 *SEM micrographs of worn surface and wear debris of different test sample*

5.1.6 Summary

Bacterial infection remains serious clinical issue in orthopedic implant, although series of prophylactic methods are available in the market. In this perspective, local sustained delivery of drugs offers a powerful tool to fight against initial bacterial colonization and delayed infection. The concept of surface modification of inner lining of acetabular cup comes handy in this effort. Present study had shown two different surface modification techniques, namely, electrostatic spray coating (ES) and chemical etching and lyophilization (CL) technique to engineer the porous surface on PE. The engineered surface impregnated with drug-loaded chitosan and investigated to understand the influence of surface morphology and pore structure on the drug delivery kinetics, mechanical and tribological behavior. Electrostatic spray coating (ES) has shown remarkable release profile up to 860 h in sustained manner, which is much longer than chemically etched surface with 626 h. However, drug delivery rate is higher in the latter case. Decrease in mechanical and tribological property, even after drug release, are the draw backs of ES surfaces, while chemically etched surface retains its mechanical and tribological behavior same as unmodified surface, after release of drugs.

CHAPTER 6

CNT Aspect Ratio – Effect on Mechanical, Tribological and Thermal Behavior on PE Composite

In order to improve the basic properties of conventional PE liner and to address the limitation of surface modification (decrease in mechanical property) of PE, CNT-PE composite was prepared. This chapter experimentally presents the effects of CNT morphology on mechanical and tribological behavior of PE composite. In addition to analyzing the effect of CNT reinforcement on mechanical and tribological behavior of PE, CNTs with different aspect ratio was also used in this study. The idea was to understand the effect of the aspect ratio of nano-fillers, if any, on the final behavior of PE.

Carbon based nanomaterials are great choice as reinforcement to ultra-high molecular weight polyethylene (PE), with potential use in orthopedic joints. While high in-plane stiffness and strength of these nanomaterials help in toughening, their weaker out-of-plane integrity is instrumental in offering lubrication for the composite structure. Tribological properties of CNT reinforced PE composite is a highly relevant aspect for potential bearing application. Only a few studies deal with the influence of CNT concentrations on wear and thermal stability of the polymer composite [241]-[247]. *All these studies explored the effect of CNT addition on the surface hardness, strength, plowing and cutting resistance on PE. The reports mostly include improvement in wear resistance and increase in coefficient of friction (COF).*

---

*Kumar, R. Manoj, et al. "**Effects of carbon nanotube aspect ratio on strengthening and tribological behavior of ultra-high molecular weight polyethylene composite**." Composites Part A: Applied Science and Manufacturing 76 (2015): 62-72.*

However, exceptions were observed by Wei et al. [246] *and Lee et al.* [247]*, who reported decrease in COF by ~20 % with addition of 5 wt.% of CNTs. This decrease in COF is attributed to the self-lubrication offered by CNTs. However, effect of aspect ratio of CNT in controlling the lubrication at polymer matrix surface is not reported. This study finds out that high aspect ratio CNTs are deeply rooted in the matrix and supplying continuous lubrication under the application of frictional force, whereas low aspect ratio CNTs are broken and coming out from the matrix. The morphological similarity of high aspect ratio CNTs to that of polymer chains help in cross linking of the polymer chains, thus leading to superior mechanical property in the composite even at low concentration.*

As mentioned earlier, not many researchers have explored the morphological effect of CNT on mechanical properties of the composite. However, to the best of the authors' knowledge, no studies exist till date on the effect of CNT morphology on wear behavior of any polymer based composites. A thorough understanding of the mechanism involved in the COF and wear resistance of different morphological CNTs, their concentration, distribution effect is required to understand the role played by morphology of reinforcement.

In order to experimentally analyze the effect of CNT morphology on mechanical and tribological behavior of PE matrix, we used two different aspect ratios of MWCNTs, with two different concentrations, as reinforcement. Ball on disc test and nano-indentation test was conducted to examine the basic properties which are required for artificial acetabular cup. Such properties include coefficient of friction (COF), specific wear rate, hardness and elastic modulus. Differential scanning calorimeter and thermos-gravimetric analysis was also carried out to study the thermal, oxidation or degradation behaviors. Analysis of the results gave us an in-sight on the causes of structural change occurring in composites, due to different aspect ratio of CNTs used as

reinforcement. Finally, the obtained results were justified based on the dominating mechanism involved in the composite.

6.1 Results and Discussion

6.1.1 Microstructural Characterization of the Composite

Fig 6.1a, b and c shows FE-SEM images of as received CNTs as well as PE powder. An inset in fig 6.1a and b clearly reveals the difference in aspect ratios of two types of CNTs used in this study. Briefly, high aspect ratio CNTs (HARC) were having outer diameter 10-12 nm and length 8-12 μm, whereas low aspect ratio CNTs (LARC) were having outer diameter 40-70 nm and length 1-3 μm. Their average aspect ratios are about 900 and 75, respectively. Probe sonication (Power-500 Watts and 20 kHz frequency) is found to be very effective in distributing the CNTs very uniformly with PE powders, irrespective of their significant difference in sizes. Fig 6.1d and e shows CNTs getting homogeneously distributed and attached to the polymer powder surface as a result of probe sonication. This is very important for effective use of the total reinforcement volume and uniform mechanical/tribological behavior of the composite.

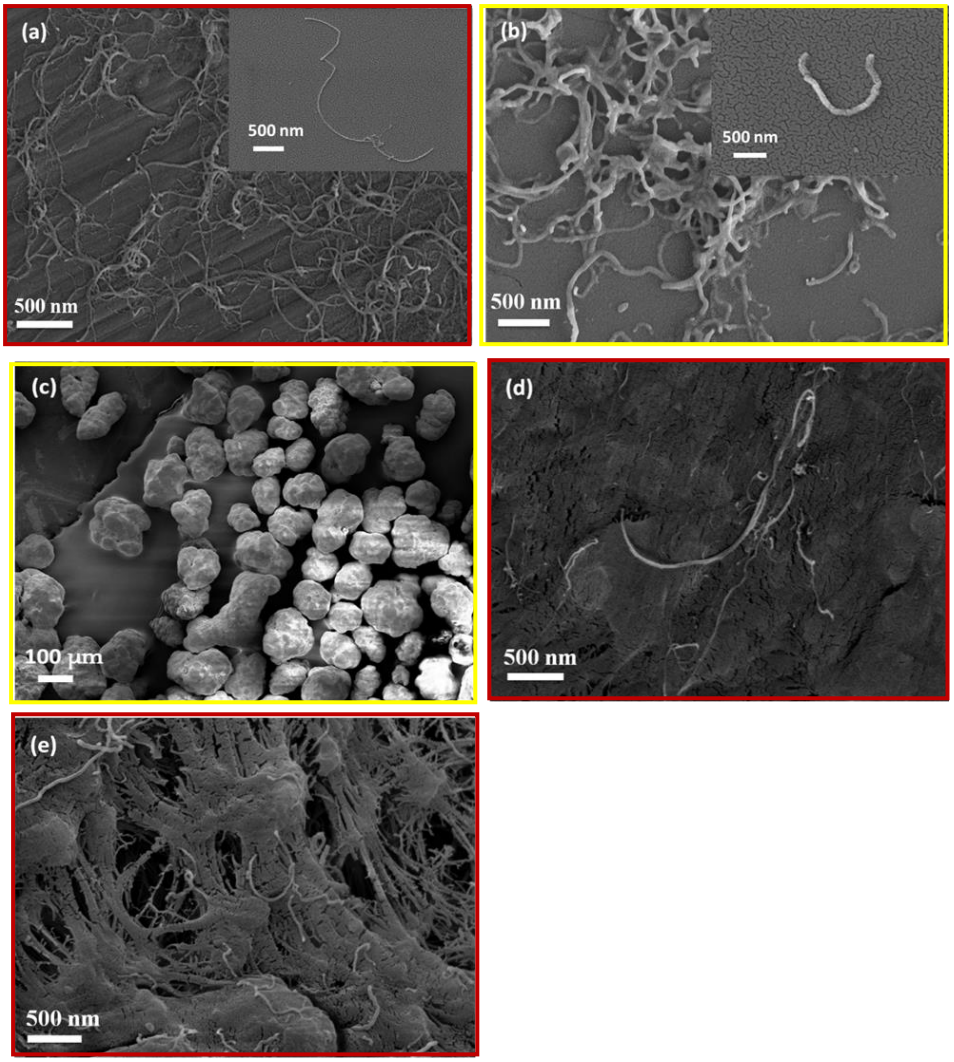

Fig. 6.1 *FE-SEM images (a) high aspect ratio CNT (HARC); (b) low aspect ratio CNT (LARC) and c) PE powder. Figure (d and e) shows the HARC and LARC dispersion on PE powder, respectively, before sintering*

The curing temperature of the polymer and composites was determined through differential scanning calorimetry (DSC) of the as-received PE powder (explained in chapter 3). The melting temperature of PE is nearly 123 °C, but it is very viscous at this point. However, proper curing and wrapping of the reinforcement phase by polymer matrix needs more flow and lesser viscosity. Thus a higher temperature of 160 °C was used for curing. This was optimized by trial and error at a range of temperatures and by observing the integrity through microscopic investigation at cross section of the cured PE pellets. Those results are included in the experimental chapter 3.

Fig 6.2a and b shows the fracture surface of the HARC and LARC composite with 0.1 wt. % reinforcement content. CNTs are nicely embedded with polymer matrix in both the composites. Both the CNTs are found to be deeply rooted in the matrix with protruded ends revealed at fracture surface, which indicates strong interfacial bonding with the polymer matrix and it helps for effective load transfer. However, the protruded ends are found to be longer in case of HARCs than in LARCs. The reason could be the lower aspect ratio of the latter, and/or uprooting of the same at higher load, as compared to the former.

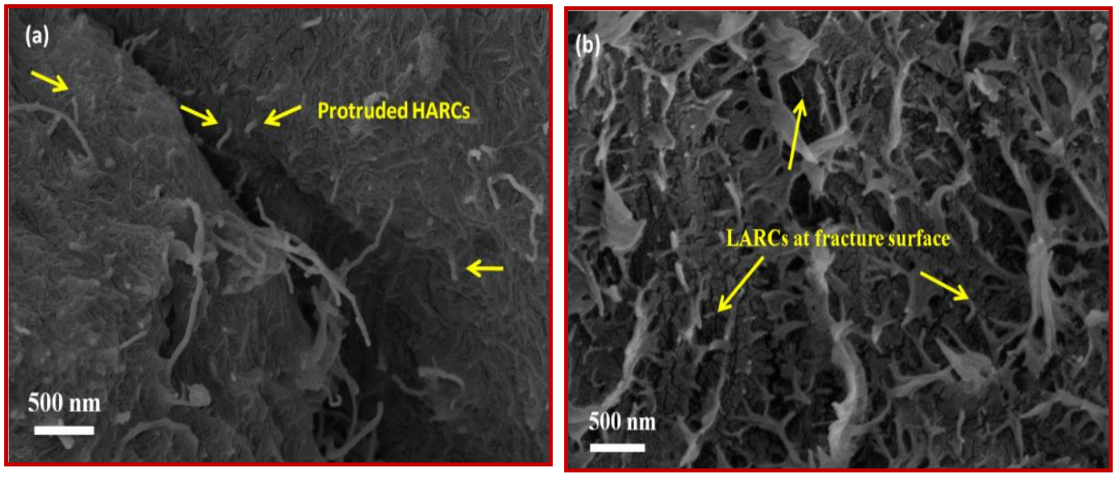

Fig. 6.2 *Fracture surface of 0.1 wt. % HARC (a) and LARC (b) composite*

6.1.2 Thermal Analysis of the Composites

Fig 6.3 shows the DSC results of the composite. The peak in the DSC curve corresponds to the melting temperature and area under the peak is equal to the enthalpy of melting. Researchers [248]-[250] have reported that CNTs can act as nucleating agent for the crystallization of polymer. Addition of 1 wt.% of MWCNT enhances the rate of crystallization up to a significant distance from their vicinity. As a result, crystallinity of polymer increases without a change in melting temperature of the composite. On the contrary, reduction in crystallinity from 58 to 48% for 5 wt.% CNT [220] and 32.5 to 27.6% for 10 wt.% of CNT [251] in PE is also reported by other

study. However, no study has reported yet the effect of aspect ratio of CNT, if any, on the crystallinity of polymer matrix composite. To understand this, DSC tests were conducted and the results were analyzed. The enthalpy of melting for pure PE, PE-0.05LARC and PE-0.1LARC is 88.1 J/g, 84.5 J/g and 70.3 J/g respectively (fig 6.3). The percentage of crystallinity was calculated by dividing the enthalpy of melting of the prepared composite with the enthalpy of fusion for 100 % crystalline PE [53], as referred in equation 1 (chapter 3). Crystallinity recorded is 30%, 29% and 25%, respectively, for PE, PE-0.05LARC and PE-0.1LARC. Addition of lower aspect ratio CNTs reduces the crystallinity of the composite to some extent, which can be explained due to following two reasons. LARCs are dispersed uniformly in PE matrix as a stiff fiber (fig 6.1e), which form, at parts, tube to tube connection and this network, at places. Such network enhances the thermal conductivity of the composite, considering excellent thermal conductivity of 3,000 W/m·K [252] for CNTs. This, in turn, increases the cooling rate of the composite during solidification, leaving less time for arrangement of the polymer chains to form crystallites. This type of behavior was also observed by other researchers [220][253]. Secondly, LARCs have higher diameter as compared to polymer chains and hence they act as obstacles and restrict the movement of chains during solidification. This may be other reason for reduction in the crystallinity of the LARC reinforced composites. PE-0.05HARCs show almost similar crystallinity of 29.76%, like PE. However, high concentration of HARCs (PE-0.1 % HARC) shows increase in crystallinity by ~3 %. One of the reasons for the latter case could be that randomly bent fibers and self-entangled flocks of high aspect ratio CNTs covering the polymer as compared to distribution in LARCs. Further, their high surface area to volume ratio increases the viscosity and nucleation sites for the crystallization in the composite and hence, crystallinity increases.

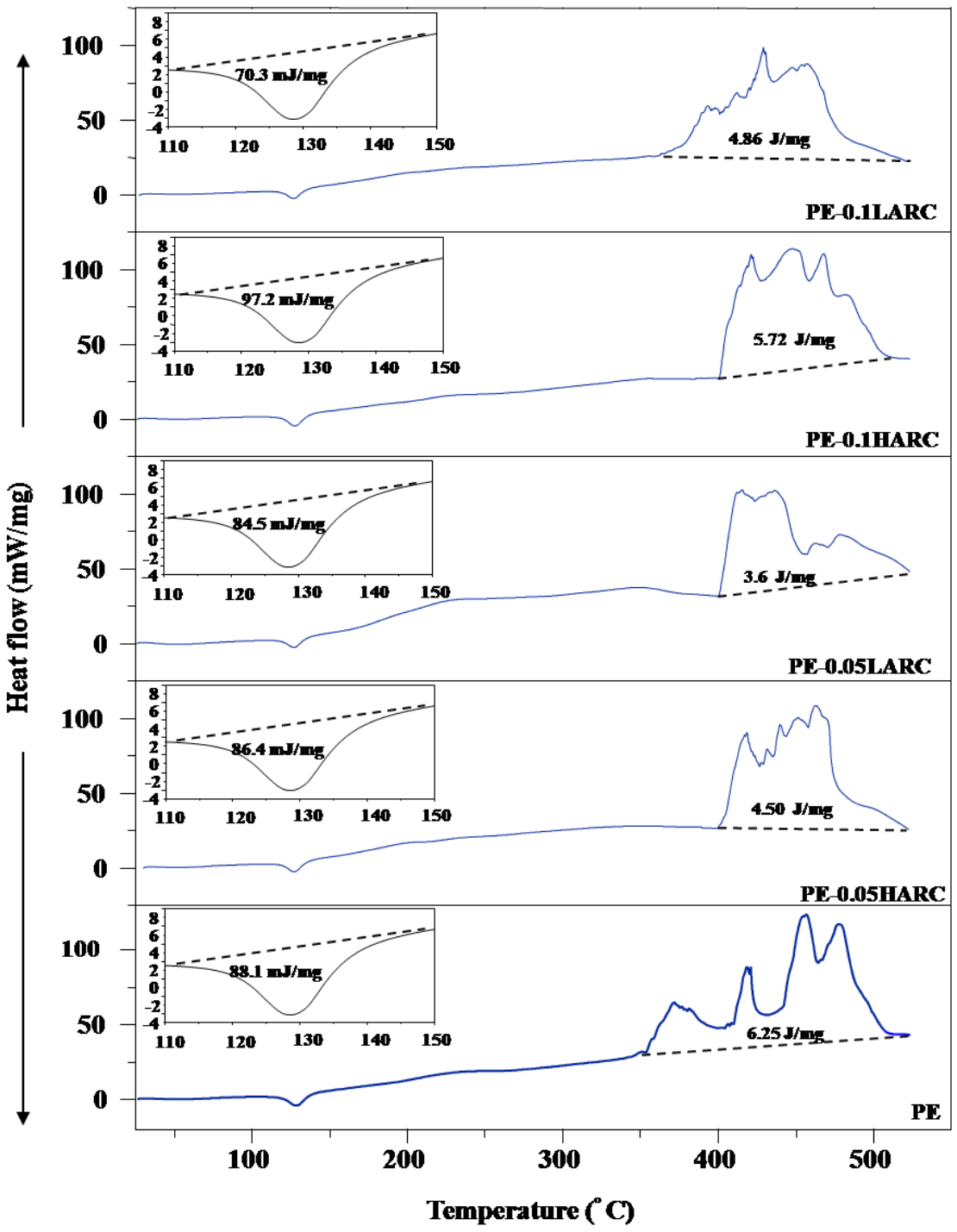

Fig. 6.3 *DSC analysis for different CNT reinforced PE and pure PE composite.*

In addition to that, HARCs are nicely embedded within matrix due to their morphological similarity with polymer chain and it is discussed in detail later in subsection (mechanical property

analysis). The higher specific heat of CNTs (C_p=0.75 $Jg^{-1}K^{-1}$ at 300 K [254] can cause a heat pool in the surrounding polymer, which thermodynamically helps rearranging the polymer chains in a manner to increase the crystallinity. But 0.05 wt.% is not a sufficient filler fraction for giving such effect and hence PE-0.05HARC has shown almost no change in crystallinity. This observation is in line with the findings of other researchers [250][255]. Therefore, aspect ratio and volume fraction of the CNTs influences the crystallinity behavior of the composite, which indirectly affects the mechanical properties.

Effect of CNT aspect ratio on thermal degradation behavior of the composites can be explained from the TGA plots presented in fig 6.4.

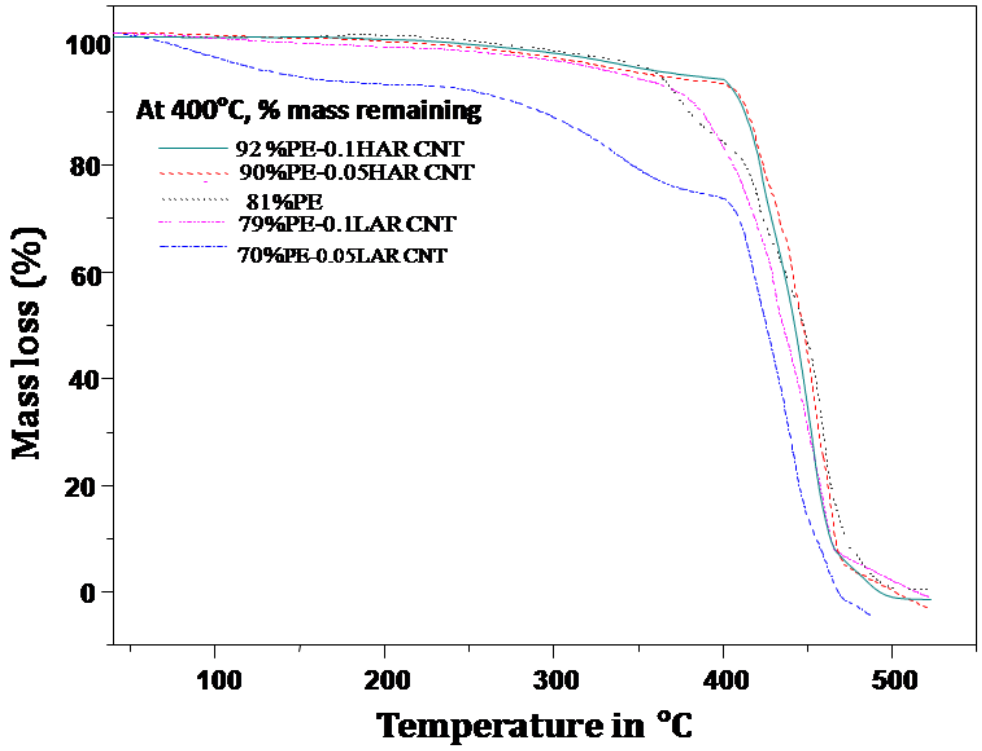

Fig. 6.4 *Thermo-gravimetric curves of composite revealing degradation loss through temperature range up to 500 °C*

It is observed that high aspect ratio carbon nanotubes reduce the amount of oxidation or degradation of the composite at higher temperature. At 400 °C the mass remaining for PE is 81.13

%, PE-0.05HARC is 90.9 % and PE-0.1HARC is 92.45%. This is due to high aspect ratio and surface area of CNTs which are sufficient to cover the polymer particles and giving protection from degradation. Further, more carbon-carbon bonds in HARCs and their self-entanglement do not allow the polymer to melt. Thirdly, HARC reinforcement also induces more crystallinity to the polymer matrix, as discussed before, which makes the structure more stable at higher temperature. As a result, HARC reinforced composite shows more stability at higher temperature as compared to pure polymer. In case of LARCs, the mass loss is much higher than PE, with a 79% remaining for PE-0.1LARC and 71% for PE-0.05LARC at 400 °C. It is due to the fact that uniformly dispersed stiff fibers expose their surface freely resulting in easy oxidation of amorphous carbon present in the CNTs and other carbonaceous impurity. Further, LARC reinforcement decreases the crystallinity by disturbing the polymer chain arrangement, which leads to increase in amorphous region. Polymer chains in amorphous regions easily degrade when it is exposed to higher temperature. Hence, more mass loss is found in composite with less concentration of LARCs as compared to pure PE. But, increasing the concentration of LARCs reduces the mass loss to some extent, because more CNTs will stabilize the composite by covering polymer and also due to the presence of more carbon-carbon bonds.

As a whole, it can be conceived that even low concentration of HARCs are also capable of significantly improving the thermal stability of polyethylene matrix. Besides, HARCs are contributing for increasing the crystallinity in the PE composite.

6.1.3 Effect of CNTs Aspect Ratio on Hardness and Elastic Modulus

The mechanical properties of the composites are evaluated through instrumented indentation technique. Fig 6.5 shows the representative load-displacement plots obtained from nano indentation test of different compositions with a depth controlled indentation mode. It can be

observed that the load required to attain 150 nm depth of indent is higher for all the CNT reinforced PE composite. Presence of CNTs in polymer matrix helps to sharing load and thus the composites show higher hardness and elastic modulus.

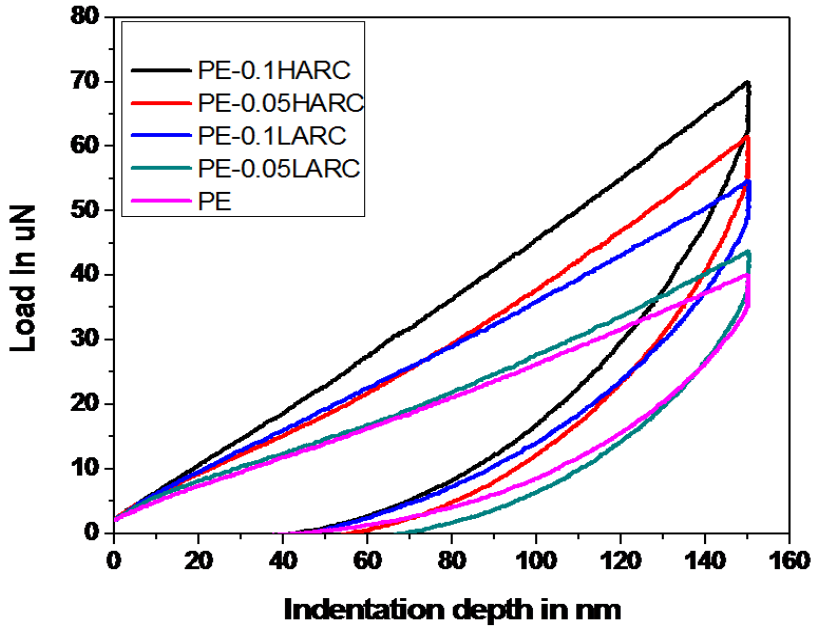

Fig. 6.5 *Representative load displacement curves obtained from nano-indentation tests for prepared composite*

Fig. 6.6 shows the average hardness and elastic modulus values and their standard deviations for at least 25 indents on each composition. Improvement in hardness and modulus is observed in the range of 3-45% and 8-42%, respectively, with increasing the concentration of different aspect ratio CNT reinforcement. PE-0.05HARC shows 13% and 29% improvement in hardness and elastic modulus as compared to pure PE. But, in case of PE-0.05LARC, a smaller improvement of 3% in hardness and 8% in elastic modulus is recorded. This result clearly indicates that HARCs have an edge over LARCs in terms of mechanical behavior of the composite. Same trend is observed in case of composite with 0.1 wt.% nano-fillers. PE-0.01HARCs show an impressive improvement of 45% in hardness and 42% in modulus, whereas the improvement in case of PE-0.1LARC is 19% in hardness and 28% in elastic modulus over pure PE.

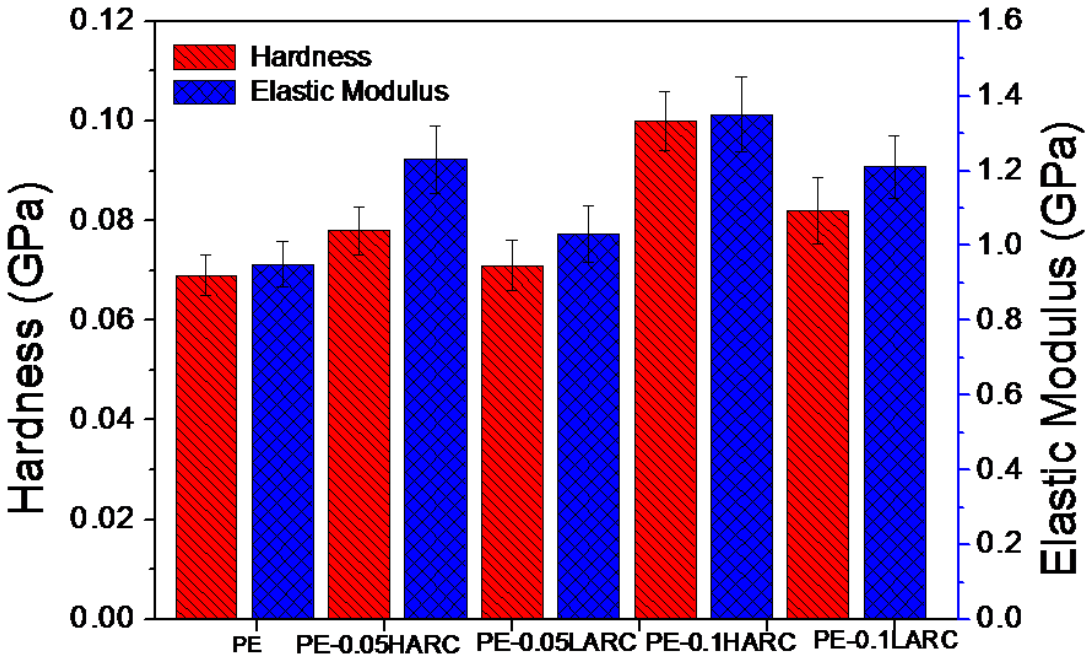

Fig. 6.6 *Hardness and Elastic modulus of different compositions obtained from nanoindentation*

Appreciable improvement in mechanical properties for composites reinforced with HARCs can be explained in terms of their high surface area to volume ratio and interfacial strength. These factors increase the load transfer efficiency to the CNT network throughout the composite uniformly and avoid the failure due to high stress concentration. Cipiriano et al. [255] have also noticed positive effect of aspect ratio of CNT on storage modulus, elastic modulus and viscoelastic property of polystyrene/CNT composite. HARCs, in the present study, have diameter of 10-12 nm, which is in much closer range to typical polymer chains with diameter range of ~1-3 nm [256]. This opens up two possibilities. Firstly, the HARCs can align themselves along polymer chains, increasing a better interfacial bond area and thus more effective load transfer. Further, due to the similar diameter and the broken C-C bonds present in CNT, they can act as cross linkers between polymer chains and making the inter-chain sliding difficult. This in turn restricts the plastic deformation and increases the strength of the polymer. In case of LARCs, due to their huge

mismatch in size (diameter) with the polymer, they cannot align or act as cross-linkers. Rather, they are potential cause of disturbance in the arrangement of polymer chains, decreasing the strength. This hypothesis is explained with the help of a schematic presented in fig 6.7.

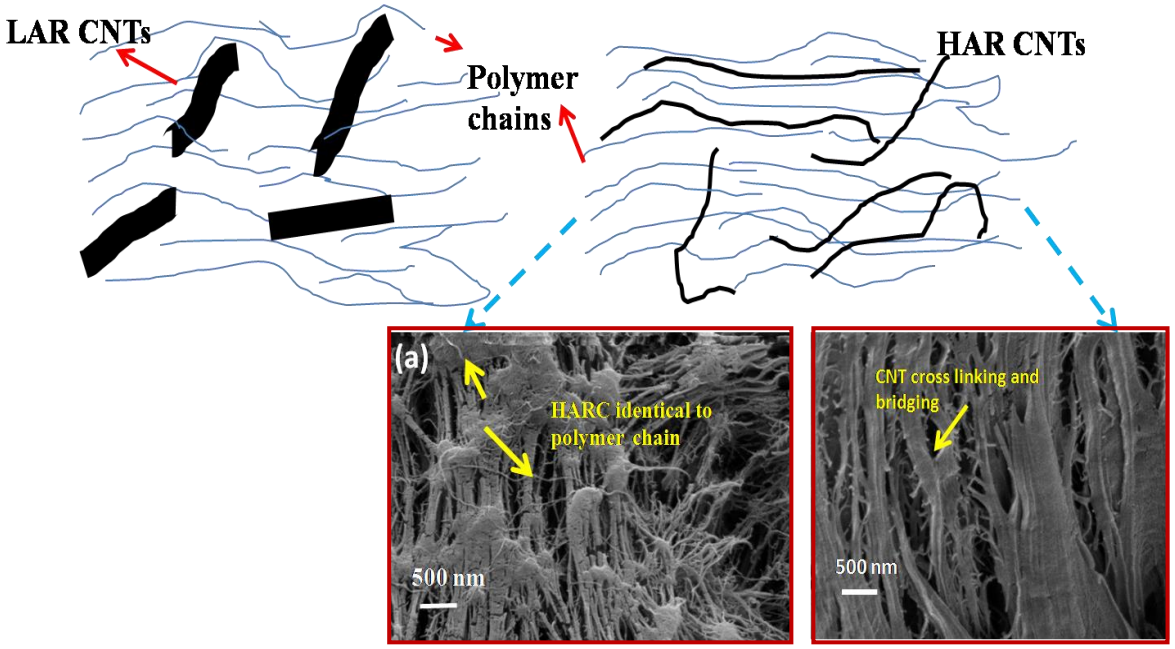

Fig. 6.7 *Graphical representation of the effect of CNT aspect ratio while interacting with polymer chains*

Further, at identical composition level, the high aspect ratio CNTs have more number of total flocks as compared to low aspect ratio CNTs, resulting in percolation network with compact structure. This increases the micro mechanical interlocking of CNT and polymer chains, holding the matrix together and restricting the movement of polymer chains through creating bridges. In case of LARCs, chances of interfacial bonding and mechanical locking are lesser due to their larger diameter and shorter length. Thus, the mechanisms of strengthening in HARCs are manifold, as compared to LARCs with only sharing of load through interface. This explains the significantly higher hardness and elastic modulus in polymer matrix with HARC reinforcement as compared to LARCs. The reinforcement potential of fibers as a function of their aspect ratio and volume fraction has been explained by some theoretical models. Amongst these, Shear lag based models

and Halphin–Tsai models are widely used. A modified form of Halpin Tsai relationship, as proposed by S. Kanagarj [250][43] and Jonathan N. et al [257], gives a simpler approach getting rid of information related to the thickness of interfacial region and fiber alignment direction. Thus, this one is more suitable for present study with randomly oriented nanotubes well adhered in the polymer matrix. In this model, both volume fraction and aspect ratio of CNT are considered to estimate the elastic modulus, as following:

$$E_C = (\eta_1 \eta_o \, E_{CNT} - E_{PE}) V_{CNT} + E_{PE} \quad \text{..... (6.1)}$$

Where, η_1 = length efficiency factor $= 1 - \dfrac{\tanh(a - 1/d)}{(a - 1/d)}$, $a = \sqrt{\dfrac{-3E_{PE}}{2E_{CNT} \ln(V_{CNT})}}$

η_o = Orientation efficiency factor = 0.2 for randomly oriented fiber, young's modulus of CNT is taken as 910 GPa [258] and for PE is 0.95 GPa obtained from this study.

The above expression is used for estimating the theoretical elastic modulus of different compositions used in this study. Fig 6.8 shows the comparison of experimental and theoretical elastic modulus for the two selected aspect ratios of CNTs. It can be observed that modified Halpin-Tsai model predicted values are in the similar range to that of the experimental values. Further, regression analysis was done to verify how this experimental result fits to the theoretical results. R^2 (coefficient of determination) values were calculated for both HARC and LARC in different volume fraction. The R^2 values for HARC are 0.822 and LARC is 0.957, which indicates linear relationship between the predicted theoretical and experimental results of the composite. Halpin Tsai equation fits very well for low volume fraction. But linear increase of modulus is predicted for higher volume fraction [257] as shown in fig 6.8. Thus, this model is a better fit for this study, as the volume fraction of reinforcement is < 0.1 wt. % in all cases. High aspect ratio CNTs have shown high modulus because a good fraction of isolated nanotubes is potentially

aligned with polymer chains, which leads to high interfacial bond and cross linking of polymer chains. Fig 6.7 clearly shows HARCs aligned along the direction of polymer chains in fracture surface of the composite. The strong coating of polymer around the CNT and their interfacial bonding can easily transfer the external load to CNTs and help in avoiding the rupturing of polymer chains as well as in minimizing the stress concentration in the composite.

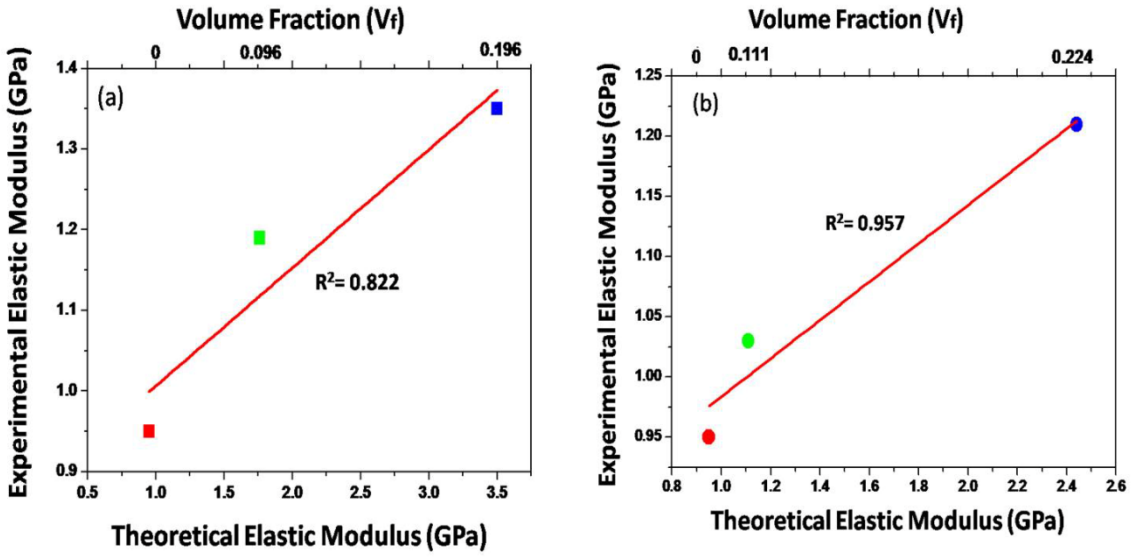

Fig. 6.8 *Regression analysis for the experimental and theoretical elastic modulus of the HARC composite (a) and LARC composite (b)*

6.1.4 Effect of CNTs Aspect Ratio on Tribological Properties

Fig 6.9 shows the average co-efficient of friction (COF) for different concentrations and aspect ratios of CNT reinforced PE composites. The COF increases from zero to peak value during running-in-period due to the influence of surface roughness and thereafter attained a steady state. It is observed that addition of CNTs to polymer remarkably reduces the friction force as compared to pure PE composite. One of the key reasons is the role played by carbon nanotubes as solid lubricants, by releasing graphene layers on wear track [259]. MWCNTs possess concentric cylindrical layers of graphene, bonded to each other with Vander Waals forces [260]. Individual cylinders of multi wall carbon nanotubes are expected to slide or rotate easily with respect to each

other because MWCNT interlayer corrugation energy is small. Therefore, it is expected that decreased friction is due to worn off CNTs acting as a lubricants, like solid powder graphite lubricants [197]. Aspect ratio of the CNTs greatly influenced the friction force irrespective of the concentration. 0.1 wt. % of HARCs and LARCs reduced the COF by 48% and 25%, respectively when compare to PE (fig 6.9). The percolation network formation of CNTs strongly depends on the aspect ratio. It is expected that the HARCs are rooted deeply on the polymer matrix and it contributes to continuous lubrication effects. Fracture surfaces of the composites have also shown longer HARCs protruding out of matrix as compared to LARCs (fig 6.2). This in turn signifies the presence of CNTs in wear track for more time. On the contrary, LARCs tend to break from the polymer matrix and get detached from the track. Thus, they cannot provide as efficient lubrication as HARCs.

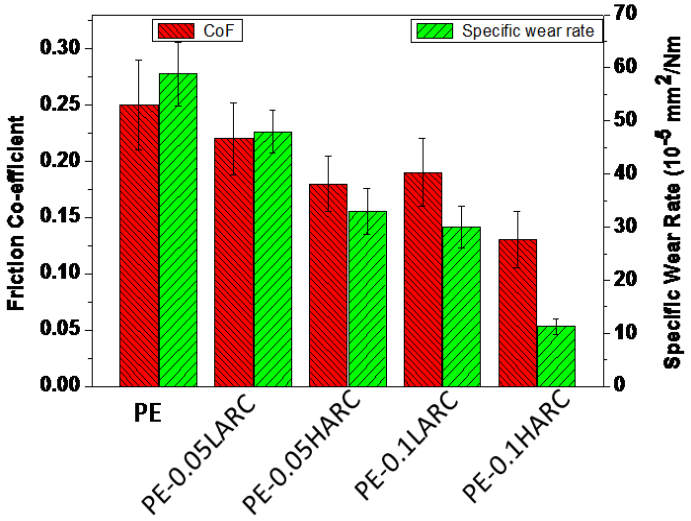

Fig. 6.9 *Variation of friction co-efficient and specific wear rate for the prepared compositions*

The surface profiles of the wear tracks were measured in the transverse direction of the sliding. Fig 6.10 presents the representative profiles of wear tracks in each composition. The average width and depth of the PE track (2.5mm and 35µm respectively) are much higher than that of PE-0.05LARC (2mm and 30µm) and PE-0.05HARC (1.5mm and 17µm). The width and depth

of the track on PE-0.1LARC is 1.5mm and 20µm, respectively as compared to those in PE-0.1HARC being 0.7mm and 4µm. Furthermore, the width and depth of the track decreased remarkably with increasing CNT concentration. Altogether, this shows significant improvement in wear resistance with CNT addition, as well as increasing aspect ratio of CNTs.

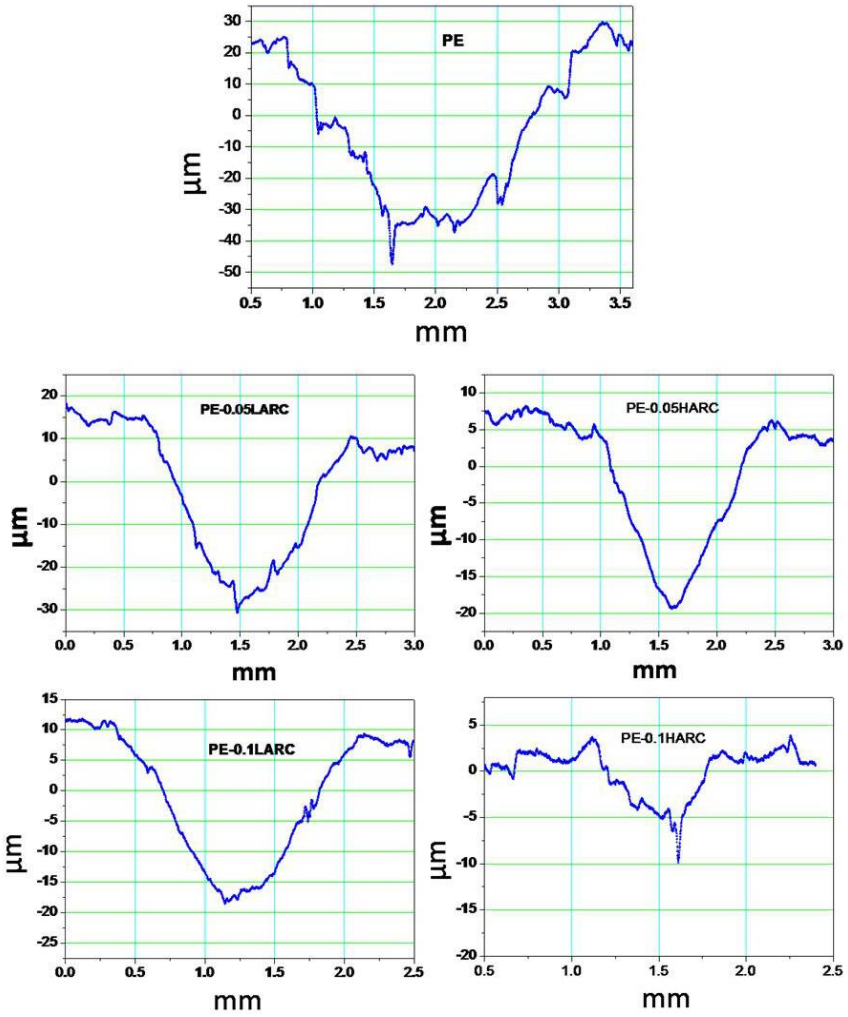

Fig. 6.10 *Wear track surface profile for the prepared composites*

The variation in specific wear rate with composition is shown in fig 6.9. Specific wear rate of PE is 76% and 18% higher than 0.05 wt.% of HARC and LARC, respectively. Besides, addition of 0.1 wt.% of HARC and 0.1wt.% of LARC improves the wear rate by 81% and 45% respectively, when compared with PE. It's interesting to note that, with same identical composition

of CNT reinforcement in PE, lot of improvement in tribological property was observed for high aspect ratio CNTs than low aspect one. This enormous improvement in wear resistance is expected to be a combined effect of increase in mechanical properties and decrease in COF.

The worn surfaces of the prepared composites were examined to understand the predominant wear mechanism (fig 6.11). The continuous sliding causes increased polymer asperities at the tribo-contact with the harder counter body. Further, the elastic plastic deformation of polymer asperity increases the deep furrows due to rubbing action and it further rolls into thin molecular sheets. This results in deeper grooves and generates wear debris on the polymer surface. Deep craters and damages on the rough wear track of PE (fig 6.11a) indicate low wear resistance of this surface. Hard asperities and compaction of wear debris (fig 6.11a′) lead to increase in COF. But, in case of CNTs reinforced composite, smoother wear track surface without broad exfoliation and micro-cracking (fig 6.11 b and c) is observed. Strong interfacial shear resistance of the CNT reinforced composite restricts the ploughing and cutting mechanism. The effective load transfer effect from polymer to CNTs suppresses the plastic deformation and cracking, which all leads to less removal of the polymer chains or particles from the composite. In addition, continuous lubrication effect from CNTs results into a smoother worn surface. During sliding the CNTs are exposed on the surface of the composite, create the interface and prevent direct contact between the counter body surfaces. All these greatly reduce the ploughing and scratching effect in the composite. This effect is predominant in case of HARCs, because these CNTs are deeply rooted with the matrix (fig 6.11c′). But, LARCs come out with the polymer coating. Hence, it fails to give continuous lubrication effect and also increases the debris in the surface (fig 6.11b′).

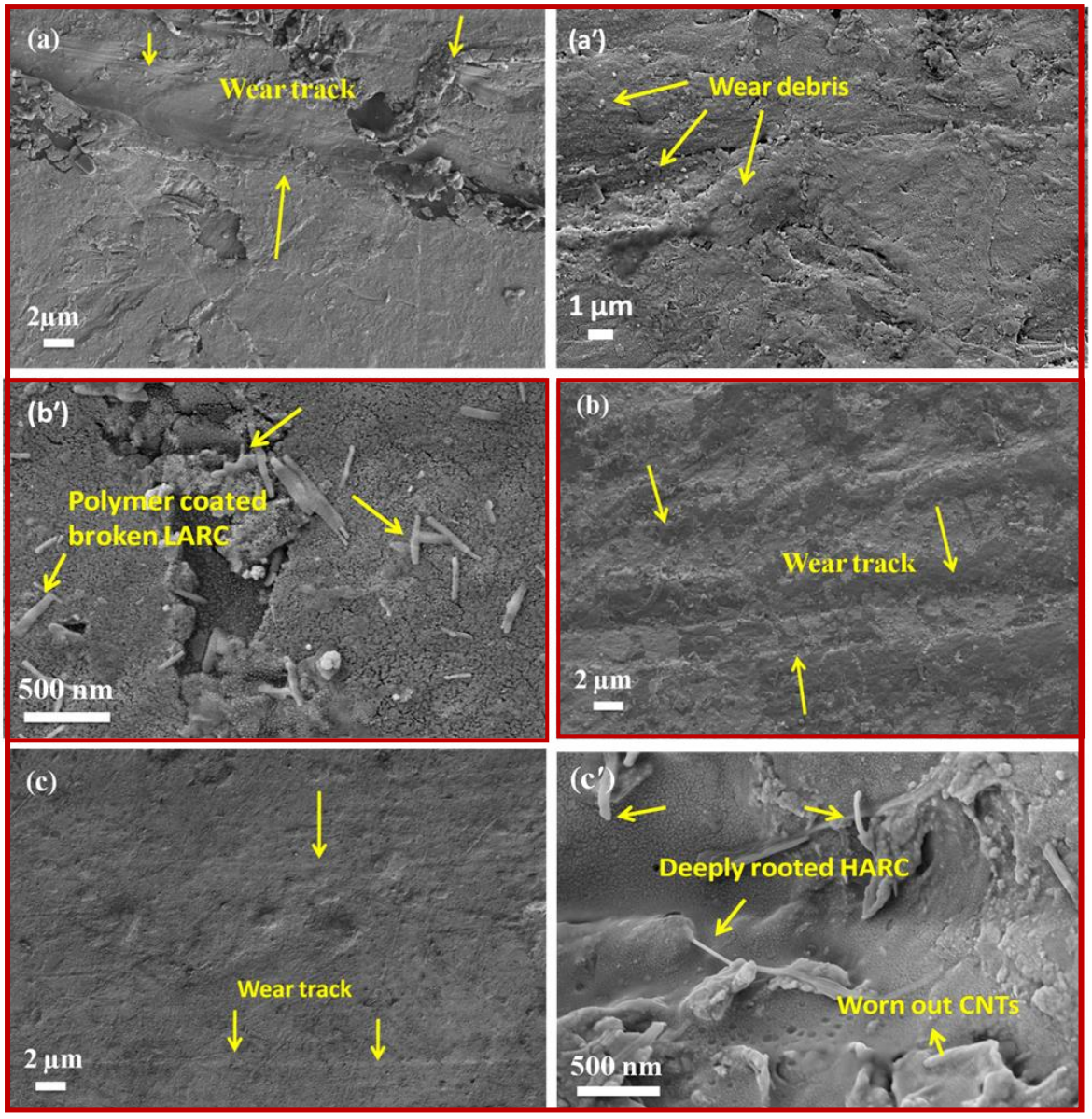

Fig. 6.11 *FE-SEM images of worn surface showing debris contained rough surface in pure PE (a and a') and smooth features in PE-0.1LARC (b-b') and PE-0.1HARC (c-c')*

While comparing the effect of CNT aspect ratio on wear behavior, HARCs are found to show significant improvement over LARCs at both the concentration. HARC composite (fig 6.10) shows shallower and smoother wear track with less width and depth as compared to LARC composite. Smoother wear tracks indicate that the tribological loss is mainly governed by adhesive wear, which results in less wear volume. The effect is more prevalent with increasing nano-filler

content, noting an impressive decrease in specific wear rate of 28% and 62% at 0.05 and 0.1 wt.% of HARC content respectively as compared to similar concentrations of LARCs (fig 6.9). The additional improvement in wear resistance for HARC reinforced composite (w.r.t. LARCs) can be explained in terms of better mechanical behavior and lower COF in the former. HARC associated with strong interfacial bonding to polymer chains and also self-entangled compact structure prevents the easy removal of debris and polymer chain movements. All the above discussions point towards the benefit of using HARCs as reinforcement in PE composite for improving tribological behavior.

6.1.5 Summary

In the present chapter, CNTs having two different aspect ratios (HAR-900 and LAR-75) were reinforced with PE matrix. Composite having higher aspect ratio of CNTs show greater hardness and elastic modulus as compared to lower aspect ratio CNTs. Differential improvement in mechanical properties of composite with HARCs and LARCs are explained in terms high surface area to volume ratio and strong interfacial bonding in the former, which increases the load transfer ability from matrix to CNT. Thermal stability of the composite containing HARCs is also better as compared to LARCs. Tribological behavior of the composites reveal significantly lower coefficient of friction and specific wear rate for HARC reinforced composites, which is the ideal requirement for its intended application in orthopedic joints. Better attachment of HARCs to polymer matrix and their morphological similarity to polymer chains are found to be important factors in fortifying their dual role as toughened and solid lubricator for polymer matrix.

CHAPTER 7

Surface Modified CNT Reinforced PE Composite

Previous chapters have described successful modification of the surface of PE and demonstrated the experimental feasibility of sustained drug delivery. But such modification causes deterioration of mechanical properties of the cup to some extent. Hence, an effort on reinforcing CNTs to PE is being presented in this chapter. The aim of this study is to enhance the initial mechanical property of the matrix and to take care of the issue related surface modification. Prepared composite surface was modified with thin porous surface layer by solvent-based etching and lyophilization technique. Drug contained chitosan is impregnated into porous surface through impregnation chamber by applying vacuum and pressure. These modified and drug loaded surfaces are characterized for mechanical and tribological properties. The drug releasing behavior of such surface and the efficacy of fighting against bacterial infection also evaluated and analyzed. Besides, in-vitro biocompatibility of surface modified CNT/PE composite is assed with osteoblasts. The findings of this study leads to a potential surface modification of acetabular cup liner in total hip implant, which can fight bacterial infection in-vivo.

Manoj Kumar R, et al. ***"Surface Modification of CNT Reinforced UHMWPE Composite for Sustained Drug Delivery"*** *Journal of Drug Delivery Science and Technology, Vol 52, 2019, Page 748-759*

7.1 Results and Discussion

7.1.1 Microstructural Characterization of Modified Porous Surface

Different aspect ratios of CNTs, with different concentration, were tried in previous chapter to get the optimized mechanical and tribological property of the PE composite [1]. The present chapter uses the best composition from that study, which is 0.1 wt.% high aspect ratio CNTs (HARC) reinforced PE composite. Briefly, the average aspect ratio of CNT (ratio of average length to diameter) and density is ~900 and 1.8 g/cm^3, respectively. HARC is having outer diameter of 10-12 nm and length of 8-12 µm (fig 7.1a). As received CNTs was dispersed uniformly in the acetone, using probe sonicator. Around 30 minutes of sonication was carried out continuously with the power of 500 watts and frequency 20 kHz to break the agglomeration of CNT. After that, PE powder was slowly added into CNT dispersed solution and was sonicated for another 30 minutes to maintain the good dispersion of CNTs in the PE matrix. Nicely dispersed and attached CNTs on PE surface were found in SEM, after drying the composite powder in hot air oven at 60 °C (fig 7.1b).

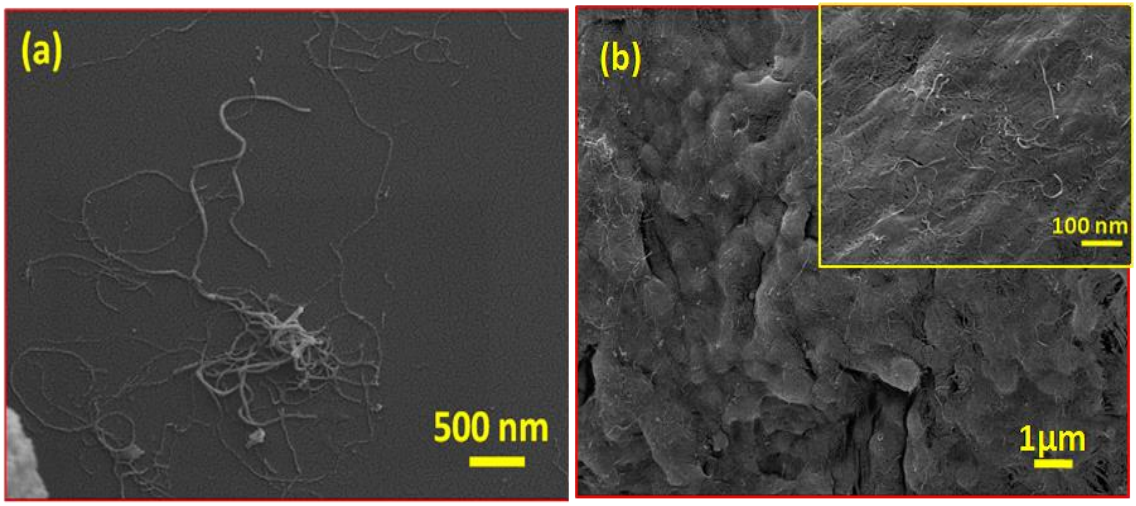

Fig. 7.1 *Shows (a) the as received HARC and (b) uniform dispersion of HARCs on PE powder*

Probe sonication has been found to be very efficient method for distributing the CNTs homogeneously with PE powder. Dispersion is important for successful utilization of the entire reinforcement volume in getting better mechanical/tribological property in the composite structure. The fracture surface of cured pellets reveals very good integrity between CNTs and PE (fig 7.2a). Polymer matrix nicely wrapped the CNTs. These deep rooted CNTs can enhance load transfer efficiency by strong interfacial bonding with the polymer matrix. Besides, addition of CNTs increases the crystallinity of the PE composite, as shown in previous studies [198][211]. More than 3% of increase in crystallinity was found by reinforcing the 0.1 wt% of CNTs [198]. Superior thermal conductivity of CNT 3000 W/mK [252] and higher aspect ratios increases the melt viscosity of polymer molecules and nucleation sites for crystallization. Excellent specific heat of CNTs (Cp = 0.75 Jg^{-1} K^{-1} at 300 K[254] generates the heat pool in the composite and thermodynamically helps in increasing the crystallinity. Overall improved crystallinity and good interfacial bonding attributes to the superior mechanical behavior of the composite. Modified chemical etching, followed by lyophilization, was used to engineer interconnected micro pores on PE surface in the previous chapter (chapter 4) [69]. Same method is used in the CNT reinforced PE composite (C-PE). Briefly, surface chemical dissolution occurs by pouring the boiling paraxylene on C-PE. Further, immediate freezing of boiling paraxylene on C-PE surface avoids full dissolution of the surface layer. During lyophilization, frozen crystal of paraxylene evaporates due to high vacuum and leaves thin porous layer on surface, as seen in fig 7.2b. An average surface porosity of C-PE is 27 ±6 %., which is 18% lesser than the porosity in PE (33 ± 5 %) (fig7.2c). Decrease in porosity was found due to matrix strength. Enhanced composite strength and 3% increased crystallinity restricts the boiling paraxylene to dissolve the surface easily.

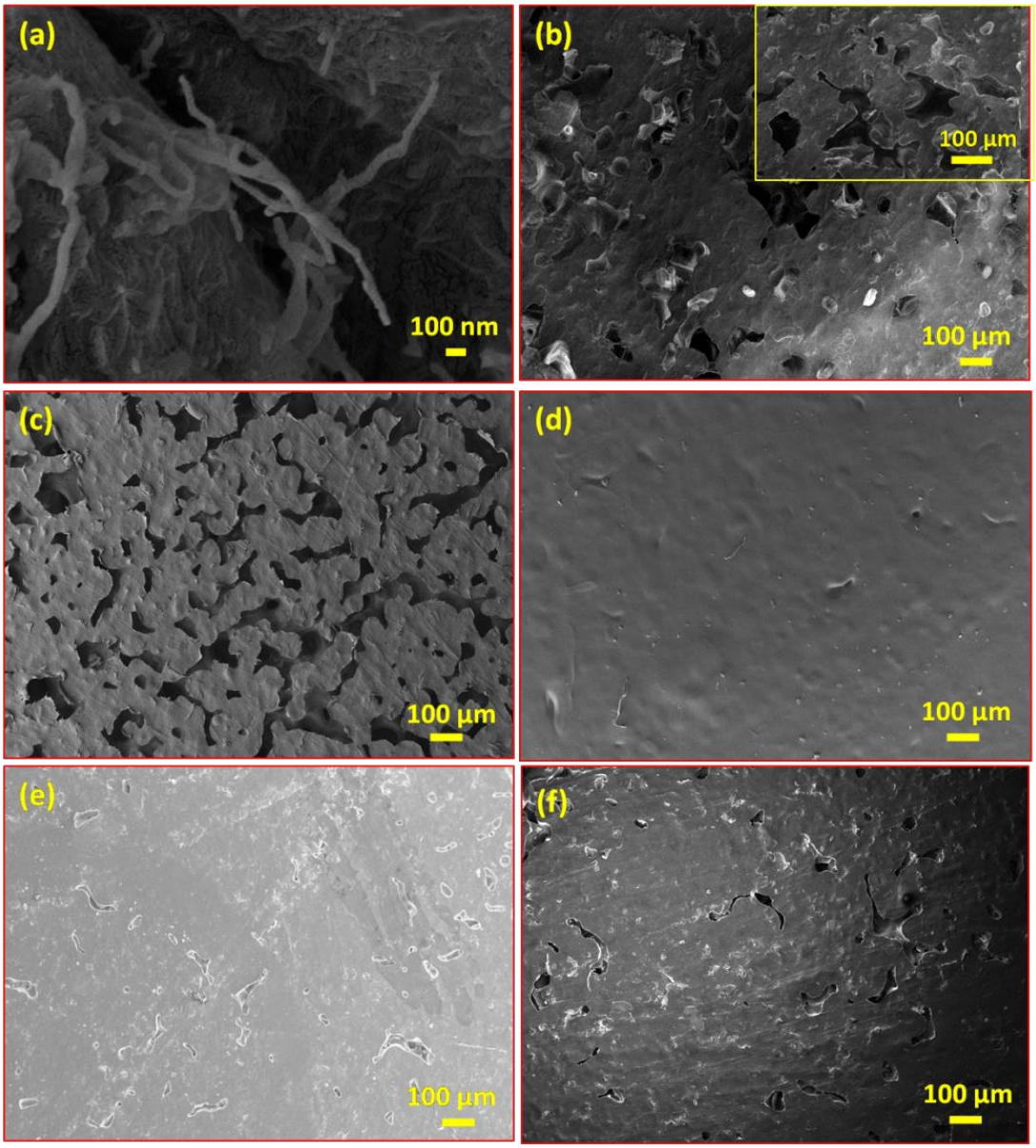

Fig. 7.2 *(a) Fracture surface of the composite; (b& C) modified C-PE surface and PE surface with micro pores; (d) drug loaded chitosan impregnated CI-C-PE surface and (e) after the drug release AD-PE surface; (f) after drug release AD-C-PE surface*

Customized impregnation chamber was used to fill the drug (gentamicin) loaded chitosan solution into micro pores. Entrapped air in pores were removed by applying 1 mbar vacuum, after which drug loaded chitosan was poured on surface to get sucked in the evacuated pores. After that 3 bar external pressure was applied on the surface to ensure effective filling of the pores. Fig 7.2d

shows the surface of drug loaded chitosan impregnated C-PE sample (CI-C-PE). The surface shows a smoother contour with no traces of open or unfilled pores. This surface modified composite is further evaluated for drug releasing kinetics, antibacterial efficacy, mechanical and tribological behavior. After the drug is released, the AD-PE surface is much smoothened with rare traces of pores as compared to AD-C-PE (fig 7.2e). Smoothened surface was found due to collapsing of the thin walls of pores during drug release kinetics. When samples were exposed to PBS for drug release study, hydrophilic and gel forming nature of chitosan starts swelling substantially inside the pores. As a result, pore walls experience large amount of compressive stress and walls deforming into thinner plates to accommodate the expanded volume. After drug release and chitosan degradation, the thin walls cannot retain their integrity and collapses. The procedure of collapsing takes place over a time period, simultaneously with degradation of chitosan [69]. This happening makes the final surface of PE smoother, reduces the volume and existence of pores (fig 7.2e). But, in case of composite surface (AD-C-PE), the existence of pores is much higher than PE after drug release (fig 7.2f). Because of higher matrix strength and thicker pores walls (fig 7.2b), some of the pore walls are not collapsed. Hence, surface of the composite after drug release (AD-C-PE) appears relatively rougher (R_a= 1.51± 0.410 µm) than PE surface (R_a=1.366 ± 0.300 µm). These differential evolutions of surface morphologies are supposed to have different effect on drug releasing, mechanical and tribological behavior, which are investigated and analyzed in following sections.

7.1.2 In Vitro Releasing Kinetics

Main interest about this surface modification and impregnation process was related to the controlled drug release for longer time to reduce the infection around the surgical area. Hence, a triplicate of samples was impregnated with 20 mg of gentamicin contained 1 ml chitosan (CI-C-

PE). Around 13 mg (65%) of gentamicin was successfully loaded on composite modified surface (CI-C-PE). Whereas, in PE modified surface got loaded with 14.1 mg (70%) of gentamicin (CI-PE) [69]. Decrease in drug loading concentration is directly attributed to surface porosity, ~18 % of lesser porosity in C-PE surface leading to 5% of decrease in drug loading capacity. Weight difference technique was used to calculate the percentage of drug loading. Fig 7.3 shows cumulative release of drug with respect to specified time. The CI-C-PE has shown a sustained release of gentamicin until 492 h (21 days) and CI-PE shown 624 h (26 days) [69]. Initial burst release, followed by a relatively slower release, is an ideal drug delivery system. This type of antibiotic release profile is highly desirable for orthopedic implant surgery. Higher amount of antibiotics is required initially to prevent infection and eradicate the bacteria from the surgical area, as well as, from implant surface. Sustained release for many weeks is essential to fight against the late infection [20].

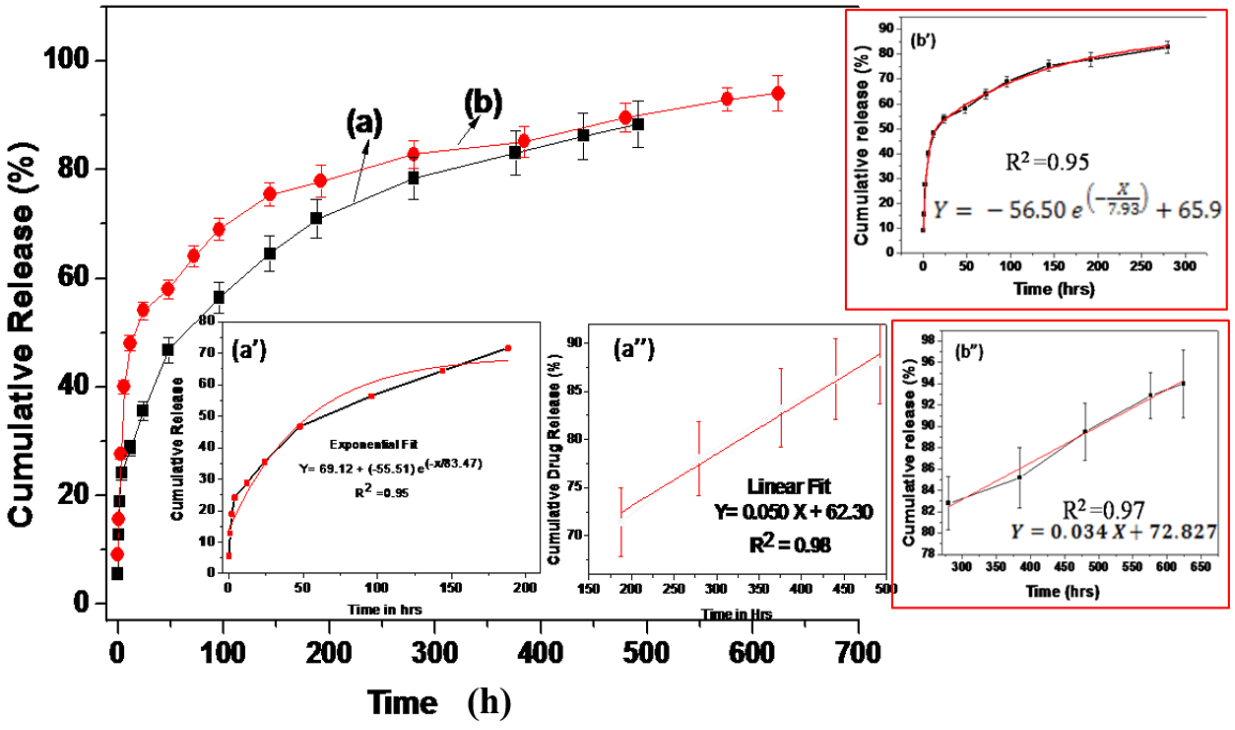

Fig. 7.3 *In vitro cumulative gentamicin release profile of (a) CI-C-PE modified surface up to 492 h and (b) CI-PE modified surface up to 624 h*

The entire release profile can be analyzed as two distinct behavioral categories. The first part denotes a burst release phase and it found up to 200 h, where the amount of gentamicin released decreases slowly with time. This typical characteristic graph is best fitted with an exponential curve fit, as seen in Fig 7.3a'. This fit indicates the domination of diffusion mechanism in the drug release profile. During this period, ~71% of drug got released in exponential manner. Second phase of release profile continues during the period of 200 to 492 h and is best fitted with linear equation (R^2 = 0.98). The slope of linear curve is used to measure the percentage of gentamicin released. It is found that ~1.257 mg (17.2 %) of gentamicin got released in continuous manner with a rate of 0.0043 mg/h. This behavior is dominated by gradual degradation of the drug-containing chitosan. The total cumulative percentage of gentamicin released from CI-C-PE was about 89% over 492 h. Same trend of drug release kinetics was found in surface modified CI-PE. Burst release phase continued up to 280 h. During this period, ~83% of drug got released in exponential manner (fig 7.3b'). It was followed by sustained release is observed during the period of 280 to 624 h. Around 1.513 mg (13.2 %) of drug is released in liner manner with a rate of 0.0043 mg/h and cumulative percentage of drug release was 94% over 624 h [69]. More sustained release behavior was observed in CI-PE as compare to composite surface, due to higher amount of drug loading capabilities and complete degradation of chitosan by collapsing most of the pores on surface (fig 7.2e). But, drug loading and releasing efficiency of CI-C-PE can be increased by trying with other synthetic biodegradable polymer. Biodegradable and non-toxic chitosan serves ideal carrier for controlled gentamicin release. Various factors may influence the kinetics gentamicin release from chitosan. Burst releasing of gentamicin can be attributed due to its high water solubility and low molecular weight. Besides, sustained gentamicin release is due to slow degradation of chitosan. During drug release, the reaction between amine groups of chitosan and

phosphate $(PO_4)^{3-}$ ions in PBS might lead to crosslinking of the chitosan, which leads to lower and sustained release of gentamicin [261]. Analysis of this section shows the surface modification effect on gentamicin loading and releasing.

7.1.3 Antimicrobial and Biocompatibility study

The antibiotic resistance test against *S. Aureus* was performed to assess the effectiveness of gentamicin release from CI-C-PE. Two third of the chronic osteomyelitis infection are caused due to gram positive bacteria (S. Aureus). Fig 7.4 reveals the antibacterial activity of CI-C-PE and CI-PE, when exposed to 5 days of S. Aureus culture. The experiment was carried out by using the agar disc diffusion method. Three different drug concentrations (10, 15 and 20 mg) were used to test the efficacy of low to high drug content to eradicate bacterial strains. All the surface modified CI-C-PE samples have displayed clear bacterial inhibition rings in agar plate (marked in yellow dotted line in fig 7.4b). Besides, no such bacteria free area was found around the unmodified C-PE. In all five days of culture, the trend of bacterial inhabitation remains same. This shows the potential importance of drug loaded CI-C-PE surface in fighting against infection. Low concentration (10 mg) of gentamicin also effectively eradicated the gram-positive bacteria around it, even when exposed to high concentrations of microbes. Besides, almost same trend of antibacterial effectiveness was found in surface modified CI-PE (fig 7.4a). The diameter of ZOI (zone of inhibition) is also changes with drug concentration (fig 7.4c). Different drug concentrations and its antibacterial efficiency are presented in fig 7.4c. The increase in antibacterial efficiency was found with increase in the drug concentration (10 to 20 mg/ml) and also with time (day 1 to day 5).

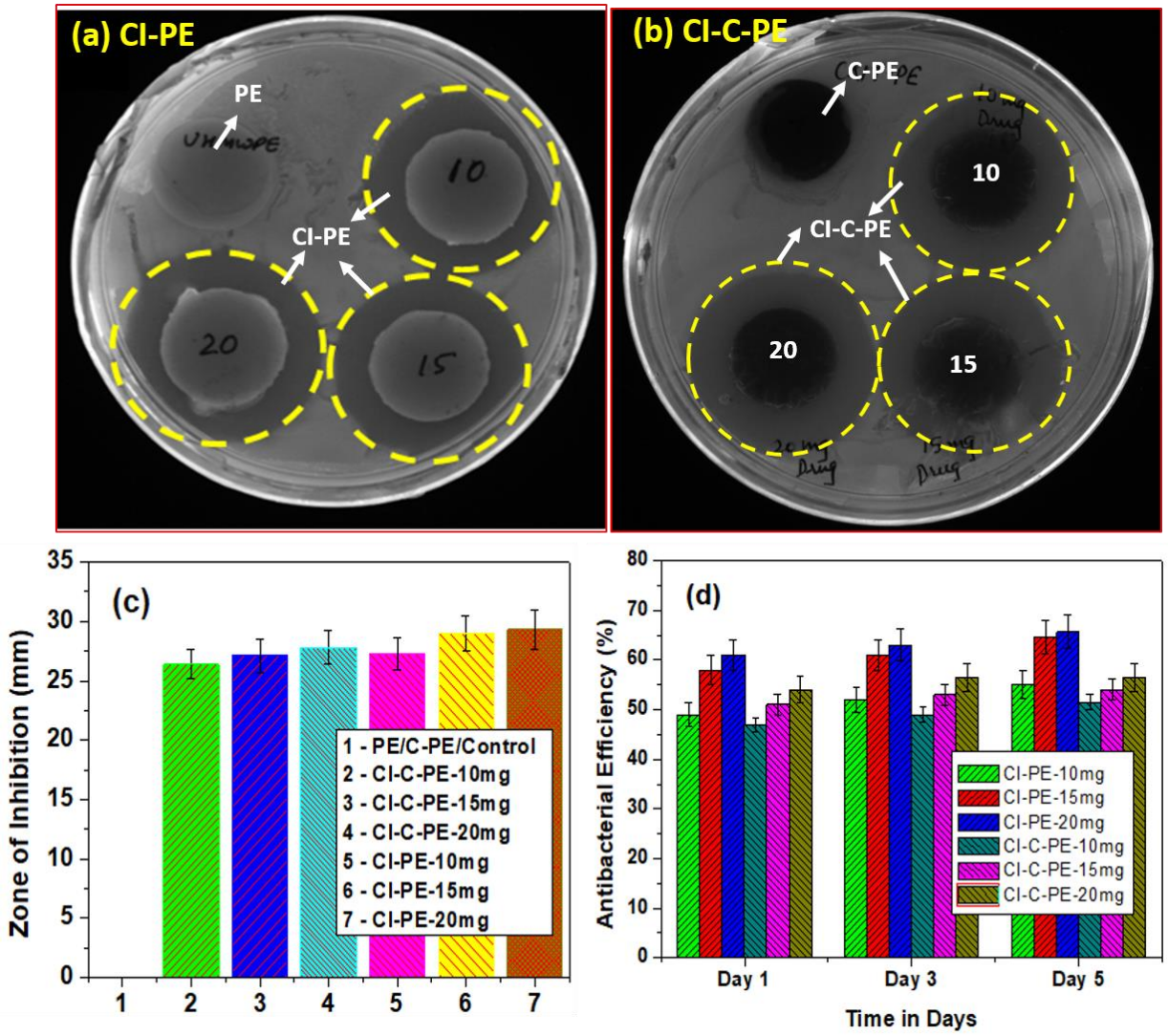

Fig. 7.4*a Shows images of agar disc diffusion test after 3 days of incubation, revealing bacterial inhabitation zones for PE and CI-PE; (b) for C-PE and CI-C-PE (10 to 20 mg concentration) respectively; (c) diameters of zone of inhibition (ZOI) of different test sample; (d) antibacterial efficiency rate with respect to time and drug concentration for CI-PE and CI-C-PE. respectively.*

SEM investigation was also done after incubation to examine the grown bacteria on each test sample. High population of bacteria growth with the passage of time was found on the surface of unmodified PE and C-PE (fig 7.5b & d). In contrast, no such bacterial cells and trace of biofilm was noticed on the drug loaded CI-PE and CI-C- PE surfaces (fig 7.5a & c) and same thing was also observed on drug loaded PE surface (5). This characterization suggests antimicrobial effectiveness of drug impregnated CI-PE and CI-C-PE implant in long run.

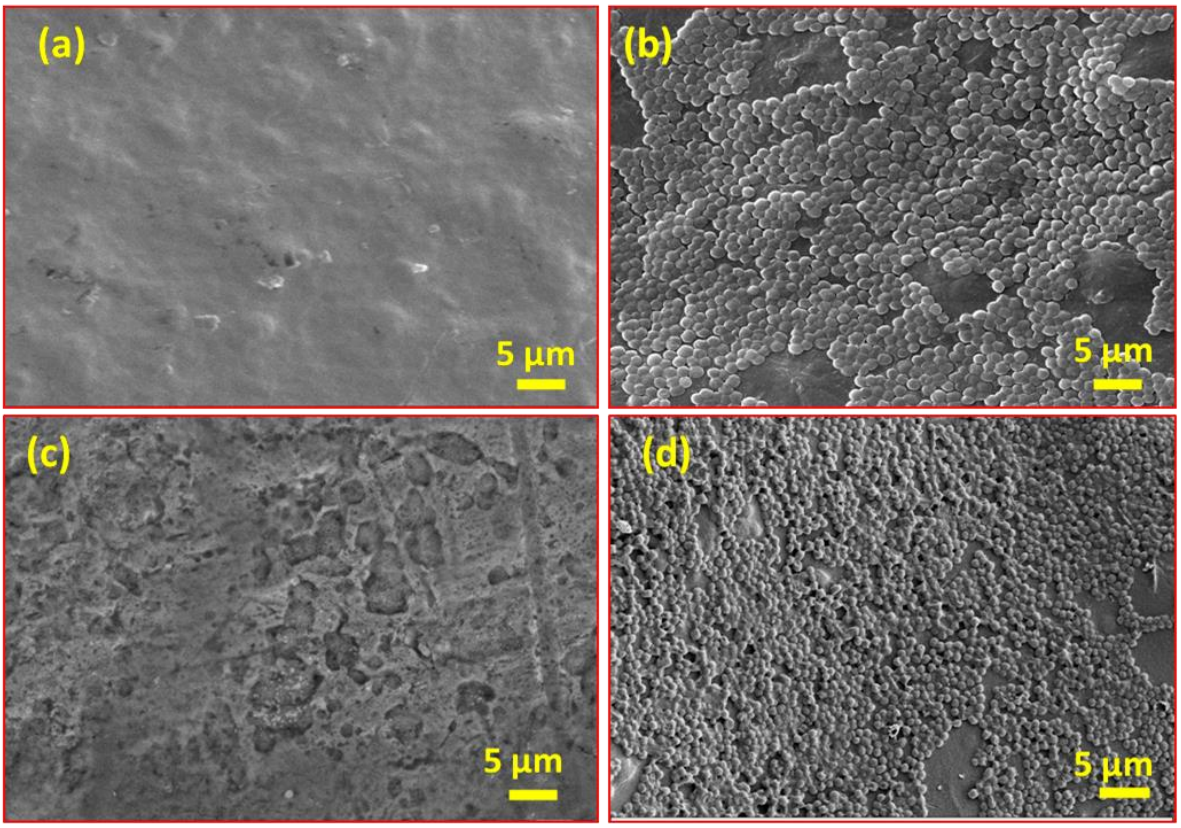

Fig. 7.5 *SEM images showing the antibacterial activity on (a & c) unmodified PE and C-PE surface and (b & d) drug loaded (20 mg/ml) CI-PE and CI-C-PE surface, for 3 days of culture.*

The surface modified implants, in the current study, are intended for orthopedic application. Therefore, it is very important to make sure that they are cytocompatible. We chose MG-63 cells for this study because they can be directed towards osteogenic differentiation. Cell survival and proliferation in the presence of the implants were evaluated through MTT assay and DAPI staining, respectively. MTT is a colorimetric assay to assess the metabolic state of cells. NAD(P)H dependent mitochondrial membrane associated oxide-reductase enzymes can reduce 3-(4,5-dimethylthiazol-2-yl)-2,5 diphenyltetrazolium bromide (MTT) to water insoluble purple formazan crystals, which are then dissolved in DMSO. Amount of formazan crystals formed is indirectly measured as its OD at 570 nm, which gives a quantitative idea of the metabolic state of the cells under treatment (here, grown on implants), relative to untreated/ control cells (here, grown on regular tissue culture surface). This can be represented as percentage cell survival. DAPI

is a fluorescent dye that stains DNA strongly by binding to the A-T rich regions. This gives blue appearance to the nucleus. Cells take up DAPI stain proportionate to the proliferation rate. Moreover, any chromosomal damage that could eventually translate to reduced cell proliferation due to experimental conditions can also be followed through this staining. Healthy living cells have a typical DAPI stained profile of their nuclei. Any deviation from this would reflect as alteration in the nuclear integrity of the cells. This will be a strong indication of lack of cytocompatibility of the biomaterial under study. Cells grown on tissue culture treated plate were taken as positive control for both the assays.

Four types of samples (implants) were used in the current study to analyze and compare the cytocompatibility results: namely, (1) PE (2) CI-PE (3) C-PE and (4) CI-C-PE. After incubating on these implants for 1, 3 and 5 days, cells show an overall survival comparable to the positive control (Fig. 6). Cells grown on PE and C-PE initially showed around 92-95% survivability after first two days of incubation, but survival rates became comparable to positive control (fig 7.6) and cells became significantly proliferative (fig 7.7 L & N) after 5 days. Our observations show overall better survival and proliferation on chitosan impregnated PE (CI-PE) and chitosan impregnated CNT-PE composite (CI-C-PE) implants (fig. 6; fig. 7, compare panels C, H, M & E, J, O with rest). Although, there is no significant difference in cell survival rates observed for CI-PE and CI-C-PE (fig. 6), the cells appear to be more proliferative when grown in the absence of CNTs. This difference is apparent after 3 and 5 days of incubation (fig 7.7; compare panels H & M with J & O). Their survivability is also higher (~108%) even compared to the control. Our observations on cell survival on the implants fall in line with those from DAPI staining of the cells' nuclei. Magnified single nuclei from a representative cell from each implant and control show a healthy nuclear integrity (fig. 8A-E). A healthy DAPI stained nucleus shows an unstained spot amidst

intense blue background. The unstained spot is the nucleolus populated by more rRNA (a type of RNA) and less DNA (fig 7.8, shown with white arrows). A dying or unhealthy nucleolus will have fragmented nucleolus. Thus, the implants are highly cytocompatible, supports cell proliferation and do not affect the nuclear integrities of the cells. Thus, it can be concluded that even after reinforcing with CNT and surface modification, the acetabular cup liner surface retains the biocompatible nature.

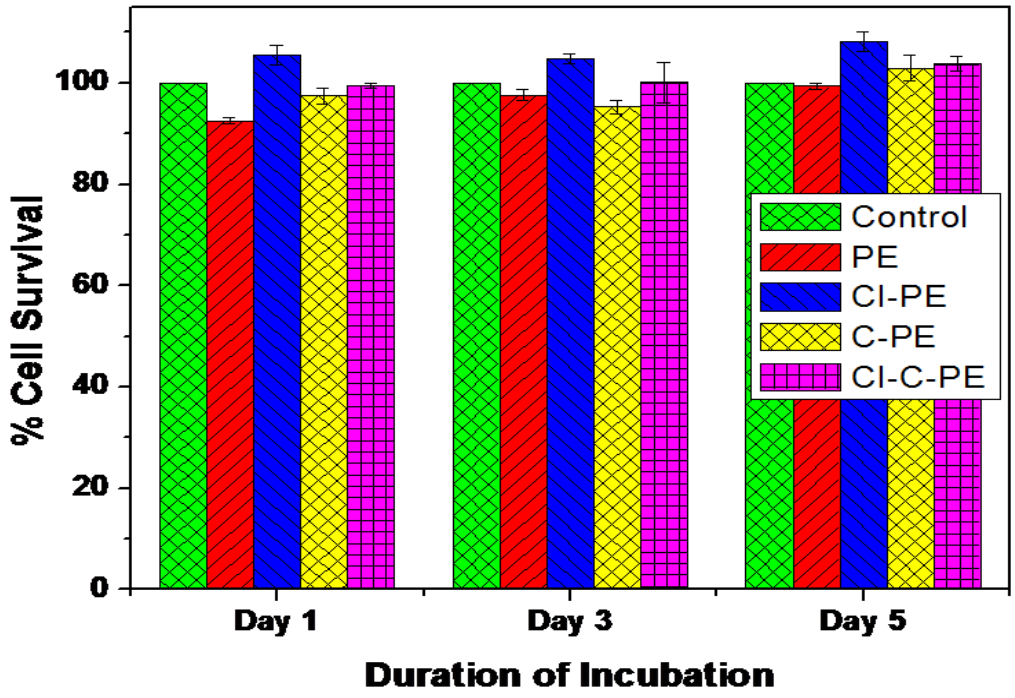

Fig. 7.6 *Cytotoxicity assay to evaluate the effect of implants on cell survival. Quantitative representations of MTT assay as % cell survival of MG-63 cells grown on different surface for 1, 3 and 5 days relative to control cells grown on regular tissue culture plastic ware. Data represents mean ± SD of 3 sets of independent experiments.*

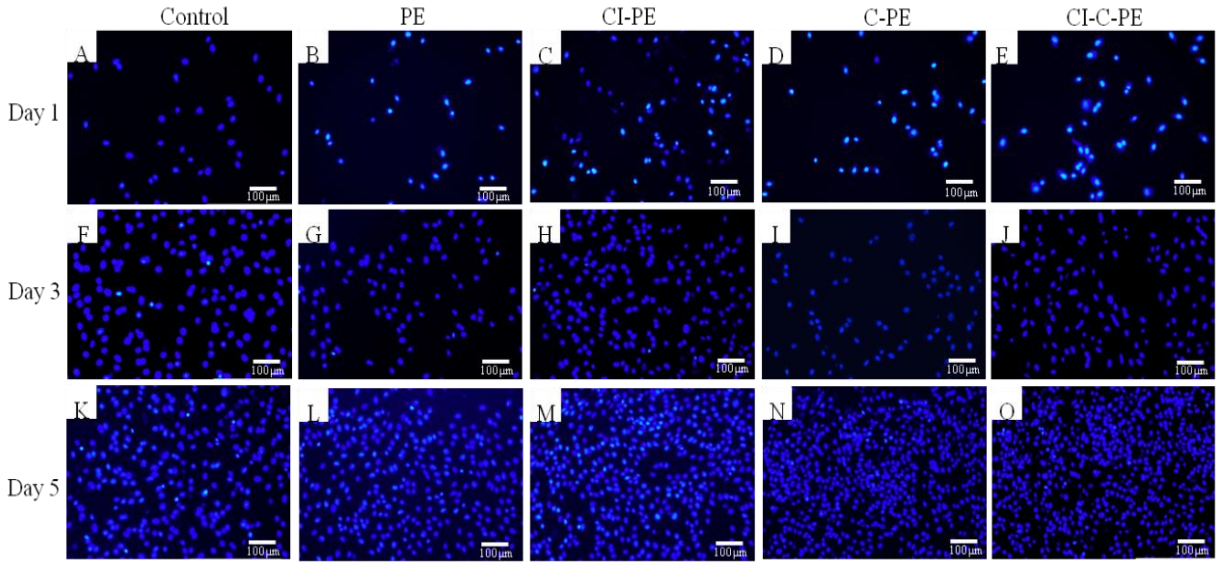

Fig. 7.7 *Nuclear staining shows the proliferation of cells over 5 days. Panels A-E, F-J and K-O shows DAPI stained nuclei of living cells after 1, 3 and 5 day of incubation without implants (A, F & K) and on implants: PE (B, G & L), CI-PE (C, H & M), C-PE (D, I & N) and CI-C-PE (E, J & O). Scale bar =100µm.*

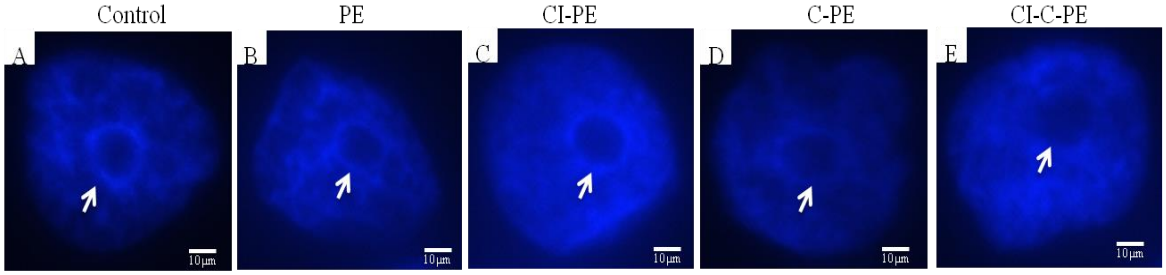

Fig. 7.8 *Nuclear staining shows the nucleolar integrity. Panels A-E, show representative single DAPI- stained nuclei from each group of cells. White arrow head in each panel points towards the intact nucleolar region pertaining to healthy cells in each case. Scale bar =10 µm.*

7.1.4 Mechanical Properties

The mechanical properties of liner in acetabular cup are significantly essential to support skeleton and to bear the body weight, as well as, frictional forces during operational condition. The hardness (H) and young's modulus (E) of different surface modified C-PE samples was measured through instrumented micro indentation technique. Fig 7.9 shows representative indentation load-displacement behavior of different surfaces. Pure PE surface has shown higher indentation depth in

the load-displacement curves, as compare to CI-C-PE, AD-C-PE and C-PE surface. The depth of penetration reached to 43 µm with the application of 2 N loads in pure PE, which is 30% (30 µm), 16% (36 µm) and 20% (34 µm) higher than C-PE, CI-C-PE and AD-C-PE, respectively. Increase in surface resistance against indentation (30%) in C-PE was found due to effective load bearing characteristics of CNT wrapped PE. Even distribution of load bearing center's in the composite effectively transfers the induced stress into matrix uniformly. Surface modified CI-C-PE has shown 14% decrease in resistance as compared to C-PE, which is due to chitosan impregnation in porous surface. But, after drug release and chitosan degradation, the surface (AD-C-PE) regains its mechanical behavior similar to C-PE. But, reinforcement of CNT shows improvement in hardness as compared to surfaces without CNTs, i.e., chitosan impregnated PE (CI-PE) and PE after drug release (AD-PE). Surface hardness of CI-PE is ~19% lesser than PE. After drug release (AD-PE), the hardness is almost similar to PE, with load displacement curves overlapping each other. However, in case of CNT reinforced composite, even after surface modification (CI-C-PE), the hardness is improved (28%) as compared to CI-PE. This was the aim for adding CNT in these modified surfaces.

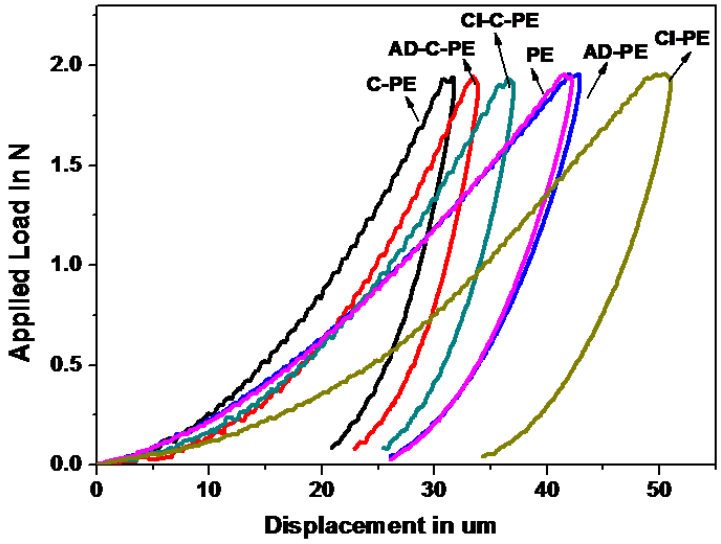

Fig. 7.9 *Representative load verses displacement plots for different test samples*

The hardness and elastic modulus for all the test samples were calculated from the slope of the unloading curve of load-displacement plots. Minimum 20 measurements were taken across the surface in each test sample. An average hardness and modulus is presented with standard deviation as error bars in fig 7.10. Around 38% and 31% increase in hardness and modulus observed in C-PE, as compared to PE. Reasons for significant improvements are the increase in crystallinity and uniform reinforcement of CNTs. Around 17% and 13% decrease in hardness and elastic modulus found in CI-C-PE, as compared to C-PE. Considerable reduction in H and E is due to chitosan impregnation on porous surface. But, when compared to PE, the H and E values of CI-C-PE are still considerably higher, by 20% and 19%, respectively. On the other hand, H and E values of CI-PE is 43% and 35% lesser, respectively, then CI-C-PE. This serves the purpose of adding CNT in the PE composite to retain the mechanical properties even after surface modification.

The mechanical properties of the surface after the drug release (AD-C-PE) are also evaluated to assess the feasibility of surface modification in practical application. The surface regains the hardness and modulus values similar to unmodified C-PE, with only 8% and 6% decrease in H and E recorded. Same trend is observed in case of AD-PE also, with only 7% and 6% decrease in H and E, respectively, as compared to PE. This can be attributed to regaining of surface morphology after drug release (fig 7.2e & f). This happens due to pore-collapsing mechanism being operational, which is explained in details in the previous chapter (chapter 5).

It is important to emphasize here that all modified surfaces of CNT–PE composite and specially the surface after drug loading (CI-C-PE) have offered better resistance against indentation than PE. This indicates that CNT reinforced acetabular cup can maintain its mechanical behavior to require level, even after modification with porous layer and impregnation with drug

containing polymer. This was the reason to reinforce the PE surface with CNTs, which is achieved successfully.

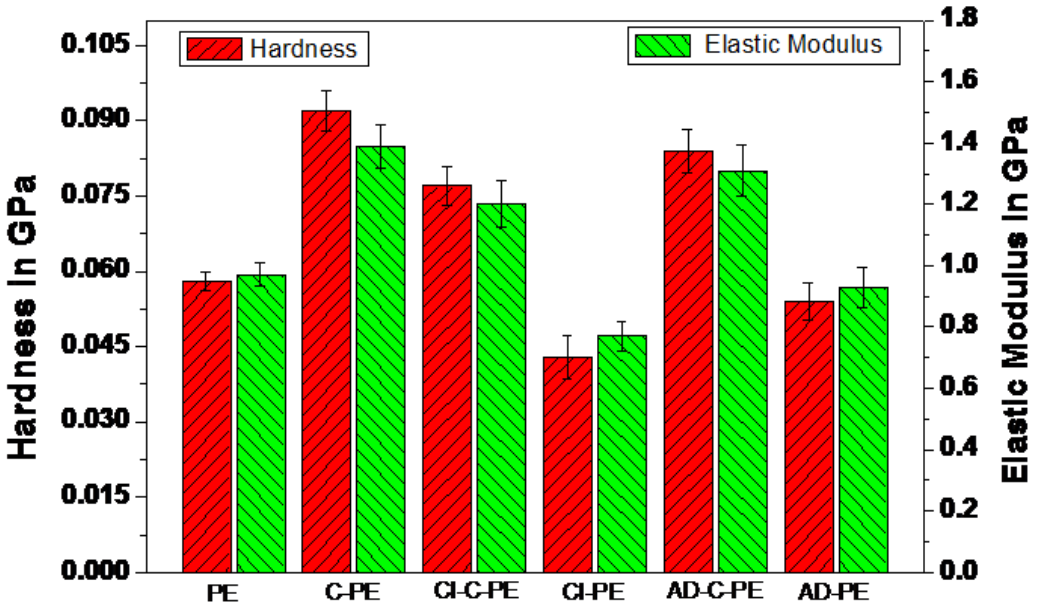

Fig. 7.10 *Represents average hardness and elastic modulus with error bars for all test samples*

7.1.5 Tribological Behaviour on Modified Surface

Hip and knee joints are the two major load-bearing parts of the human body, which are continuously experiencing severe dynamic frictional forces during limb movement. The inner lining of the acetabular cup and femoral head are the two mating parts of the total hip implant, which are continuously facing sever frictional forces during limb actions. Therefore, it is essential to consider the tribological performance of all surface modified C-PE composite, which is being projected for acetabular cup liner. Fig 7.11 demonstrates the variation in friction coefficient (CoF) and specific wear rate for different test surface.

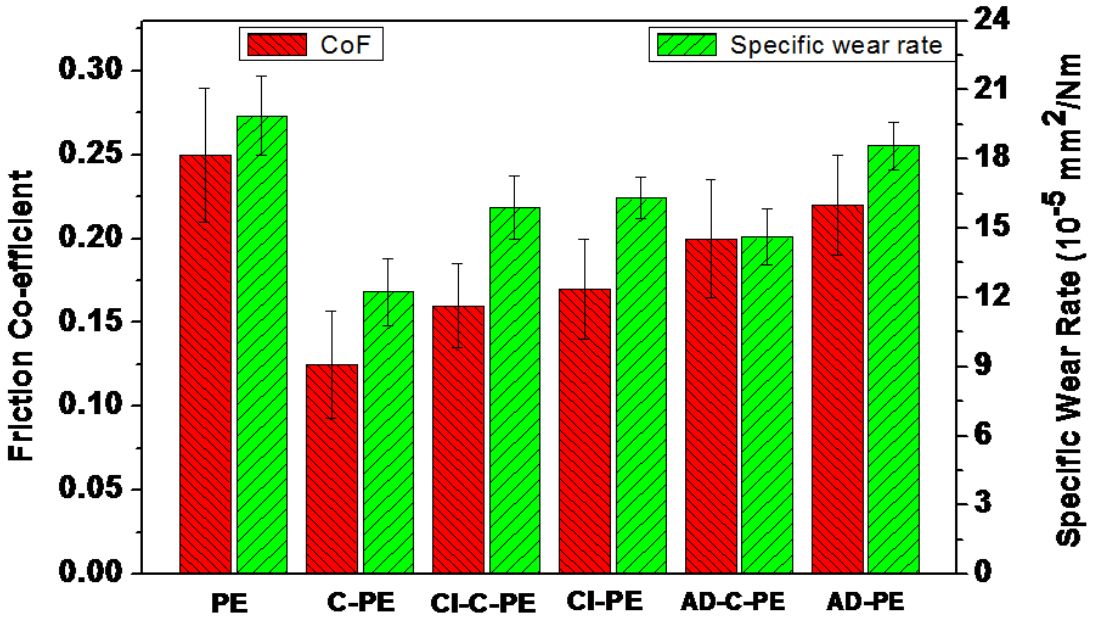

Fig 7.11 *Coefficient of friction and specific wear rate for different test surfaces*

Initially, during ~150 m sliding distance, continuous increase in friction coefficient was observed, followed by attaining of steady state. Reinforcing the 0.1 wt.% of CNT in PE brings down the friction coefficient significantly. More than 48% of decrease in CoF was observed in C-PE than PE, due to self-lubricating nature of CNTs [211]. During the rubbing action, the broken CNTs act as a solid layered graphite lubricant, resulting in lower friction [198]. Chitosan impregnated CI-C-PE and drug released AD-C-PE have also shown 36% and 20% decrease in friction coefficient than PE. On other hand, same trend is noticed for CI-PE and AD-PE, with ~ 27% and 8% decrease in CoF, as compared to PE. Overall, impregnated chitosan (drug loaded) helps as lubricating agent by avoiding the stick-slip mechanism [69] and thus helps in reducing the CoF of CI-C-PE and CI-PE further. In both the cases (CI-C-PE & CI-PE), impregnated chitosan was the key factor for reducing the friction coefficient. Whereas, after drug releasing, by comparing both AD-C-PE and AD-PE, AD-C-PE had shown ~11% decrease in CoF than AD-PE.

Reason for the reduced CoF in AD-C-PE is the left over pores on the surface and CNTs solid lubrication mechanism.

Fig 7.12 shows the 2D line profile across the worn surface of PE, C-PE, CI-C-PE, CI-PE, AD-C-PE and AD-PE. Total volume of material removed from the surface during test and corresponding wear rate were calculated using 2D line profile. The average specific wear rate and its standard deviation are represented as error bar in bar chart fig 7.11. Lowest wear rate was observed in C-PE, which is the combined effect of low friction and good mechanical properties. Furthermore, the improved crystallinity with the addition of CNTs plays a key role in tribological performance. According to an energy-based model, wear rate of PE is mainly dependent on energy dissipation. Crystalline phase shown good damping and fatigue nature by dissipating the applied load [262]. Thus, increasing crystallinity in C-PE facilitate energy dissipation mechanism and reduces the wear rate [211]. Worn surface characteristics also supported self-lubricating mechanism, offered by CNTs fig 7.13b. Deep rooted CNTs suppress the plastic deformation and cracking on the surface during rubbing, which leads less removal of material. But in PE, deep furrows were generated due to continuous elastic plastic deformation of the polymer asperity fig 7.13a, which further ends up with abrasive wear mechanism. Combined effect of higher CoF and lower hardness and modulus decreases the wear resistance of PE surface. CI-C-PE and AD-C-PE have also shown 20% and 26% improvement in wear rate as compared to PE.

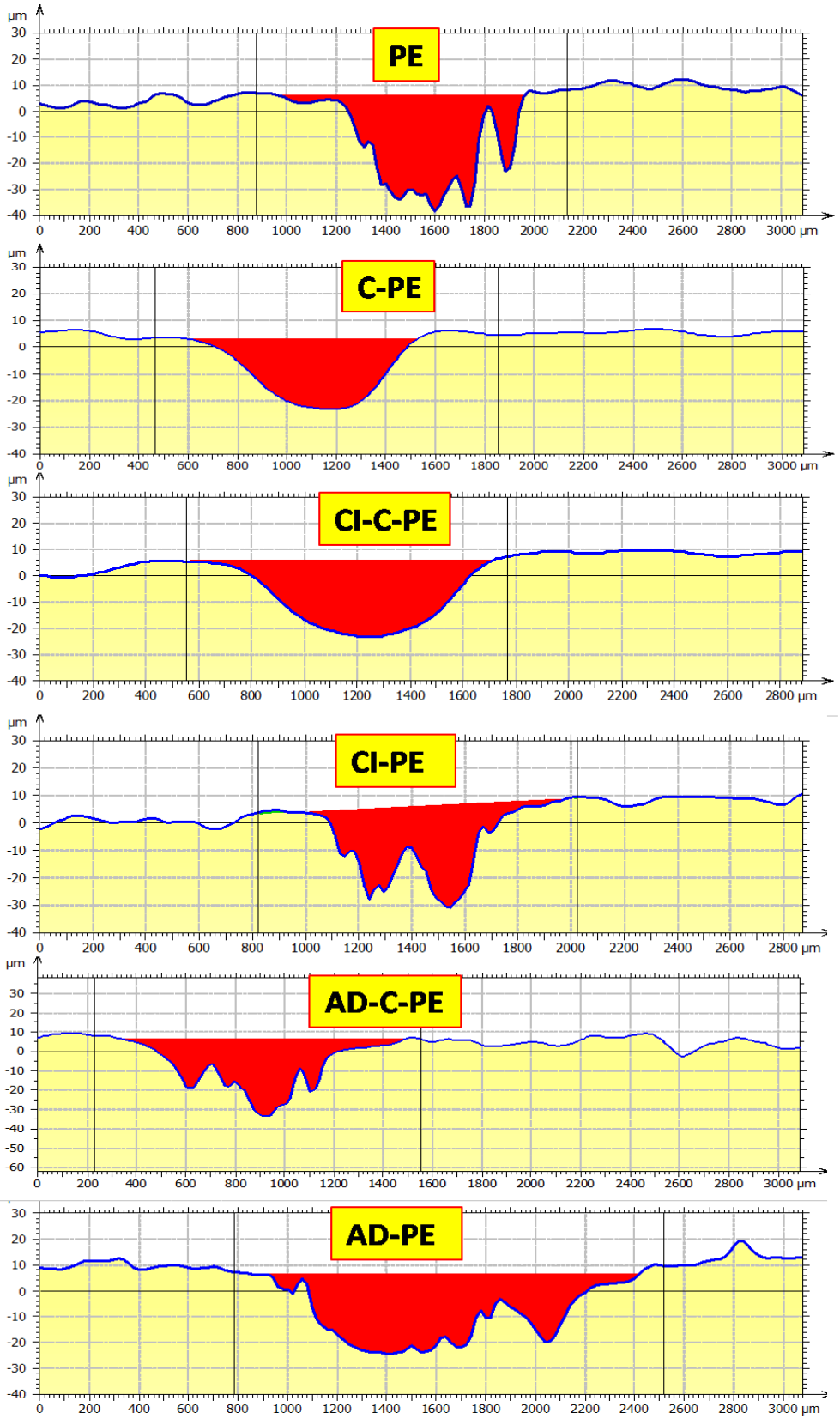

Fig. 7.12 *Shows the 2D line wear profiles across the worn surfaces*

Same trend was noticed for CI-PE and AD-PE; ~19% and 5% improvement in wear rate was recorded against PE. Worn surface of chitosan impregnated CI-C-PE and CI-PE has shown mild adhesion and abrasion Fig 7.13c& d. During tribo-contact, large extent of chitosan film transfers to counter body surface. As a result, CI-C-PE and CI-PE surface is protected from rough wear and it was shown clearly in chapter 4 [69].

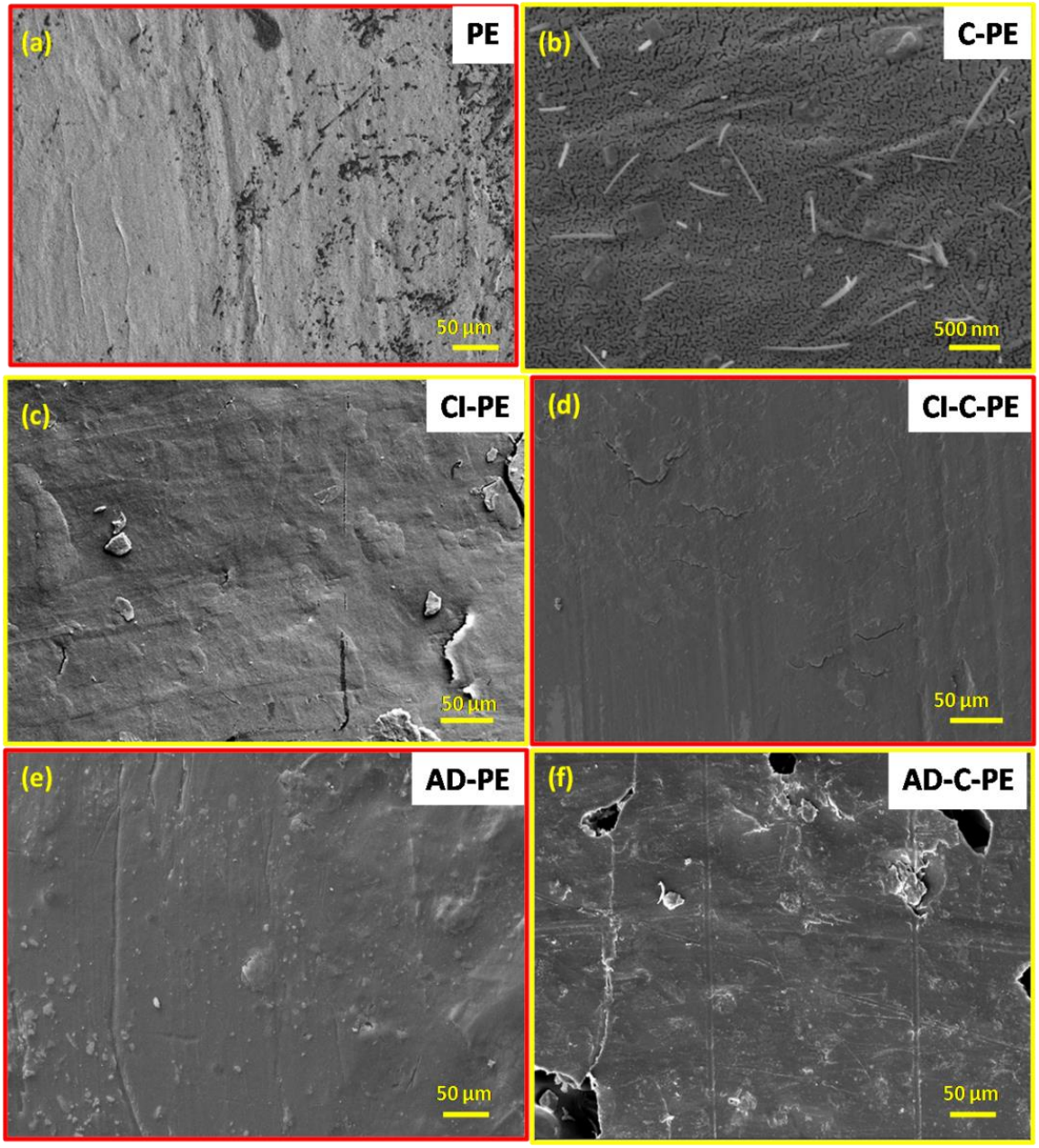

Fig. 7.13 *FE-SEM images of different test samples worn surfaces: (a) PE, (b) C-PE, (c) CI-PE, and (d) CI-C-PE, (e) AD-PE and (f) AD-C-PE respectively*

Fig 7.13f shows the morphology of worn surface after drug release (AD-C-PE), revealing some traces of pores and debris. Debris induced abrasive wear mechanism, increasing the wear rate by 14% as compare to C-PE. Same type of wear mechanism is identified in AD-PE, with wear rate almost similar to PE (fig 7.13e). During drug release, pores were collapsed and turned similar to PE surface with traces of tiny debris.

In short, all surface modified CNT-PE composite have shown remarkable improvement in tribological property, as compared to unmodified PE and modified PE (CI-PE). CNT reinforced acetabular cup can maintain its wear behavior to required level, even after incorporating the therapeutic agents into modified surface. It's an additional benefit for acetabular cup for reducing antibacterial infection. Drug eluting CNT reinforced PE composite is expected to perform well as part of fully weight bearing acetabular liner.

7.1.6 Summary

In this study, CNTs reinforced PE composite are prepared and surface is modified through modified chemical etching technique. Interconnected micro pores were effectively filled with gentamicin contained chitosan and this modified surface was evaluated for drug release kinetics. Sustained release of gentamicin up to 492 h (21 days) successfully eradicated the bacteria and avoids the initial infection around the surgical area. Besides, biocompatibility results fortify the candidature of surface modified CNT composite for clinical use. Addition of 0.1 wt.% CNTs to PE reduced the friction coefficient and specific wear rate by 48% and 36%, respectively, as compare to pure PE. The hardness and elastic modulus of the C-PE composite increased by 37% and 31%, respectively, due to presence of effective load sharing centers. Besides, implants after drug loading and releasing shown improved mechanical and tribological behavior, as compared to unmodified and modified PE surface. Thus, surface modified CNT-PE composite (CI-C-PE) liner of acetabular

cup is predicted to perform better than PE, both mechanically and biologically. But, modified PE (CI-PE) has shown comparatively better drug release (624 h) than CI-C-PE (492 h). The difference in drug release was mainly due to morphology of surface pores.

CHAPTER 8

Conclusions and Future Scope

8.1 Conclusions

This thesis has explored the possibility of developing the conventional PE acetabular cup liner into drug eluting liner for reducing the bacterial infection around the surgical area. In this regard, dissertation presents a complete analysis on surface modification of PE and CNT-PE composite, in terms of surface morphology for loading and delivering the drugs and mechanical, tribological and biological behavior to judge its potential for orthopedic application. Two different surface modification techniques, such as, modified chemical etching technique and electrostatic spray coating technique are used to engineer thin porous surface layer on PE. Porous surface layer is filled with drug containing chitosan using the impregnation chamber. An in-vitro antibacterial efficacy proves the success of surface modification in terms of drug loading and releasing kinetics. Besides, significant improvement in tribological performance enhances the interest in surface modification of acetabular cup liner.

To address the issue with the mildly inferior mechanical property of the modified PE surface, different aspect ratio of MWCNTs is used as reinforcement in PE composite. High aspect ratio CNTs had shown the better mechanical, tribological and thermal degradation behavior than low aspect ratio CNTs. This CNT-PE composite liner can reduce the wear debris by providing low friction. Wear debris are known for inducing osteolytic condition and leading to implant loosening problem. Modified chemical etching technique is used to engineer the interconnected micro pores on the surface of high aspect ratio CNT reinforced PE composite. Thereafter, effective loading of drug contained chitosan within pores was performed. These surface modified liners were evaluated for mechanical, tribological and antibacterial behavior. Modified surface of composite has shown

sustained release of drug and eradicated bacteria around it. Comparing all the results with surface modified PE liner, it is found that surface modified composite liner could be the promising alternative to conventional PE liner for total hip joint replacement, though the period of drug release should be improved further, which is possible. In this regard, Suhardi, V. et al. [47] have also developed drug-eluting UHMWPE with highly eccentric drug clusters. The vancomycin (drug) powder was mechanically mixed with GUR1020 UHMWPE powder and consolidated by compression moulding at 170 °C and 20 MPa, for 5 min. The resulting consolidated sample had shown sustained release of vancomycin up to 500 h and retaining the mechanical and wear properties of clinically used UHMWPE joint prostheses. The antibiotic eluting UHMWPE led to complete bacterial eradication and the absence of detectable systemic effects. But, it is a composite method (vancomycin blended with UHMWPE), during the curing (170 °C) process, the drug may get loses its effective antibacterial property due to temperature and even it may affect the structural integrity of the composite. Besides, entrapped drug inside the composite is not releasing until composite degrade or wear out. But, in our current technique only surface modified and loaded the drug effectively through impregnation process at room temperature. As a result, any type of drug can be used without damaging its physical property. Effective drug delivery and antibacterial efficacy can be expected along with improved tribological property. However, it is important to emphasize the need for further studies to understand the in vivo behavior of this new drug eluting PE liner, prior to their clinical use.

The following are the specific conclusions drawn out of the present work.

- A modified chemical etching and lyophilization technique is used to engineer the surface of PE to deliver the drug in sustained manner for eradicating the initial bacterial infection

around surgical area. The concept of surface modification of the inner lining material of the acetabular cup brings additional functionalities and capabilities to meet the future demand.

- A modified chemical etching technique is developed, which offers uniform interconnected micro porosity on PE surface. Boiling paraxylene dissolves the surface preferentially, and creating pores during lyophilization. Customized impregnation system can fill drug contained chitosan solution into pores successfully. This modified surface releases the drug in controlled manner up to 624 h (26 days). Complete release profile has two distinct behavioral categories, with initial burst release up to 280 h, followed by sustained release till 624 h. It is an ideal drug delivery system to control the initial infection, as well as, delayed infection. Modified surface has shown good antibacterial behavior against Staphylococcus aureus and cytocompatibility with MG-63 cells. Chitosan impregnation reduces the frictional force and wear rate by 26% and 19%, respectively, as compared to PE. Besides, decrease in hardness (27%) and elastic modulus (20%) was noticed for the same. But it is interesting to observe the regaining of mechanical and tribological property after drug releasing (26 days). During drug release, surface is modified by degrading of chitosan and collapsing of pores.

- Electrostatic spray coating technique was also used to construct the thin porous coating layer on PE substrate. Very strong integrity between porous coating and substrate was noticed after curing, because both substrate and coating material are same (PE). Uniform and highly interconnected porosity characteristics increased the drug loading efficiency by ~82% and drug releasing kinetic up to 860 h (35 days), which is much longer than modified chemical etching technique (626 h) and loading efficiency of ~70% ± 3 (14.02 ± 0.5 mg). However, both techniques had shown almost similar antibacterial behavior. Besides,

chitosan impregnated surface of both the techniques had shown almost similar decrease in mechanical and tribological property. But after drug release, chemically etched surface regains its property similar to unmodified PE surface, while decrease in mechanical and tribological property was noticed for electrostatic spray coating technique. This is the big drawback for electrostatic spray coating technique.

- In order to enhance the basic properties of conventional PE liner and to address the limitation of surface modification (decrease in mechanical property) of liner, CNT-PE composite was prepared. Two nominal concentrations of 0.05 wt.% and 0.1 wt.% of different aspect ratio of CNTs (HAR-900 and LAR-75) were reinforced in PE matrix. It was found that high aspect ratio of CNTs (HARCs) have shown remarkable improvement in mechanical, tribological and thermal degradation properties as compared to low aspect ratio of CNTs (LARCs). Besides, the effect is more prevalent with increasing nano filler content. An increase in HARC content from 0.05 to 0.1 wt.% improved the specific wear rate by 28% to 62% respectively, as compared to PE. But, similar trend of improvement was not observed in case of LARCs composite. A reason for the former case is morphological similarity between HARCs and polymer chains. In addition to this, differential improvement in hardness, elastic modulus and crystallinity is observed in composite. Strong interfacial bonding increases the possibility of load transfer centers from matrix to CNT and CNT to matrix in the composite.
- Chemical etching technique is used to engineer thin porous surface layer on 0.1 wt% reinforced HARCs composite. Modified surface of composite (drug loaded) gives sustained release of drug up to 492 h (21 days), whereas the same in unreinforced PE is 624 h (26 days). Reasons for the former case are directly related surface morphology and drug

loading efficiency ~13 mg (65%). Both surface modified composite and PE shown good antibacterial characteristics and effectively eradicated the bacteria. Surface modified CNT composite liner can maintain its mechanical and tribological behavior even in sever service condition. This was the reason to reinforce the PE surface with CNTs, which is achieved successfully. Besides, positive in-vitro biocompatibility results and the absence of detectable systemic effects secure the candidature of surface modified CNT composite liner for clinical use. Besides, drug release kinetics can be tailored in sustained manner by using other drug carrier such as PCL, PLA and PLGA. Cross linking the drug carriers will also be the solution to ovoid the burst and fast release rate.

8.2 Scope for future work

The aim of the current research was to explore the potential of surface modified PE liner as drug eluting implant without compromising the required property to inhibit initial infection around the surgical area. The criteria for judgment were the effect of surface modification on drug delivery kinetics, antibacterial effectiveness, biological, mechanical and tribological properties of the surface. The findings of this study establish surface modified CNT-PE composite liner to be potential alternative for clinically used PE liner. However, some of the topics need further investigations to progress towards the clinical translation of CNT-PE liner. Following is a tentative list of recommendations for the same.

- In the present work, natural biodegradable polymer, such as, chitosan has been used as drug carrier, while the study can be extended by using other biodegradable polymer such as PLGA, PDLG, PCL, PLA, collagen for further enhancing the drug release kinetics for longer period to take care of delayed infection.
- Combination of two biodegradable polymer and drugs can be used for tailoring the antibacterial efficacy.
- Cross linking of the drug carriers will also extend the research work towards reducing the burst and fast drug delivery kinetics
- Different wear conditions, such as, reciprocating sliding, lubricated sliding (bovine serum) and multidirectional wear simulator can be used to study the modified surface tribological behavior. Besides, study can be extending to predict the biological activity of wear debris.
- In-vitro cytocompatibility test was carried out in present study to check the primary biocompatible nature of modified surface. Analyzing the in-vivo performance of surface modified PE liner is a recommended work towards translation.

- Modifying the other hip replacement parts, such as, femoral stems (metal parts) and impregnating the drugs in similar method for eradicating complete bacterial infection.
- Reinforcing other than CNTs, such as hollocite nano clay (HNT) to PE for improving the mechanical and tribological property
- Vacuum impregnation technique can be used to any drug eluting implants for effectively controlling the release kinetics.

LIST OF PUBLICATIONS

Patent

- Debrupa Lahiri, **Manoj Kumar R**, Partha Roy. "Orthopedic metallic implant for sustained drug release', received the provisional patent no **'201711024735'.** from Indian patent office

Book Chapter

- "Medical Applications of Hierarchical Composites", **Manoj Kumar R**, K. Agrawal, D. Lahiri, in "Hybrid and Hierarchical Composite Materials", Editors: C.-S. Kim, C. Randow, T. Sano, Springer, ISBN: 978-3-319- 12867-2

Published Papers

1. **R. Manoj Kumar**, S. Sharma, B.V.M. Kumar, D. Lahiri, "Effects of Carbon Nanotube Aspect Ratio on Strengthening and Tribological Behaviour of Ultra High Molecular Weight Polyethylene Composite", **Composites A**, Vol. 76, 2015, pp. 62-72. **(Journal Impact Factor: 6.28)** (http://www.sciencedirect.com/science/article/pii/S1359835X1500161X)
2. S. Singh, **R. Manoj Kumar**, K.K. Kuntal, P. Gupta, S. Das, R. Jayaganthan, P. Roy, D. Lahiri, "Sol–Gel Derived Hydroxyapatite Coating on Mg-3Zn Alloy for Orthopedic Application", **JOM**, Vol. 67, 2015, pp. 702- 712. **(Journal Impact Factor: 2.30)** (http://link.springer.com/article/10.1007/s11837-015-1364-1)
3. K. Saini, **R.M. Kumar**, D. Lahiri, I. Lahiri, "Quantifying Bonding Strength of CuO Nanotubes with Substrate Using Nano-Scratch Technique", **Nanotechnology**, Vol. 26, 2015, pp. 305701. **(Journal Impact Factor: 3.39)** (https://www.ncbi.nlm.nih.gov/pubmed/26148461)
4. **R Manoj Kumar,** Kuntal KK, Singh S, Gupta P, Bhushan B, Gopinath P, Lahiri D. "Electrophoretic deposition of hydroxyapatite coating on Mg–3Zn alloy for orthopaedic application" **Surface and Coatings Technology**, Vol. 287, 2016, pp. 82-92. **(Journal Impact Factor: 3.2)** (http://www.sciencedirect.com/science/article/pii/S0257897215305168)
5. Kumar, Raj, **R. Manoj Kumar**, Debrupa Lahiri, and Indranil Lahiri. "Thermally reduced graphene oxide film on soda lime glass as transparent conducting electrode." **Surface and Coatings Technology**, Vol. 309, 2017, pp 931-937. **(Journal Impact Factor: 3.2)** (http://www.sciencedirect.com/science/article/pii/S0257897216310581)
6. **R Manoj Kumar,** Pallavi Gupta, Sandan Kumar Sharma, Akshat Mittal, Manish Shekhar, Vijayesh Kumar, B.V. Manoj Kumar, Partha Roy, Debrupa Lahiri. "Sustained drug release from surface modified UHMWPE for acetabular cup lining in total hip implant" Journal of **Materials Science and Engineering C**, Vol 77, 2017, pp 649-661.**(Journal Impact Factor: 4.96)** (http://www.sciencedirect.com/science/article/pii/S0928493116313145)

7. Ankita Bisht, Mukul Srivastava, **R. Manoj Kumar**, Indranil Lahiri, DebrupaLahiri. "Strengthening mechanism in graphene nanoplatelets reinforced aluminium composite fabricated through spark plasma sintering" **Materials Science and Engineering A,** Vol 695, 2017, pp 20-28. **(Journal Impact Factor: 4.09)** (http://www.sciencedirect.com/science/article/pii/S0921509317304513)
8. Kumar, Raj; **R. Manoj Kumar**; Bera, Parthasarathi; Lahiri, Debrupa; Lahiri, Indranil. "Temperature-time dependent transmittance, sheet resistance and bonding energy of reduced graphene oxide on soda lime glass" **Journal of Applied Surface Science,** Vol 425, 2017, pp 558-563 **(Journal Impact Factor: 5.15)** https://www.sciencedirect.com/science/article/pii/S0169433217318792
9. Jaiswal Satish, **R. Manoj Kumar**, Pallavi Gupta, Murali K, Partha Roy, Debrupa Lahiri. "Mechanical, Corrosion and Biocompatibility Behaviour of Mg-3Zn-HA Biodegradable Composites for Orthopaedic Fixture Accessories." **Journal of the Mechanical Behavior of Biomedical Materials** (2017), Vol 78, pp 442-454. **(Journal Impact Factor: 3.42)** https://www.sciencedirect.com/science/article/pii/S1751616117305180
10. **R. Manoj Kumar,** Kanike Rajesh, Swati Haldar, Pallavi Gupta, K. Murali, Partha Roy, and Debrupa Lahiri. "Surface modification of CNT reinforced UHMWPE composite for sustained drug delivery." **Journal of Drug Delivery Science and Technology** (2019). Vol 52, pp 748-759. **(Journal Impact Factor: 2.62)** https://www.sciencedirect.com/science/article/pii/S1773224719302503
11. Raj Kumar; **R. Manoj Kumar**; Debrupa Lahiri; Indranil Lahiri. "Measurement of bonding strength of thermally reduced graphene oxide with soda lime glass using nanoscratch technique" Journal of **Materials Today Proceedings,** Vol 5, Issue 8, 2018, pp 16338-16345 **(Journal Impact Factor: 0.83)** https://www.sciencedirect.com/science/article/pii/S2214785318310836
12. Bisht, Ankita, **R. Manoj Kumar**, Kinshuk Dasgupta, and Debrupa Lahiri. "Spatial distribution of nanodiamond and its effect on mechanical behaviour of epoxy based composite using 2D modulus mapping." **Mechanics of Materials** 135 (2019): 114-128. https://www.sciencedirect.com/science/article/pii/S0167663619301103

Submitted Papers

1. ***R. Manoj Kumar***, Kanike Rajesh, Swati Haldar, *Debrupa Lahiri. "Surface modification of UHMWPE for sustained drug delivery by electrostatic spray coating method for orthopaedic application" first review has been submitted in* ***Materials Science and Engineering C***

2. *Rajesh K,* ***R.Manoj Kumar****,* Swati Haldar, *Partha Roy, Debrupa Lahiri. "Surface modification of Ti metallic implants for sustained drug delivery application" under review in* ***ACS Applied Biomaterals.***

Honors and Awards

- Received young scientists international travel support to visit Imperial collage of London, UK from Science and Engineering Research Board (SERB), Established under Department of Science and Technology (DST), Government of India.
- Received young scientists international travel support to attend International conference at Dubai, UAE from CSIR, Government of India.
- Received "second best oral presentation award" in Material Science at IIM-ATM, 2015, organized during 13-16, November 2015 at Coimbatore, India.
- Article on our work published in Health Care Times magazine in May 2017 issue

Conferences

1. **Manoj Kumar R**, S.K. Sharma, A.D. Ray, D. Natu, S. Tikko, B.V. Manoj Kumar, D. Lahiri, "Effects of Carbon Nano Tube Morphology on Tribological Behaviour of UHMWPE Composite for Total Hip Joint", International conference on Polymeric Biomaterials, Bioengineering and Biodiagnostics, New Delhi, India, 27 – 30 Oct., 2014.
2. **Manoj Kumar R**, A.D. Ray, D. Natu, S. Tikko, D. Lahiri, "CNT-UHMWPE Composite for Orthopeadic Application", 2nd National conference on Recent Advances in Mechanical Engineering (NCRAME-2014), G.B. Pant Engineering College, Uttarakhand, India, 26 – 27 Sept., 2014.
3. **Manoj Kumar R**, S.K. Sharma, D. Ray, D. Natu, S. Tikko, B.V. Manoj Kumar, D. Lahiri, "Carbon Nanotube/Ultra High Molecular Weight Polyethylene Composite for Hip Joint – Influence of CNT Morphology on Wear Behavior", 52nd Annual Technical Meeting of Indian Institute of Metals, Pune, India, 12-15 Nov., 2014.
4. **Manoj Kumar R, S**andan Kumar Sharma, Vijayesh Kumar, B.V. Manoj Kumar, Debrupa Lahiri"Surface modification of ultra-high molecular weight polyethylene for drug eluting orthopaedic implant applications"53nd Annual Technical Meeting of Indian Institute of Metals, Coimbatore. Indian, 13th-16th Nov., 2015
5. **Manoj Kumar R,** Praveen Kumar Gupta, Debrupa Lahiri "Study on Mechanical and Tribological Properties of Graphene Nanoplatelet Reinforced Ultra High Molecular Weight polyethylene Composite" 53nd Annual Technical Meeting of Indian Institute of Metals, Coimbatore. India, 13th-16th Nov., 2015
6. **Manoj Kumar R**, Kishor Kumar Kuntal, Sanjay Singh, Pallavi Gupta, Bharat Bhushan, P. Gopinath, Debrupa Lahiri. "Electrophoretic Coating of Nanostructured Hydroxyapatite on Mg-3Zn Alloy for Orthopaedic Application" International Conference on Metals and Materials Research (ICMR 2016) at Indian Institute of Science, Bangalore, India. 20 -22 June 2016.
7. **Manoj Kumar R,** Pallavi Gupta, Sandan Kumar Sharma, Vijayesh Kumar, B.V. Manoj Kumar, Partha Roy, Debrupa Lahiri**.** "Surface modification of ultra high molecular weight

polyethylene for drug eluting orthopaedic implant applications" 3rd International Conference on Bio-Tribology (ICoBT 2016) at Imperial College London, London, UK, 11-14 September 2016

8. **Manoj Kumar R,** Pallavi Gupta, Debrupa Lahiri "Sustained Drug Release from Surface Modified UHMWPE for Drug Eluting Orthopeadic Applications"54 Annual Technical Meeting of Indian Institute of Metals, IIT Kanpur, Indian, 13th-16th Nov., 2016.
9. Kumar, Raj, **R. Manoj Kumar**, Debrupa Lahiri, and Indranil Lahiri. "Measuring the bonding strength of thermally reduced grapheen oxide on soda lime glass using nano scratch technology" International Conference on Material Sciences (SCICON' 16), Coimbatore, India, 19-21st December 2016.
10. Raj Kumar, **Manoj Kumar R.** Debrupa Lahiri, Indranil Lahiri. "Quantification of temperature-time dependent bonding strength of thermally reduced graphene oxide with soda lime glass as transparent conducting electrode" 2nd International Conference on Soft Materials (ICSM-2016), Jaipur 14-16th December 2016.
11. **R. Manoj Kumar**, Pallavi Gupta, Partha Roy, Debrupa Lahiri. "Surface Modified Drug Releasing Total Hip Implant" 2017 TMS Annual Meeting and Exhibition, February 26 – March 2, 2017, San Diego, CA
12. A. Bisht, **R. Manoj. Kumar**, K. Dasgupta, D. Lahiri, "Effect of introduction of nanodiamond on the mechanical behaviour of epoxy matrix under tensile stress", Nanoyantrika, Thiruvananthapuram, India, 17th-20th September 2017.
13. **R. Manoj Kumar,** S. Jaiswal, D. Lahiri, "Nanodynamic Mechanical and Tribological Behaviour of Graphene Nanoplatelet Reinforced Ultra High Molecular Weight Polyethylene Composite" Nanoyantrika, Thiruvananthapuram, India, 17th-20th Sept. 2017.
14. **R. Manoj Kumar,** Debrupa Lahiri "Surface Modification of CNT Reinforced UHMWPE Composite for Sustained Drug Delivery" Biological Engineering Society (BES), IIT Roorkee, India, 24th November 2017
15. **R Manoj Kumar**, Debrupa Lahiri "Nanodynamic Mechanical and Tribological Behavior of GNPs Reinforced UHMWPE composite" International conference on recent advances in materials and manufacturing technologies (IMMT 2017), Dubai, UAE, 28 to 29th November 2017
16. **R Manoj Kumar**, Pallavi Gupta, Debrupa Lahiri "Sustained drug delivery from surface Modified CNT-UHMWPE Composite**"** International conference on advances in materials and processing: challenges and opportunities (AMPCO'17), IIT Roorkee, India 30th Nov to 2nd Dec 2017
17. Krishna Saini, **Manoj Kumar R**, Debrupa Lahiri, Indranil Lahiri, "Bonding Strength of CuO NT with substrate", 7th Bangalore India Nano, Bangalore, India, Dec. 4-6, 2014
18. **R. Manoj Kumar** participated in the conference on "Scientific Validation of Traditional Knowledge-II" conducted by IPR chair, department of management studies, IIT Roorkee from Feb.24-25, 2017

REFERENCES

[1] P. K. Chu and X. Liu, *Biomaterials fabrication and processing handbook*. Taylor & Francis, 2008.

[2] "Biomaterials Market | Growth | Size | Analysis (2017-2022)." [Online]. Available: https://www.mordorintelligence.com/industry-reports/global-biomaterials-market-industry. [Accessed: 11-Mar-2018].

[3] "Indian Orthopedic Devices Market A $2.4 Bn Opportunity Succeeding in the Evolving Landscape," 2016.

[4] L. Murphy and C. G. Helmick, "The Impact of Osteoarthritis in the United States," *Orthop. Nurs.*, vol. 31, no. 2, pp. 85–91, 2012.

[5] R. Pivec, A. J. Johnson, S. C. Mears, and M. A. Mont, "Hip arthroplasty.," *Lancet (London, England)*, vol. 380, no. 9855, pp. 1768–77, Nov. 2012.

[6] J. A. Pachore, S. V Vaidya, C. J. Thakkar, H. K. P. Bhalodia, and H. M. Wakankar, "ISHKS joint registry: A preliminary report.," *Indian J. Orthop.*, vol. 47, no. 5, pp. 505–9, Sep. 2013.

[7] P. Drees, A. Eckardt, R. E. Gay, S. Gay, and L. C. Huber, "Mechanisms of Disease: molecular insights into aseptic loosening of orthopedic implants," *Nat. Clin. Pract. Rheumatol.*, vol. 3, no. 3, pp. 165–171, Mar. 2007.

[8] Z. Song, L. Borgwardt, N. Høiby, H. Wu, T. S. Sørensen, and A. Borgwardt, "Prosthesis infections after orthopedic joint replacement: the possible role of bacterial biofilms.," *Orthop. Rev. (Pavia).*, vol. 5, no. 2, pp. 65–71, Jun. 2013.

[9] S. A. Lie, G. Hallan, O. Furnes, L. I. Havelin, and L. B. Engesæter, "Isolated acetabular liner exchange compared with complete acetabular component revision in revision of primary uncemented acetabular components," *J. Bone Joint Surg. Br.*, vol. 89-B, no. 5, pp. 591–594, May 2007.

[10] S. D. Ulrich *et al.*, "Total hip arthroplasties: what are the reasons for revision?," *Int. Orthop.*, vol. 32, no. 5, pp. 597–604, Oct. 2008.

[11] D. Fabi *et al.*, "Metal-on-Metal Total Hip Arthroplasty: Causes and High Incidence of Early Failure," *Orthopedics*, vol. 35, no. 7, pp. e1009–e1016, Jul. 2012.

[12] S. Veerachamy, T. Yarlagadda, G. Manivasagam, and P. K. Yarlagadda, "Bacterial adherence and biofilm formation on medical implants: A review," *Proc. Inst. Mech. Eng. Part H J. Eng. Med.*, vol. 228, no. 10, pp. 1083–1099, Oct. 2014.

[13] M. Geetha, A. K. Singh, R. Asokamani, and A. K. Gogia, "Ti based biomaterials, the ultimate choice for orthopaedic implants – A review," *Prog. Mater. Sci.*, vol. 54, no. 3, pp. 397–425, May 2009.

[14] R. Yunus Basha, S. K. T.S., and M. Doble, "Design of biocomposite materials for bone tissue regeneration," *Mater. Sci. Eng. C*, vol. 57, pp. 452–463, Dec. 2015.

[15] G. D. Ehrlich *et al.*, "Engineering approaches for the detection and control of orthopaedic biofilm infections.," *Clin. Orthop. Relat. Res.*, no. 437, pp. 59–66, Aug. 2005.

[16] S. B. Goodman, Z. Yao, M. Keeney, and F. Yang, "The future of biologic coatings for orthopaedic implants.," *Biomaterials*, vol. 34, no. 13, pp. 3174–83, Apr. 2013.

[17] J. Raphel, M. Holodniy, S. B. Goodman, and S. C. Heilshorn, “Multifunctional coatings to simultaneously promote osseointegration and prevent infection of orthopaedic implants,” *Biomaterials*, vol. 84, pp. 301–314, Apr. 2016.

[18] E. M. Greenfield, Y. Bi, A. A. Ragab, V. M. Goldberg, J. L. Nalepka, and J. M. Seabold, “Does endotoxin contribute to aseptic loosening of orthopedic implants?,” *J. Biomed. Mater. Res.*, vol. 72B, no. 1, pp. 179–185, Jan. 2005.

[19] S. M. Kurtz, E. Lau, H. Watson, J. K. Schmier, and J. Parvizi, “Economic Burden of Periprosthetic Joint Infection in the United States,” *J. Arthroplasty*, vol. 27, no. 8, pp. 61-65.e1, Sep. 2012.

[20] M. Gimeno *et al.*, “A controlled antibiotic release system to prevent orthopedic-implant associated infections: An in vitro study,” *Eur. J. Pharm. Biopharm.*, vol. 96, pp. 264–271, 2015.

[21] L. Bernard, P. Hoffmeyer, M. Assal, P. Vaudaux, J. Schrenzel, and D. Lew, “Trends in the treatment of orthopaedic prosthetic infections,” *J. Antimicrob. Chemother.*, vol. 53, no. 2, pp. 127–129, Jan. 2004.

[22] G. A. Ayliffe, “Role of the environment of the operating suite in surgical wound infection.,” *Rev. Infect. Dis.*, vol. 13 Suppl 10, pp. S800-4.

[23] K. A. Poelstra, N. A. Barekzi, A. M. Rediske, A. G. Felts, J. B. Slunt, and D. W. Grainger, “Prophylactic treatment of gram-positive and gram-negative abdominal implant infections using locally delivered polyclonal antibodies.,” *J. Biomed. Mater. Res.*, vol. 60, no. 1, pp. 206–15, Apr. 2002.

[24] S. Veerachamy, T. Yarlagadda, G. Manivasagam, and P. K. Yarlagadda, “Bacterial adherence and biofilm formation on medical implants: A review,” *Proc. Inst. Mech. Eng. Part H J. Eng. Med.*, vol. 228, no. 10, pp. 1083–1099, Oct. 2014.

[25] H. Liu *et al.*, “Antibacterial and anti-biofilm activities of thiazolidione derivatives against clinical staphylococcus strains,” *Emerg. Microbes Infect.*, vol. 4, no. 1, pp. e1–e1, Jan. 2015.

[26] P. Stoodley *et al.*, “Molecular and imaging techniques for bacterial biofilms in joint arthroplasty infections.,” *Clin. Orthop. Relat. Res.*, no. 437, pp. 31–40, Aug. 2005.

[27] A. Trampuz and A. F. Widmer, “Infections associated with orthopedic implants,” *Curr. Opin. Infect. Dis.*, vol. 19, no. 4, pp. 349–356, Aug. 2006.

[28] A. J. Tande and R. Patel, “Prosthetic joint infection.,” *Clin. Microbiol. Rev.*, vol. 27, no. 2, pp. 302–45, Apr. 2014.

[29] H. Willenegger and B. Roth, “[Treatment tactics and late results in early infection following osteosynthesis].,” *Unfallchirurgie*, vol. 12, no. 5, pp. 241–6, Oct. 1986.

[30] J. S. Price, A. F. Tencer, D. M. Arm, and G. A. Bohach, “Controlled release of antibiotics from coated orthopedic implants.,” *J. Biomed. Mater. Res.*, vol. 30, no. 3, pp. 281–6, Mar. 1996.

[31] Z. Ruszczak and W. Friess, “Collagen as a carrier for on-site delivery of antibacterial drugs.,” *Adv. Drug Deliv. Rev.*, vol. 55, no. 12, pp. 1679–98, Nov. 2003.

[32] M. ZILBERMAN and J. ELSNER, “Antibiotic-eluting medical devices for various applications,” *J. Control. Release*, vol. 130, no. 3, pp. 202–215, Sep. 2008.

[33] P. Wu and D. W. Grainger, “Drug/device combinations for local drug therapies and infection prophylaxis,” *Biomaterials*, vol. 27, no. 11, pp. 2450–2467, Apr. 2006.

[34] S. B. Trippel, “Antibiotic-impregnated cement in total joint arthroplasty.,” *J. Bone Joint Surg. Am.*, vol. 68, no. 8, pp. 1297–302, Oct. 1986.

[35] E. Sanchez-Rexach, E. Meaurio, and J. R. Sarasua, “Recent developments in drug eluting devices with tailored interfacial properties,” *Adv. Colloid Interface Sci.*, vol. 249, pp. 181–191, 2017.

[36] D. Stengel, K. Bauwens, J. Sehouli, A. Ekkernkamp, and F. Porzsolt, “Systematic review and meta-analysis of antibiotic therapy for bone and joint infections,” *Lancet Infect. Dis.*, vol. 1, no. 3, pp. 175–188, Oct. 2001.

[37] H. Wahlig, E. Dingeldein, R. Bergmann, and K. Reuss, “The release of gentamicin from polymethylmethacrylate beads. An experimental and pharmacokinetic study.,” *J. Bone Joint Surg. Br.*, vol. 60-B, no. 2, pp. 270–5, May 1978.

[38] S. F. Hoff, R. H. Fitzgerald, and P. J. Kelly, “The depot administration of penicillin G and gentamicin in acrylic bone cement.,” *J. Bone Joint Surg. Am.*, vol. 63, no. 5, pp. 798–804, Jun. 1981.

[39] “American Joint Replacement Registry 2016 Annual Report Third AJRR Annual Report on Hip and Knee Arthroplasty Data.”

[40] M. Stigter, J. Bezemer, K. De Groot, and P. Layrolle, “Incorporation of different antibiotics into carbonated hydroxyapatite coatings on titanium implants, release and antibiotic efficacy,” *J. Control. Release*, vol. 99, no. 1, pp. 127–137, 2004.

[41] S. K. Nandi, P. Mukherjee, S. Roy, B. Kundu, D. K. De, and D. Basu, “Local antibiotic delivery systems for the treatment of osteomyelitis - A review,” *Mater. Sci. Eng. C*, vol. 29, no. 8, pp. 2478–2485, 2009.

[42] S. Radin, J. T. Campbell, P. Ducheyne, and J. M. Cuckler, “Calcium phosphate ceramic coatings as carriers of vancomycin,” *Biomaterials*, vol. 18, no. 11, pp. 777–782, 1997.

[43] D. Neut, R. J. B. Dijkstra, J. I. Thompson, C. Kavanagh, H. C. van der Mei, and H. J. Busscher, “A biodegradable gentamicin-hydroxyapatite-coating for infection prophylaxis in cementless hip prostheses,” *Eur. Cells Mater.*, 2015.

[44] F. Pishbin *et al.*, “Electrophoretic Deposition of Gentamicin-Loaded Bioactive Glass / Chitosan Composite Coatings for Orthopaedic Implants,” 2014.

[45] E. M. Brach Del Prever, A. Bistolfi, P. Bracco, and L. Costa, “UHMWPE for arthroplasty: past or future?,” *J. Orthop. Traumatol.*, vol. 10, no. 1, pp. 1–8, Mar. 2009.

[46] S. M. Kurtz, O. K. Muratoglu, M. Evans, and A. A. Edidin, “Advances in the processing, sterilization, and crosslinking of ultra-high molecular weight polyethylene for total joint arthroplasty.,” *Biomaterials*, vol. 20, no. 18, pp. 1659–88, Sep. 1999.

[47] V. J. Suhardi *et al.*, “A fully functional drug-eluting joint implant,” *Nat. Biomed. Eng.*, vol. 1, no. 6, pp. 1–11, 2017.

[48] J. (Johan) Bellemans, M. D. Ries, and J. (Jan) Victor, *Total knee arthroplasty : a guide to get better performance*. Springer, 2005.

[49] S. Ramakrishna, J. Mayer, E. Wintermantel, and K. W. Leong, “Biomedical applications of polymer-composite materials: a review,” *Compos. Sci. Technol.*, vol. 61, no. 9, pp. 1189–1224, Jul. 2001.

[50] D. Lahiri *et al.*, “Graphene nanoplatelet-induced strengthening of ultrahigh molecular weight polyethylene and biocompatibility in vitro.,” *ACS Appl. Mater. Interfaces*, vol. 4, no. 4, pp. 2234–41, May 2012.

[51] S. S. Moreno, “Carbon Reinforced UHMWPE Composites for Orthopaedic Applications Characterization and Biological Response to Wear Particles,” *Luleå Univ. Technol.*, 2013.

[52] P. K. Levangie, C. C. Norkin, and P. K. Levangie, *Joint structure and function : a comprehensive analysis*. F.A. Davis Co, 2011.

[53] S. M. Kurtz, *UHMWPE biomaterials handbook : ultra-high molecular weight polyethylene in total joint replacement and medical devices*. .

[54] b Domingos Lusitâneo Pier Macuvele a *et al.*, “Advances in ultra high molecular weight polyethylene/hydroxyapatite composites for biomedical applications: A brief review,” *Mater. Sci. Eng. C*, vol. 76, pp. 1248–1262, 2017.

[55] D. M. Rein, R. L. Khalfin, Y. Cohen, K. Shuster, and E. Zussman, “Electrospinning of Ultrahigh-Molecular-Weight Polyethylene Nanofibers,” pp. 11–16, 2007.

[56] L. D. I. Silvio, “Biodegradable drug delivery system for the treatment of bone infection and repair,” vol. 0, pp. 653–658.

[57] I. Armentano, M. Dottori, E. Fortunati, S. Mattioli, and J. M. Kenny, “Biodegradable polymer matrix nanocomposites for tissue engineering: A review,” *Polym. Degrad. Stab.*, vol. 95, no. 11, pp. 2126–2146, Nov. 2010.

[58] B. Clarke, “Normal bone anatomy and physiology.,” *Clin. J. Am. Soc. Nephrol.*, vol. 3 Suppl 3, no. Suppl 3, pp. S131-9, Nov. 2008.

[59] M. Kazemzadeh-Narbat, “Local Delivery of Antimicrobial Peptides From Titanium Surface for the Prevention of Implant-Associated,” *Tesis*, no. March, pp. 1–190, 2013.

[60] R. Florencio-Silva, G. R. da S. Sasso, E. Sasso-Cerri, M. J. Simões, and P. S. Cerri, “Biology of Bone Tissue: Structure, Function, and Factors That Influence Bone Cells.,” *Biomed Res. Int.*, vol. 2015, p. 421746, Jul. 2015.

[61] C. Bonifasi-Lista and E. Cherkaev, “Identification of bone structure from effective measurements,” in *III European Conference on Computational Mechanics*, Dordrecht: Springer Netherlands, 2006, pp. 551–551.

[62] S. L. Teitelbaum, “Osteoclasts: What Do They Do and How Do They Do It?,” *Am. J. Pathol.*, vol. 170, no. 2, pp. 427–435, Feb. 2007.

[63] K. Balani, Y. Chen, S. P. Harimkar, N. B. Dahotre, and A. Agarwal, “Tribological behavior of plasma-sprayed carbon nanotube-reinforced hydroxyapatite coating in physiological solution,” *Acta Biomater.*, vol. 3, no. 6, pp. 944–951, Nov. 2007.

[64] S. R. Bakshi, K. Balani, T. Laha, J. Tercero, and A. Agarwal, “The nanomechanical and nanoscratch properties of MWNT-reinforced ultrahigh-molecular-weight polyethylene coatings,” *JOM*, vol. 59, no. 7, pp. 50–53, Jul. 2007.

[65] V. Everts *et al.*, "The Bone Lining Cell: Its Role in Cleaning Howship's Lacunae and Initiating Bone Formation," *J. Bone Miner. Res.*, vol. 17, no. 1, pp. 77–90, Jan. 2002.

[66] M. A. F. Afzal, S. Kalmodia, P. Kesarwani, B. Basu, and K. Balani, "Bactericidal effect of silver-reinforced carbon nanotube and hydroxyapatite composites," *J. Biomater. Appl.*, vol. 27, no. 8, pp. 967–978, May 2013.

[67] L. F. Bonewald, "The amazing osteocyte," *J. Bone Miner. Res.*, vol. 26, no. 2, pp. 229–238, Feb. 2011.

[68] S. L. Dallas, M. Prideaux, and L. F. Bonewald, "The Osteocyte: An Endocrine Cell … and More," *Endocr. Rev.*, vol. 34, no. 5, pp. 658–690, Oct. 2013.

[69] R. Manoj Kumar *et al.*, "Sustained drug release from surface modified UHMWPE for acetabular cup lining in total hip implant," *Mater. Sci. Eng. C*, vol. 77, pp. 649–661, 2017.

[70] J. Pachore, S. Vaidya, C. Thakkar, H. K. Bhalodia, and H. Wakankar, "ISHKS joint registry: A preliminary report," *Indian J. Orthop.*, vol. 47, no. 5, p. 505, Sep. 2013.

[71] T. J. Levingstone, "Optimisation of Plasma Sprayed Hydroxyapatite Coatings," 2008.

[72] H. C. Amstutz, P. Grigoris, M. R. Safran, M. J. Grecula, P. A. Campbell, and T. P. Schmalzried, "Precision-fit surface hemiarthroplasty for femoral head osteonecrosis. Long-term results.," *J. Bone Joint Surg. Br.*, vol. 76, no. 3, pp. 423–7, May 1994.

[73] S. Yousef, A. Visco, G. Galtieri, D. Nocita, and C. Espro, "Wear behaviour of UHMWPE reinforced by carbon nanofiller and paraffin oil for joint replacement," *Mater. Sci. Eng. C*, vol. 73, pp. 234–244, Apr. 2017.

[74] T. J. Levingstone, M. Ardhaoui, K. Benyounis, L. Looney, and J. T. Stokes, "Plasma sprayed hydroxyapatite coatings: Understanding process relationships using design of experiment analysis," *Surf. Coatings Technol.*, vol. 283, pp. 29–36, 2015.

[75] T. calcium Phosphate, E. Shells, B. Cements, Hydroxyapatite, and B. Relevantions, "Self Setting Bone Cement Formulations Based on Egg shell Derived TetraCalcium Phosphate BioCeramics," *Bioceram. Dev. Appl.*, vol. 05, no. 01, pp. 1–6, Apr. 2015.

[76] K. Søballe and R. J. Friedman, "Calcium Hydroxyapatite in Total Joint Arthroplasty," in *Human Biomaterials Applications*, Totowa, NJ: Humana Press, 1996, pp. 137–167.

[77] L. L. Hench and Ö. Andersson, "BIOACTIVE GLASSES," in *An Introduction to Bioceramics*, WORLD SCIENTIFIC, 1993, pp. 41–62.

[78] F. Chai, J. C. Hornez, N. Blanchemain, C. Neut, M. Descamps, and H. F. Hildebrand, "Antibacterial activation of hydroxyapatite (HA) with controlled porosity by different antibiotics," *Biomol. Eng.*, vol. 24, no. 5, pp. 510–514, 2007.

[79] J.-C. Hornez, F. Chai, N. Blanchemain, A. Lefèvre, M. Descamps, and H. F. Hildebrand, "Biocompatibility Improvement of Pure Hydroxyapatite (Ha) with Different Porosity."

[80] A. Trampuz and A. F. Widmer, "Infections associated with orthopedic implants," *Curr. Opin. Infect. Dis.*, vol. 19, no. 4, pp. 349–356, Aug. 2006.

[81] A. Trampuz and A. F. Widmer, "Infections associated with orthopedic implants," *Curr. Opin. Infect. Dis.*, vol. 19, no. 4, pp. 349–356, Aug. 2006.

[82] A. F. Widmer, "New Developments in Diagnosis and Treatment of Infection in Orthopedic

Implants," *Clin. Infect. Dis.*, vol. 33, no. s2, pp. S94–S106, Sep. 2001.

[83] S. Veerachamy, T. Yarlagadda, G. Manivasagam, and P. K. Yarlagadda, "Bacterial adherence and biofilm formation on medical implants: a review.," *Proc. Inst. Mech. Eng. H.*, vol. 228, no. 10, pp. 1083–99, Oct. 2014.

[84] Chee Meng Pang, Peiying Hong, and Huiling Guo, and W.-T. Liu*, "Biofilm Formation Characteristics of Bacterial Isolates Retrieved from a Reverse Osmosis Membrane," 2005.

[85] G. Cheng, Z. Zhang, S. Chen, J. D. Bryers, and S. Jiang, "Inhibition of bacterial adhesion and biofilm formation on zwitterionic surfaces," *Biomaterials*, vol. 28, pp. 4192–4199, 2007.

[86] D. Losic, M. S. Aw, A. Santos, K. Gulati, and M. Bariana, "Titania nanotube arrays for local drug delivery : recent advances and perspectives," pp. 103–127, 2015.

[87] M. Zilberman and J. J. Elsner, "Antibiotic-eluting medical devices for various applications," *J. Control. Release*, vol. 130, no. 3, pp. 202–215, 2008.

[88] A. Fahr and X. Liu, "Drug delivery strategies for poorly water-soluble drugs," *Expert Opin. Drug Deliv.*, vol. 4, no. 4, pp. 403–416, Jul. 2007.

[89] H. Liu and T. J. Webster, "Ceramic/polymer nanocomposites with tunable drug delivery capability at specific disease sites," *J. Biomed. Mater. Res. Part A*, vol. 9999A, no. 3, p. NA-NA, Jun. 2009.

[90] M. G. House *et al.*, "Expression of an Extracellular Calcium-Sensing Receptor in Human and Mouse Bone Marrow Cells," *J. Bone Miner. Res.*, vol. 12, no. 12, pp. 1959–1970, Dec. 1997.

[91] R. Vaishya, M. Chauhan, and A. Vaish, "Bone cement," *J. Clin. Orthop. Trauma*, vol. 4, pp. 157–163, 2013.

[92] K. Kanellakopoulou and E. J. Giamarellos-Bourboulis, "Carrier systems for the local delivery of antibiotics in bone infections.," *Drugs*, vol. 59, no. 6, pp. 1223–32, Jun. 2000.

[93] D. A. Wininger and R. J. Fass, "MINIREVIEW Antibiotic-Impregnated Cement and Beads for Orthopedic Infections," *Antimicrob. Agents Chemother.*, vol. 40, no. 12, pp. 2675–2679, 1996.

[94] M. Nottrott, "Acrylic bone cements Influence of time and environment on physical properties," 2010.

[95] S. J. Breusch and H. Malchau, "The Well-Cemented Total Hip Arthroplasty Theory and Practice."

[96] L. I. Havelin, B. Espehaug, S. E. Vollset, and L. B. Engesaeter, "The effect of the type of cement on early revision of Charnley total hip prostheses. A review of eight thousand five hundred and seventy-nine primary arthroplasties from the Norwegian Arthroplasty Register.," *J. Bone Joint Surg. Am.*, vol. 77, no. 10, pp. 1543–50, Oct. 1995.

[97] P. Smitham *et al.*, "Bone cement: perioperative issues, orthopaedic applications and future developments," 2014.

[98] M. Arora, E. K. Chan, S. Gupta, and A. D. Diwan, "Polymethylmethacrylate bone cements and additives: A review of the literature," *World J. Orthop.*, vol. 4, no. 2, p. 67, Apr. 2013.

[99] K. W. Lye, H. Tideman, M. A. W. Merkx, and J. A. Jansen, “Bone cements and their potential use in a mandibular endoprosthesis.,” *Tissue Eng. Part B. Rev.*, vol. 15, no. 4, pp. 485–96, Dec. 2009.

[100] B. Magnan, M. Bondi, T. Maluta, E. Samaila, L. Schirru, and C. Dall’Oca, “Acrylic bone cement: current concept review,” *Musculoskelet. Surg.*, vol. 97, no. 2, pp. 93–100, Aug. 2013.

[101] E. J. Harper, “Bioactive bone cements.”

[102] W. E. BROWN, L. C. Chow, and W. E. Brown, “A new calcium phosphate, water-setting cement.” 01-Jan-1986.

[103] J. Zhang, W. Liu, V. Schnitzler, F. Tancret, and J. M. Bouler, “Calcium phosphate cements for bone substitution: Chemistry, handling and mechanical properties,” *Acta Biomater.*, vol. 10, no. 3, pp. 1035–1049, 2014.

[104] M. P. Ginebra, C. Canal, M. Espanol, D. Pastorino, and E. B. Montufar, “Calcium phosphate cements as drug delivery materials,” *Adv. Drug Deliv. Rev.*, vol. 64, no. 12, pp. 1090–1110, 2012.

[105] J. A. Planell, *Bone repair biomaterials*. Woodhead, 2009.

[106] G. Fernandez de Grado *et al.*, “Bone substitutes: a review of their characteristics, clinical use, and perspectives for large bone defects management,” *J. Tissue Eng.*, vol. 9, p. 204173141877681, Jan. 2018.

[107] J. Tritz *et al.*, “Designing a three-dimensional alginate hydrogel by spraying method for cartilage tissue engineering,” *Soft Matter*, vol. 6, no. 20, p. 5165, Oct. 2010.

[108] R. J. Narayan, R. D. Boehm, and A. V. Sumant, “Medical applications of diamond particles & surfaces,” *Mater. Today*, vol. 14, no. 4, pp. 154–163, Apr. 2011.

[109] A. Hoppe, N. S. Güldal, and A. R. Boccaccini, “A review of the biological response to ionic dissolution products from bioactive glasses and glass-ceramics,” *Biomaterials*, vol. 32, no. 11, pp. 2757–2774, Apr. 2011.

[110] K. Rezwan, Q. Z. Chen, J. J. Blaker, and A. R. Boccaccini, “Biodegradable and bioactive porous polymer/inorganic composite scaffolds for bone tissue engineering,” *Biomaterials*, vol. 27, no. 18, pp. 3413–3431, Jun. 2006.

[111] M. Bohner and G. Baroud, “Injectability of calcium phosphate pastes,” *Biomaterials*, vol. 26, no. 13, pp. 1553–1563, May 2005.

[112] E. Landi, S. Martorana, A. Tampieri, S. Guicciardi, and C. Melandri, “Carbonated-Apatite/Gelatine Porous Scaffolds for Bone Replacement,” *Key Eng. Mater.*, vol. 361–363, pp. 547–550, Nov. 2007.

[113] S. P. Adiga, C. Jin, L. A. Curtiss, N. A. Monteiro-Riviere, and R. J. Narayan, “Nanoporous membranes for medical and biological applications,” *Wiley Interdiscip. Rev. Nanomedicine Nanobiotechnology*, vol. 1, no. 5, pp. 568–581, Sep. 2009.

[114] M. P. Ginebra, T. Traykova, and J. A. Planell, “Calcium phosphate cements as bone drug delivery systems: A review,” *J. Control. Release*, vol. 113, no. 2, pp. 102–110, 2006.

[115] A. Tampieri, G. Celotti, E. Landi, M. Sandri, N. Roveri, and G. Falini, “Biologically

inspired synthesis of bone-like composite: Self-assembled collagen fibers/hydroxyapatite nanocrystals," *J. Biomed. Mater. Res.*, vol. 67A, no. 2, pp. 618–625, Nov. 2003.

[116] M. J. Penner, B. A. Masri, and C. P. Duncan, "Elution characteristics of vancomycin and tobramycin combined in acrylic bone-cement.," *J. Arthroplasty*, vol. 11, no. 8, pp. 939–44, Dec. 1996.

[117] V. Alt *et al.*, "An in vitro assessment of the antibacterial properties and cytotoxicity of nanoparticulate silver bone cement," *Biomaterials*, vol. 25, no. 18, pp. 4383–4391, Aug. 2004.

[118] Z. Shi, K. G. Neoh, E. T. Kang, and W. Wang, "Antibacterial and mechanical properties of bone cement impregnated with chitosan nanoparticles," *Biomaterials*, vol. 27, no. 11, pp. 2440–2449, Apr. 2006.

[119] J. A. Goodell, A. B. Flick, J. C. Hebert, and J. G. Howe, "Preparation and release characteristics of tobramycin-impregnated polymethylmethacrylate beads.," *Am. J. Hosp. Pharm.*, vol. 43, no. 6, pp. 1454–61, Jun. 1986.

[120] K. Adams, L. Couch, G. Cierny, J. Calhoun, and J. T. Mader, "In vitro and in vivo evaluation of antibiotic diffusion from antibiotic-impregnated polymethylmethacrylate beads.," *Clin. Orthop. Relat. Res.*, no. 278, pp. 244–52, May 1992.

[121] D. Neut, J. G. E. Hendriks, J. R. Van Horn, R. S. Z. Kowalski, H. C. Van Der Mei, and H. J. Busscher, "Antimicrobial Efficacy of Gentamicin-Loaded Acrylic Bone Cements with Fusidic Acid or Clindamycin Added."

[122] F. R. Dimaio, J. J. O'halloran, and J. M. Quale, "In Vitro Elution of Ciprofloxacin from Polymet h ylme t hacry lat e Cement Beads."

[123] K. E. Marks, C. L. Nelson, and E. P. Lautenschlager, "Antibiotic-impregnated acrylic bone cement.," *J. Bone Joint Surg. Am.*, vol. 58, no. 3, pp. 358–64, Apr. 1976.

[124] H. van de Belt *et al.*, "Surface roughness, porosity and wettability of gentamicin-loaded bone cements and their antibiotic release.," *Biomaterials*, vol. 21, no. 19, pp. 1981–7, Oct. 2000.

[125] M. R. Virto, P. Frutos, S. Torrado, and G. Frutos, "Gentamicin release from modified acrylic bone cements with lactose and hydroxypropylmethylcellulose.," *Biomaterials*, vol. 24, no. 1, pp. 79–87, Jan. 2003.

[126] B. Picknell, L. Mizen, and R. Sutherland, "Antibacterial activity of antibiotics in acrylic bone cement.," *J. Bone Joint Surg. Br.*, vol. 59, no. 3, pp. 302–7, Aug. 1977.

[127] B. A. Masri, C. P. Duncan, C. P. Beauchamp, N. J. Paris, and J. Arntorp, "Effect of varying surface patterns on antibiotic elution from antibiotic-loaded bone cement.," *J. Arthroplasty*, vol. 10, no. 4, pp. 453–9, Aug. 1995.

[128] H. Wahlig, E. Dingeldein, R. Bergmann, and K. Reuss, "The release of gentamicin from polymethylmethacrylate beads. An experimental and pharmacokinetic study.," *J. Bone Joint Surg. Br.*, vol. 60-B, no. 2, pp. 270–5, May 1978.

[129] V. R., C. M., and V. A., "Bone cement," *J. Clin. Orthop. Trauma*, vol. 4, no. 4, pp. 157–163, 2013.

[130] R. R. Roberts *et al.*, "The Use of Economic Modeling to Determine the Hospital Costs

Associated with Nosocomial Infections," *Clin. Infect. Dis.*, vol. 36, no. 11, pp. 1424–1432, Jun. 2003.

[131] J. Ricci *et al.*, "Biological mechanisms of calcium sulfate replacement by bone." Em2 Inc., pp. 332–344, 2000.

[132] S. Bose and S. Tarafder, "Calcium phosphate ceramic systems in growth factor and drug delivery for bone tissue engineering: A review," *Acta Biomater.*, vol. 8, no. 4, pp. 1401–1421, 2012.

[133] D. Yu, J. Wong, Y. Matsuda, J. L. Fox, W. I. Higuchi, and M. Otsuka, "Self-Setting Hydroxyapatite Cement: A Novel Skeletal Drug-Delivery System for Antibiotics," *J. Pharm. Sci.*, vol. 81, no. 6, pp. 529–531, Jun. 1992.

[134] T. Higuchi, "Mechanism of sustained-action medication. Theoretical analysis of rate of release of solid drugs dispersed in solid matrices," *J. Pharm. Sci.*, vol. 52, no. 12, pp. 1145–1149, Dec. 1963.

[135] M. P. Ginebra, T. Traykova, and J. A. Planell, "Calcium phosphate cements: Competitive drug carriers for the musculoskeletal system?," *Biomaterials*, vol. 27, no. 10, pp. 2171–2177, 2006.

[136] J. C. Doadrio, D. Arcos, M. V. Cabañas, and M. Vallet-Regí, "Calcium sulphate-based cements containing cephalexin," *Biomaterials*, vol. 25, no. 13, pp. 2629–2635, Jun. 2004.

[137] L. S. Nair and C. T. Laurencin, "Biodegradable polymers as biomaterials," *Prog. Polym. Sci.*, vol. 32, no. 8–9, pp. 762–798, Aug. 2007.

[138] K. Rezwan, Q. Z. Chen, J. J. Blaker, and A. R. Boccaccini, "Biodegradable and bioactive porous polymer/inorganic composite scaffolds for bone tissue engineering," *Biomaterials*, vol. 27, no. 18, pp. 3413–3431, Jun. 2006.

[139] L. Tan, X. Yu, P. Wan, and K. Yang, "Biodegradable Materials for Bone Repairs: A Review," *J. Mater. Sci. Technol.*, vol. 29, no. 6, pp. 503–513, Jun. 2013.

[140] S. COMMANDEUR, H. M. M. VAN BEUSEKOM, and W. J. VAN DER GIESSEN, "Polymers, Drug Release, and Drug-Eluting Stents," *J. Interv. Cardiol.*, vol. 19, no. 6, pp. 500–506, Dec. 2006.

[141] L. Di Silvio, R. G. Courteney-Harris, and S. Downes, "The use of gelatin as a vehicle for drug and peptide delivery," *J. Mater. Sci. Mater. Med.*, vol. 5, no. 11, pp. 819–823, Nov. 1994.

[142] G. J. S. Dawes, L. E. Fratila-Apachitei, K. Mulia, I. Apachitei, G.-J. Witkamp, and J. Duszczyk, "Size effect of PLGA spheres on drug loading efficiency and release profiles," *J. Mater. Sci. Mater. Med.*, vol. 20, no. 5, pp. 1089–1094, May 2009.

[143] T. Ling *et al.*, "Improvement of drug elution in thin mineralized collagen coatings with PLGA-PEG-PLGA micelles," *J. Biomed. Mater. Res. Part A*, vol. 101, no. 11, p. n/a-n/a, Nov. 2013.

[144] M. Aviv, I. Berdicevsky, and M. Zilberman, "Gentamicin-loaded bioresorbable films for prevention of bacterial infections associated with orthopedic implants," *J. Biomed. Mater. Res. Part A*, vol. 83A, no. 1, pp. 10–19, Oct. 2007.

[145] S. C. von Plocki *et al.*, "Biodegradable Sleeves for Metal Implants to Prevent Implant-

Associated Infection: An Experimental In Vivo Study in Sheep," *Vet. Surg.*, vol. 41, no. 3, p. n/a-n/a, Jan. 2012.

[146] M. LUCKE *et al.*, "Systemic versus local application of gentamicin in prophylaxis of implant-related osteomyelitis in a rat model," *Bone*, vol. 36, no. 5, pp. 770–778, May 2005.

[147] H. Gollwitzer, K. Ibrahim, H. Meyer, W. Mittelmeier, R. Busch, and A. Stemberger, "Antibacterial poly(D,L-lactic acid) coating of medical implants using a biodegradable drug delivery technology.," *J. Antimicrob. Chemother.*, vol. 51, no. 3, pp. 585–91, Mar. 2003.

[148] J. A. Lyndon, B. J. Boyd, and N. Birbilis, "Metallic implant drug/device combinations for controlled drug release in orthopaedic applications," *J. Control. Release*, vol. 179, pp. 63–75, Apr. 2014.

[149] H. Gollwitzer, K. Ibrahim, H. Meyer, W. Mittelmeier, R. Busch, and A. Stemberger, "Antibacterial poly(D,L-lactic acid) coating of medical implants using a biodegradable drug delivery technology," *J. Antimicrob. Chemother.*, vol. 51, no. 3, pp. 585–591, Mar. 2003.

[150] K. de Groot, J. G. C. Wolke, and J. A. Jansen, "Calcium phosphate coatings for medical implants," *Proc. Inst. Mech. Eng. Part H J. Eng. Med.*, vol. 212, no. 2, pp. 137–147, Feb. 1998.

[151] D. Arcos and M. Vallet-Regí, "Bioceramics for drug delivery," *Acta Mater.*, vol. 61, no. 3, pp. 890–911, Feb. 2013.

[152] S. V. Dorozhkin and M. Epple, "Biological and Medical Significance of Calcium Phosphates," *Angew. Chemie Int. Ed.*, vol. 41, no. 17, pp. 3130–3146, Sep. 2002.

[153] W. L. Jaffe and D. F. Scott, "Total hip arthroplasty with hydroxyapatite-coated prostheses.," *J. Bone Joint Surg. Am.*, vol. 78, no. 12, pp. 1918–34, Dec. 1996.

[154] M. Dusková *et al.*, "Bioactive Glass-Ceramics in Facial Skeleton Contouring," *Aesthetic Plast. Surg.*, vol. 26, no. 4, pp. 274–283, Jul. 2002.

[155] L. Tan, X. Yu, P. Wan, and K. Yang, "Biodegradable Materials for Bone Repairs: A Review," *J. Mater. Sci. Technol.*, vol. 29, no. 6, pp. 503–513, Jun. 2013.

[156] K. De Groot, R. Geesink, C. P. A. T. Klein, and P. Serekian, "Plasma sprayed coatings of hydroxylapatite," *J. Biomed. Mater. Res.*, vol. 21, no. 12, pp. 1375–1381, Dec. 1987.

[157] K. A. Gross and C. C. Berndt, "Thermal processing of hydroxyapatite for coating production.," *J. Biomed. Mater. Res.*, vol. 39, no. 4, pp. 580–7, Mar. 1998.

[158] S.-J. Ding, "Properties and immersion behavior of magnetron-sputtered multi-layered hydroxyapatite/titanium composite coatings," *Biomaterials*, vol. 24, no. 23, pp. 4233–4238, Oct. 2003.

[159] L. Clèries, E. Martínez, J. . Fernández-Pradas, G. Sardin, J. Esteve, and J. . Morenza, "Mechanical properties of calcium phosphate coatings deposited by laser ablation," *Biomaterials*, vol. 21, no. 9, pp. 967–971, May 2000.

[160] S. Kačiulis *et al.*, "Surface analysis of biocompatible coatings on titanium," *J. Electron Spectros. Relat. Phenomena*, vol. 95, no. 1, pp. 61–69, Aug. 1998.

[161] P. Li, K. de Groot, and T. Kokubo, "Bioactive Ca10(PO4)6(OH)2−TiO2 composite coating prepared by sol-gel process," *J. Sol-Gel Sci. Technol.*, vol. 7, no. 1–2, pp. 27–34, Aug. 1996.

[162] Y. Han, T. Fu, J. Lu, and K. Xu, “Characterization and stability of hydroxyapatite coatings prepared by an electrodeposition and alkaline-treatment process,” *J. Biomed. Mater. Res.*, vol. 54, no. 1, pp. 96–101, Jan. 2001.

[163] P. Habibovic, F. Barrè, C. A. Van Blitterswijk, K. De Groot, and P. Layrolle, “Biomimetic Hydroxyapatite Coating on Metal Implants.”

[164] K. Duan, Y. Fan, and R. Wang, “Electrolytic deposition of calcium etidronate drug coating on titanium substrate,” *J. Biomed. Mater. Res.*, vol. 72B, no. 1, pp. 43–51, Jan. 2005.

[165] J. Xiao, Y. Zhu, Y. Liu, Y. Zeng, and F. Xu, “An asymmetric coating composed of gelatin and hydroxyapatite for the delivery of water insoluble drug,” *J. Mater. Sci. Mater. Med.*, vol. 20, no. 4, pp. 889–896, Apr. 2009.

[166] E. P. Avés *et al.*, “Hydroxyapatite coating by sol–gel on Ti–6Al–4V alloy as drug carrier,” *J. Mater. Sci. Mater. Med.*, vol. 20, no. 2, pp. 543–547, Feb. 2009.

[167] H. Thomazeau and F. Langlais, “[Antibiotic release by tricalcic phosphate bone implantation. In vitro and in vivo pharmacokinetics of different galenic forms].,” *Chirurgie*, vol. 121, no. 9–10, pp. 663–6, Jan. 1997.

[168] S. Radin, J. T. Campbell, P. Ducheyne, and J. M. Cuckler, “Calcium phosphate ceramic coatings as carriers of vancomycin.,” *Biomaterials*, vol. 18, no. 11, pp. 777–82, Jun. 1997.

[169] H. Wahlig, E. Dingeldein, R. Bergmann, and K. Reuss, “The release of gentamicin from polymethylmethacrylate beads. An experimental and pharmacokinetic study.,” *J. Bone Joint Surg. Br.*, vol. 60-B, no. 2, pp. 270–5, May 1978.

[170] S. F. Hoff, R. H. Fitzgerald, and P. J. Kelly, “The depot administration of penicillin G and gentamicin in acrylic bone cement.,” *J. Bone Joint Surg. Am.*, vol. 63, no. 5, pp. 798–804, Jun. 1981.

[171] F. Chai, J.-C. Hornez, N. Blanchemain, C. Neut, M. Descamps, and H. F. Hildebrand, “Antibacterial activation of hydroxyapatite (HA) with controlled porosity by different antibiotics,” *Biomol. Eng.*, vol. 24, no. 5, pp. 510–514, Nov. 2007.

[172] M. Stigter, K. de Groot, and P. Layrolle, “Incorporation of tobramycin into biomimetic hydroxyapatite coating on titanium.,” *Biomaterials*, vol. 23, no. 20, pp. 4143–53, Oct. 2002.

[173] E. M. Brach Del Prever, A. Bistolfi, P. Bracco, and L. Costa, “UHMWPE for arthroplasty: past or future?,” *J. Orthop. Traumatol.*, vol. 10, no. 1, pp. 1–8, Mar. 2009.

[174] S. M. Kurtz, *UHMWPE biomaterials handbook : ultra-high molecular weight polyethylene in total joint replacement and medical devices*. .

[175] R. Jamjah, G. H. Zohuri, M. Javaheri, M. Nekoomanesh, S. Ahmadjo, and A. Farhadi, “Synthesizing UHMWPE Using Ziegler-Natta Catalyst System of MgCl 2 (ethoxide type)/ TiCl 4 /tri-isobutylaluminum.”

[176] D. L. P. Macuvele *et al.*, “Advances in ultra high molecular weight polyethylene/hydroxyapatite composites for biomedical applications: A brief review,” *Mater. Sci. Eng. C*, vol. 76, pp. 1248–1262, Jul. 2017.

[177] E. Enqvist, *Carbon Nanofiller Reinforced UHMWPE for Orthopaedic Applications*. .

[178] S. M. Kurtz, O. K. Muratoglu, M. Evans, and A. A. Edidin, “Advances in the processing,

sterilization, and crosslinking of ultra-high molecular weight polyethylene for total joint arthroplasty.," *Biomaterials*, vol. 20, no. 18, pp. 1659–88, Sep. 1999.

[179] S. B. Goodman, "Wear particles, periprosthetic osteolysis and the immune system.," *Biomaterials*, vol. 28, no. 34, pp. 5044–8, Dec. 2007.

[180] H. C. Amstutz, P. Campbell, N. Kossovsky, and I. C. Clarke, "Mechanism and clinical significance of wear debris-induced osteolysis.," *Clin. Orthop. Relat. Res.*, no. 276, pp. 7–18, Mar. 1992.

[181] S. S. Moreno, *Carbon Reinforced UHMWPE Composites for Orthopaedic Applications Characterization and Biological Response to Wear Particles*. 2013.

[182] G. Lewis, "Properties of crosslinked ultra-high-molecular-weight polyethylene.," *Biomaterials*, vol. 22, no. 4, pp. 371–401, Feb. 2001.

[183] K. Park, S. Mishra, G. Lewis, J. Losby, Z. Fan, and J. B. Park, "Quasi-static and dynamic nanoindentation studies on highly crosslinked ultra-high-molecular-weight polyethylene.," *Biomaterials*, vol. 25, no. 12, pp. 2427–36, May 2004.

[184] A. Bistolfi, M. B. Turell, Y.-L. Lee, and A. Bellare, "Tensile and tribological properties of high-crystallinity radiation crosslinked UHMWPE," *J. Biomed. Mater. Res. Part B Appl. Biomater.*, vol. 90B, no. 1, pp. 137–144, Nov. 2008.

[185] M. Narkis, A. Tzur, A. Vaxman, and H. G. Fritz, "Some properties of silane-grafted moisture-crosslinked polyethylene," *Polym. Eng. Sci.*, vol. 25, no. 13, pp. 857–862, Sep. 1985.

[186] M. L. Shofner, V. N. Khabashesku, and E. V. Barrera, "Processing and Mechanical Properties of Fluorinated Single-Wall Carbon Nanotube−Polyethylene Composites," *Chem. Mater.*, vol. 18, no. 4, pp. 906–913, Feb. 2006.

[187] W. Wood, B. Li, and W.-H. Zhong, "Influence of phase morphology on the sliding wear of polyethylene blends filled with carbon nanofibers," *Polym. Eng. Sci.*, vol. 50, no. 3, pp. 613–623, Mar. 2010.

[188] S. Xu and X. W. Tangpong, "Review: Tribological behavior of polyethylene-based nanocomposites," *J. Mater. Sci.*, vol. 48, no. 2, pp. 578–597, Jan. 2013.

[189] S. A. Mirsalehi, A. Khavandi, S. Mirdamadi, M. R. Naimi-Jamal, and S. M. Kalantari, "Nanomechanical and tribological behavior of hydroxyapatite reinforced ultrahigh molecular weight polyethylene nanocomposites for biomedical applications," *J. Appl. Polym. Sci.*, vol. 132, no. 23, p. n/a-n/a, Jun. 2015.

[190] M. Deng and S. W. Shalaby, "Properties of self-reinforced ultra-high-molecular-weight polyethylene composites.," *Biomaterials*, vol. 18, no. 9, pp. 645–55, May 1997.

[191] S. R. Bakshi, J. E. Tercero, and A. Agarwal, "Synthesis and characterization of multiwalled carbon nanotube reinforced ultra high molecular weight polyethylene composite by electrostatic spraying technique."

[192] D. Lahiri *et al.*, "Graphene Nanoplatelet-Induced Strengthening of UltraHigh Molecular Weight Polyethylene and Biocompatibility In vitro," *ACS Appl. Mater. Interfaces*, vol. 4, no. 4, pp. 2234–2241, Apr. 2012.

[193] A. Gupta *et al.*, "Compression Molded Ultra High Molecular Weight Polyethylene–

Hydroxyapatite–Aluminum Oxide–Carbon Nanotube Hybrid Composites for Hard Tissue Replacement," *J. Mater. Sci. Technol.*, vol. 29, no. 6, pp. 514–522, Jun. 2013.

[194] D. A. Baker, R. S. Hastings, and L. Pruitt, "Study of fatigue resistance of chemical and radiation crosslinked medical grade ultrahigh molecular weight polyethylene.," *J. Biomed. Mater. Res.*, vol. 46, no. 4, pp. 573–81, Sep. 1999.

[195] E. W. Wong, P. E. Sheehan, C. M. Lieber, W. A. de de Heer WA, T. F. Kelly, and R. S. Ruoff, "Nanobeam Mechanics: Elasticity, Strength, and Toughness of Nanorods and Nanotubes," *Science (80-.).*, vol. 277, no. 5334, pp. 1971–1975, Sep. 1997.

[196] Yu, Lourie, Dyer, Moloni, Kelly, and Ruoff, "Strength and breaking mechanism of multiwalled carbon nanotubes under tensile load," *Science*, vol. 287, no. 5453, pp. 637–40, Jan. 2000.

[197] B. B. Johnson, M. H. Santare, J. E. Novotny, and S. G. Advani, "Wear Behavior of Carbon Nanotube/High Density Polyethylene Composites.," *Mech. Mater.*, vol. 41, no. 10, pp. 1108–1115, Oct. 2009.

[198] R. Manoj Kumar, S. K. Sharma, B. V. Manoj Kumar, and D. Lahiri, "Effects of carbon nanotube aspect ratio on strengthening and tribological behavior of ultra high molecular weight polyethylene composite," *Compos. Part A Appl. Sci. Manuf.*, vol. 76, pp. 62–72, 2015.

[199] N. Saito *et al.*, "Safe Clinical Use of Carbon Nanotubes as Innovative Biomaterials," *Chem. Rev.*, vol. 114, no. 11, pp. 6040–6079, Jun. 2014.

[200] N. W. Shi Kam, T. C. Jessop, P. A. Wender, and H. Dai, "Nanotube Molecular Transporters: Internalization of Carbon Nanotube−Protein Conjugates into Mammalian Cells," *J. Am. Chem. Soc.*, vol. 126, no. 22, pp. 6850–6851, Jun. 2004.

[201] S. L. Ruan, P. Gao, X. G. Yang, and T. X. Yu, "Toughening high performance ultrahigh molecular weight polyethylene using multiwalled carbon nanotubes," *Polymer (Guildf).*, vol. 44, no. 19, pp. 5643–5654, Sep. 2003.

[202] M. A. Samad and S. K. Sinha, "Mechanical, thermal and tribological characterization of a UHMWPE film reinforced with carbon nanotubes coated on steel," *Tribol. Int.*, vol. 44, no. 12, pp. 1932–1941, Nov. 2011.

[203] S. Bal and S. S. Samal, "Carbon nanotube reinforced polymer composites—A state of the art," *Bull. Mater. Sci.*, vol. 30, no. 4, pp. 379–386, Aug. 2007.

[204] D. Qian, D. Qian, E. C. D. A, R. Andrews, and T. Rantell, "Load transfer and deformation mechanisms in carbon nanotube-polystyrene composites," *Appl. Phys. Lett.*, pp. 2868--2870, 2000.

[205] M. R. Ayatollahi, S. Shadlou, M. M. Shokrieh, and M. Chitsazzadeh, "Effect of multi-walled carbon nanotube aspect ratio on mechanical and electrical properties of epoxy-based nanocomposites," *Polym. Test.*, vol. 30, no. 5, pp. 548–556, Aug. 2011.

[206] D. Wu, L. Wu, W. Zhou, Y. Sun, and M. Zhang, "Relations between the aspect ratio of carbon nanotubes and the formation of percolation networks in biodegradable polylactide/carbon nanotube composites," *J. Polym. Sci. Part B Polym. Phys.*, vol. 48, no. 4, pp. 479–489, Feb. 2010.

[207] W. Zhang, R. C. Picu, and N. Koratkar, “The effect of carbon nanotube dimensions and dispersion on the fatigue behavior of epoxy nanocomposites,” *Nanotechnology*, vol. 19, no. 28, p. 285709, Jul. 2008.

[208] Z. Wei, Y.-P. Zhao, S. L. Ruan, P. Gao, and T. X. Yu, “A study of the tribological behavior of carbon-nanotube-reinforced ultrahigh molecular weight polyethylene composites,” *Surf. INTERFACE Anal. Surf. Interface Anal*, vol. 38, pp. 883–886, 2006.

[209] J.-H. Lee, J. Kathi, K. Y. Rhee, and J. H. Lee, “Wear properties of 3-aminopropyltriethoxysilane-functionalized carbon nanotubes reinforced ultra high molecular weight polyethylene nanocomposites,” *Polym. Eng. Sci.*, vol. 50, no. 7, pp. 1433–1439, Jul. 2010.

[210] X. Wu, J. Zhang, C. Wu, G. Wang, and P. Jiang, “Study on tribological properties of UHMWPE irradiated by electron beam with TMPTMA and TPGDA as crosslinking agents,” *Wear*, vol. 297, no. 1–2, pp. 742–751, 2013.

[211] J. Fang *et al.*, “Freeze-drying method prepared UHMWPE/CNTs composites with optimized micromorphologies and improved tribological performance,” *J. Appl. Polym. Sci.*, vol. 132, no. 18, pp. 1–7, 2015.

[212] X. Ren, X. Q. Wang, G. Sui, W. H. Zhong, M. A. Fuqua, and C. A. Ulven, “Effects of carbon nanofibers on crystalline structures and properties of ultrahigh molecular weight polyethylene blend fabricated using twin-screw extrusion,” *J. Appl. Polym. Sci.*, vol. 107, no. 5, pp. 2837–2845, Mar. 2008.

[213] G. Sui, W. H. Zhong, X. Ren, X. Q. Wang, and X. P. Yang, “Structure, mechanical properties and friction behavior of UHMWPE/HDPE/carbon nanofibers,” *Mater. Chem. Phys.*, vol. 115, no. 1, pp. 404–412, May 2009.

[214] M. J. Martínez-Morlanes, F. J. Medel, M. D. Mariscal, and J. A. Puértolas, “On the assessment of oxidative stability of post-irradiation stabilized highly crosslinked UHMWPEs by thermogravimetry,” *Polym. Test.*, vol. 29, no. 4, pp. 425–432, Jun. 2010.

[215] P. Gill, T. T. Moghadam, and B. Ranjbar, “Differential scanning calorimetry techniques: applications in biology and nanoscience.,” *J. Biomol. Tech.*, vol. 21, no. 4, pp. 167–93, Dec. 2010.

[216] S. M. Kurtz, *The UHMWPE handbook : ultra-high molecular weight polyethylene in total joint replacement*. Academic Press, 2004.

[217] M. a L. I. Golozar and R. Bagheri, “High-Density Polyethylene Coating on Carbon Steel by an Electrostatic Powder Spray System,” pp. 5–7, 1998.

[218] L. K. Prasad, J. M. Keen, J. S. Lafountaine, J. Maincent, R. O. Williams, and J. W. McGinity, “Electrostatic powder deposition to prepare films for drug delivery,” *J. Drug Deliv. Sci. Technol.*, vol. 30, pp. 501–510, 2015.

[219] S. Singh, V. K. Meena, M. Sharma, and H. Singh, “Preparation and coating of nano-ceramic on orthopaedic implant material using electrostatic spray deposition,” *Mater. Des.*, vol. 88, pp. 278–286, 2015.

[220] S. R. Bakshi, J. E. Tercero, and a. Agarwal, “Synthesis and characterization of multiwalled carbon nanotube reinforced ultra high molecular weight polyethylene composite by

electrostatic spraying technique," *Compos. Part A Appl. Sci. Manuf.*, vol. 38, no. 12, pp. 2493–2499, Dec. 2007.

[221] M. Zouari, M. Kharrat, M. Dammak, and M. Barletta, "Scratch resistance and tribological performance of thermosetting composite powder coatings system: A comparative evaluation," *Surf. Coatings Technol.*, vol. 263, pp. 27–35, 2015.

[222] E. Torlak and M. Nizamlioğlu, "Antimicrobial effectiveness of chitosan-essential oil coated plastic films against foodborne pathogens," *J. Plast. Film Sheeting*, vol. 27, no. 3, pp. 235–248, Jul. 2011.

[223] T. Mosmann, "Rapid colorimetric assay for cellular growth and survival: application to proliferation and cytotoxicity assays.," *J. Immunol. Methods*, vol. 65, no. 1–2, pp. 55–63, Dec. 1983.

[224] W. C. Oliver and G. M. Pharr, "An improved technique for determining hardness and elastic modulus using load and displacement sensing indentation experiments," *J. Mater. Res.*, vol. 7, no. 06, pp. 1564–1583, Jun. 1992.

[225] T. Whelan, *Polymer Technology Dictionary*. Dordrecht: Springer Netherlands, 1994.

[226] K. S. Whiteley, T. G. Heggs, H. Koch, R. L. Mawer, and W. Immel, "Polyolefins," in *Ullmann's Encyclopedia of Industrial Chemistry*, Weinheim, Germany: Wiley-VCH Verlag GmbH & Co. KGaA, 2000.

[227] F. Pishbin *et al.*, "Electrophoretic Deposition of Gentamicin-Loaded Bioactive Glass/Chitosan Composite Coatings for Orthopaedic Implants," *ACS Appl. Mater. Interfaces*, vol. 6, no. 11, pp. 8796–8806, Jun. 2014.

[228] S. Honary, M. Maleki, and M. Karami, "The effect of chitosan molecular weight on the properties of alginate/ chitosan microparticles containing prednisolone," *Trop. J. Pharm. Res.*, vol. 8, no. 1, pp. 53–61, Feb. 2009.

[229] W. C. Oliver and G. M. Pharr, "An improved technique for determining hardness and elastic modulus using load and displacement sensing indentation experiments," *J. Mater. Res.*, vol. 7, no. 06, pp. 1564–1583, Jun. 1992.

[230] *,† Shao-Feng Wang, † Lu Shen, *,‡ and Wei-De Zhang, and Y.-J. Tong§, "Preparation and Mechanical Properties of Chitosan/Carbon Nanotubes Composites," 2005.

[231] M. P. Fernández-Ronco *et al.*, "Improving the wear resistance of UHMWPE implants by in situ precipitation of hyaluronic acid using supercritical fluid technology," *J. Supercrit. Fluids*, vol. 95, pp. 204–213, Nov. 2014.

[232] C. H. Navarro, K. J. Moreno, A. Arizmendi-Morquecho, A. Chávez-Valdez, and S. García-Miranda, "Preparation and tribological properties of chitosan/hydroxyapatite composite coatings applied on ultra high molecular weight polyethylene substrate," *J. Plast. Film Sheeting*, vol. 28, no. 4, pp. 279–297, Oct. 2012.

[233] N. K. Myshkin, M. I. Petrokovets, and A. V. Kovalev, "Tribology of polymers: Adhesion, friction, wear, and mass-transfer," *Tribol. Int.*, vol. 38, no. 11–12, pp. 910–921, Nov. 2005.

[234] B. J. Briscoe and S. K. Sinha, "Wear of polymers," *Proc. Inst. Mech. Eng. Part J J. Eng. Tribol.*, vol. 216, no. 6, pp. 401–413, Jun. 2002.

[235] S. Bahadur, "The development of transfer layers and their role in polymer tribology," *Wear,*

vol. 245, no. 1–2, pp. 92–99, Oct. 2000.

[236] L. Pichavant, G. Amador, C. Jacqueline, B. Brouillaud, V. Héroguez, and M.-C. Durrieu, “pH-controlled delivery of gentamicin sulfate from orthopedic devices preventing nosocomial infections,” *J. Control. Release*, vol. 162, no. 2, pp. 373–381, Sep. 2012.

[237] L. Di Silvio and W. Bonfield, “Biodegradable drug delivery system for the treatment of bone infection and repair.,” *J. Mater. Sci. Mater. Med.*, vol. 10, no. 10/11, pp. 653–8.

[238] R. Mustaffa, M. R. Yusof, F. Othman, and A. Rahmat, “DRUG RELEASE STUDY OF POROUS HYDROXYAPATITE COATED GENTAMYCIN-AS DRUG DELIVERY SYSTEM,” *Regen. Res.*, vol. 1, no. 2, pp. 61–67, 2012.

[239] Y. M. Yang, W. Hu, X. D. Wang, and X. S. Gu, “The controlling biodegradation of chitosan fibers by N-acetylation in vitro and in vivo,” *J. Mater. Sci. Mater. Med.*, vol. 18, no. 11, pp. 2117–2121, Nov. 2007.

[240] T. Jiang *et al.*, “Chitosan–poly(lactide-co-glycolide) microsphere-based scaffolds for bone tissue engineering: In vitro degradation and in vivo bone regeneration studies,” *Acta Biomater.*, vol. 6, no. 9, pp. 3457–3470, Sep. 2010.

[241] S. Kanagaraj, M. T. Mathew, A. Fonseca, M. S. A. Oliveira, and J. A. O. Simões, “Tribological characterisation of carbon nanotubes / ultrahigh molecular weight polyethylene composites : the effect of sliding distance,” vol. 4, 2010.

[242] S. R. Bakshi, K. Balani, T. Laha, J. Tercero, and A. Agarwal, “The Nanomechanical and Nanoscratch Properties of MWNT- Reinforced Ultrahigh-Molecular- Weight Polyethylene Coatings,” no. July, pp. 50–53, 2007.

[243] M. A. Samad and S. K. Sinha, “Mechanical, thermal and tribological characterization of a UHMWPE film reinforced with carbon nanotubes coated on steel,” *Tribol. Int.*, vol. 44, no. 12, pp. 1932–1941, Nov. 2011.

[244] H.-J. Park, J. Kim, Y. Seo, J. Shim, M.-Y. Sung, and S. Kwak, “Wear behavior of in situ polymerized carbon nanotube/ultra high molecular weight polyethylene composites,” *Macromol. Res.*, vol. 21, no. 9, pp. 965–970, Apr. 2013.

[245] Y.-S. Zoo, J.-W. An, D.-P. Lim, and D.-S. Lim, “Effect of Carbon Nanotube Addition on Tribological Behavior of UHMWPE,” *Tribol. Lett.*, vol. 16, no. 4, pp. 305–309, May 2004.

[246] Z. Wei, Y. Zhao, S. L. Ruan, P. Gao, and T. X. Yu, “A study of the tribological behavior of carbon-nanotube-reinforced ultrahigh molecular weight polyethylene composites,” pp. 883–886, 2006.

[247] J. Lee, J. Kathi, K. Y. Rhee, and J. H. Lee, “Wear Properties of 3-Aminopropyltriethoxysilane- Functionalized Carbon Nanotubes Reinforced Ultra High Molecular Weight Polyethylene Nanocomposites,” 2010.

[248] E. Assouline *et al.*, “Nucleation ability of multiwall carbon nanotubes in polypropylene composites,” *J. Polym. Sci. Part B Polym. Phys.*, vol. 41, no. 5, pp. 520–527, Mar. 2003.

[249] J. N. Coleman *et al.*, “High Performance Nanotube-Reinforced Plastics: Understanding the Mechanism of Strength Increase,” *Adv. Funct. Mater.*, vol. 14, no. 8, pp. 791–798, Aug. 2004.

[250] S. Kanagaraj, F. R. Varanda, T. V. Zhil’tsova, M. S. a. Oliveira, and J. a. O. Simões,

"Mechanical properties of high density polyethylene/carbon nanotube composites," *Compos. Sci. Technol.*, vol. 67, no. 15–16, pp. 3071–3077, Dec. 2007.

[251] T. McNally *et al.*, "Polyethylene multiwalled carbon nanotube composites," *Polymer (Guildf).*, vol. 46, no. 19, pp. 8222–8232, Sep. 2005.

[252] P. Kim, L. Shi, A. Majumdar, and P. L. Mceuen, "Thermal Transport Measurements of Individual Multiwalled Nanotubes," vol. 87, 2001.

[253] M. B. Turell and A. Bellare, "A study of the nanostructure and tensile properties of ultra-high molecular weight polyethylene.," *Biomaterials*, vol. 25, no. 17, pp. 3389–98, Aug. 2004.

[254] N. R. Pradhan, H. Duan, J. Liang, and G. S. Iannacchione, "The specific heat and effective thermal conductivity of composites containing single-wall and multi-wall carbon nanotubes," *Nanotechnology*, vol. 20, no. 24, p. 245705, Jun. 2009.

[255] B. H. Cipiriano *et al.*, "Effects of aspect ratio of MWNT on the flammability properties of polymer nanocomposites," *Polymer (Guildf).*, vol. 48, no. 20, pp. 6086–6096, Sep. 2007.

[256] D. I. Bower, "An Introduction to Polymer Physics."

[257] J. N. Coleman, U. Khan, W. J. Blau, and Y. K. Gun'ko, "Small but strong: A review of the mechanical properties of carbon nanotube–polymer composites," *Carbon N. Y.*, vol. 44, no. 9, pp. 1624–1652, Aug. 2006.

[258] B. . Demczyk *et al.*, "Direct mechanical measurement of the tensile strength and elastic modulus of multiwalled carbon nanotubes," *Mater. Sci. Eng. A*, vol. 334, no. 1–2, pp. 173–178, Sep. 2002.

[259] D. Lahiri, V. Singh, A. K. Keshri, S. Seal, and A. Agarwal, "Carbon nanotube toughened hydroxyapatite by spark plasma sintering: Microstructural evolution and multiscale tribological properties," *Carbon N. Y.*, vol. 48, no. 11, pp. 3103–3120, Sep. 2010.

[260] Cumings and Zettl, "Low-friction nanoscale linear bearing realized from multiwall carbon nanotubes," *Science*, vol. 289, no. 5479, pp. 602–4, Jul. 2000.

[261] Y. Zhang and M. Zhang, "Calcium phosphate/chitosan composite scaffolds for controlledin vitro antibiotic drug release," *J. Biomed. Mater. Res.*, vol. 62, no. 3, pp. 378–386, Dec. 2002.

[262] R. Colaço, M. P. Gispert, A. P. Serro, and B. Saramago, "An energy-based model for the wear of UHMWPE," *Tribol. Lett.*, vol. 26, no. 2, pp. 119–124, Mar. 2007.